

# **DAMPING OF POWER SYSTEM OSCILLATIONS USING FACTS DEVICES**

**THESIS**

*Submitted in fulfillment of the requirement of the degree of*

**DOCTOR OF PHILOSOPHY**

*to*

***YMCA UNIVERSITY OF SCIENCE & TECHNOLOGY***

*by*

**POONAM GUPTA**

Registration No. YMCAUST/02/2010

*Under the Supervision of*

**S.K. AGARWAL  
PROFESSOR**

**NARENDRA KUMAR  
PROFESSOR**



**Electrical Department**

**Faculty of Engineering and Technology**

**YMCA University of Science & Technology**

**Sector-6, Mathura Road, Faridabad, Haryana, India**

**DECEMBER 2014**



## **DEDICATION**

This dissertation is lovingly dedicated to my husband, Parveen Singhal and children Priyanka and Rishi. My husband's support, encouragement, and constant love has sustained me throughout my research. Also, my children have always been understanding and readily shared their time with my research activities for which I feel blessed and contented at the end of this enriching journey.

## **DECLARATION**

I hereby declare that this thesis entitled **DAMPING OF POWER SYSTEM OSCILLATIONS USING FACTS DEVICES** by **POONAM GUPTA**, being submitted in fulfillment of the requirements for the Degree of Doctor of Philosophy in **ELECTRICAL ENGINEERING** under Faculty of **ENGINEERING AND TECHNOLOGY** of **YMCA University of Science & Technology** Faridabad, during the academic year 2014, is a bona fide record of my original work carried out under guidance and supervision of **S.K. AGARWAL, PROFESSOR, ELECTRONICS DEPARTMENT** and **NARENDRA KUMAR, PROFESSOR, ELECTRICAL DEPARTMENT** and has not been presented elsewhere.

I further declare that the thesis does not contain any part of any work which has been submitted for the award of any degree either in this university or in any other university.

(Poonam Gupta)

Registration No. YMCAUST/02/2010

## **CERTIFICATE**

This is to certify that this Thesis entitled “**DAMPING OF POWER SYSTEM OSCILLATIONS USING FACTS DEVICES**” by **POONAM GUPTA**, submitted in fulfillment of the requirement for the Degree of Doctor of Philosophy in **ELECTRICAL ENGINEERING** under Faculty of Engineering and Technology of YMCA University of Science & Technology, Faridabad, during the academic year 2014, is a bonafide record of work carried out under our guidance and supervision.

We further declare that the thesis does not contain any part of any work which has been submitted for the award of any degree either in this university or in any other university.

S.K. AGARWAL

**PROFESSOR**

Department of Electronics Engg.

YMCA University of Science & Technology

Faridabad

NARENDRA KUMAR

**PROFESSOR**

Department of Electrical Engg.

Delhi Technological University

New Delhi

Dated:

## ACKNOWLEDGEMENT

I take this opportunity to express my sincere gratitude towards my supervisors **Prof. S.K.Agarwal/Prof. Narendra Kumar** for their intensive and sincere guidance, encouragement and inspiration given to me throughout my period of research and giving me the opportunity to work in this area. I am also thankful to them for providing me with the necessary computational facilities to build up the thesis. It would never be possible for me to take this thesis to this level without their innovative ideas and their rentless support.

I express my deep sense of gratitude to our Vice Chancellor Lt General (Retired) Shri K.S. Yadava, for his useful considerations and discussions.

My heartfelt gratitude and indebtedness are due to my family members especially my husband, daughter and son for their never fading love and encouragement and bearing with me during the research period.

I also thank all those who helped me directly or indirectly in the successful completion of my thesis.

(Poonam Gupta)

Registration No. YMCAUST/02/2010

## **ABSTRACT**

Today there is a huge demand of electric energy due to rapid and fast industrialization and urbanization and still growing continuously and has adversely affected the quality of power supply. In order to provide reliable and secure power system, there is a lot of pressure on the electric utilities. Power system network at international level is growing and becoming complex day by day and finding difficulty in maintaining the synchronism between the machines. Though deregulation in electricity market could be the solution but due to environmental constraints and further any new investment in laying of new lines and new generating units are always costly. Hence the need arises for the increase in the power flow in the existing transmission lines without overloading them, keeping the stability of the power system at all period of time and for giving electricity at cheaper rates. Before 80's, mechanical controllers were there for series and shunt compensation. For series compensation, mechanically switched capacitors were used, but these devices had the disadvantage of slow operation and less reliability. Advancement in the field of power electronics gave the solution to the above problems. The Electric Power Research Institute (EPRI) introduced FACTS technology in 80's. A number of FACTS devices like SVC, STACOM, TCSC, UPFC, IPFC and many more came into existence to enhance the power flow in the existing transmission lines. Apart from this, these devices have many other applications also like tie line control, dynamic voltage stability, damping of power system oscillations and damping of sub-synchronous resonance. This is possible due to provision of both real and reactive power control for series and shunt compensation by these FACTS devices and thereby provide highly reliable and secure power system under various contingencies like loss of generation, varying loads and loss of line by maintaining the stability and damping the power oscillations quickly. Hence these devices have completely replaced the historic mechanical controllers due to high speed of operation and high reliability. Each FACTS device has a controller and proper designing and optimization of controller parameters is the topic of today's research. Many researchers are working on these FACTS controllers for enhancing the power system performance by fast mitigation of power system oscillations. Many FACTS controllers have been designed and modelled, but still the electric utilities keep on relying on the conventional PI controllers for the

FACTS devices due to their simplicity and easy to optimize its parameters. But the conventional methods of optimizing their parameters are time consuming and sometimes deteriorate the performance. Hence need arises to go for some alternative methods.

All these factors gave the motivation to develop the suitable FACTS controllers and find ways to optimize the controller parameters suitably for the enhancement of the power system stability. In the present thesis, work has been carried out with three major FACTS controllers. Static Var compensator (SVC, a Shunt controller), Thyristor controlled series compensator (TCSC, a series controller) and Unified power flow controller (UPFC, a combined series-shunt controller). Proper controllers were designed and modelled keeping in mind that the dynamics of a power system has the following basic features:

1. Synchronous tie has the typical behavior that the machines go out of synchronism if the power transfer in the lines reached the line limits.
2. The power system dynamics is represented by nonlinear equations and under contingencies, there is a larger variation in machine angle  $\delta$  since power transfer in lines is proportional to  $\sin \delta$ .

Due to the above factors, there is a lot of pressure on the electric utilities to provide the stability to the power system. There are four stabilities to be considered in power system- Small signal stability, Dynamic stability, Transient stability and Voltage stability. A lot of research is going on for the enhancement of these stabilities.

Keeping all these in mind, SVC controller (a shunt controller) has been developed for voltage stability, dynamic stability and transient stability enhancement in the multi-machine system. An auxiliary SVC controller has also been developed for enhancing the small signal stability. The controller parameters are optimized first by conventional technique and then by Swarm intelligence techniques. Various algorithms implemented are Particle Swarm Optimization (PSO) and its variants, Bacterial Foraging Optimization (BFO) and Hybrid BF-PSO. An evolutionary technique i.e Genetic Algorithm (GA) has also been applied. Simulation results reveal the efficacy of Hybrid BF-PSO algorithm over other algorithms. This hybrid technique is the synergy of two



algorithms which take the advantages of both in searching the global optima in the m-dimensional search space.

TCSC (a series controller) has been developed for the enhancement of small signal stability of the SMIB system. The controller parameters are optimized by PSO algorithm and the simulations depict the robustness of PSO based controllers over the conventionally tuned controllers. Another control strategy has been developed for developing the TCSC controller and has been applied for the transient stability enhancement of an SMIB system for different levels of series compensation.

Coordination control of SVC and TCSC has also been implemented for transient stability enhancement of a multi-machine system.

UPFC (combined series and shunt controller) has been designed and modelled and implemented for the transient stability enhancement of an SMIB system under different contingencies. All Swarm intelligence algorithms and GA have been implemented in optimizing the controller parameters. The Simulation results validates the robustness of AI based controllers over the conventional ones. A different approach has also been implemented for the designing and modelling of UPFC controller and the same has been implemented for damping out local and inter area mode of oscillations in a multi-machine system. The controller parameters are optimized by both conventional method and PSO. PSO based UPFC controllers damp the power oscillations very fast and thereby enhances the transient stability of the multi-machine power system. All Simulations are carried out with MATLAB Simulink and MATLAB coding.

The work carried out has thus justified the topic of the thesis. The 21<sup>st</sup> century will certainly see a revolution in the control philosophy with a motivation towards intelligent FACTS controllers for the performance enhancement of the existing complex power system.

# CONTENTS

Dedication	i
Candidate's Declaration	ii
Certificate of the supervisor	iii
Acknowledgement	iv
Abstract	v
Table of contents	viii
List of tables	xiii
List of figures/graphs	xiv
List of acronyms	xxix
Body of the thesis	1
References	194
Appendices	204
Brief Bio-Data of the research scholar	211
List of publications out of thesis	212

# TABLE OF CONTENTS

	<b>Page No.</b>
<b>CHAPTER – 1</b>	
<b>INTRODUCTION</b>	
1.1 General	1
1.2 Literature Review	2
1.3 Application of Static VAR Systems	2
1.3.1. Power Transfer Capability Enhancement	3
1.3.2. Prevention of voltage collapse	4
1.3.3. SVC for Dynamic Performance Enhancement	5
1.3.4. SVC for Transient Performance Enhancement	7
1.3.5. Damping of Sub synchronous Resonance in Power System	8
1.4 Application of TCSC	9
1.5 Application of UPFC	10
1.5.1. Power Transmission Capability Enhancement	10
1.5.2. Dynamic Performance Enhancement	11
1.5.3. Enhancement of Transient Stability	11
1.6 Applications of other FACTS Controllers	12
1.7 Objective and scope of the thesis	13
1.8 Chapter wise distribution of the thesis	15
1.9 Discussion	16
<b>CHAPTER – 2</b>	
<b>FACTS DEVICES AND CONTROL</b>	
2.1. General	17
2.2. FACTS devices	17
2.3. Shunt connected controllers	18
2.3.1. Static VAR compensator (SVC)	18
2.3.2. STATCOM	21

2.3.3. Advantages of STATCOM over SVC	22
2.4. Series Controllers	23
2.4.1. Thyristor Controlled Series Capacitor (TCSC)	23
2.4.2. Advantages of TCSC over Conventional Series Capacitor	24
2.4.3. Static Synchronous Series Compensator (SSSC)	24
2.5. Shunt and Series Controller	25
2.5.1. Unified Power Flow Controller (UPFC)	25
2.6. Combined series – series controller	26
2.6.1 Inter Line Power Flow Controller (IPFC)	26
2.7. FACTS control	26
2.8. Discussion	27

## **CHAPTER – 3**

### **CONTROL STRATEGIES FOR OPTIMIZATION**

3.1 General	28
3.2 Conventional techniques	29
3.3 Ziegler Nichols, a conventional technique	29
3.4 Soft computation techniques	30
3.5 Swarm intelligence algorithm	30
3.6 Particle swarm optimization	31
3.6.1. Algorithm	32
3.6.2. Flow chart of PSO	33
3.7. PSO-Shrinkage factor with time varying inertia weight approach (PSO-TVIWA)	34
3.8. Advanced adaptive particle swarm optimization (PSO-TVAC)	35
3.9. PSO and its variants: issues	35
3.10. Bacterial foraging optimization	36
3.10.1 Algorithm	37
3.10.2 Flow chart	38
3.10.3 Bacterial foraging: issues	39

3.11. Hybrid BFO-particle swarm optimization	39
3.11.1. Hybrid BFO-particle swarm optimization with time varying acceleration coefficients	40
3.12. Genetic algorithm	40
3.12.1. Genetic algorithm: issues	42
3.13. Formulation of an objective function	43
3.14 Discussions	43

## **CHAPTER 4**

### **STATIC VAR COMPENSATOR FOR PERFORMANCE ENHANCEMENT OF POWER SYSTEM**

4.1. Introduction	45
4.2. System Model -1	46
4.2.1 System Description	46
4.2.2 SVC controller	47
4.2.3 TCSC controller	47
4.2.4 Simulation results	47
4.2.5 Discussion	54
4.3. System Model-2	55
4.3.1 System Description	55
4.3.2 Generator Model	56
4.3.3 Linearized Model	58
4.3.4 Linearized model of SMIB system	60
4.3.5 Modeling of SVC Controller	60
4.3.6 Auxiliary SVC Controller	63
4.3.7 Linearized Model of SMIB System with PID Damped SVC Controller	64
4.4 Simulations	64

4.5 Implementation Of Swarm Intelligence Techniques for Optimization Of Parameters Of Auxiliary SVC Controller	65
4.5.1 Objective Function	65
4.5.2 Simulation results with PSO and its variant based SVC Controller	66
4.5.3 Simulation results with BFO based auxiliary SVC Controller	78
4.5.4 Simulation results with Hybrid BF-PSO based auxiliary SVC Controller	81
4.5.5 Simulation results with Genetic Algorithm based auxiliary SVC Controller	84
4.5.6 Discussion	88

## **CHAPTER 5**

### **THYRISTOR CONTROLLED SERIES COMPENSATOR FOR PERFORMANCE ENHANCEMENT OF POWER SYSTEM**

5.1. Introduction	90
5.2 System Model -1	92
5.2.1 System Description	92
5.2.2 TCSC Controller Structure	93
5.2.3 Simulation Results with 20 percent series compensation	94
5.2.4 Simulation Results with 50 percent series compensation	97
5.2.5 Simulation Results with 80 percent series compensation	99
5.2.6 Discussion	102
5.3. System Model-II	102
5.3.1 TCSC Controller Structure	103
5.3.2 Simulation Results	103
5.3.3 Discussion	107
5.4. System Model-III	108
5.4.1 Linearized Model of SMIB	108
5.4.2 TCSC Controller	110
5.4.3 Simulation Results	111

5.4.4 Optimizing the parameters of TCSC Controller using Particle swarm optimization for steady state stability enhancement	116
5.4.5 Discussion	120

## **CHAPTER-6**

### **PERFORMANCE ENHANCEMENT OF POWER SYSTEM USING UNIFIED POWER FLOW CONTROLLER**

6.1 Introduction	121
6.2 UPFC Basic Operation and characteristics	123
6.3 Case Study	125
6.3.1 Modelling of SMIB System connected with UPFC Controller	126
6.4 Control Schemes for PI Controller of UPFC	131
6.5 Implementation of Swarm Intelligence Techniques for Optimization of UPFC Controller Parameters	132
6.6 Objective Function	132
6.7 Simulation Results	133
6.8 Discussion	170
6.9 Modelling of Multi-Machine System	171
6.10 Power Injection Model of UPFC	172
6.11 UPFC Dynamic Model	176
6.12 Procedure for Multi-Machine Power System Simulation	177
6.13 Implementation of Particle Swarm Optimization for Optimization	179
6.14 Formulation of an Objective Function	179
6.15 Simulations	180
6.16 Discussion	190

## **CHAPTER-7**

### **CONCLUSION**

7.1 General	191
7.2 Overall Assessment	192
7.3 Future Scopes	193

## LIST OF TABLES

<b>Tables</b>	<b>Page No</b>
Table 1: Comparison of Eigen Value Report with and without SVC Controller.	48
Table 2: Eigen values of the system with or without SVC controller	49
Table 3 Comparison chart with respect to settling time	78
Table 4 Comparison in settling time between various AI techniques based auxiliary SVC Controller	88
Table 5: Active and Reactive Power Flow in Line with and without TCSC controller	106
Table 6: Comparison of Eigen value Report with and without TCSC Controller.	106
Table 7: Eigenvalues of the system with or without TCSC controller	107
Table 8: Comparison in settling time between various AI techniques based UPFC Controller in an SMIB system for 40MW generator loading under 3-phase fault condition.	170



## LIST OF FIGURES

<b>Figure</b>	<b>Page No.</b>
Fig. 2.1 (FC-TCR) type SVS	19
Fig. 2.2 Characteristics of SVS (FC-TCR) configuration	20
Fig. 2.3 TSC-TCR type SVS	20
Fig. 2.4 TCSC structure	23
Fig.2.5 Unified Power Flow Controller	25
Fig. 3.1 Flow Chart of PSO	33
Fig. 3.2 Unit Walk of a Bacteria indicating Tumble and swim in chemotaxis step	37
Fig. 3.3 Flow Chart of BFO	38-39
Fig. 3.4 Block Diagram Representation of Genetic Algorithm	42
Fig. 4.1 Single line diagram of multi machine bus system with both SVC and TCSC controller	46
Fig. 4.2 Representation of SVC controller	47
Fig. 4.3 Representation of TCSC controller	47
Fig. 4.4 Voltage stability margin without and with SVC Controller at bus number 5	48
Fig.4.5 Voltage Magnitude Profile without and with SVC Controller connected at bus 5	48
Fig 4.6.1 Inter area mode of oscillation with and without SVC controller ( $\delta_2 - \delta_1$ )	50
Fig. 4.6.2 Inter area mode of oscillation with and without SVC controller ( $\delta_2 - \delta_3$ )	50
Fig. 4.6.3 Inter area mode of oscillation with and without SVC controller ( $\delta_3 - \delta_2$ )	51
Fig.4.6.4. Deviation in active power in machine1 with and without SVC controller	51
Fig. 4.6.5 Deviation in active power in machine2 with and without SVC controller	52

Fig. 4.6.6 Deviation in active power in machine3 with and without SVC controller	52
Fig. 4.7.1 Inter area mode of oscillation with SVC controller and with both SVC and TCSC controller ( $\delta_2 - \delta_1$ )	53
Fig. 4.7.2 Inter area mode of oscillation with SVC controller and with both SVC and TCSC controller ( $\delta_3 - \delta_1$ )	53
Fig. 4.7.3 Intra area mode of oscillation with SVC controller and with both SVC and TCSC controller ( $\delta_3 - \delta_2$ )	54
Fig 4.8 Single Machine Infinite bus system connected with SVC controller	55
Fig. 4.9 Equivalent circuit of stator of generator	56
Fig. 4.10 Generator connected to infinite bus-bar through transmission line	57
Fig. 4.11 Linearized model of SMIB system	60
Fig. 4.12 Representation of TCR model	61
Fig. 4.13 Transfer function representing measuring block	62
Fig. 4.14 Transfer function representing voltage regulator	62
Fig. 4.15 Representation of SVC controller using different modules	63
Fig. 4.16 SVC controller with auxiliary signal	63
Fig. 4.17 SMIB system with auxiliary SVC controller	64
Fig.4.18.1 Time response of rotor angle without and with conventionally tuned SVC controller	67
Fig.4.18.2 Time response of speed variation without and with conventionally tuned SVC controller	67
Fig.4.18.3 Time response of variation in generator terminal voltage without and with conventionally tuned SVC controller	68
Fig. 4.19.1: Time response of variation in rotor angle with conventionally tuned and with PSO based SVC controller	68
Fig. 4.19.2: Time response of speed deviation with conventionally tuned and with PSO based SVC controller	69
Fig. 4.19.3: Time response of variation in generator terminal voltage with conventionally tuned and with PSO based SVC controller	69

Fig. 4.20.1: Time response of variation in rotor angle with conventionally tuned auxiliary SVC controller and with PSO based SVC controller	70
Fig. 4.20.2: Time response of speed deviation with conventionally tuned and with PSO based SVC controller	70
Fig. 4.20.3: Time response of variation in generator terminal voltage with conventionally and with PSO based SVC controller	71
Fig. 4.21.1 Time response of variation in rotor angle with conventionally tuned and with PSO based auxiliary SVC controller	71
Fig. 4.21.2: Time response of speed deviation with conventionally tuned and with PSO based auxiliary SVC controller	72
Fig. 4.21.3: Time response of variation in generator terminal voltage with conventionally tuned and with PSO based auxiliary SVC controller	72
Fig. 4.22.1 Time response of variation in rotor angle with PSO based and with PSO-SFIWA based auxiliary SVC controller	73
Fig. 4.22.2 Time response of speed deviation with PSO based and with PSO-SFIWA based auxiliary SVC controller	73
Fig. 4.22.3 Time response of variation in generator terminal voltage with PSO based and with PSO-SFIWA based auxiliary SVC controller	74
Fig. 4.23.1 Time response of variation in rotor angle with PSO--SFIWA based and with PSO-TVAC based auxiliary SVC controller	75
Fig. 4.23.2 Time response of speed deviation with PSO-SFIWA based and with PSO-TVAC based auxiliary SVC controller	75
Fig. 4.23.3 Time response of variation in generator terminal voltage with PSO-SFIWA based and with PSO-TVAC based auxiliary SVC controller	76
Fig. 4.24.1 Time response of variation in rotor angle without, with PSO based SVC controller and with PSO-TVAC based auxiliary	76

SVC controller	
Fig. 4.24.2 Time response of speed deviation without, with PSO based SVC controller and with PSO-TVAC based auxiliary SVC controller	77
Fig. 4.24.3 Time response of variation in generator terminal voltage without, with PSO based SVC controller and with PSO-TVAC based auxiliary SVC controller	77
Fig. 4.25.1 Time response of variation in rotor angle with conventionally tuned and with BFO based auxiliary SVC controller	79
Fig. 4.25.2 Time response of speed deviation with conventionally tuned and with BFO based auxiliary SVC controller	79
Fig. 4.26.1 Time response of variation in rotor angle with BFO based SVC controller and with BFO based auxiliary SVC controller	80
Fig. 4.26.2 Time response of speed deviation with BFO based SVC controller and with BFO based auxiliary SVC controller	80
Fig. 4.26.3 Time response of variation in generator terminal voltage with BFO based SVC controller and with BFO based auxiliary SVC controller	81
Fig. 4.27.1 Time response of variation in rotor angle with Hybrid BF-PSO based and with conventionally tuned auxiliary SVC controller	82
Fig. 4.27.2 Time response of speed deviation with Hybrid BF-PSO based auxiliary SVC controller and with conventionally tuned auxiliary SVC controller	82
Fig. 4.28.1 Time response of variation in rotor angle with Hybrid BF-PSO based SVC controller and with Hybrid BF-PSO based auxiliary damped SVC controller	83
Fig. 4.28.2 Time response of speed deviation with Hybrid BF-PSO based SVC controller and with Hybrid BF-PSO based auxiliary damped SVC controller	83
Fig. 4.28.3 Time response of variation in generator terminal voltage with Hybrid BF-PSO based SVC controller and with Hybrid	84

	BF-PSO based auxiliary damped SVC controller	
Fig. 4.29.1	Time response of variation in rotor angle with conventionally tuned and with GA based auxiliary SVC controller	85
Fig. 4.29.2	Time response of speed deviation angle with conventionally tuned and with GA based auxiliary SVC controller	85
Fig. 4.30.1	Time response of variation in rotor angle with GA based SVC controller and with GA based auxiliary SVC controller	86
Fig. 4.30.2	Time response of speed deviation with GA based SVC controller and with GA based auxiliary SVC controller	86
Fig. 4.31.1	Time response of variation in rotor angle without, with GA Based SVC Controller and with GA based auxiliary SVC controller	87
Fig. 4.31.2	Time response of speed deviation without, with GA Based SVC Controller and with GA based auxiliary SVC controller	87
Fig. 5.1	Single line diagram of an SMIB system with TCSC connected between bus 2 and bus 3.	93
Fig. 5.2	Representation of TCSC controller.	94
Fig.5.1.1	Time response of power angle with and without TCSC controller for 20% series compensation	95
Fig.5.1.2	Time response of speed variation with and without TCSC controller for 20% series compensation	95
Fig.5.1.3	Time response of variation in active power with and without TCSC controller for 20% series compensation	96
Fig.5.1.4	Time response of variation in reactive power with and without TCSC controller for 20% series compensation	96
Fig.5.1.5	Time response of Generator terminal voltage with and without TCSC controller for 20% series compensation	97
Fig.5.2.1	Time response of speed deviation with and without TCSC controller for 50% series compensation	97
Fig.5.2 .2	Time response of power angle with time with and without	98

TCSC controller for 50% series compensation	
Fig.5.2.3 Time response of active power variation with and without TCSC controller for 50% series compensation	98
Fig.5.2.4 Time response of variation in Reactive power with and without TCSC controller for 50% series compensation	99
Fig.5.2.5 Time response of variation in Generator terminal voltage with and without TCSC controller for 50% series compensation	99
Fig.5.3.1 Time response of power angle with and without TCSC controller for 80% series compensation	100
Fig.5.3.2 Time response of speed deviation with and without TCSC controller for 80% series compensation	100
Fig.5.3.3 Time response of variation in active power with and without TCSC controller for 80% series compensation	101
Fig.5.3.4 Time response of variation in reactive power with and without TCSC controller for 80% series compensation	101
Fig.5.3.5 Time response of variation in generator terminal voltage without and with TCSC controller for 80% series compensation	102
Fig 5.4 Single line diagram of SMIB system connected with TCSC Controller	103
Fig. 5.5 Single line diagram of representation of TCSC controller	103
Fig. 5.6.1 Time response of variation in delta with and without TCSC controller.	104
Fig. 5.6.2 Time response of variation in rotor mechanical angle with and without TCSC controller	104
Fig. 5.6.3 Time response of speed deviation without TCSC controller	105
Fig. 5.6.4 Time response of speed deviation with TCSC controller	105
Fig. 5.7 Single line representation of study system	108
Fig 5.8 Representation of TCSC controller structure	110
Fig. 5.9 Single line diagram of linearized model of SMIB with TCSC Controller	111
Fig.5.10.1 Time response of rotor deviation without and with conventionally tuned TCSC controller	112
Fig.5.10.2 Time response of speed deviation without and with conventionally tuned TCSC controller	112

Fig.5.10.3 Time response of variation in generator terminal voltage without and with conventionally tuned TCSC controller	113
Fig.5.10.4 Time response of variation in active power without and with conventionally tuned TCSC controller	113
Fig. 5.11.1 Time response of rotor angle variation without and with conventionally tuned TCSC controller	114
Fig. 5.11.2 Time response of speed deviation without and with conventionally tuned TCSC controller	114
Fig. 5.11.3 Time response of variation in generator terminal voltage without and with conventionally tuned TCSC controller	115
Fig. 5.12.1 Time response of rotor angle variation without and with conventionally tuned TCSC controller (with one line outage)	115
Fig. 5.12.2 Time response of speed deviation without and with conventionally tuned TCSC controller (with one line outage)	116
Fig. 5.13.1 Time response of rotor angle variation with conventionally tuned and PSO based TCSC controller	117
Fig. 5.13.2 Time response of speed deviation with conventionally tuned and PSO based TCSC controller	117
Fig. 5.13.3 Time response of generator terminal voltage with conventionally tuned and PSO based TCSC controller	118
Fig.5.13.4 Time response of variation in active power with conventionally tuned and PSO based TCSC controller	118
Fig. 5.14.1 Time response of rotor angle variation with conventionally tuned TCSC controller and PSO based TCSC controller	119
Fig. 5.14.2 Time response of speed deviation with conventionally tuned and PSO based TCSC controller	119
Fig. 5.14.3 Time response of generator terminal voltage with conventionally tuned and PSO based TCSC controller	120
Fig. 6.1 Circuit diagram of unified power flow controller	123

Fig. 6.2 Elementary control functions of UPFC: (a)Voltage Regulation, (b)Series compensation, (c)Angle regulation and (d) Multi-function power flow control	124
Fig. 6.3 Representation of Single Machine connected to an Infinite Bus system.	125
Fig. 6.4 d-q representation of series converter	128
Fig. 6.5 UPFC Controller with SMIB System in PQ Mode	129
Fig.6.6 d-q representation of shunt converter	130
Fig. 6.7.1 Time response of Power angle without and with conventionally tuned UPFC controller (for 40 MW load with 3-Phase fault)	134
Fig. 6.7.2 Time response of speed deviation without and with conventionally tuned UPFC controller (for 40 MW load with 3-Phase fault)	134
Fig. 6.7.3 Time response of active power without and with conventionally tuned UPFC controller (for 40 MW load with 3-Phase fault)	135
Fig. 6.7.4 Time response of reactive power without and with conventionally tuned UPFC controller (for 40 MW load with 3-Phase fault)	135
Fig. 6.7.5 Time response of variation in active power without and with conventionally tuned UPFC controller (for 40 MW load with 3-Phase fault)	136
Fig. 6.7.6 Time response of variation in reactive power without and with conventionally tuned UPFC controller (for 40 MW load with 3-Phase fault)	136
Fig. 6.7.7 Time response of variation in Generator terminal voltage without and with conventionally tuned UPFC controller (for 40 MW load with 3-Phase fault)	137
Fig. 6.7.8 Time response of variation in dc capacitor voltage with conventionally tuned UPFC controller (for 40 MW load with 3-Phase fault)	137
Fig. 6.7.9 Time response of variation in d-axis series voltage injection with conventionally tuned UPFC controller (for 40 MW load with 3-Phase fault)	138
Fig. 6.7.10 Time response of variation in q-axis series voltage injection with conventionally tuned UPFC controller (for 40 MW load with 3-Phase fault)	138
Fig. 6.8.1 Time response of Power angle without and with conventionally tuned UPFC controller (for 80 MW load with 3-Phase fault)	139
Fig. 6.8.2 Time response of speed deviation without and with conventionally	139



tuned UPFC controller (for 80 MW load with 3-Phase fault)	
Fig. 6.9.1 Time response of Power angle without and with conventionally tuned UPFC controller (for 100 MW load with 3-Phase fault)	140
Fig. 6.9.2 Time response of speed deviation without and with conventionally tuned UPFC controller (for 100 MW load with 3-Phase fault)	140
Fig. 6.10.1 Time response of Power angle without and with conventionally tuned UPFC controller (for 40 MW with line outage)	141
Fig. 6.10.2 Time response of speed deviation without and with conventionally tuned UPFC controller (for 40 MW with line outage)	141
Fig. 6.11.1 Time response of Power angle without and with conventionally tuned UPFC controller (for 120 MW load with line outage)	142
Fig. 6.11.2 Time response of speed deviation without and with conventionally tuned UPFC controller (for 120 MW load with line outage)	142
Fig. 6.12.1 Time response of Power angle with conventionally tuned UPFC controller (with line outage for 150 MW load)	143
Fig. 6.12.2 Time response of speed deviation with conventionally tuned UPFC controller (with line outage for 150 MW load)	143
Fig. 6.12.3 Time response of Machine angle without UPFC controller (with line outage for 150 MW load)	144
Fig 6.13.1 Time response of Power angle with conventionally tuned and BFO based UPFC controller (for 40 MW load with 3-Phase fault)	145
Fig 6.13.2 Time response of speed deviation with conventionally tuned and BFO based UPFC controller (for 40 MW load with 3-Phase fault)	145
Fig 6.13.3 Time response of generator terminal voltage with conventionally tuned and BFO based UPFC controller (for 40 MW load with 3-Phase fault)	146
Fig 6.13.4 Time response of active power with conventionally tuned and BFO based UPFC controller (for 40 MW load with 3-Phase fault)	146
Fig 6.14.1 Time response of Power angle with conventionally tuned and BFO based UPFC controller (for 80 MW load with 3-Phase fault)	147
Fig 6.14.2 Time response of speed deviation with conventionally tuned and BFO based UPFC controller (for 80 MW load with 3-Phase fault)	147

Fig 6.15.1 Time response of Power angle with conventionally tuned and BFO based UPFC controller (for 120 MW load with 3-Phase fault)	148
Fig 6.15.2 Time response of speed deviation with conventionally tuned and BFO based UPFC controller (for 120 MW load with 3-Phase fault)	148
Fig 6.16.1 Time response of Power angle with BFO based UPFC controller (for 150 MW load with 3-Phase fault)	149
Fig 6.16.2 Time response of speed deviation with BFO based UPFC controller (for 150 MW load with 3-Phase fault)	149
Fig 6.17.1 Time response of Power angle with conventionally tuned UPFC controller (for 160 MW with line outage)	150
Fig 6.17.2 Time response of Power angle with BFO based UPFC controller for 160 MW with line outage)	150
Fig 6.17.3 Time response of speed deviation with conventionally tuned UPFC controller(for 160 MW with line outage)	151
Fig 6.17.4 Time response of speed deviation with BFO based UPFC controller (for 160 MW with line outage)	151
Fig 6.18.1 Time response of Power angle with BFO based UPFC (for 170 MW with line outage)	152
Fig 6.18.2 Time response of speed deviation with BFO based UPFC (for 170 MW with line outage)	152
Fig. 6.19.1 Time response of Power angle with conventionally tuned and PSO based UPFC controller (for 40 MW load with 3-Phase fault)	153
Fig. 6.19.2 Time response of speed deviation with conventionally tuned and PSO based UPFC controller (for 40 MW load with 3-Phase fault)	154
Fig. 6.20.1 Time response of Power angle with conventionally tuned and PSO based UPFC controller (for 80 MW load with 3-Phase fault)	154
Fig. 6.20.2 Time response of speed deviation with conventionally tuned and PSO based UPFC controller (for 80 MW load with 3-Phase fault)	155
Fig. 6.21.1 Time response of Machine angle with conventionally tuned and PSO based UPFC controller (for 120 MW load with 3-Phase fault)	156

Fig. 6.21.2 Time response of speed deviation with conventionally tuned and PSO based UPFC controller (for 120 MW load with 3-Phase fault)	156
Fig. 6.22.1 Time response of Machine angle with PSO based UPFC controller (for 140 MW load with 3-Phase fault)	157
Fig. 6.22.2 Time response of speed deviation with PSO based UPFC controller (for 140 MW load with 3-Phase fault)	157
Fig. 6.23.1 Time response of Power angle with PSO based UPFC controller (for 160 MW load with line outage)	158
Fig. 6.23.2 Time response of speed deviation with PSO based UPFC controller (for 160 MW load with line outage)	158
Fig. 6.23.1 Time response of Power angle with PSO based UPFC controller (for 170 MW load with line outage)	159
Fig. 6.23.2 Time response of speed deviation with PSO based UPFC controller (for 170 MW load with line outage)	159
Fig. 6.24.1 Time response of Power angle with conventionally tuned and Hybrid BF-PSO based UPFC controller(for 40 MW load with 3-Phase fault)	160
Fig. 6.24.2 Time response of speed deviation with conventionally tuned and Hybrid BF-PSO based UPFC controller(for 40 MW load with 3-Phase fault)	161
Fig. 6.25.1 Time response of Power angle with conventionally tuned and Hybrid BF-PSO based UPFC controller(for 80 MW load with 3-Phase fault)	161
Fig. 6.25.2 Time response of speed deviation with conventionally tuned and Hybrid BF-PSO based UPFC controller(for 80 MW load with 3-Phase fault)	162
Fig. 6.26.1 Time response of Power angle with conventionally tuned and Hybrid BF-PSO based UPFC controller(for 120 MW load with 3-Phase fault)	162
Fig. 6.26.2 Time response of speed deviation with conventionally tuned and Hybrid BF-PSO based UPFC controller(for 120 MW load with 3-Phase fault)	163
Fig. 6.27.1 Time response of Machine angle with Hybrid BF-PSO based UPFC controller(for 160 MW load with 3-Phase fault)	163
Fig. 6.27.2 Time response of speed deviation with Hybrid BF-PSO based UPFC controller(for 160 MW load with 3-Phase fault)	164

Fig. 6.29.1 Time response of Power angle with Hybrid BF-PSO based UPFC controller(for 170 MW load with line outage)	164
Fig. 6.29.2 Time response of speed deviation with Hybrid BF-PSO based UPFC controller(for 1670 MW load with line outage)	165
Fig. 6.30.1 Time response of Power angle with conventionally tuned and GA based UPFC controller(for 40 MW load with 3-Phase fault)	166
Fig. 6.30.2 Time response of speed deviation with conventionally tuned and GA based UPFC controller(for 40 MW load with 3-Phase fault)	166
Fig. 6.31.1 Time response of Power angle with conventionally tuned and GA based UPFC controller(for 120 MW load with 3-Phase fault)	167
Fig. 6.32.2 Time response of speed deviation with conventionally tuned and GA based UPFC controller(for 120 MW load with 3-Phase fault)	167
Fig. 6.32.1 Time response of power angle with GA based UPFC controller (for 160 MW load with line outage)	168
Fig. 6.32.2 Time response of speed deviation with GA based UPFC controller (for 160 MW load with line outage)	168
Fig. 6.33.1 Time response of power angle with GA based UPFC controller (for 170 MW load with line outage)	169
Fig. 6.33.2 Time response of speed deviation with GA based UPFC controller (for 170 MW load with line outage)	169
Fig. 6.34 Single line diagram of Multi-machine power system with UPFC Controllers	172
Fig 6.35 Two voltage source model of UPFC	173
Fig.6.36 Voltage source representation of series converter	173
Fig.6.37 Current source representation of series converter	174
Fig.6.38 Representation of series converter with equivalent load form	175
Fig. 6.39 Power Injection model of UPFC	176
Fig. 6.40 Phasor representation	177
Fig. 6.41 Time response of speed deviation ( $w_2-w_1$ ) (Inter area mode oscillations without and with conventionally tuned UPFC controllers)	180
Fig. 6.42 Time response of speed deviation ( $w_3-w_1$ ) (Inter area mode oscillations	180

without and with conventionally tuned UPFC controllers)	
Fig.6.43 Time response of speed deviation ( $w_3-w_2$ ) (Intra area mode oscillations without and with conventionally tuned UPFC controllers))	181
Fig. 6.44 Time response of power angle ( $\delta_1 - \delta_2$ ) without and with conventionally tuned UPFC controllers	181
Fig. 6.45 Time response of power angle ( $\delta_2 - \delta_3$ ) (without and with conventionally tuned UPFC controllers)	182
Fig. 6.46 Time response of machine angle deviation ( $\delta_1 - \delta_3$ ) (without and with conventionally tuned UPFC controllers)	182
Fig. 6.47 Time response of speed deviation ( $w_2-w_1$ ) (with conventionally tuned and with PSO based UPFC controllers)	183
Fig. 6.48 Time response of speed deviation ( $w_3-w_1$ ) (with conventionally tuned and with PSO based UPFC controllers)	183
Fig. 6.49 Time response of speed deviation ( $w_3-w_2$ ) (with conventionally tuned and with PSO based UPFC controllers)	184
Fig 6.50 Time response of power angle ( $\delta_1 - \delta_2$ )(with conventionally tuned and with PSO based UPFC controllers)	184
Fig. 6.51 Time response of power angle ( $\delta_1 - \delta_3$ )(with conventionally tuned and with PSO based UPFC controllers)	185
Fig.6.52 Time response of power angle ( $\delta_2 - \delta_3$ )(with conventionally tuned and with PSO based UPFC controllers)	185
Fig. 6.53 Time response of Generator terminal voltage deviation( $v_2-v_1$ ) (with conventionally tuned and with PSO based UPFC controllers)	186
Fig. 6.54 Time response of Generator terminal voltage deviation ( $v_3-v_1$ ) (with conventionally tuned and with PSO based UPFC controllers)	186
Fig.6.55 Time response of Generator terminal voltage deviation ( $v_3-v_2$ ) (with conventionally tuned and with PSO based UPFC controllers)	187
Fig. 6.56 Time response of in phase component of series voltage injection of UPFC 1(with conventionally tuned and with PSO based UPFC controllers)	187

Fig. 6.57 Time response of quadrature component of series voltage injection of UPFC 1(with conventionally tuned and with PSO based UPFC controllers)	188
Fig. 6.58 Time response of quadrature component of series voltage injection of UPFC 2(with conventionally tuned and with PSO based UPFC controllers)	188
Fig. 6.59 Time response of in phase component of series voltage injection of UPFC 2(with conventionally tuned and with PSO based UPFC controllers)	189
Fig. 6.60 Time response of D.C voltage of UPFC-1(with conventionally tuned and with PSO based UPFC controllers)	189
Fig. 6.61 Time response of D.C voltage of UPFC-2(with conventionally tuned and with PSO based UPFC controllers)	190

## ACRONYMS

The following table describes the significance of various abbreviations and acronyms used throughout the thesis.

Abbreviation	Meaning
FACTS	Flexible AC Transmission System
SVC	Static Var compensator
STATCOM	Static Synchronous Compensator
TCSC	Thyristor controlled series compensator
TCPST	Thyristor controlled phase shifting transformer
UPFC	Unified Power Flow Controller
FC-TCR	Fixed capacitor- Thyristor Controlled Reactor
TCR	Thyristor Controlled Reactor
AI	Artificial Intelligence
SSSC	Static Synchronous Series Compensator
PSAT	Power System Analysis Tool
EHV	Extra high voltage
DFL	direct feedback
DQLF	Decoupled – Quadratic Load Flow
POD	Power Oscillation Damping
SSR	Sub-Synchronous Resonance
SIMO	single input multi output
IMDU	Induction machine damping unit
PSO	Particle Swarm Optimization
SMIB	Single machine infinite bus
FLC	Fuzzy logic controller
GA	Genetic Algorithm
BFO	Bacterial Foraging Optimization
BF-PSO	Bacterial Foraging- Particle Swarm Optimization
SVS	Static Var Systems

SPS	Static phase shifter
TSC-TCR	Thyristor switched capacitor- Thyristor Controlled Reactor
GTO	Gate turns off thyristors
SCR	Silicon controlled rectifier
ZN	Ziegler Nichols
PSO-TVAC	Particle Swarm Optimization-Time Varying Acceleration
PSO-SFIWA	Coefficient
AVR	Particle Swarm Optimization-Shrinkage Factor Inertia Weight
PI	Approach
HTG	Automatic voltage regulator
TCSR	Proportional Integral
TCSC	Hydraulic Turbine Governor
TSSR	Thyristor-controlled series reactor
ANN	Thyristor-controlled series capacitor
	Thyristor-switched series reactor
	Artificial Neural Networks



# CHAPTER 1

## INTRODUCTION

### 1.1 GENERAL

Modern interconnected power systems comprise a number of generators, a large electrical power network and a variety of loads. Such a complex system is vulnerable to sudden faults, load changes and disturbances of uncertain nature resulting in instability. The electric power network comprises of long distance transmission lines, transformers and associated auxiliary devices for power control. The power transmission network is an important element of the power system which is responsible for causing instability, sudden voltage collapse and power oscillations during transient conditions and has received considerable attention. Recently to improve power system performance flexible AC transmission systems (FACTS) are being developed and researched. The FACTS envisage the use of solid state power converter technology to obtain fast and reliable control of line flow in a transmission line. In an electrical power transmission system, a FACTS device has the greatest advantage in damping out the power system oscillations and thus enhances the transient stability performance by controlling the real and reactive power flow during fault conditions. FACTS device are classified into two categories; the shunt type comprises of the static VAR compensator (SVC) and the static synchronous compensator (STATCOM) whereas the series type includes the thyristor controlled series compensator (TCSC) and the thyristor controlled phase shifting transformer (TCPST). The shunt devices negotiate reactive power with the system and thereby bus voltage magnitude is controlled. On the other hand the series devices provide fast control of the real power flow in a transmission line. The unified power flow controller (UPFC) is the most versatile of the FACTS family which combines both shunt and series feature. The main objective of the UPFC is to add a variable series voltage which modulates reactance of the line for controlling the flow of power in the transmission line.

The FACTS device either use thyristor-switched capacitor and reactor (TCR-FC) to achieve reactive series and shunt compensation, or take use of line-commutated inverters as synchronous voltage sources in altering the existing transmission line voltage and thus power flow be controlled. The family of compensators based on TCR-FC is SVC and TCSC

whereas the STATCOM, TCPST and UPFC belong to the synchronous voltage source category. The TCR-FC type device compensates the line voltage by controlling the current through a reactor. STATCOM with its converter control presents a variable magnitude and phase angle synchronous voltage source to the power system. On the contrary, TCPST injects a series controllable voltage source with an angle of  $\pi / 2$  to the bus voltage. The UPFC with two voltage source converters connected via a dc capacitor is able to inject controllable series voltage to the line where the angle varies between  $0-2\pi$ . Further the shunt converter can inject variable reactive power to the bus. By regulating the power flow in a transmission line by FACTS device, full exploitation of the existing transmission line without overheating [1] as well as damping of electromechanical oscillations in a power system [1-2] is possible. The satisfactory performance of FACTS device largely depends upon its control system design. Conventionally controlled PI regulators normally used for the control of FACTS devices system design may not perform satisfactorily at different operating conditions and disturbances. To provide good control and transient stability enhancement over an extensive range of system operating conditions, AI Techniques based FACTS controllers can be one of the real solution.

## **1.2 LITERATURE REVIEW**

In the present chapter a comprehensive review of the developments in the area of FACTS application for improving the power system performance has been presented. The emphasis has been given on the recent advances made in the field of SVC, TCSC and UPFC application in power system. The application of other FACTS controllers like static synchronous series compensator (SSSC) and static synchronous compensator (STATCOM) have been highlighted.

## **1.3 APPLICATIONS OF STATIC VAR SYSTEM**

The applications of SVC in long-distance power system has received much attention by researchers in recent years. Due to its ability to provide fast and continuous reactive power and voltage control, SVC can be incorporated for the performance enhancement of power system network. The work reported in literature in the area of SVC application has been classified as follows

- (a) Power transmission capability enhancement
- (b) Prevention of voltage collapse
- (c) Dynamic performance enhancement
- (d) Enhancement of transient stability
- (e) Damping of sub synchronous resonance

### **1.3.1 Power Transfer Capability Enhancement**

It has been theoretically demonstrated [5] that the steady state power transfer over a transmission line can be doubled if the voltage at the midpoint is maintained at a constant level. SVC can be incorporated for enhancement of power flow capability of a line but when it is used to permit a high power transfer over a long distance, the possibility of instability must be recognized.

Abdel- Aty Edris [6] demonstrated the usefulness of static VAR compensator (SVC) for voltage support at the load side to increase the load-ability of radial transmission lines. In order to analyze the efficacy of SVC controller, a general formula has been formulated relating the sensitivity of receiving end voltage to shunt compensation and for that Radial links of different lengths of transmission line, voltages along with different types of loads had been considered.

The formula developed has been implemented for obtaining the gain of the regulator used in designing the control model of SVC along with the steady state load ability limits of radial transmission lines at different loads.

M. H. Haque [7] has applied both shunt and series compensation techniques in order to maximize the power transfer in a high voltage A.C transmission lines. The researcher has also defined the maximum limit of the receiving end current to flow beyond which it cannot be enhanced due to instability in voltage.

Md. Nazmus Sahadat [8] has presented the effect of various values of susceptance of SVC controller for an enhancement of bus voltage profile and ability of active power flow in transmission lines. Modeling of SVC has not been done, only the existing model of SVC in PSAT tool box has been analyzed.

C. Bulac [9] has described the feasibility of incorporating FACTS devices in the electrical power grid in the South-Eastern part of Romania for increasing its ability to transfer the power to its other parts.

### 1.3.2 Prevention of Voltage Collapse

Owing to deficit reactive power in Transmission line and due to large and continuously varying loads on the power system network causes voltage instability and is defined by load voltage noose contours. In today's scenario, power system transmission lines are operating at high power levels, hence lead to reduction in voltage stability margin and due to which utilities are using compensating devices. Fast voltage stability is obtained by using SVC. Static VAR system is a latest power electronic device used for smooth and continuous control of reactive power as desired. It can either be inductive or capacitive depending upon the requirement of the system.

R. L. Hauth et. al. [10, 11] have illustrated through various systems studies, the application of SVC in controlling over voltages, improving transient stability power limits and prevention of voltage instability. Studies showed that the SVC performed as intended to regulate the steady state voltage swings. T.S Bhatti and D.P. Kothari [12] described the compensation scheme of a radial transmission system keeping in view of two objectives.

(i) Voltage profile at the receiving end terminals might be held constant

(ii) The load factor might be maintained at unity. The method of finding the specification of both the compensators one at the midpoint and other at the receiving end was described using power balance equation.

S. C Tripathy and B. Viswanathan [13] presented a strategy for the control of extra high voltage lines which is series compensated. Voltage stability analysis is carried out assuming the uncertainties in power flow due to continuous varying load. He has also suggested that the instability in the voltage in long E.H.V lines be reduced by using series compensation.

J. G. Mayordomo et. al [14] demonstrated that to avoid the variation of voltage due to load variation at the buses by connecting SVC at respective buses. TCR connected in SVC regulates the reactive power compensation needed for stabilizing the voltage at the buses.

Huayuan Chen et.al [15] discussed the application of nonlinear SVC for the improvement in the voltage stability. The new SVC controller designed on direct feedback linearization (DFL) techniques has significantly increased the stability margin of the voltage. D. Thukarum et.al [16] presented a methodology for finding out the exact location and required rating of SVC controller for system voltage stability improvement.

Trang Phuong nam [17] has proposed the practical method for choice and placement of SVC in power market for voltage control in real time and hence improves the efficiency of power system.

M.A. Kamarposhti in his paper [18] has investigated IEEE-14 bus system for analyzing the significant voltage stability using various FACTS controllers like TCSC, UPFC, STATCOM and SVC. Power System analysis toolbox has been used for the investigation. But the paper deserves further investigation with different parameter values of FACTS Controllers.

M. Sailaja Kumari [19] has proposed Decoupled – Quadratic Load Flow (DQLF) technique for optimizing the Static VAR compensator parameters connected in the IEEE 14 bus system. This modified model gives much faster response than the conventional Fast Decoupled load flow model. The time required for optimization is very less.

O. L. Bekri [20] has investigated the IEEE 6-bus system for voltage stability analysis using both series (TCSC) and shunt (SVC) FACTS devices. Larger voltage stability limit is achieved in SVC as compare to TCSC device.

### **1.3.3 SVC for Dynamic Performance Enhancement**

Static VAR system is known to extend the stability limit and improve system damping when connected at the intermediate points of a transmission line. S. C. Kapoor [21] proposed that an automatic static compensator shunt connected at synchronous generator terminals using an appropriate control strategy yielded superior dynamic stability than that of a conventional or dual excited machine. A state space mathematical model for the proposed system was formulated and dynamic stability limits for various studies were obtained using eigenvalue technique. However the proposed scheme is powerful but deserves further investigation for its transient stability.

For analyzing the effectiveness of SVC controller for voltage support and mitigating low frequency oscillations, K. Ramar and A. Srinivas [22] has developed a model. A single machine infinite bus system with SVC has been taken as case study. The authors also investigated the efficacy of SVC over conventional Power system stabilizer (PSS) in regard to voltage support and damping of power oscillations.

Nelson Martins and L .T. G. Lima [23] presented the work relating to the location of SVC taking into account various factors such as dynamic voltage support, capability of damping electro mechanical and sub synchronous oscillations. The proposed algorithm attempted to provide an answer to the problems of finding the best location for the sole purpose of damping electromechanical oscillations.

E. Lerch et al [24] presented an innovative SVC control for mitigating the power oscillations in the power system network. The researcher has implemented the phase angle signal for SVC control which is derived from the local measurement of electrical parameters of the bus where SVC is located. This control has considerably mitigate the power oscillations effectively even under severe contingencies and maintain the system under stability limits. Apart from damping of oscillations, SVC controller has also increased the power transfer capability of the network.

K. R Padiyar and R. K. Varma [25] have proposed a new SVC auxiliary controller which has used the computed internal frequency (CIF) as the controlling signal which provides shunt compensation in the transmission line at the midpoint of the line and thus increases the power flow in the line along with damping of torsional oscillations. Dynamic stability has been analyzed using Eigen value analysis. The damping torque results were co-related with those obtained from Eigen value analysis. However this study needs transient stability investigations to test the system performance under large disturbance conditions over a wide operation range.

Shun Lee and Chun Chang Liu [26] investigated an output feedback SVC for damping the electromechanical oscillations of synchronous generator. The SVC controller is designed. Both Eigen value and transient analysis is carried out for various operating conditions to justify the usefulness of the designed controller.

E. Z. Zhou [27] developed a control strategy for transient stability enhancement employing equal area criterion. SVC controller is based on discrete methodology. On the basis of change in power flow in line, reactive power change is obtained at some specified points. The author proposed that the SVC control approach and the developed theory could also be applicable for the mitigation of power oscillations in actual power system network and can be applied to solve practical power system damping.

A.R. Messina et. al [27,29] presented a comprehensive analysis of the SVC in a large interconnected power system and control design was based on Eigen value analysis. Linearization is done for designing the model.

Poonam Singhal [30] presented an auxiliary SVC controller for enhancement of Dynamic stability. No Transient analysis is been carried out.

#### **1.3.4 SVC for Transient Performance Enhancement**

SVC with some auxiliary signals in addition to voltage feedback is very effective for improving power system dynamic and transient stability. The auxiliary signals may be change in active power, reactive power, bus frequency, and rotor speed, phase angle derivative of reactive power and active power and combination of these signals. The measurement of generator frequency deviations is difficult in a single machine or multi machine power system particularly when SVC is placed at the midpoint of transmission line. But other parameter can be conveniently and locally measured.

R. M. Mathur and A. E Hammad [31] presented a theoretical model for designing TCR. The most attractive feature of the new design was that it produced less harmonics and cost effective due to savings in filtering and valves. The study was further extended to analyze the performance of thyristor valves under an assumed overvoltage situation. Finally an efficient model for transient stability simulation was proposed.

Y. Y. Hsu et.al [32] demonstrated the coordinated applications of PSS and SVC for dynamic stability improvement of a longitudinal power system. An analytical approach was developed for determination of PSS parameters. The effectiveness of the coordinated scheme was demonstrated using time domain simulations.

A.S.R Murthy et. al [33] has attempted to use deviation of reactive power as auxiliary control signal for SVC. The auxiliary controller parameters were obtained using eigenvalue analysis and by employing the criterion that the damping factor of the two sensitive eigenvalues was made nearly equal. The power system performance (with SVS with and without auxiliary control) and with fixed susceptance had been studied using digital simulation under fault conditions.

P.K. Muttik [34] has described the importance of the Armidale SVC from ALSTOM for the NSW-Queensland interconnection project to provide steady-state, dynamic, voltage and transient stability along with voltage control.

N. A. Mohamed Kamari [35] has implemented the Evolutionary Programming (EP) in getting the optimized values of integral gain  $k_i$  and proportional gain,  $k_p$  of SVC controller. She has also validated the results by doing eigenvalue analysis and computation of synchronizing and damping torque coefficients (KS and KD) value which validate the effectiveness of defined scheme for rotor angle stability.

Y. P. Wang [36], has optimized the PI controller of SVC using Genetic Algorithm

R. Sadikovic [37] has investigated the residue method for the adaptive tuning of Power Oscillation Damping (POD) Controller parameters for FACTS Devices for different operating conditions. TCSC and UPFC FACTS devices are considered for analysis. Kalman filtering technique has been applied for online detection of electromechanical oscillations.

### **1.3.5 Damping of Sub Synchronous Resonance in Power System**

Sub synchronous resonance in a series compensated power system is defined in [1] as a phenomenon when there is an exchange of energy between mechanical turbine generator system and electrical network at one or more of the natural frequencies of the combined system below the power frequency. The problem of SSR was experienced for the first time at Mohave power plant in Southern Nevada. Two incidents of shaft failures were reported in Dec 1970 and Oct. 1971. Since then efforts are going on undertaken by many researchers in developing new controllers for damping the SSR [38, 39] and to find out the permissible range of series compensation levels. Many FACTS controllers are gaining importance due to their application in mitigating the SSR problems arises out of series compensation of the long transmission lines.

A.E Hammad and M.E.L. Sadek [40] presented a new concept for controlling SVC controller for efficient damping of SSR oscillations. In addition to it, bus voltage is also controlled. Eigen value analysis has been carried out. IEEE SSR benchmark model has been implemented for the investigation.



Shun Lee and Chun –Change Liu [41] proposed new scheme for design of a static VAR controller based on single input multi output (SIMO) for stabilizing torsional oscillations. They suggested that the proposed SVC controller could easily be realized by a multi proportion integral (MPI) controller. Six rotor mass system has been considered. Speed of turbines and generator is taken as the signal fed to the SVC controller in order to stabilize torsional oscillations. Eigenvalue analysis is done for different loading conditions and different series compensation levels, transient stability, simulation, FFT analysis for system behavior were also performed to validate the efficacy of the suggested controller.

A. F. Abdou [42] investigated the effectiveness of SVC Controller in stabilizing multi-mode torsional oscillations of SSR of a large turbine generator and thus enhances the transient stability. Two control signals, generator terminal voltage and Generator speed are used in generating correct triggering angle for SVC by controlling the number of SVC capacitors connected. The suggested SVC controller is very active in damping the SSR modes of the power system network.

Li- wang et. al [43] presented the results of a study on the utilization of shunt reactors for damping of common torsional mode interactions of a series compensated power system. The IEEE second benchmark model has been employed to investigate the unstable SSR modes interactions. A unified approach based on modal control theory has been proposed for the design of PID shunt reactor controllers so that all the torsional modes in the study system were stabilized.

Paper [44] has analyzed the effect of an Induction machine damping unit for damping out the Sub-synchronous resonance which is coupled to the shaft of turbo-generator set. The author has investigated that IMDU unit alone is capable of damping Sub-synchronous resonance effectively without the need of controller. Apart from this, rating and location of IMDU unit is also being investigated.

Keshavan, in his paper [45] proposed the computed internal voltage as an auxiliary control signal to control the STATCOM connected at the middle of the transmission line for damping out the Sub-synchronous resonance.

#### **1.4 APPLICATIONS OF TCSC**

The basic Thyristor-Controlled Series Capacitor scheme, proposed in 1986 by Vithayathil with others as a method of "rapid adjustment of network impedance," By controlling series reactance of

line, TCSC is able to enhance the Power transmission capability of the transmission line and damping of the power swings from local and inter-area oscillations. At sub-synchronous frequencies, TCSC presents an inherently resistive–inductive reactance, due to which the sub-synchronous oscillations cannot be sustained in this situation and consequently get damped. A lot of work has been reported in the above area of TCSC application. Alberto [46] has proposed the design of hierarchical TCSC controller for both steady state stability and dynamic stability enhancement.

A.O. Anele [47] has developed the mathematical model of TCSC for studying its steady state behavior. Paper has emphasized on selection of appropriate values of Capacitance and Inductance of TCSC for getting flexibility in enhancing the power flow in the Transmission lines. No real time implementation has been done in any power system network. TCSC Controller has been designed in paper [48] using reduced system model for power flow control, transient stability enhancement and damping of inter-area oscillations.

## **1.5 APPLICATIONS OF UPFC**

UPFC has an important function of providing the stability control by damping out the power system oscillations, thus leads to the improvement in the transient stability of power system network. Independent control of active and reactive power can be achieved by series voltage injection and reactive current in shunt. UPFC is capable of controlling individually or simultaneously the three line parameters- phase angle, impedance and line voltage which regulates the flow of power in the transmission line. The work reported in literature in the area of UPFC application has been classified as follows:

- 1 Power transmission capability enhancement
- 1 Dynamic performance enhancement
- 2 Enhancement of transient stability

### **1.5.1 Power Transmission Capability Enhancement**

A.M. Kulkarni [49] has suggested a control method for UPFC to control the flow of active power through transmission line using transient simulation.

H.W. Nagani [50] has defined various control strategies for FACTS Controller for the enhancement of steady and dynamic stability under both normal and abnormal conditions. UPFC Controller is developed and successfully illustrate the load flow control.

Arnez [51] has done the brief analysis of both the series injected voltage and the shunt reactive current of UPFC for controlling the transmittable line flow in a line. The simulation results justify the capabilities of UPFC in increasing and modifying the line flow.

Paper [52] has designed Fuzzy logic based UPFC Controller instead of using PI regulator for Power Flow Control and Stability Enhancement. Response curves for machine angle and speed deviation have not been analyzed.

S. Rai [53] has found the suitable location for UPFC in a multi-machine system for congestion management. Stability index has been implemented to determine the crucial lines during the period of congestion.

R.S.Lubis [54] has done a mathematical modeling for the GUPFC having one shunt converter and two or more series converters which control both the line flow and voltage of the bus.

### **1.5.2 Dynamic performance enhancement**

M.A. Abido [55] has investigated the dynamic stability enhancement of a weakly connected system by using Supplementary Controller of UPFC. Particle Swarm Optimization (PSO) technique is applied to controller for effective damping of low frequency oscillation.

In 1999, Wang developed two UPFC models [56, 57] which have been converted into the linearized model.

E.Babaei [58] has optimized the UPFC Controller parameters using PSO and GA for improving the dynamic response and the stability of the SMIB system.

### **1.5.3 Enhancement of Transient Stability**

E. Gholipour [59] has suggested a new identification method based on local measurement and on State variable for controlling the series part of the UPFC for transient stability of the system and to achieve first swing stability.

S. Koul [60] has investigated the effectiveness of Predictive controller for damping out the low frequency oscillations and thus leads to the enhancement of small signal stability of SMIB system and compared the performance of the Predictive controller with the controller based on phase compensation technique.

R.C. Eberhart [61] has compared the performance of Particle Swarm Optimization using an Inertia weight with the PSO with Constriction factor. Five benchmark functions are used for the comparison and paved the way for applying these technique in optimizing the controller parameters for stability enhancement of power system.

G.K. Venayagamoorthy [62] has proposed the PSO based approach for the design of PI controller of UPFC in a multi-machine power system for time domain stability. The simulation results indicate that the system is not stable after 5 sec even with PSO based controller.

Kazemi, in his paper [63] proposed a controller which includes both Fuzzy logic (FLC) and conventional kp plus conventional ki to the FACTS devices in damping intra and inter area modes of oscillation. The proposed controller takes the advantage of both FLC and conventional PI controller and simulation is performed in a multi-machine power system.

D. Mondal [64] has compared the effectiveness of PSO based SVC controller with its Genetic Algorithm (GA) based Performance. Results revealed that both PSO and GA handle the proposed optimization problem with ease and produce good results. But results could have been better if the author could have used dynamic inertia weight approach, moreover response of machine angle has not been provided. Conventional technique must be implemented first and then comparison should have been made with PSO and GA based controller.

M. Zarghami [65] has determined the various operating points of UPFC. Eigenvalue analysis has been carried out to find the best operating point for stability purpose.

## **1.6 APPLICATION OF OTHER FACTS CONTROLLERS**

Several FACTS controllers have been designed and used in practical power system network. These comprises of static synchronous compensator (STATCOM), Thyristor controlled series capacitor (TCSC), static phase shifter (SPS), Static Synchronous Series compensator (SSSC), and unified Power Flow controller (UPFC). These controllers have

been used for improving voltage stability, dynamic stability, load balancing and damping power system oscillations.

G. Li et. al. [66] designed an optimal controller to work on wide range of series compensation in transmission networks of interconnected power system. The suggested controller was designed for the damping of inter area oscillations.

H. F. Wang [67] proposed a SSSC controller to damp power system oscillations.

Y. L. Kang [68] et. al. used static phase shifter. Both phase angle and magnitude of phase shifter were controlled for the enhancement of dynamic stability of the power system.

W.M. Korani [69] has proposed the hybrid BF-PSO algorithm for PID tuning. The proposed scheme takes the advantage of both the algorithm for achieving better optimized value. But the proposed scheme has not been implemented for power system stability enhancement and secondly the acceleration coefficients of PSO parameters have been taken as fixed values instead of variable which is needed for better search and fine tuning of global minima.

A. Muruganand [70] has designed a new active and reactive power coordination controller for a interline power flow controller (IPFC & UPFC) for equalizing both real and reactive power flow between the lines in order to relieve the burden on the line by transferring power from it to under loaded lines.

A.F.Abdou [71] has investigated the effect of STATCOM for both transient stability improvement and stabilizing multi-mode torsional oscillations.

S. R. Khuntia [72] has designed the fuzzy based SSSC controller and comparison is then made with PSO based Controller for transient stability enhancement. The simulation results reveal the effectiveness of fuzzy based SSSC controller over PSO technique.

## **1.7 OBJECTIVE AND SCOPE OF THE THESIS**

An exhaustive list of references has been presented. However it is observed that the control of SVC and UPFC has not been demonstrated over wide operating range. It requires an effective SVC and UPFC Controllers to be developed which can be applicable over a large operational range for performance enhancement of power system. Optimizing the controller parameters is very important for damping power system oscillations which needs to be investigated. In the present literature it is seen that many authors have implemented

FACTS Technology for stability enhancement of power system network. Different models have been proposed for FACTS Controllers by different researchers. They have used conventional techniques for optimizing the controller parameters. Many researchers have gone for Eigenvalue analysis for analyzing stability. Though concept of artificial intelligent techniques came more than a decade before as seen from the literature review but implementation of this technique in power sector for performance enhancement of power system in real time operation, designing the AI based Controllers and for optimizing the parameters of FACTS Controllers using various AI techniques has become the topic of research. For system stability, decreasing the settling time of oscillation is very important. Many researchers have implemented only basic Particle Swarm Optimization and basic Bacterial Foraging Optimization technique for controller parameters optimization. As a result controllers used are less sensitive towards power transients. Hence FACTS Controllers models which can damp the power system oscillations effectively and efficiently and provide Steady State stability, Dynamic stability and Transient stability are required to be developed. Different auxiliary FACTS controllers based on AI techniques, especially on the advanced adaptive swarm intelligent and evolutionary techniques are to be tried for damping Power system oscillations to evaluate the performance of SMIB system and multi-machine system.

The goal of this thesis is to study the capability of FACTS devices, such as Static Var Compensator (SVC), Thyristor Controlled Series Compensator (TCSC) and Unified Power Flow Controller (UPFC) for damping of Power System oscillations. Thesis comprises of designing, modelling and optimization of Controller Parameters. Various control schemes based on different methods for damping of power system oscillations using various FACTS controllers have been implemented. The present thesis provides several new concepts in designing intelligent controllers for series and shunt connected FACTS devices in an SMIB system and multi-machine environment. Eigenvalue analysis has been carried out for dynamic stability enhancement. For steady state stability and transient stability enhancement over a wide range of working conditions, parameters of controllers are optimized by conventional methods, Particle Swarm Optimization and its Variants, Bacterial Foraging Optimization, Hybrid methods of Optimization and Genetic Algorithm. The robustness of each approach is discussed and validated through Simulation Results.

## **1.8 CHAPTER WISE DISTRIBUTION OF THE THESIS**

A chapter wise distribution of the work done in this thesis is described as follows:

Chapter 1 presents the introduction part of the thesis, an exhaustive review of literature giving the major areas of application of various FACTS controllers like SVC, TCSC, STATCOM, SSSC and UPFC in power system for improvement of Steady state, dynamic and transient stability of the system, Damping of Power system oscillations and Voltage regulation, the aim of the thesis and the chapter wise distribution of thesis.

In Chapter 2, the recent developments in the area of emerging technology of FACTS devices have been presented and also highlights the applications of FACTS controllers for Performance enhancement of power system.

In chapter 3, various Artificial Intelligent Techniques, in particular Swarm Intelligent Techniques have been described like basic Particle Swarm Optimization, Advanced Adaptive Particle Swarm Optimization, Bacterial Foraging Optimization, Hybrid BFO-Particle Swarm Optimization and Genetic Algorithm. These algorithms have been implemented in optimizing the FACTS controller parameters for enhancement of the performance of the power system.

In chapter 4, Enhancement of Voltage stability, Dynamic Performance using Eigenvalue analysis and Transient stability analysis have been carried out in a multi-machine system with SVC Controller and the coordinated control of TCSC and SVC controller in PSAT environment using Simulink. Modeling of SMIB system with auxiliary SVC controller has been carried out. Linearized model of SMIB system equipped with auxiliary SVC Controller has been developed. The auxiliary signal is fed through PID controller and act as a supplementary control signal to SVC. The parameters of auxiliary SVC controller are then optimized both by using Conventional method and Swarm Intelligent Techniques. Simulation results are compared for effective damping of Power System Oscillations and thus enhancement of small signal stability of power system.

In chapter 5, damping of power swings and improving the power transfer capability of power system in single machine infinite bus system equipped with TCSC controller in PSAT environment has been analyzed. Variable reactance model of TCSC controller has been developed and study its effectiveness in damping of electromechanical oscillations in SMIB system for different levels of series compensation of transmission line. The simulation is carried out in MAT LAB Simulink environment. Finally a linearized model of SMIB system equipped with TCSC Controller has been

developed and then Controller parameters of TCSC are optimized both by conventional method and AI technique, in particularly the Particle Swarm Optimization technique for enhancement of steady state performance of the power system.

In chapter 6, SMIB system connected with UPFC Controller is designed and modeled in MATLAB coding. The parameters of UPFC Controller are then optimized using both by conventional method and by various Swarm intelligent techniques for effective damping of power system oscillations, thereby enhancing the transient stability in real time operation. Modelling is also carried out for multi-machine system connected with UPFC controllers. Particle Swarm Optimization technique is implemented for optimizing the parameters of UPFC controllers for enhancement of transient performance of the multi-machine system.

Chapter 9 describes the concluding remarks, a brief review of the investigations carried out in this thesis and suggestions for future work are also highlighted.

## **1.9 DISCUSSION**

In the present chapter a comprehensive review of the development in the area of FACTS devices application to power system has been presented. The emphasis is given on the recent advances taken place in this area. It is observed in the literature that the FACTS devices like TCSC, SVC, UPFC, STATOM and SSSC are finding increasing application in the modern power systems for its secure and reliable operation.



## **CHAPTER - 2**

### **FACTS DEVICES AND CONTROL**

#### **2.1 GENERAL**

Today the existing power system network is very complex due to large interconnections. With ever increasing interconnections and stressed operating conditions, the secure and stable operation has become a challenging task. In the present pace of power system restructuring, electric utilities have to compete in the power market where many constraints restrict them in increasing the power transmission facilities like economic and environmental factors. These constraints are responsible for to limit the full exploitation of existing transmission corridors. Due to the above limitations, it was felt to regulate those factors which are responsible for increase in the power flow in the existing lines and to design those regulating devices. The main factors over which the line flow depends are voltage of the bus, line resistance and machine angle. Since voltage depends upon the reactive power, hence shunt compensation technique was adopted. Similarly by controlling the series reactance of line, power flow can be regulated, thus series compensation technique was used. Thus the main aim of series and shunt compensation is to support the voltage of transmission lines and thus improve the voltage profile of the transmission line during disturbances in both loads and generation and to achieve a secure and stable operation by improving the power transfer capability of lines. The shunt and series compensation techniques are the most attractive thrust areas of research. Initially the mechanically controlled systems were used for compensation. The speed of operation of mechanically switched devices is slower and these devices wear out quickly hence cannot be operated frequently.

#### **2.2 FACTS DEVICES**

The power transfer in an interconnected power system is inhibited by transient stability, voltage stability, small signal stability and sub-synchronous resonance. These factors do not permit the full utilization of existing transmission lines. FACTS devices are very effective and capable of enhancing the power transfer capability, reduce system losses and flexible line flow control through transmission lines while maintaining reliability and power system stability. The problem of sub synchronous resonance which threatened the

series compensation technology some years back has been successfully tackled using FACTS controllers like Static Var System (SVS), Thyristor controlled series compensation (TCSC), Static phase shifter (SPS) and Static synchronous series compensator (SSSC) [22,73,74]. IEEE has given the definition of FACTS as follows:

“Alternating current transmission systems incorporating power electronic based and other static controllers to enhance controllability and increase power transfer capability”.

The FACTS technology does not comprise of one single unit of power regulator. It is a family of many controllers which can either be used alone or in coordination with other controllers in order to regulate those power system parameters like voltage, phase angle and current so that power transmission can be enhanced along with the damping of sub-frequency oscillations which can break the rotor-generator shaft and leads to the loss of reliability and security. On the basis of how the FACTS controllers are connected to the A.C system, they are classified as:

- Series connected controllers
- Shunt connected controllers
- Combined shunt and series connected controllers
- Combined series – series controllers

## **2.3 SHUNT CONNECTED CONTROLLERS**

### **2.3.1 Static VAR Compensator (SVC)**

SVC's are used to control the voltage profile under load variations, enhance the power flow capability of the line and improve the stability of the power system. They can be used for damping power system oscillations incorporating some auxiliary signals [75, 76, 77,]. SVC's are first generation FACTS controllers which are likely to revolutionize power transmission in the near future. These are also used for power factor compensation of dynamic loads such as steel mills and arc furnaces and load balancing [19]. They can provide better control of power flow on parallel path which is important in relatively tight mesh networks.

There are mainly two types of static VAR compensators configuration which are used in power system. A continuous control over the capacitive and inductive range of reactive power can be

achieved from either of the two SVS configurations, FC-TCR or TSC-TCR. It has been reported by Gyugyi et al [43] that while the steady state characteristics and response of both the compensators are identical for small voltage perturbations, the operating behavior of TSC-TCR is characterized by low losses and reduced harmonic contents.

### FC-TCR (Fixed Capacitor-Thyristor Controlled Reactor) Type SVS

The elementary structure of (FC-TCR) type SVS is shown in Fig. (2.1).

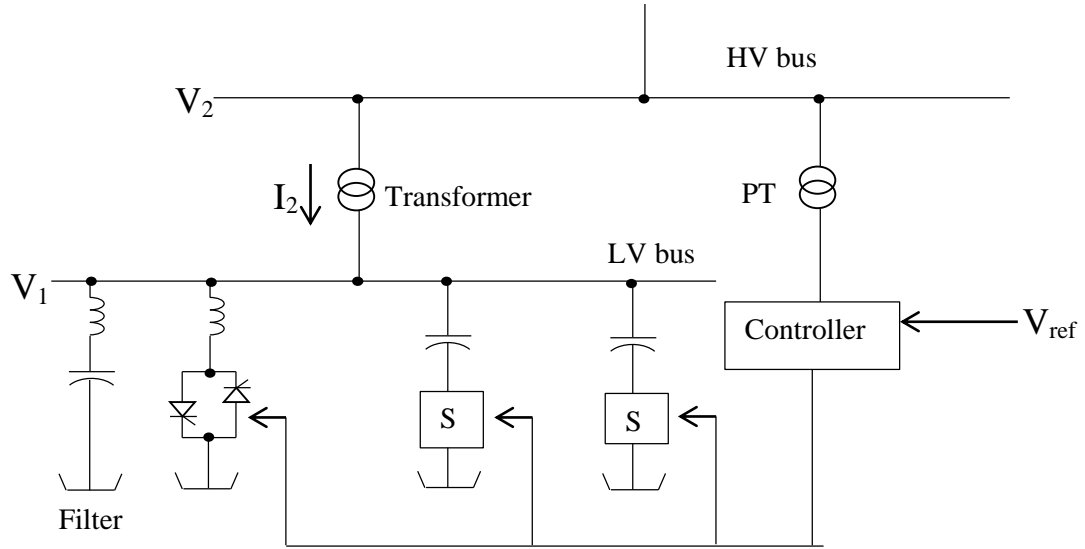


Fig. 2.1 (FC-TCR) type SVS

By controlling the firing angle of the SCR's, the inductive current can be varied. The fundamental inductive current can be expressed as a function of firing angle  $\alpha$  as represented by following equation

$$I_L = \frac{V}{\omega L} \left( 1 - \frac{2\alpha}{\pi} - \frac{\sin 2\alpha}{\pi} \right) \quad (2.1)$$

The fixed capacitor connected in parallel to TCR act as a harmonic suppressor. It provides low impedance path to the dominant harmonics generated by TCR. TCR acts as variable reactive admittance which is expressed in terms of firing angle  $\alpha$  as

$$B_L = \frac{1}{\omega L} \left( 1 - \frac{2\alpha}{\pi} - \frac{\sin 2\alpha}{\pi} \right) \quad (2.2)$$

### SVS Steady State Control Characteristics

The VI operating range of the FC-TCR VAR generator is defined by maximum attainable inductive and capacitive admittances by the current and voltage ratings of the power components. Fig. 2.2 shows the steady state control characteristics of SVS (FC-TCR) configuration.

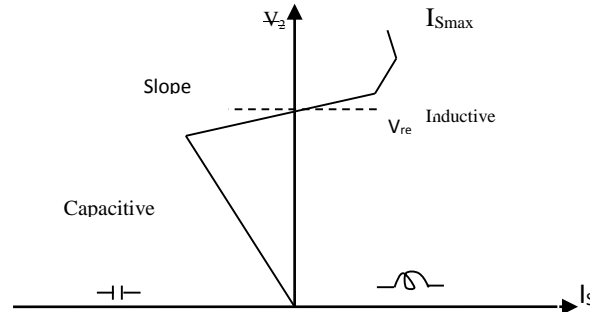


Fig. 2.2 Characteristics of SVS (FC-TCR) configuration

For severe under voltage, the SVS gets transformed into an equivalent fixed capacitor having susceptance  $(B_{L_{min}} - B_C)$  while for large over voltages it reduces to an equivalent shunt reactor of susceptance  $(B_{L_{max}} - B_C)$ . The slope of SVS control characteristics essentially represents a compromise between SVS rating and voltage stabilizing requirement. The slope of control characteristics is typically kept at 3.5%.

### Thyristor– Switched Capacitor, Thyristor Controlled Reactor Type SVS (TSC-TCR) Configuration.

A basic single phase TSC-TCR arrangement and its control scheme is shown in Fig 2.3.

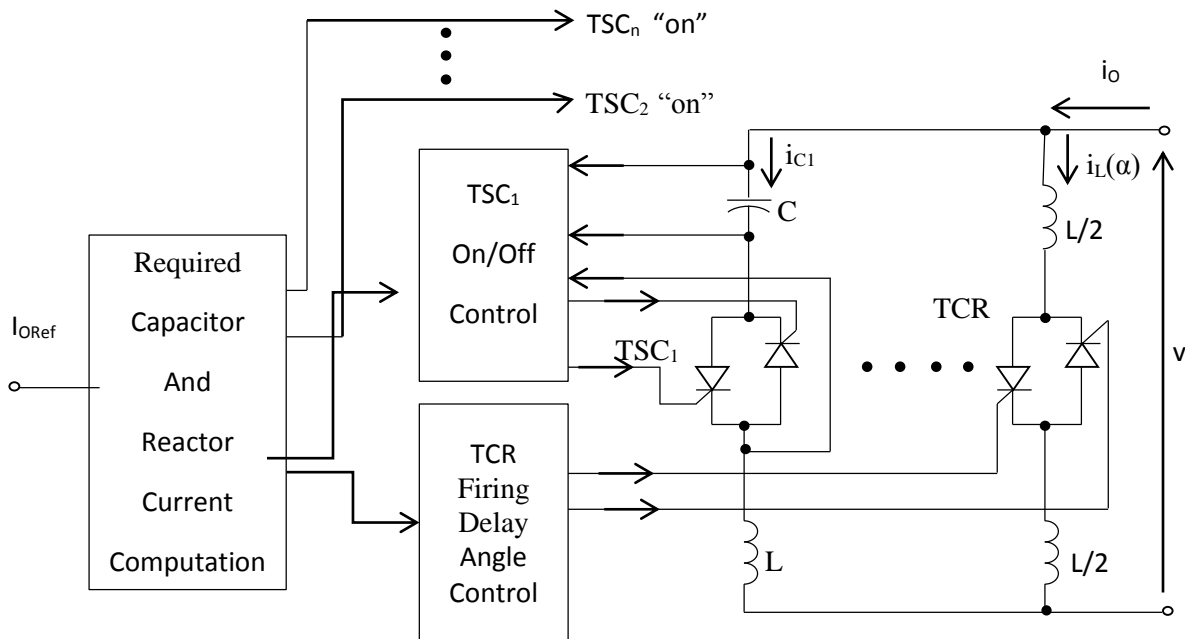


Fig. 2.3 TSC-TCR type SVS

It comprises of n TSC parallel branches for a given range of capacitor output connected in parallel with one TCR and harmonic filters for filtering TCR generated harmonics. The number of branches depend upon the maximum var output, current rating and operating voltage level of thyristor valves. At line frequency, the capacitive filters generate reactive power of about 11 to 30 % of TCR MVAR rating.

The SVS characteristics within control range defined by slope reactance  $X_{SL}$  as given as

$$V = V_0 + X_{SL}I_S \quad (2.3)$$

The slope  $X_{SL}$  has a significant effect on the performance of SVS. A large value of  $X_{SL}$  makes SVS less responsive. The value of  $X_{SL}$  is determined by steady state gain of voltage regulator and current feedback.

### **Applications of Static VAR Compensators**

Due to virtue of the ability of SVC's to deliver continuous and fast control of voltage and reactive power, SVS has many applications in regard to the performance enhancement of the power system. They are characterized as:

- Control voltage profile
- Avoid voltage collapse
- Improves the transient stability
- Mitigation of power system oscillations
- Balancing the unbalanced loads
- Eliminating voltage flicker
- Damping sub-synchronous resonance
- Power factor improvement
- Loss reduction
- Enhancement of power transfer capability

### **2.3.2 STATCOM**

Static synchronous compensator belongs to second generation FACTS device and is based on voltage source converter using gate turns off thyristors (GTO'S) and is being used for high power applications. The applications of STATCOM are almost the same as those of SVC.

STATCOM provides both active and reactive power exchange while SVC provides only reactive power exchange. By altering the magnitude of output voltage, reactive power is injected or

absorbed by the converter. This reactive power can be exchanged between the inverters and AC system. The current in DC capacitor is zero under steady state. A small amount of harmonic current flows through the DC capacitor to counter balance the harmonic voltages at the AC terminals.

In STATCOM, exchange of active power is possible between the A.C supply system and voltage source converters. It is possible by having the control on phase angle of the voltage injected by voltage source converter with respect to A.C supply voltage. This can be achieved only by using a suitable D.C energy storage device such as battery or superconducting magnet. Apart from this, this device is also capable of providing both type of reactive compensation (inductive and capacitive) and is able to control output current which is independent of AC system voltage. At any system voltage, STATCOM is able to supply full inductive or capacitive output current while the output current of SVC depends on the system voltage. Thus at low system voltage, SVC is able to provide low output current. Hence STATCOM is superior to SVC on the pretext of improvement in voltage and transient stability enhancement. Hence STATCOM may be used to handle peak power demand and prevent power interruptions. The STATCOM has the ability to damp the power system oscillations in the network by supplying or absorbing the reactive power as per the need.

### **2.3.3 Advantages of STATCOM over SVC**

The capability of providing maximum compensating current at reduced system voltage enables the STATCOM to provide better dynamic compensation in compare to SVC of higher rating.

- STATCOM is more operational in compare to SVC in enhancing the transient stability of the power system.
- For the same stability margin, the rating of STATCOM is lower than that of SVC.
- Size and cost of STATCOM is smaller as compared to SVC.

A.H.M.A. Rahim [78] developed a robust STATCOM voltage controller for power system damping. The first high power STATCOM was commissioned in 1995 in U.S. A. used for line compensation.

## **2.4 SERIES CONTROLLERS**

### **2.4.1 Thyristor Controlled Series Capacitor (TCSC)**

First three phase TCSC was installed at 230 KV Kayanta substation in Arizona under Western Area Power administration (WAPA) in October 1992. The installation permitted a flat and fast control of (capacitive) reactance through phase control of TCR. The device

was equipped with a 15 ohm capacitor bank that was connected in parallel with a TCR. In 1993 another installation of three phase TCSC was done at 500 kV Slatt substation in Oregon under Bonneville power administration. TCSC structure used had six modules placed in series are controlled to vary capacitive reactance from 1.4 ohm to -16 ohm [1].

### Working of TCSC

TCSC is represented as shown below in fig (2.4) which shows two modules connected in series.

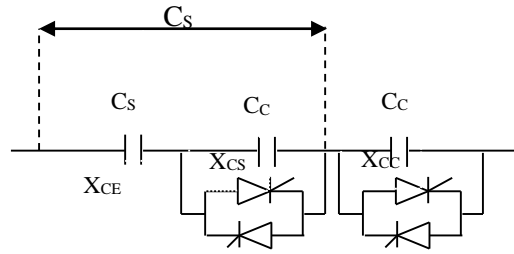


Fig. 2.4 TCSC structure

No. of modules depend upon requirement. TCSC may be used in conjunction with fixed series capacitors to reduce the cost, TCSC has three operating modes which are as:

(i) By Passed:

In this mode valves are fired at  $0^0$  to make them conducting for  $180^0$  and the inductive reactive current that flows in reactor is continuous and sinusoidal. Most of the line current flows through the TCR with little current flowing through the capacitor. TCSC operating in this mode is used mainly for capacitor protection against over-voltages.

(ii) With blocking Thyristor Valve mode:

In this scheme of operation, gating pulses to the SCR's are blocked and there will be no current flowing through TCR. The reactance of TCSC will be same as that of fixed capacitor connected in parallel. This operating mode also known as waiting mode is generally avoided.

(iii) Vernier control mode:

In this scheme of operation, the SCR's are fired between  $(\alpha_{min} < \alpha < 180)$ , such that they conduct partially. The effective value for TCSC reactance increases as  $\alpha$  is reduced below  $180^0$  and maximum for  $\alpha = \alpha_{min}$ . Where  $\alpha_{min}$  is above the value of  $\alpha$  corresponding to the parallel resonance of TCR and capacitor at fundamental frequency. Vernier control generally works in the capacitive region only.

### **2.4.2 Advantages of TCSC over Conventional Series Capacitor**

TCSC has high speed control capability which enables rapid control of power flow in response to contingencies. TCSC increases power transfer capability. It improves the transient stability by providing damping for system swing modes. TCSC can increase the effective impedance of series compensating capacitor. This increase of effective impedance is due to additional voltage, the TCR produces across the capacitor by repetitive charge reversals. TCSC is neutral to sub-synchronous resonance. The operation of TCSC using constant reactance control using Vernier mode is sufficient to avoid torsional interaction which is a serious problem with fixed series compensation. In India, FACTS technology may provide an important solution to the present power crisis where increased electrification is resulting in the need for effective use of power system. High degree of series compensation is possible with TCSC without the fear of SSR.

### **2.4.3 Static Synchronous Series Compensator (SSSC)**

Static synchronous series compensator (SSSC) was proposed in 1989 by Gyugyi. It is a static synchronous generator which is operated as a series reactive power compensator, if no external battery source is used. The controllable output voltage injected is in quadrature with the line current. This injected voltage either increases or decreases the overall reactive voltage drop across the line and thus power flow in the line is controlled. This device can also be implemented for temporary active power compensation by connecting the external battery energy source and thus provide enhanced dynamic behavior. SSSC is similar to STATCOM except that SSSC is connected in series with the line to provide series compensation by injecting the small amount of voltage in series with line while STATCOM is connected in shunt with the line to provide shunt compensation by injecting the current in the line.

### **Characteristics of S.S.S.C**

The S.S.S.C. has the following features:

1. Increase in power flow due to SSSC is almost constant and nearly independent of power angle ( $\delta$ ), but at  $\delta=0^0$  the series compensation has no effect on the power flow.
2. S.S.S.C can generate a controlled reactive voltage which is independent of magnitude of line current.



3. X/R ratio can be made high even for high degree of series compensation with S.S.S.C due to its capability to compensate the resistance in a transmission line.
  4. S.S.S.C has wider control range than the series capacitor. Even the reverse power flow is possible with S.S.S.C just by reversing the polarity of injected voltage ( $v_{q_1}$ ).
- S.S.S.C. does not cause electrical resonance in the line and hence S.S.S.C. is expected to be SSR neutral.

## 2.5 SHUNT AND SERIES CONTROLLER

### 2.5.1 Unified Power Flow Controller (UPFC)

Unified Power Flow Controller (UPFC) comprises of a shunt and series controller connected back to back through dc link capacitor [1]. For controlling the voltage and power flow control in a 132 kV long transmission line in U.S.A., the first UPFC designed and manufactured by Westinghouse Electric Corporation was commissioned in 1998 at the Inez station of the American Electric Power (AEP) in Kentucky. It was a joint venture of EPRI and AEP.

#### Functional Block Diagram and Phasor Diagram of U.P.F.C.

Functional block diagram of UPFC is shown in Fig 2.5.

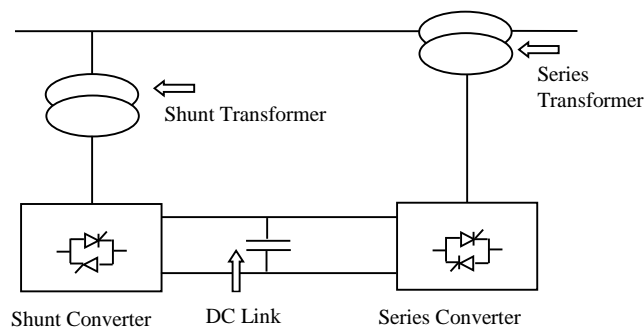


Fig.2.5 Unified Power Flow Controller

U.P.F.C. is capable of controlling independently or simultaneously all the parameters like impedance, phase angle and voltage which affect the line flow in the transmission line. Both active and reactive line flows can be controlled by this device. Hence UPFC is considered as a strong device for the cost management in effective exploitation of individual transmission lines due to independent control of both the real and reactive power

flow and leads to the enhancement of active power transfer with minimum losses in the line.

## **2.6 COMBINED SERIES – SERIES CONTROLLER**

### **2.6.1 Inter Line Power Flow Controller (IPFC)**

Interline Power flow controller (IPFC) came into existence to tackle the problem of compensating a number of transmission lines at a given substation by Gyugyi with Sen and Schauder in 1998. It comprises of series combination of static synchronous series compensators. This arrangement allow to equalize both real and reactive power flow between the lines, reduce the burden of overloaded lines, to provide compensation against resistive line voltage drops and subsequently the demand of reactive power as it has the capability to directly transfer real power between the compensated lines by controlling reactive series compensation of each individual line. Thus increases the effectiveness of the overall compensating system for dynamic disturbances and is highly effective at a multilined substation for power transmission management.

## **2.7 FACTS CONTROL**

The FACTS devices are exploited to regulate the line flow in the transmission lines. The shunt devices regulate the line flow by controlling the voltage magnitude at the buses, whereas the series converter injection modulates the line reactance for fast power flow control. By regulating the power flow in a transmission line, the speed of oscillations of the generators can be damped effectively. In practice the series connected FACTS devices are controlled through active power flow error whereas the shunt devices through bus voltage error. The series reactive compensation is able to reduce only the effective line reactance  $X$  and leads to the reduction of the effective  $X/R$  ratio and thus increase the reactive power flow and also losses in the line [1]. Hence there is a need to regulate the resistance of the transmission line to keep  $X/R$  ratio at a desired value. The requirement of simultaneous control of reactive and resistance of the transmission line can be accomplished by injecting in-phase and quadrature voltage components with the line current, respectively. These components can be generated by the UPFC by regulating the phase angle and magnitude of the added voltage source. Therefore active and reactive power error are used to control the quadrature and in-phase component, respectively.

Also, for shunt current control and series voltage injection, UPFC uses voltage source converters (VSCs) connected through a common D.C link capacitor as shown in fig. 2.2. Individual control of reactive power (injection or absorption) can be achieved in this device. The shunt converter solves the problem of circulating the real power demand of series converter through the D.C link. The literature covers the exact balancing of real power between the converters of the UPFC represented by injection model but in practice this condition can never be attained. Hence precaution is taken that there shall not be the real power mismatch and is made possible by modifying the injection model of UPFC.

## **2.8 DISCUSSION**

In leading countries, due to structural reformation of the electricity market, electric utilities are undergoing rapid changes. In the recent trend of deregulation in the electricity market, there is a need of flexible power load flow control and which has been attained by innovative power electronic technology. This chapter describes the effectiveness of various FACTS devices which are proved to be capable of enhancing the power transfer capability and flexible control of power flow through transmission lines while maintaining stability and reliability of power system. Hence it is being concluded that due to the fast control action of FACT devices, they is a good option for utilizing them in power system damping enhancement.

# **CHAPTER - 3**

## **CONTROL STRATEGIES FOR OPTIMIZATION**

### **3.1 GENERAL**

The most important principles in the world is to search for an optimal state. One can define the optimization as the mathematical process to achieve maximum or minimum of the output either by altering the device characteristics or the inputs. In order to go for optimization, objective function or cost function or fitness function need to be defined and computed. Optimization act as an instrumental in tackling the difficult or unsolvable problems. They are classified into various categories: one/multi-dimensional optimization, Trial and error optimization, Dynamic optimization, Static optimization and constrained/unconstrained optimization and Global optimization.

In hit and trial optimization technique, the output is affected without having knowledge about the limitations that yield the output during processes. During optimization, objective function or cost function is described by the mathematical formula. Problems having one variable requires one dimensional optimization, while multi variable problem requires multi-dimensional optimization approach. The optimization problem becomes clumsy with an increase in the number of dimensions. Another optimization algorithms are dynamic and static optimization. The former technique is time dependent, whereas the latter technique is independent of time. The static problems are difficult to solve for getting the finest solutions but by adding the time as a new dimension, the challenge of solving dynamic problems further increases. A limited number of possible outputs are produced in a discrete variable optimization, whereas unlimited number of possible outcomes are produced in continuous variable optimization. Variables generally have constraints. Variable equalities and inequalities are included in the objective function in the constrained optimization problems while in the unconstrained optimization, the variable is permitted to take any arbitrary value. A constrained optimization problem can be converted into an unconstrained one through the conversion of variables. In global optimization, main aim is to find the global optima which can either be maxima or minima. Parameters or designs for components are computed by optimization and then are enforced into action either by machines or by the human beings.

Economic Load Dispatch and optimal power flow problems are being solved using conventional method of optimization and its response is based on the equality and inequality constraints of the system.

As the complexity of the system increases, Conventional methods are no longer effective and helpful and these methods can handle the system up to a certain limits. Moreover these techniques are time consuming and may not give good results even for a simple system. Hence there is a great need to develop more intelligent and helpful techniques.

For this purpose, we have soft computing techniques like Genetic Algorithm (G.A.), Particle Swarm Optimization (PSO) and their integration have been developed and applied for optimization.

G.A. are used for optimization using normal search.

According to the complexity of systems, the following techniques may be used for system optimization:-

1. Less Complex Systems (Conventional Techniques)
2. Medium Complex Systems (Soft Computation Techniques like Genetic Algorithm, Particle Swarm Optimization, Bacterial Foraging Optimization and their hybrid techniques.

### **3.2 CONVENTIONAL TECHNIQUES**

For finding the optimum solution and unconstrained maxima and minima of continuous and differentiable factors, we have classical or conventional optimization techniques.

These are analytical methods and for locating the optimum solutions, they use differential calculus. Because of the presence of objective functions which are not continuous and differentiable, the classical methods have a limited scope.

### **3.3 ZIEGLER NICHOLS, A CONVENTIONAL TECHNIQUE**

The Ziegler- Nichols tuning method was introduced by John Ziegler and Nathaniel Nichols in 1942. It is a heuristic method for tuning PID controller. It is a closed loop tuning technique that is performed manually. While tuning with this method dynamic characteristics of the system are represented by the gain of Proportional controller and the

period of oscillation of the system. It usually determine the ultimate gain and period by the following method:

1. Only proportional controller is considered and the integral and derivative mode of the feedback controller are turned off.
2. The proportional gain is increased or reduced till the loop oscillates with constant amplitude keeping the controller in closed loop. The value of the gain that produces sustained oscillation is recorded. In order to obtain the final gain value and to prevent the loop, going to unstable, small increments in gain are made.
3. The period of oscillation is measured and recorded as  $T$ , the ultimate period.
4. Change the integral and derivative gains till oscillations are decayed substantially.

For the best response of the close loop, Z-N method specifies a decay ratio to one-fourth. The decay ratio is the ratio of the amplitude of two consecutives oscillations. It may be independent of the input and should depend only on the roots of the characteristic equation for the closed loop.

However, there are some few drawbacks to this technique: getting the closed loop to cycle continuously is a time-taking process and there is always a risk that oscillations will grow beyond stability. There is no procedure to calculate the magnitude of oscillations of a system.

### **3.4 SOFT COMPUTATION TECHNIQUES**

According to professor Zaden, Soft Computation is an emerging technique for parallel computation of the remarkable ability of the human mind to learn about the environment of uncertainty and imprecision.

For computing optimization techniques, the aim is to develop a computer or a machine which will work in a similar way like human brain does.

### **3.5 SWARM INTELLIGENCE ALGORITHM**

Swarm Intelligence is a branch of nature inspired by Artificial Intelligence and is linked to the collective behavioral study and emergent properties of complex, self-organized, decentralized system with social structure.

The collective intelligence seems to provide insight into meta-heuristics by evolving from the behavior of a group of social insects for example in the insect community, there are limited self-capabilities but many complex tasks can be performed for their survival.

Without any supervisor or controller, problems requiring detailed planning like finding and storing food, selecting and picking materials for future usage can be done.

Since its origin in 1980, Swarm Intelligence Algorithm has been studied and used wisely in fields such as economic analysis and decision making, biology and industry and power sectors.

This technique can be used for solving multi objective optimization and constraint optimization problems. Various algorithms are Particle Swarm optimization and its variants, Bacterial Foraging optimization and hybrid BFO-particle swarm optimization, ant colony optimization and many more.

### **3.6 PARTICLE SWARM OPTIMIZATION**

PSO was presented by Eberhart and Kennedy in 1995 [22]. It is an analytical & stochastic based optimization technique and can be used for optimization problems that are partially irregular, noisy and dependent on time etc. It is emerged from swarm intelligence and is established on the research of a flock of bird and fish movement behavior. The particle swarm optimization comprises of a swarm of particles representing birds that are initialized with a population of random candidate solution in the multidimensional search space. During their flying movement, they follow the best trajectory according to their personal best flying experience (pbest) & best flying experience of the group (gbest). During this process, each particle modifies its position & velocity according to shared information to follow the best trajectory which leads to optimum solution. This technique being simple requires very few parameters to be determined. This search is based on probabilistic, rather than deterministic transition rules. The choice of PSO parameters can have a colossal impact on optimization performance. Going for PSO parameters that yield good performance have therefore been the subject of much research.

### 3.6.1 Algorithm

Step 1: Initialize the number of particles  $n$ , minimum and maximum limits for the  $d$ -dimension search space  $\theta_{\max}$ ,  $\theta_{\min}$  and  $i_{\max}$ .

Step2: Set initial position of particles  $\theta_i^k$

Where,

$$\theta_i^k = \theta_{\min} + (\theta_{\max} - \theta_{\min}) * rand( ) \quad (3.1)$$

Step 3: Set initial velocity  $\lambda_i$  of particles

$$\lambda_{id}^k = \lambda_{\min} + (\lambda_{\max} - \lambda_{\min}) * rand( ) \quad (3.2)$$

Where,

$$\lambda_{\max} = 0.1 * (\theta_{\max} - \theta_{\min}) \quad (3.3)$$

$$\lambda_{\min} = -0.1 * (\theta_{\max} - \theta_{\min}) \quad (3.4)$$

Step 4: Select initial  $p_{ibest}^k$ ,  $g_{best}^k$

Step5: calculate cost function  $f(x_i)$  taking initial position into consideration.

Step 6: If  $f(\theta_i) > f(p_{ibest}^k)$

Then

Update the value of  $\theta_i^k$  by  $p_{ibest}^k$

Else

retain the  $p_{ibest}^k$  as  $p_{ibest}^k$

end if;

Step 7: If  $f(p_{ibest}^k) > f(g_{best}^k)$

Then

Update value of  $p_{ibest}^k \rightarrow g_{best}^k$

Else

go to step 8.

step 8: If

maximum number of iterations has been done

then

store  $g_{best}^k$  as best position value.

Else

Increase order of iteration by one.



Update particle velocity & position:

$$\lambda_i^{k+1} = \lambda_i^k + a1 * rand1(pbest_i^k - \theta_i^k) + a2 * rand2(gbest^k - \theta_{id}^k) \quad (3.5)$$

$$\theta_i^{k+1} = \theta_i^k + \lambda_i^{k+1} \quad (3.6)$$

Where, a1 and a2 represents the acceleration factors, *rand1* and *rand2* represents distributed random numbers between (0, 1). First part of equation (3.5) depicts the previous velocity of the particle, the second part is a positive cognitive component & third part is a positive social component as described in [23].

If  $\lambda \leq \lambda_{\min}$  then  $\lambda = \lambda_{\min}$  and If  $\lambda \geq \lambda_{\max}$  then  $\lambda = \lambda_{\max}$

Repeat Step 4 to step 7

Else if,

End.

### 3.6.2 Flow Chart of PSO

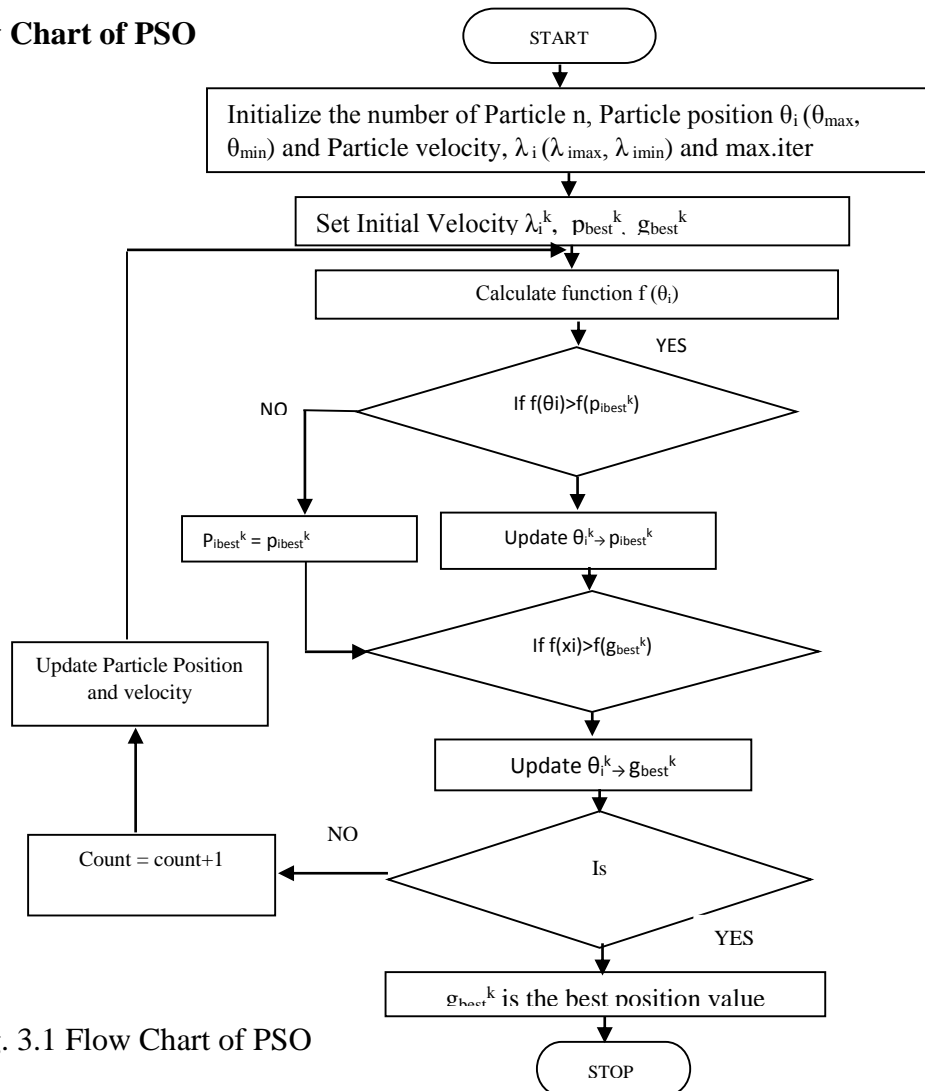


Fig. 3.1 Flow Chart of PSO

### 3.7 PSO-SHRINKAGE FACTOR WITH TIME VARYING INERTIA WEIGHT APPROACH (PSO-TVIWA)

The conventional PSO has the drawback of premature convergence & problem of stagnation. This can be overcome by incorporating additional factor called inertia weight factor  $w$ , whose concept has been explained by Shi & Eberhart [21] in order to achieve the balance between local & global search during the iteration process of an optimization problem. Inertia weight plays an important role in controlling the exploitation and exploration capability of algorithm. For enhancement of performance index of conventional PSO algorithm, one can adjust the inertia weight  $w$ , the value of which is linearly reduced during the iterations. Typical values of  $w_{\max}$  &  $w_{\min}$  are 0.9 & 0.4 respectively. Since there is a need of vast random search in multi-dimensional search space initially & at later stage when problem is converging to best solution, fine tuning is required. Due to dynamic behavior of  $w$ , this technique can be named as PSO-TVIWA as described in paper [20]. The inertia weight  $w$  is an inertia weight factor which controls the exploitation and exploration of the search space by adjusting the velocity dynamically and it is a function of iteration time and mathematically,

$$w = w_{\max} - \left( (w_{\max} - w_{\min}) / \text{iter max} \right) \text{iter} \quad (3.7)$$

This technique had some limitations of not converging towards global minima. In order to converge efficiently and to avoid outburst of the particle swarm, an additional new parameter called shrinkage factor/constriction factor  $S$  has been proposed by Clerc et al [24, 25]. Mathematical representation of updated particle velocity and position using shrinkage factor is given as follows:

$$\lambda_{id}^{k+1} = S \left( w * \lambda_{id}^k + a1 * \text{rand1} (pbest_i^k - \theta_{id}^k) + a2 * \text{rand2} (gbest^k - \theta_{id}^k) \right) \quad (3.8)$$

$$\theta_{id}^{k+1} = \theta_{id}^k + \lambda_{id}^{k+1} \quad (3.9)$$

$\theta_{id}^k$  is the previous position of the particle and  $\lambda_{id}^{k+1}$  is the updated particle velocity.

Mathematically, Shrinkage factor has been represented as

$$S = \frac{2}{|2 - \varphi - \sqrt{\varphi^2 - 4\varphi}|} \quad (3.10)$$

$$\varphi = a1 + a2 \quad \& \quad \varphi > 4$$

Normally, values of  $a_1$  and  $a_2$  lie from 0.5 to 2.05. For  $a_1=a_2=2.05$ , the computed value of  $S=0.73$ . These values can be changed according to the optimization problem.

### 3.8 ADVANCED ADAPTIVE PARTICLE SWARM OPTIMIZATION

This strategy has the advantage of both fast convergence as well as fine tuning to global minima [28]. In optimizing to global maxima, an important role is played by both cognitive part and social interaction part of velocity. In order to increase the randomness at the initial stage, value of  $a_1$  is made larger than  $a_2$ . This allows particle to search the optima in the whole  $d$ -dimensional search space. Due to premature convergence, lower value of  $a_1$  can lead to trapping into local minima. Whereas, higher value of  $a_2$  than  $a_1$  is desired at later stage to enhance the social interaction and hence converges efficiently to global minima. Hence this technique is also called as PSO with time varying acceleration coefficients (PSO-TVAC). It is mentioned here that this algorithm is used with time varying inertia weight factor.

Mathematically updated particle velocity and position is represented as:

$$\lambda_{id}^{k+1} = (w * \lambda_{id}^k + a_1' * rand1(pbest_i^k - \theta_{id}^k) + a_2' * rand2(gbest^k - \theta_{id}^k)) \quad (3.11)$$

$$\theta_{id}^{k+1} = \theta_{id}^k + \lambda_{id}^{k+1} \quad (3.12)$$

where modified  $a_1'$  and  $a_2'$  are mathematically represented as [26, 28]:

$$a_1' = ((a_1f - a_2i) * k / K_{max}) + a_1i \quad (3.13)$$

$$a_2' = ((a_2f - a_1i) * k / K_{max}) + a_2i \quad (3.14)$$

$a_1i$ ,  $a_2i$ ,  $a_1f$  and  $a_2f$  are initial and final values of  $a_1$  and  $a_2$  respectively. Normally  $a_1$  varies from 2.5 to 0.5 and  $a_2$  varies from 0.5 to 2.5 over the full range of search.  $K_{max}$  represents maximum iteration.

### 3.9 PSO AND ITS VARIANTS: ISSUES

Proper implementation of PSO is required while designing AI controllers. The following issues are to be considered while optimizing the controller parameters employing Particle swarm optimization.

Deciding the number of particles is an important issue in an optimization problems. Large number of particles increases the converging rate while small number of particles leads to premature convergence and leads to trapping into local minima.

Global search for optimal solution firmly depends on the right selection of acceleration coefficients  $a_1$  and  $a_2$ . Larger values of  $a_1$  and  $a_2$  makes the search completely random in nature and problem may not converge and smaller values may lead to trapping into local minima.

The maximum and minimum limit values of the dimensional search space also affects the search of global minima. Wrong selection of limits can lead to incorrect results.

Proper selection of shrinkage factor and inertia weight is required to avoid the outburst of the particle swarm.

### **3.10 BACTERIAL FORAGING OPTIMIZATION**

To optimize the variables effectively and efficiently, BFO turns out to be a very effective AI technique. BFO technique is motivated by the pattern shown by animals that have successful foraging strategies (locating, handling & ingesting food). The author in [\[18, 22\]](#) explains the biology & physics of E. coli bacteria & applies that in adaptive controller. The control system of these E. coli bacteria can be explained by five operations: Chemotaxis, Swarming, Reproduction, Elimination and Dispersal. In this technique a cluster of bacteria moves in search of food and away from toxic elements. In chemotaxis step, the bacteria swims and tumbles in its entire life span. With the help of flagella, the nutrients concentration is computed at its initial position before tumbling. If the bacteria gets more nutrients in that direction then it will swim in the same direction and if less, then tumbles and finds new direction. Half of them which are healthier reproduce and remaining die out. The new born then also go under chemotaxis step & again healthier bacteria survive and weaker die out but bacteria population remains constant. During this process, the healthy bacteria attract other healthy bacteria which are quite away from them & repel those which are weaker; this takes the variable to best possible value, which is called swarming effect.

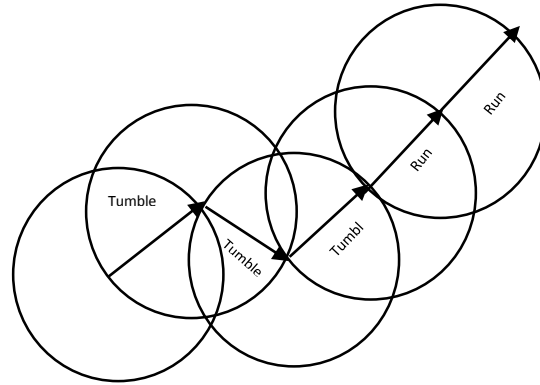


Fig. 3.2 Unit Walk of a Bacteria indicating Tumble and swim in chemotaxis step

### 3.10.1 Algorithm

1. Initialize the dimension of search space, number of bacteria, chemotaxis steps, swim steps, reproduction steps, elimination & dispersal steps, probability of elimination & run length unit  $U(i) i=1,2,\dots,S$ ,  $\theta^i$  (initial position of bacterium). Cell to cell attractant & repellant parameters.

2. Initialize elimination dispersal loop control,  $d=d+1$

3. Check  $d=N_{ed}$ , stop else continue

4. Initialize reproduction loop count  $r=r+1$

5. Check  $r < N_{re}$ , continue else go to step 2

6. Initialize chemotaxis loop count  $c=c+1$

7. Check  $c < N_c$  continue else go to step 4

i) Compute fitness value of objective function,  $F$  for each bacterium  $i$ ,  $F(i, c, r, d) = F(i, c, r, d) + S_{cc}$

Where  $S_{cc} = \sum [-d_{attractant} \exp(-w_{attractant} \sum (\theta_m - \theta_m^i)^2)] + \sum [h_{repellant} \exp(-w_{repellant} \sum (\theta_m - \theta_m^i)^2)]$

ii) Check  $F(i, c, r, d) < F(i, c-1, r, d)$ , save it.

iii) Tumble: Generate a random vector  $\alpha(i)$  in range  $(-1, 1)$ .

iv) Move:  $x^i(c+1, r, d) = x^i(c, r, d) + U_i \alpha(i) / (\alpha^T(i) \alpha(i))^{1/2}$ .

v) Again compute  $F(i, c+1, r, d)$  & compare, if least continue, else Tumble.

8. Initialize swim loop counter  $N=N+1$

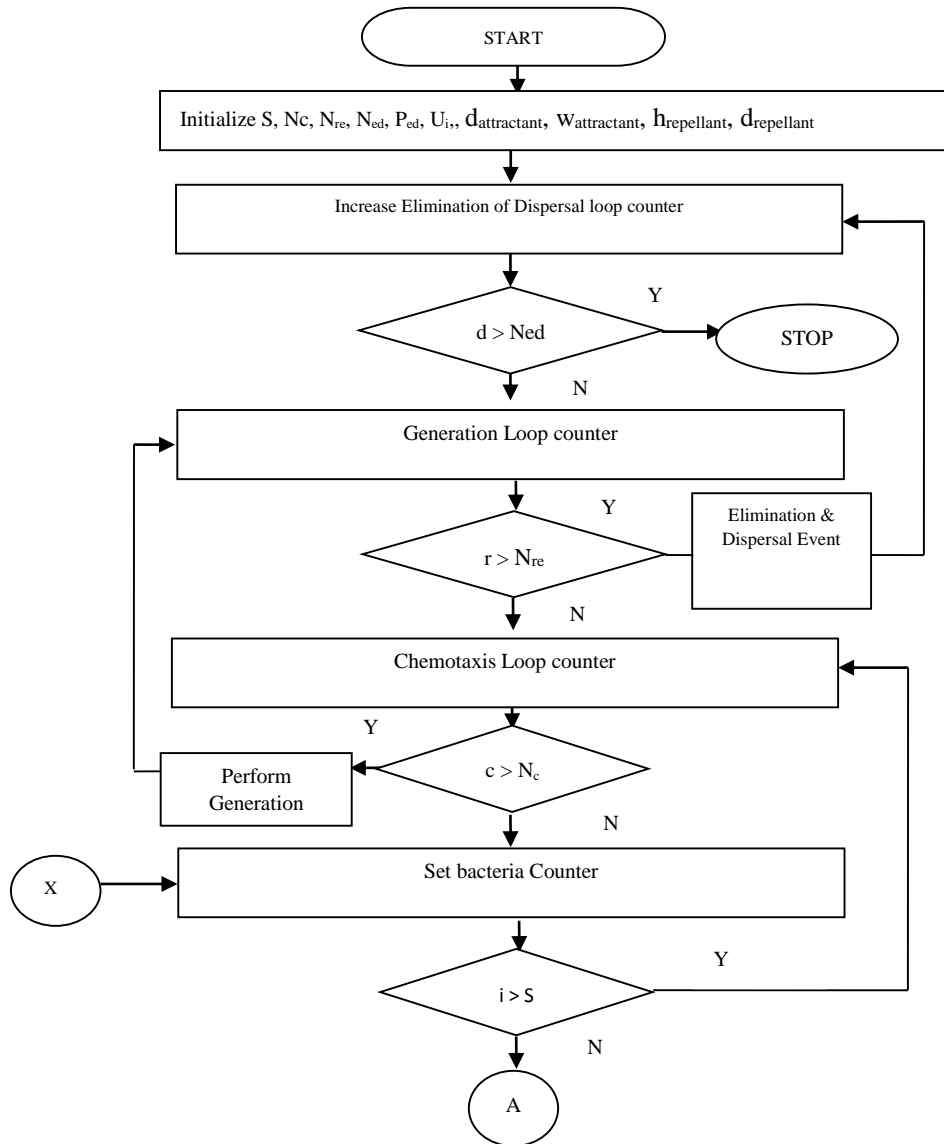
9. Check  $N < N_s$  go to 7(iv) else tumble.

10. Perform Reproduction of healthy bacteria.

11. Perform Elimination & dispersal.

12. Continue the process till the maximum computations are over.

### 3.10.2 Flow Chart



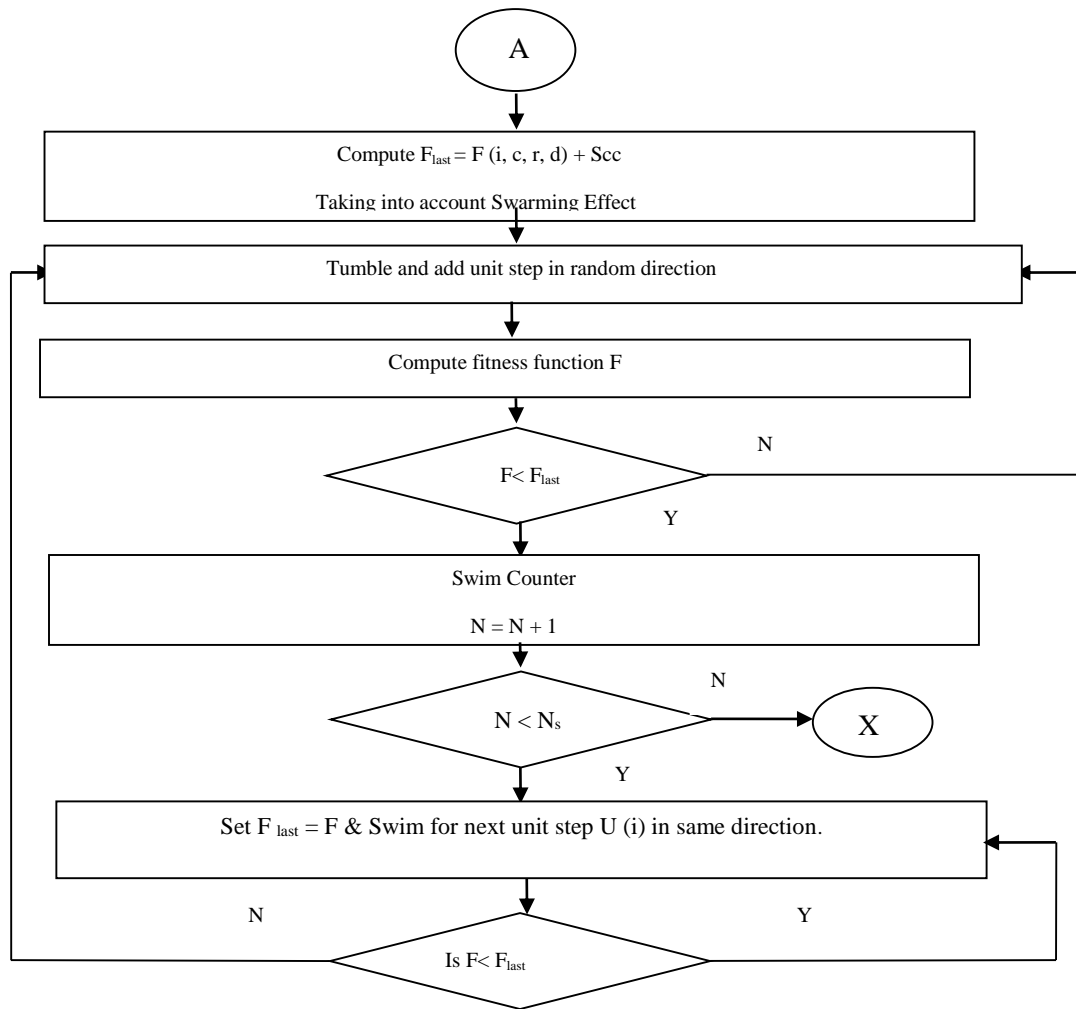


Fig. 3.3 Flow Chart of BFO

### 3.10.3 Bacterial Foraging: Issues

Deciding the number of bacteria, probability of elimination and dispersal, selection of swim length is the area of research.

### 3.11 HYBRID BFO-PARTICLE SWARM OPTIMIZATION

It takes advantage of both Bacterial Foraging and Particle Swarm Optimization Techniques in searching the global minima.

In every chemotaxis step, Personal best position of each bacteria and global best position of all bacteria is computed and velocity is upgraded according to personal best experience and social interaction experience as discussed in PSO.

$\alpha(i)$  =Velocity

Updated velocity

$$\lambda_i^{k+1} = \lambda_i^k + a1 * rand1(pbest_i^k - \theta_{id}^k) + a2 * rand2(gbest^k - \theta_{id}^k) \quad (3.15)$$

New position of bacteria is computed as

$$\theta^i(c+1,r,d) = \theta^i(c,r,d) + U_i \alpha(i) / (\alpha^T(i) \alpha(i))^{1/2} \quad (3.16)$$

### 3.11.1 Hybrid BFO-Particle Swarm Optimization With Time Varying Acceleration Coefficients.

This technique provides both wide area search initially and fine tuning while reaching near global minima. Initial wide area search is possible by keeping larger value of a1 and lower value of a2 and for fine tuning, a2 is made larger than a1. Thus by continuous modifying the values of a1 and a2 of PSO parameters along with elimination and dispersal event of BFO, global minima can be achieved effectively.

Updated velocity

$$\lambda_i^{k+1} = \lambda_i^k + a1' * rand1(pbest_i^k - \theta_{id}^k) + a2' * rand2(gbest^k - \theta_{id}^k) \quad (3.17)$$

Where

$$a1' = ((a1f - a2i) * k / K_{max}) + a1i \quad (3.18)$$

$$a2' = ((a2f - a1i) * k / K_{max}) + a2i \quad (3.19)$$

Keep the updated velocity=  $\alpha(i)$  and compute the updated position of Bacteria in the next step of Chemotaxis event under BFO algorithm as under:

$$\theta^i(c+1,r,d) = \theta^i(c,r,d) + U_i \frac{\alpha(i)}{\alpha^T(i) \alpha(i)^{1/2}} \quad (3.20)$$

### 3.12 GENETIC ALGORITHM

Genetic algorithms are adaptive algorithms for finding the global optimum solution for an optimization problem. Genetic Algorithm is one of the family members of Evolutionary



algorithms (EAs), which are the population-based Meta heuristic optimization algorithms that use biology-inspired mechanisms and based on Darwin's theory of the survival of the fittest. It was first developed by Holland. Hard and complex problems are being solve in a very efficient, very fast and with reliability and solve the complexity of the real-time controllers effectively. Genetic algorithms (GAs) may contain a chromosome, a gene, a set of population, fitness, fitness function, generation, mutation and selection. Genetic algorithms (GAs) begin with a set of solutions represented by chromosomes, called population or the parents. Solutions from one population are taken and used to form a new population called off-springs with the possibility that the new population will be better than the old one according to Darwin's theory. Selection is being made based on their fitness values. It will continue till the specific condition is achieved. Algorithmically, the basic genetic algorithm (GAs) is outlined as below:

1. Create a random population. It can either be of genes or chromosomes.
2. Compute the fitness of each member of the population.
3. Retain some fittest parents according to elitism criteria.
4. Repeat the following steps to create a new population.
  - i) According to the fitness values, 2 parents are selected from a population. The Parent having larger fitness function are more likely to be selected.
  - ii) According to crossover probability (GA operator), a new child is obtained by the cross over operation of the selected parents.
  - iii) Mutation (another GA operator) is applied to a new child according to the mutation probability.
  - iv) The new children created, form the new population.
4. Go to step 2 and continue.
5. If the end condition is satisfied, stop, and return the best solution in current population else continue.

Representation of Genetic Algorithm technique using block diagram is shown in fig 3.4.

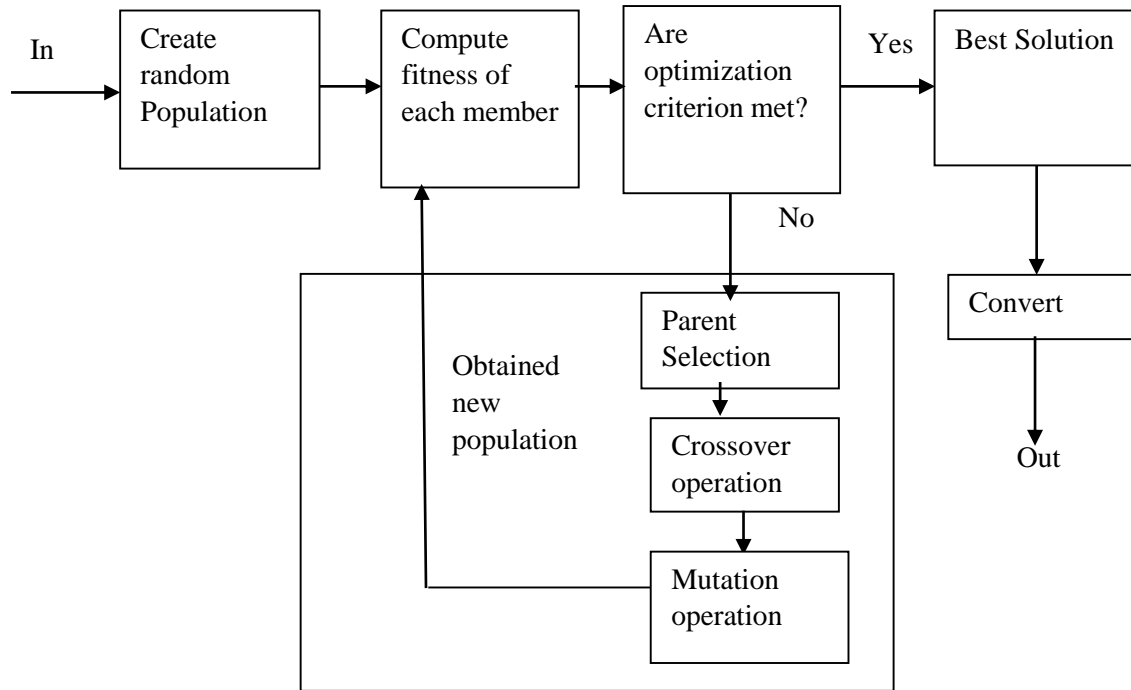


Fig. 3.4 Block Diagram Representation of Genetic Algorithm

### 3.12.1 Genetic Algorithm: Issues

Proper implementation of Genetic Algorithm is required for effective optimization of plant parameters. The following issues are to be considered while optimizing the plant parameters employing Genetic algorithm.

Selection of population size plays a vital role in optimization problems. Generally 20 to 30 chromosomes are considered as the population size. Large population size increases the converging rate while small population leads to premature convergence and leads to the deterioration of performance of GA.

Wrong selection of crossover rates leads to the premature convergence and to avoid it, around 90 percent crossover rate is commonly considered.

Low mutation rate of about 1 percent is usually preferred to get the optimized solution by GA. As discussed earlier, Mutation is a GA operator and is responsible for global search of the solution and it is implemented by altering the numerical value of the chromosome by artificial means from 1 to 0 or vice versa. Larger mutation rate makes the search completely random in nature and problem may not be converged or can trap into local

minima, hence generally avoided. Thus small mutation rates are preferred by the researchers.

During application of genetic algorithms in plant optimization problems, another important problem is in deciding the selection technique for the selection of good population having more fitness value. Roulette wheel and Rank selection techniques are better in compare to other selection techniques.

From the above explanation, it can be concluded that Genetic algorithms (GAs) play a vital role in power system stability applications by optimizing the controller parameters using this technique. Contribution of many researchers have already been highlighted in literature review.

### **3.13 FORMULATION OF AN OBJECTIVE FUNCTION**

In all the swarm optimization techniques discussed above, need the formulation of an objective function which is based on the optimization parameters. It is a mathematical representation of denoting the relationship between the output and the control variables. The requirement for optimal solution is to minimize the objective function. Generally Integral Time Square Error (ITSE), Integral Time Absolute Error (ITAE) or Integral Square Error (ISE) are considered for the formulation of an objective function.

### **3.14 DISCUSSION**

Correct implementation of a particular AI techniques for optimizing the parameters of Controllers for power system stability is a broad area for research in present scenario of large and complex interconnected power system which is subjected to sudden faults, overloads and other contingencies, since Conventional techniques are not only time consuming but also fails to handle complex systems. Hence swarm intelligent and other evolutionary techniques are being extensively used by many researchers in designing the AI controllers or optimizing the controller parameters for performance enhancement of the power system in real time and for many other applications in various fields as already discussed in literature survey. Every technique has got its own merits and demerits. Hence Synergy of two techniques has been tried for getting better results. Hybrid technique has been implemented in this thesis also for optimization of controller parameters and the

simulations yield good results. Though it is too early to say which technique is the best but the 21<sup>st</sup> century will certainly see a revolution in the control philosophy with a motivation towards intelligent FACTS controllers for the performance enhancement of the existing complex power.

# **CHAPTER 4**

## **STATIC VAR COMPENSATOR FOR PERFORMANCE ENHANCEMENT OF POWER SYSTEM**

### **4.1 INTRODUCTION**

The demand of electricity is increasing day by day due to large interconnected system. To fulfill the demand needs increased transmission capabilities. This causes transmission lines to get overstressed and sometimes go beyond thermal limits and subsequently get damaged. But laying of new transmission lines is not an easy task due to financial and environmental constraints. Also due to the inclusion of modern excitation system, use of high rating machines and long transmission lines, modern power system faces various stability issues like Steady State stability, Dynamic stability & Transient stability. Various efforts have been put on for the enhancement of these stabilities as they are major concerns in the modern power system. Hence need of flexible AC transmission system (FACTS) devices to be installed for better utilization of existing transmission lines. Many constraints like voltage stability, transient stability and small signal stability restricts the power transmission in an integrated power system. By installing the FACTS devices, the burden on the transmission line is reduced, increased loadability, enhancement of power system stability, improvement in voltage profile, low system losses and thus leads to provide secure and stable power system network. Static VAR compensator (SVC), one of the oldest member of the FACTS devices plays an important role in overcoming these shortcomings. Installation of SVC leads to voltage enhancement and increases the tolerance limit of the voltage, effective damping of power system oscillations and thus overcome the stability issues in the power system network.

However, for the performance enhancement of the power system, design of effective SVC controller is required. To predict the performance behavior of SVC controller, the exact knowledge of the system and its accurate modeling is required under any contingencies or under abnormal conditions. In the literature, the SVC and system models reported vary from the most simplistic representation of both AC system and SVC [10, 79] to detailed representation of generator, network and SVC [\[25\]](#).

In the present chapter, initially study is being carried out with Multi Machine system with SVC and with coordinated control of both SVC and TCSC controllers for voltage stability, dynamic stability and Transient stability enhancement. The system is modelled in PSAT i.e. power system analysis toolbox and finally a detailed linearized system model [4] is developed for the study system consisting of a generator supplying power to an infinite bus over a long distance double circuit transmission lines. The SVC is located at the generator bus. An auxiliary signal to SVC Controller is incorporated in the system model to study the damping effect and overall performance enhancement of power system. Various swarm intelligent techniques like Particle Swarm Optimization and its variants, Bacterial Foraging Optimization and Hybrid BFO-Particle Swarm Optimization along with Genetic Algorithm, an evolutionary technique are implemented for optimizing various parameters of controller for better stability enhancement of the power system network. AI based auxiliary SVC controller found to be better than the conventionally tuned controller. Hybrid technique found to be the most effective technique.

## 4.2 SYSTEM MODEL -1

### 4.2.1 System Description

Three generator with nine bus system is considered for case study as depicted in fig. 4.1. The parameters of the system are given in appendix A.

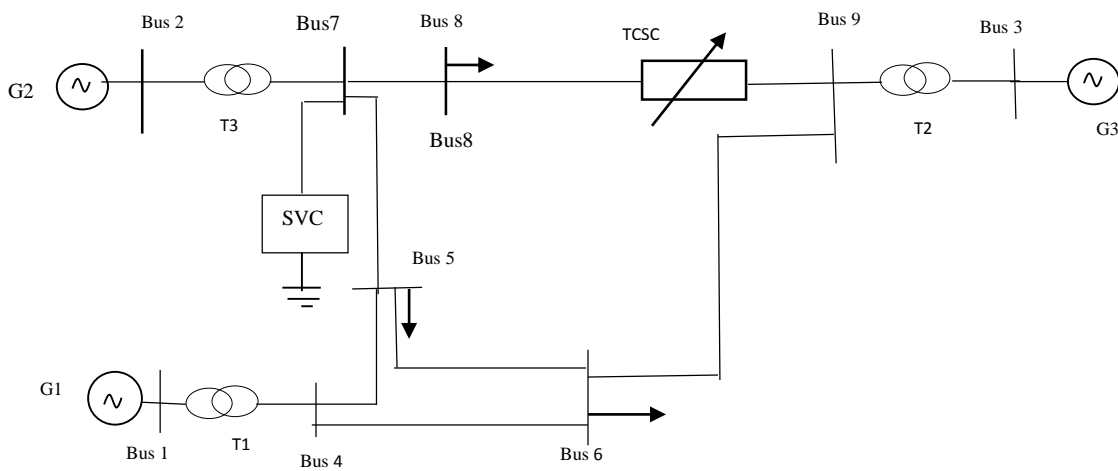


Fig. 4.1 Single line diagram of multi machine bus system with both SVC and TCSC controller

### 4.2.2 SVC Controller

The following configuration is used for representing the SVC controller. The nonlinear relationship between  $B$  and  $\sigma$  has been ignored. The lead lag terms are taken as zero. The parameters of controller are given in appendix A.

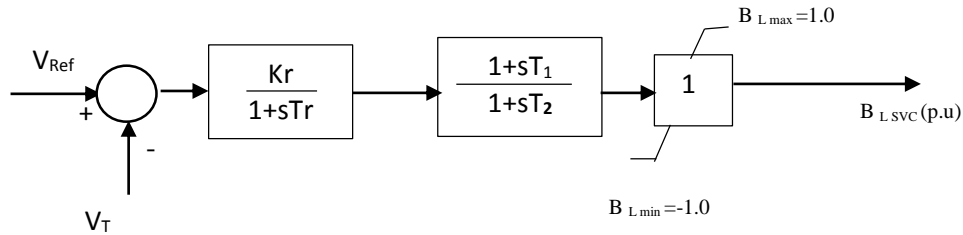


Fig. 4.2 Representation of SVC controller

### 4.2.3 TCSC Controller

The following configuration is used for representing the TCSC controller. The parameters of controller are given in appendix A.

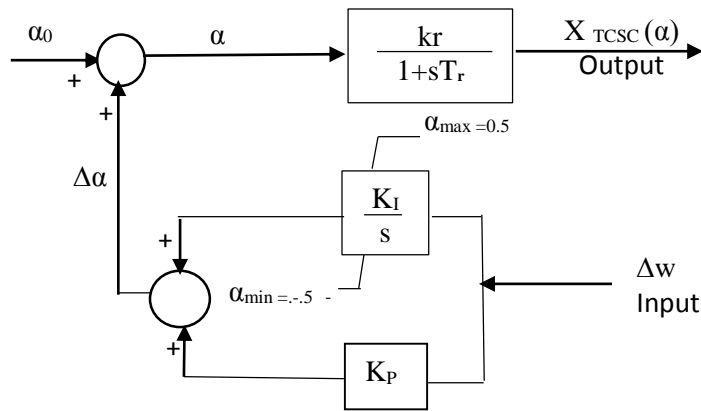


Fig. 4.3 Representation of TCSC controller

### 4.2.4 Simulation Results

**Case 1:** The computer simulations are carried out with and without SVC controller at all buses and observed that buses 5 and 6 needs voltage support, thus SVC was placed at bus number 5 for analyzing the voltage stability and dynamic stability of the multi-machine system. The results shown in fig. 4.4 and 4.5 reveal that SVC provide the necessary reactive power compensation and enhances the voltage stability margin of all buses and improve the voltage profile of bus number 5 and 6 respectively.

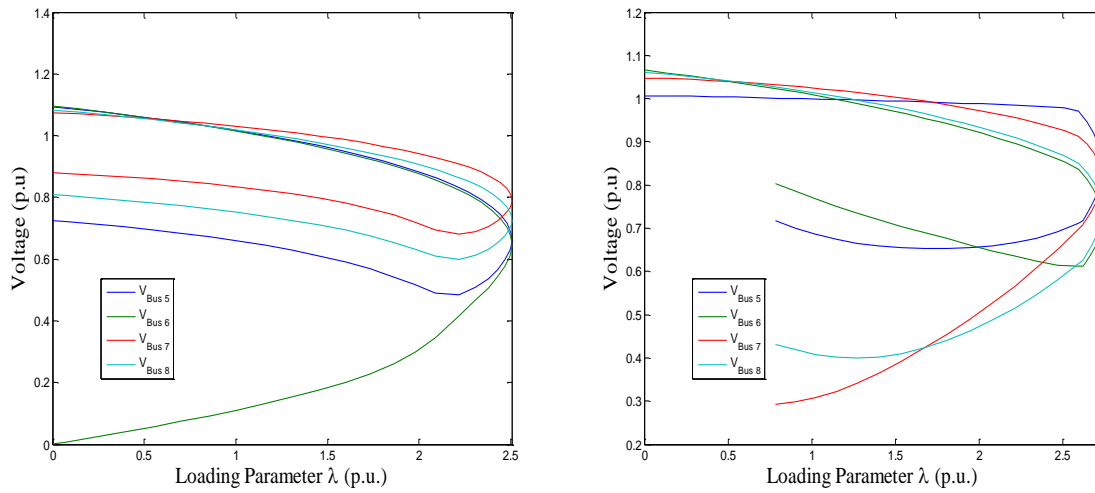


Fig. 4.4 Voltage stability margin without and with SVC Controller at bus number 5

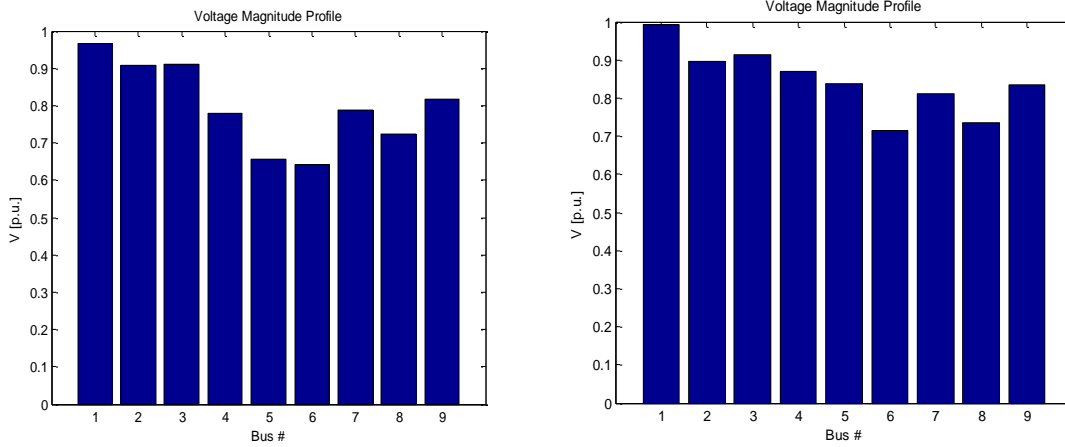


Fig.4.5 Voltage Magnitude Profile without and with SVC Controller connected at bus 5

**Table 1:** Comparison of Eigen Value Report with and without SVC Controller.

STATISTICS	Without SVC Controller	With SVC Controller
Dynamic Order	24	25
Negative Eigen	22	23
Positive Eigen	0	0
Real Eigen	10	9
Complex Pair	7	8
Zero Eigen	2	2



**Table 2:** Eigen values of the system with or without SVC controller

Without SVC controller	With SVC controller
-1000+j0	-1000±j0
-1000+j0	-1000±j0
-1000+j0	-1000±j0
-1.1453 ±j11.0007	-1.0465 ±j11.077
-0.34491±j 6.0299	-5.2036 ±j7.8055
-5.2864±j7.9172	-5.2929±j7.9201
-5.2537±j7.8774	-0.28999 ±j6.0723
-5.1083 ±j 5.1661	-5.1058±j5.1596
-3.6364 ±j0	-3.818 ±j 0
-2.8435 ±j0	-2.2951±j0
-0.62695±j.77896	-0.83231 ±j1.1351
-0.53311 ±j.57136	-0.56149 ±j0.65773
-0.56242±j. 65528	-0.52102 ±j0.56282
0±j0	0±j0
-3.2258±j0	-3.2258 ±j0
-----	-0.5137 ±j0

**Case 2:** The transient stability analysis is carried out by creating three phase fault at bus number 6 for 0.2 sec and with SVC controller connected at bus number 7. Inter area mode of oscillations and machine power oscillations are investigated with and without SVC controller. The Simulation results justify that SVC controller is effective in mitigating the power system oscillations as depicted in fig. 4.6.1 to 4.6.6.

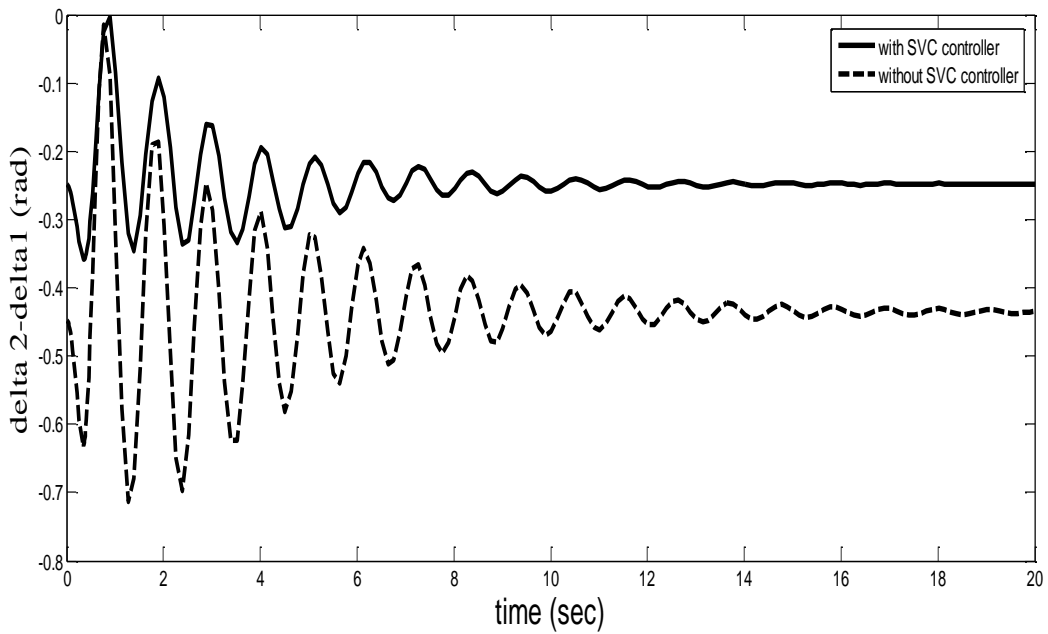


Fig 4.6.1 Inter area mode of oscillation with and without SVC controller (delta 2-delta1)

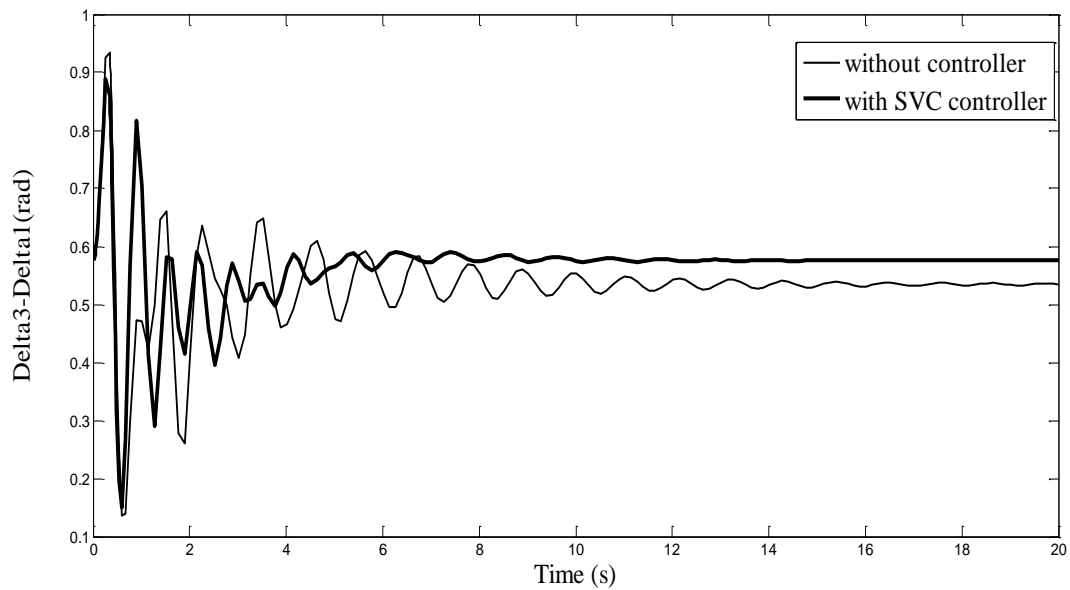


Fig. 4.6.2 Inter area mode of oscillation with and without SVC controller (delta 3-delta1)

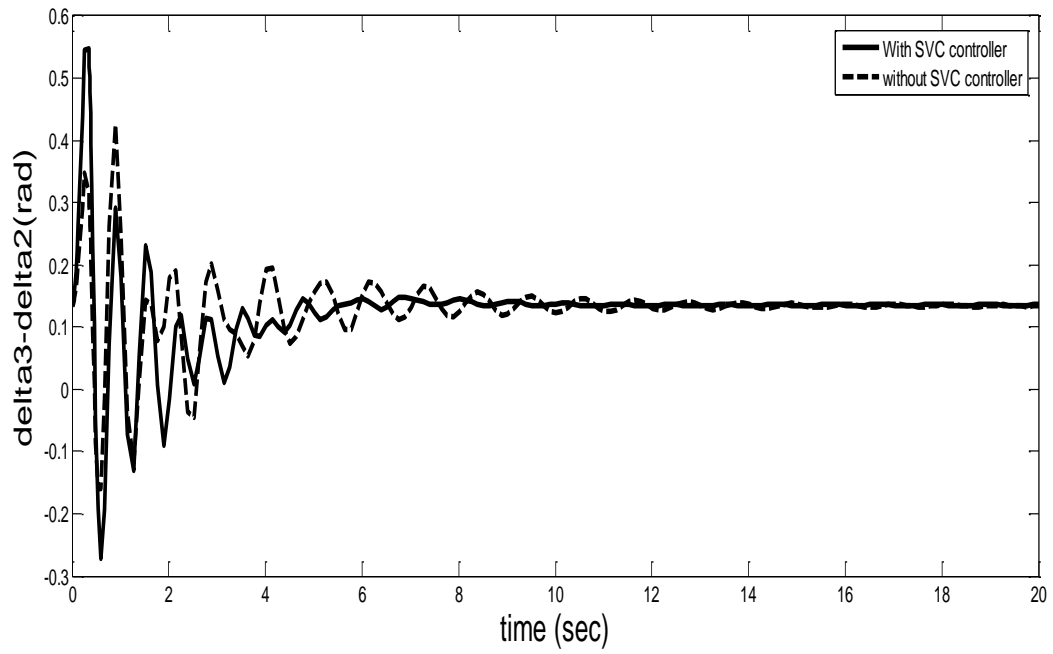


Fig. 4.6.3 Intra area mode of oscillation with and without SVC controller ( $\delta_3 - \delta_2$ )

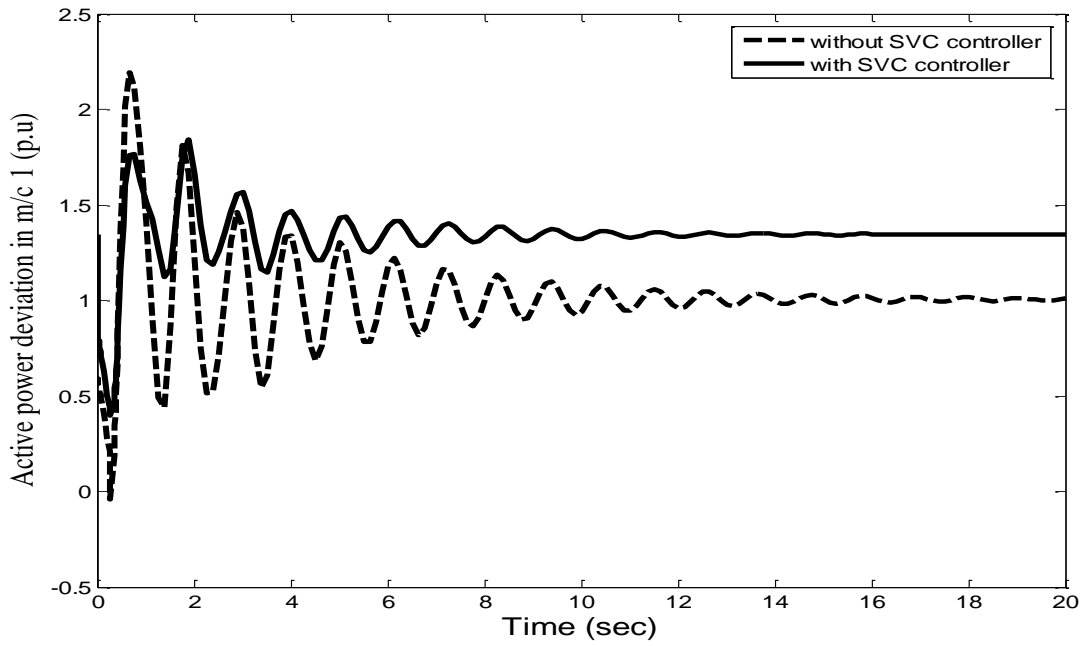


Fig.4.6.4 Deviation in active power in machine1 with and without SVC controller

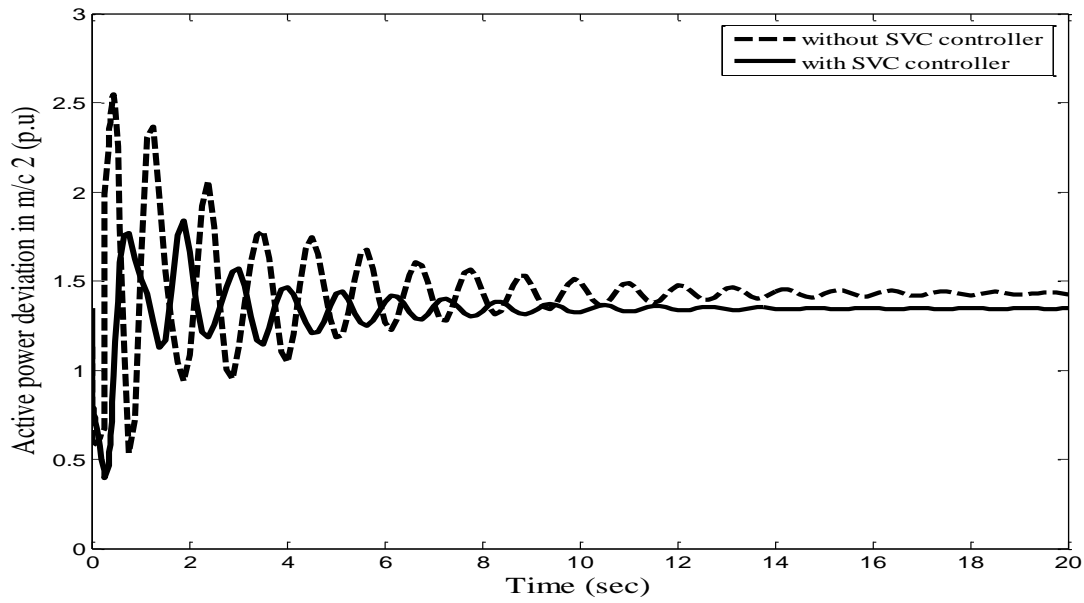


Fig. 4.6.5 Deviation in active power in machine2 with and without SVC controller

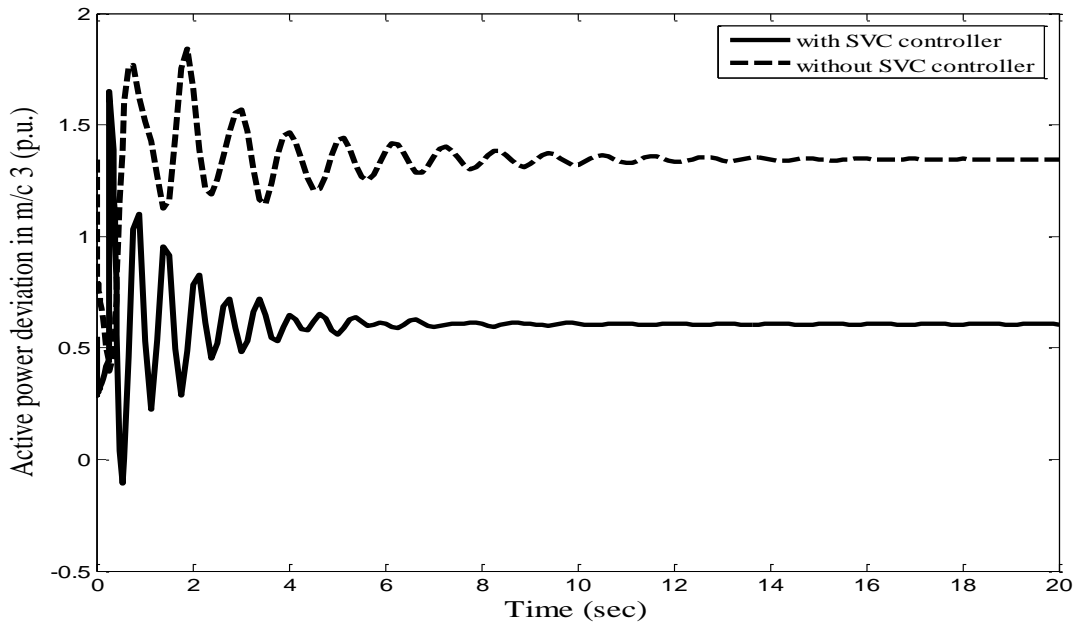


Fig. 4.6.6 Deviation in active power in machine3 with and without SVC controller

**Case 3:** The transient stability is further analyzed by the coordination control of two FACTS controllers (SVC and TCSC). SVC controller is connected at bus number 7 and TCSC controller between buses 8 and 9. The effectiveness of the proposed coordination

control scheme is depicted in fig. 4.7.1 to 4.7.3 in damping out the power system oscillations.

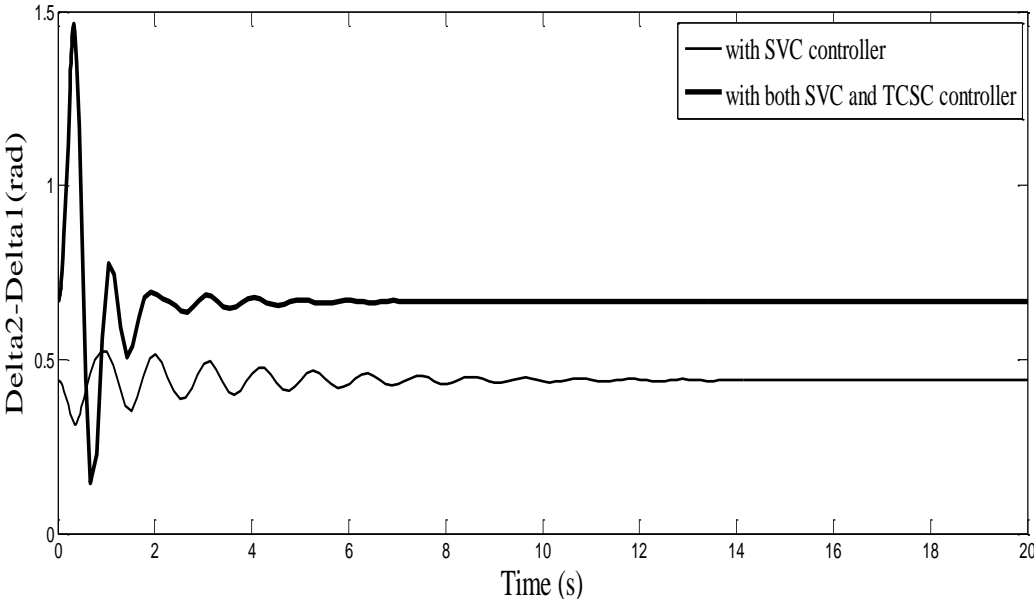


Fig. 4.7.1 Inter area mode of oscillation with SVC controller and with both SVC and TCSC controller (delta 2-delta1)

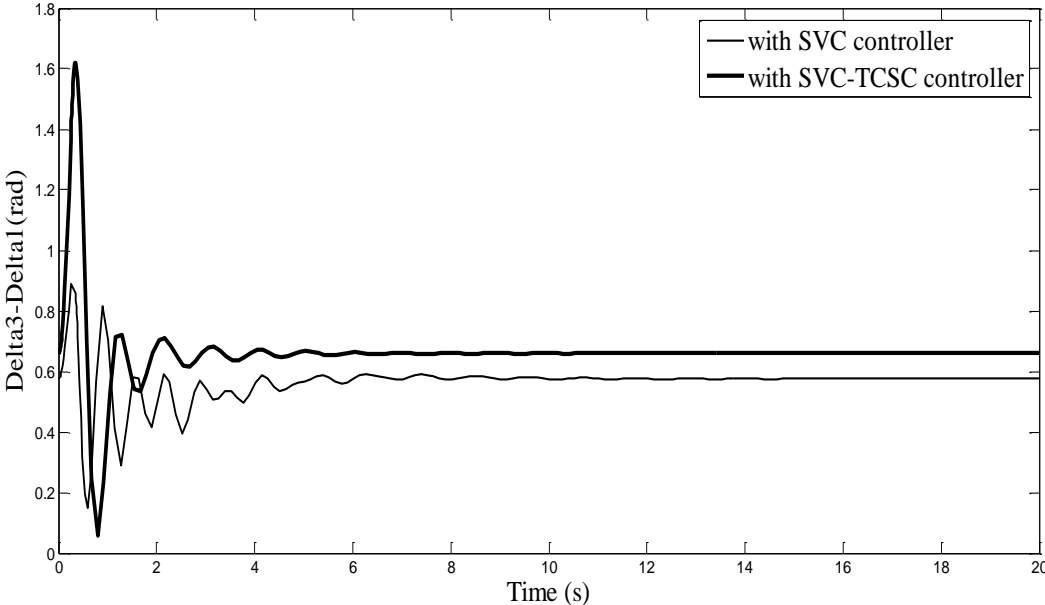


Fig. 4.7.2 Inter area mode of oscillation with SVC controller and with both SVC and TCSC controller (delta 3-delta1)

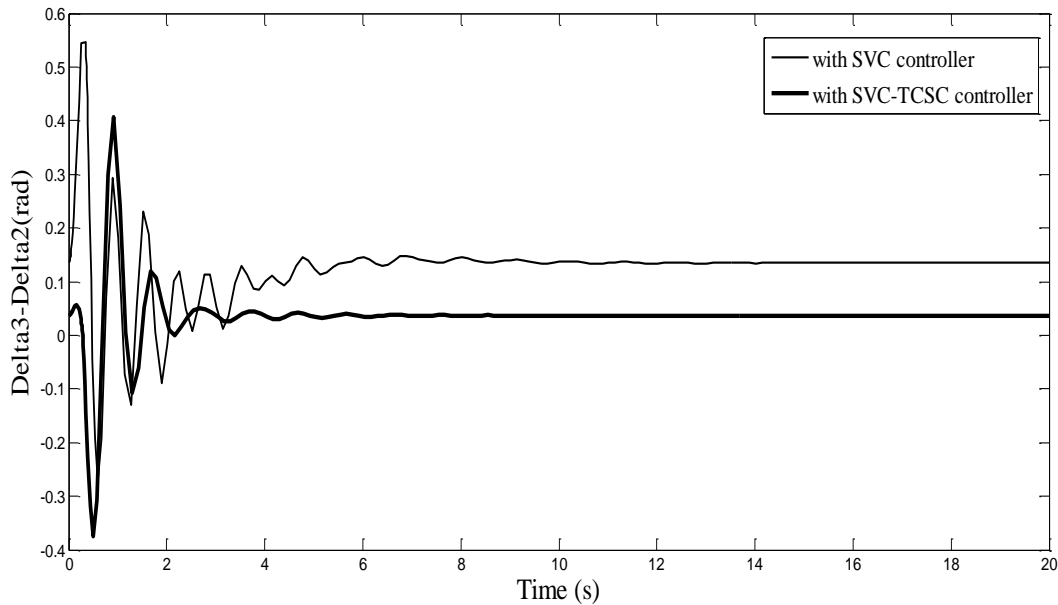


Fig. 4.7.3 Intra area mode of oscillation with SVC controller and with both SVC and TCSC controller (delta 3-delta2)

#### 4.2.5 Discussion

It is observed from the simulation results that buses 5, 6, and 8 are identified as the weakest buses needing MVAR support as depicted from the histogram shown in fig 4.5. SVC is connected at the weakest bus number 5. It is observed from figure 4.4 that by connecting SVC at bus number 5, voltage profile has been improved and the voltage stability margin has been increased. The maximum loading point where the system Jacobin is singular, is at  $\lambda = 2.505$  p.u without SVC controller and with SVC controller, it has been increased. The dynamic stability behavior of the network is analyzed on the basis of Eigenvalue analysis. Table 1 and 2 gives the comparison of Eigenvalue Report with and without SVC controller. For stability of the system, the poles must lie on the left half of the s-plane. It means that all Eigenvalues should either be zero or negative. Though the base case model (without SVC controller) is also stable as indicated in Eigen value analysis but with SVC controller, Eigenvalues are more negative. No Eigenvalue lies in the right hand side of the s-plane as shown in table 2. Hence the system is more stable. The transient analysis is carried out by creating three phase fault at bus number 6. It is observed clearly from figure 4.6.1-4.6.6 that system takes longer time period for the rotor angle and power oscillations to settle

down without any controller but by connecting SVC at bus number 7, these inter area oscillations and power oscillations mitigate quite fast and effectively but by coordination control of SVC and TCSC controllers, these inter area oscillations are damped much faster than that with SVC controller alone as observed in fig.4.7.1 to 4.7.3, thus enhances the transient stability of the power system network. Since system damping factor, D is taken as zero, hence system is taking more time to stabilize.

### 4.3 SYSTEM MODEL-2

#### 4.3.1 System Description

The study system comprises of a generating station supplying bulk power to an infinite bus bar over a long distance transmission line. The generating station is represented by an equivalent synchronous generator and the large power system is represented as an infinite bus. The proposed study system consists of four 555MVA, 24kV, 60 Hz thermal units which are connected to infinite bus system through two parallel transmission lines. The generators are to be modeled as a single equivalent generator. All the parameters of generator are expressed in p.u on 2220 MVA, 24 kV base. The resistance of the transmission line is neglected. A synchronous machine is represented by model 1.1, considering field winding in the d-axis and in q axis, only one damper winding is considered. Also, the armature resistance of the machine is neglected and the excitation system is represented by a single time-constant system.

SVC is located at the generator bus. The single line diagram of the study system is shown in figure 4.8. The SVC is assumed to be of switched capacitor thyristor controlled reactor type configuration. All system parameters are given in Appendix B.

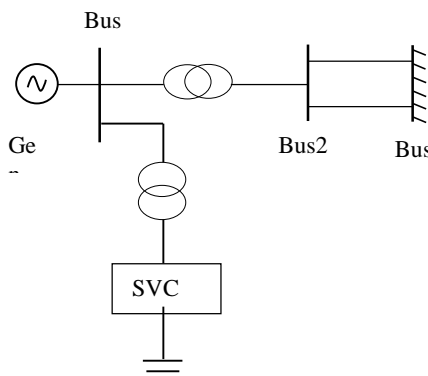


Fig 4.8 Single Machine Infinite bus system connected with SVC controller

### 4.3.2 Generator Model

Stator Equations:

$$v_q = E'_q + x'_d i_d \quad \text{and} \quad v_d = E'_d - x'_q i_q \quad (4.1)$$

Where  $v_d$  and  $v_q$  are defined w. r. t. machine reference frame (Park's reference frame).  $E'_q$  and  $E'_d$  are generator internal voltage behind the machine impedance  $Z_a$ .

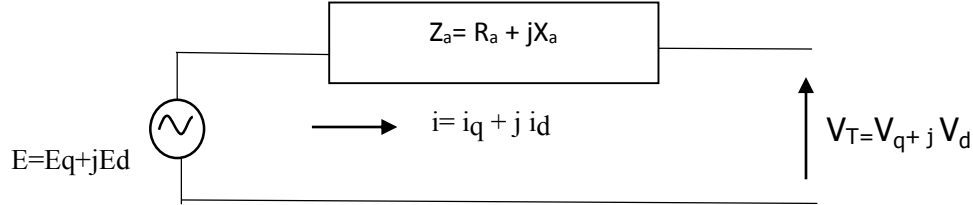


Fig. 4.9 Equivalent circuit of stator of generator

Rotor Mechanical Equations:

$$\frac{d\delta}{dt} = w_B (w - 1) \quad (4.2)$$

According to Swing equation,

$$M \frac{d^2\delta}{dt^2} + D \frac{d\delta}{dt} + K\delta = P_m - P_e \quad (4.3)$$

Where  $\delta$ =rotor angle of synchronous generator,  $K$ =spring constant=0,  $D$ =damping

Mechanical power is related to rotor mechanical torque, hence  $P_m \cong T_m$

Electrical power is related to electrical torque, so  $P_e \cong T_e$

Let  $p = \frac{d}{dt}$  and since  $p\delta = w$

Therefore, Equation (3) is represented as

$$pw = \frac{1}{M} [T_m - T_e - Dw] \quad (4.4)$$

Where

$$T_e = -(x'_q - x'_d) i_q i_d + E'_q i_q \quad (4.5)$$

Field Winding and Excitation Equations:



$$pE'_q = \frac{1}{T_{do}} [E_{fd} - E'_q + (x_d - x'_d) i_d] \quad (4.6)$$

Where  $E_{fd}$  = d-axis field excitation voltage

$$pE_{fd} = \frac{(K_E (V_{Ref} - V_T)) - E_{fd}}{T_E} \quad (4.7)$$

Where  $V_T$  is generator terminal voltage,  $K_E$  and  $T_E$  are excitation gain regulator and excitation time constant respectively.

Equations for SMIB system are computed by considering the following figure:

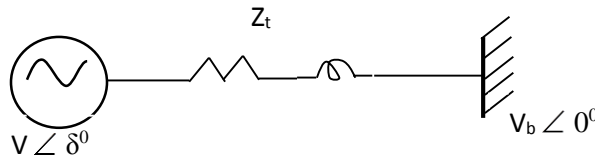


Fig. 4.10 Generator connected to infinite bus-bar through transmission line

Generator, G is connected to infinite bus through long transmission line having resistance  $R_T$  and reactance  $X_T$ .  $R_T$  is assumed to be negligible, hence taken as zero.

Voltage Equation can be written as

$$V \angle \delta = I(0 + jx_T) \angle \delta + V_b \angle 0^\circ \quad (4.8)$$

In d-q frame of reference,

$$(v_q + jv_d) \angle \delta = (i_q + j i_d) (jx_T) \angle \delta + V_b \angle 0 \quad (4.9)$$

$$(v_q + jv_d) = (i_q + j i_d) (jx_T) + V_b \angle -\delta \quad (4.10)$$

$$v_q = V_b \cos \delta - x_T i_d \quad \text{and} \quad v_d = x_T i_q - V_b \sin \delta \quad (4.11)$$

On equating equations 4.1 and 4.11,

$$V_b \cos \delta - x_T i_d = x'_d i_d + E'_q \quad (4.12)$$

$$x_T i_q - E_b \sin \delta = -x_q i_q \quad (4.13)$$

$$\begin{bmatrix} x_T + x_d' & \dots & 0 \\ 0 & \dots & -(x_T + x_q') \end{bmatrix} \begin{bmatrix} i_d \\ i_q \end{bmatrix} = \begin{bmatrix} V_b \cos \delta - E_q' \\ -V_b \sin \delta \end{bmatrix} \quad (4.14)$$

$$i_d = \frac{1}{x_d' + x_T} [(E_b \cos \delta - E_q')] \quad (4.15)$$

$$i_q = \frac{1}{x_q' + x_T} [E_b \sin \delta] \quad (4.16)$$

### 4.3.3 Linearized Model

The linearized model is obtained by linearizing the above nonlinear equations and algebraic equations around an operating point. Linearized current equations are:

$$\Delta i_d = a_1 \Delta \delta + a_2 \Delta E_q' \quad \Delta i_q = a_3 \Delta \delta + a_4 \Delta E_q' \quad (4.17)$$

$$a_1 = \frac{1}{x_d' + x_T} [- (V_b \sin \delta_0)] \quad a_2 = - \frac{1}{(x_d' + x_T)} \quad (4.18)$$

$$a_3 = \left[ \frac{E_b \cos \delta_0}{(x_q' + x_T)} \right], \quad a_4 = 0 \quad (4.19)$$

Linearized voltage equations are:

$$\begin{aligned} \Delta v_q &= \Delta i_d x_d' + \Delta E_q' \\ \Delta v_d &= -x_q \Delta i_q + \Delta E_d' \end{aligned} \quad (4.20)$$

On putting the values of  $\Delta i_d$  and  $\Delta i_q$ , voltage equations are represented as:

$$\begin{aligned} \Delta v_q &= x_d' a_1 \Delta \delta + (1 + a_2 x_d') \Delta E_q' \\ \Delta v_d &= \Delta E_d' - x_q a_4 \Delta E_q' - x_q a_3 \Delta \delta \end{aligned} \quad (4.21)$$

Linearized rotor equations are:

$$p \Delta \delta = w_B \Delta w \quad (4.22)$$

$$p \Delta w = \frac{1}{M} [- D \Delta w + \Delta T_m - \Delta T_e] \quad (4.23)$$

$$\Delta T_e = [\Delta E'_{q0} - (x'_q - x'_d)j_{d0}] \Delta i_q - (x'_q - x'_d)j_{q0} \Delta i_d + i_{q0} \Delta E'_q$$

$$\Delta T_e = K_2 \Delta E'_q + K_1 \Delta \delta \quad (4.24)$$

$$\text{where.....} K_1 = \{E'_{q0} a_4 + i_{q0} - (x'_q - x'_d)j_{q0} a_2\} a_3 - ((x'_q - x'_d)j_{q0} a_1$$

$$K_2 = i_{q0} + E'_{q0} a_4 - (x'_q - x'_d)j_{q0} a_2 \quad (4.25)$$

Linearized field winding equations are:

$$p \Delta E'_q = \frac{1}{T'_{do}} [\Delta E_{fd} + (x_d - x'_d) \Delta i_d - \Delta E'_q] \quad (4.26)$$

On putting the value of  $\Delta i_d$  in above equation and taking Laplace Transform, we have

$$[1 + sT'_{do} K_3] \Delta E'_q = K_3 \Delta E_{fd} - K_3 K_4 \Delta \delta$$

$$\text{where.....} K_3 = \frac{1}{[1 - (x_d - x'_d) a_2]} \quad (4.27)$$

$$K_4 = -(x_d - x'_d) a_1$$

On linearizing the generator terminal voltage,

$$v_T = v_q + jv_d$$

$$\Delta v_T = \frac{v_{q0}}{v_{T0}} \Delta v_q + \frac{v_{d0}}{v_{T0}} \Delta v_d \quad (4.28)$$

On putting the values of  $\Delta v_q$  and  $\Delta v_d$  in above equation, we have

$$\Delta v_T = K_5 \Delta \delta + K_6 \Delta E'_q \quad (4.29)$$

$$K_5 = \left( \frac{v_{q0}}{v_{T0}} \right) x'_d a_1 - \left( \frac{v_{d0}}{v_{T0}} \right) x'_q a_3 \quad (4.30)$$

$$K_6 = \left( \frac{v_{q0}}{v_{T0}} \right) (1 + x'_d a_2) - \left( \frac{v_{d0}}{v_{T0}} \right) x'_q a_4 \quad (4.31)$$

#### 4.3.4 Linearized Model of SMIB System

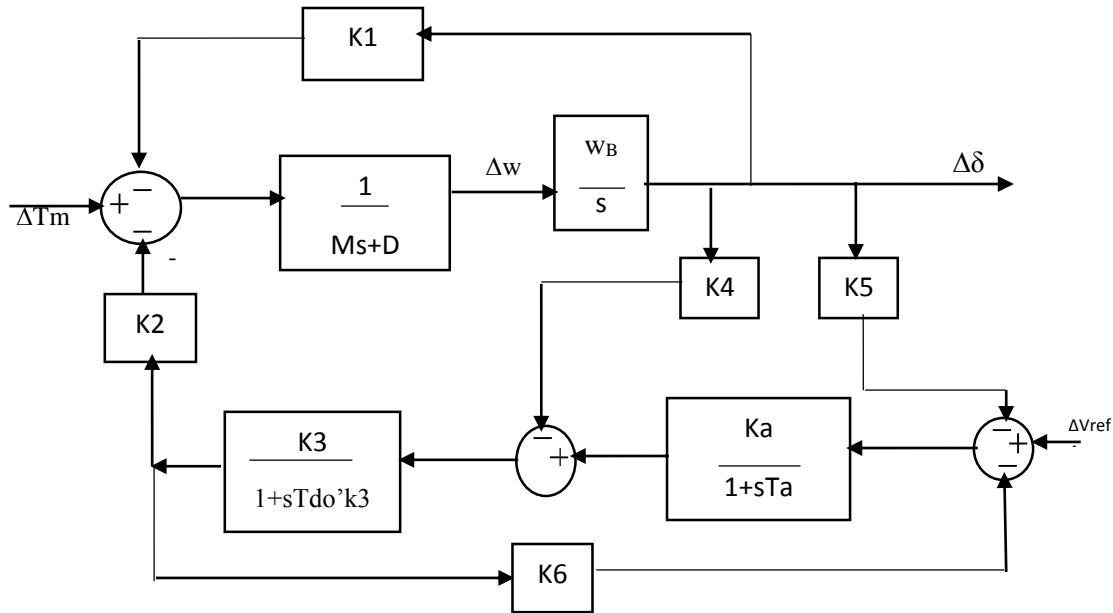


Fig. 4.11 Linearized model of SMIB system

#### 4.3.5 Modeling of SVC Controller

The basic CIGRE model of SVC controller [3] consists of a measurement block, voltage regulator block & thyristor susceptance control block for simulation of SVC control loop stability & SVC response time. This model is a fundamental frequency model & suitable for continuous control of SVC. SVC has a reactive/current/susceptance regulator so that SVC can return back to a desired steady state operating point.

In short Stability model of SVC is obtained by developing the mathematical model of each functional block [ku, cigre].

1. TCR (Thyristor Controlled Reactor) block for control of Susceptance
2. Voltage Regulator block
3. Measuring Block

##### Model of TCR block

Thyristor controlled reactor (TCR) comprises of a reactor connected in series with bidirectional thyristor switches which conduct for every alternate half cycle based on firing angle  $\alpha$ .

For  $\alpha=90^\circ$ , thyristor conducts fully.

Current is sinusoidal and reactive in nature.

$90^\circ < \alpha < 180^\circ$ , thyristor conducts partially and for  $0^\circ < \alpha < 90^\circ$  thyristor are not allowed due to production of asymmetrical current.

Let  $\sigma$  be the conduction angle which is related to firing angle  $\alpha$  as

$$\sigma = 2(\pi - \alpha)$$

Instantaneous Current  $i$  is given by

$$i = \begin{cases} \frac{\sqrt{2}V}{X_L} (\cos \alpha - \cos wt) & \text{for } \alpha < wt < \alpha + \sigma \\ 0 & \text{for } \alpha + \sigma < wt < \alpha + \pi \end{cases} \quad (4.32)$$

And the fundamental component of current  $I_f$  can be computed from Fourier analysis as:

$$I_f = \left( \frac{\sigma - \sin \sigma}{\pi} \right) \frac{V}{X_L} \quad (4.33)$$

The effective inductance of the reactor increases on increasing  $\alpha$  (decrease in  $\sigma$ ) due to decrease in current  $I_f$ .

Hence TCR can be considered as a controllable susceptance.

$$B(\alpha) = \frac{I_f}{V} = \frac{\sigma - \sin \sigma}{\pi X_L} = \frac{2(\pi - \alpha) + \sin 2\alpha}{\pi X_L} \quad (4.34)$$

Thus model of TCR block must represent the variation of reactor susceptance which is a function of  $\alpha$ , the firing angle. Since there is a non-linearity between  $B$  and  $\sigma$ , hence also need linearizing circuit to compensate this nonlinear relationship. The CIGRE model showing Thyristor firing delays is being used in this module.

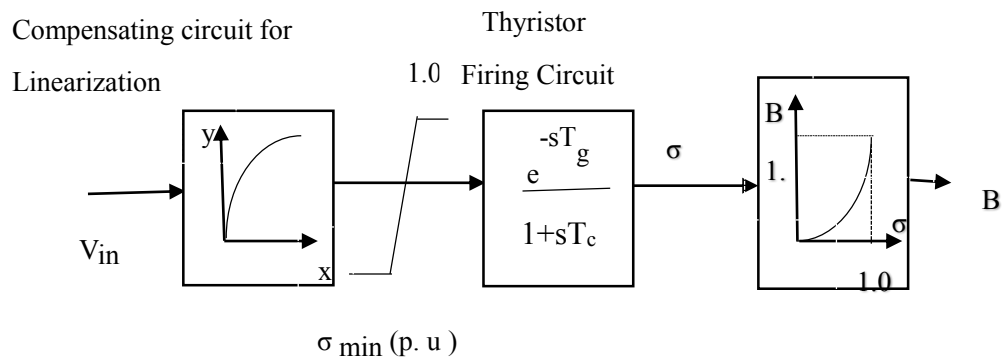


Fig. 4.12 Representation of TCR model

Limiting values of reactive susceptance are determined by limiting values of conduction angle  $\sigma$ .

Typical values of  $B_{LMAX}=1\text{p.u}$  and  $B_{LMIN}=0.02\text{ p.u}$ .  $T_g$  represents the gating transport delay, value of which is 1msec and  $T_c$  is the time constant represents the effect of thyristor firing sequence control, value of which ranges between 3-6msec. For ideal conditions, when nonlinearity is fully compensated,  $T_g$  and  $T_c$  can be omitted.

### Measuring Block

This block comprises of instrument transformer, signal conditioners, A/D converters and rectifiers. Three phase voltage and current are measured from the bus at which SVC is connected and are converted into dc control signals. Thus this block is represented by a single low pass filter having  $T_f$  as time constant whose value ranges between 1-10msec. It can be represented by the following block diagram.

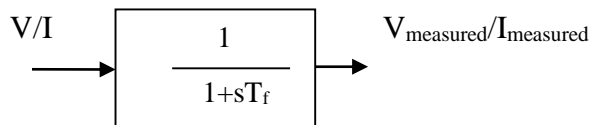


Fig. 4.13 Transfer function representing measuring block

### Voltage Regulator Block

It is basically a proportional type regulator where  $K_a$  is the gain of the regulator & is reciprocal of the slope setting of SVC & which can be set between 5% & 1% on the SVC base.  $T_a$  is the regulator time constant which is taken between 20 & 150 ms. PI controller is being used in some voltage regulator circuit to provide fast response and when high gain is required lead lag compensator followed by AVR block. Here  $T_1$  and  $T_2$  parameters of lead lag compensator are taken as zero. The generic AVR control block is defined by the transfer function:

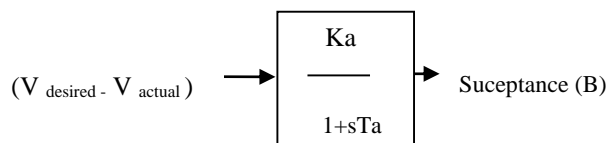


Fig. 4.14 Transfer function representing voltage regulator

### Dynamic Model of SVC

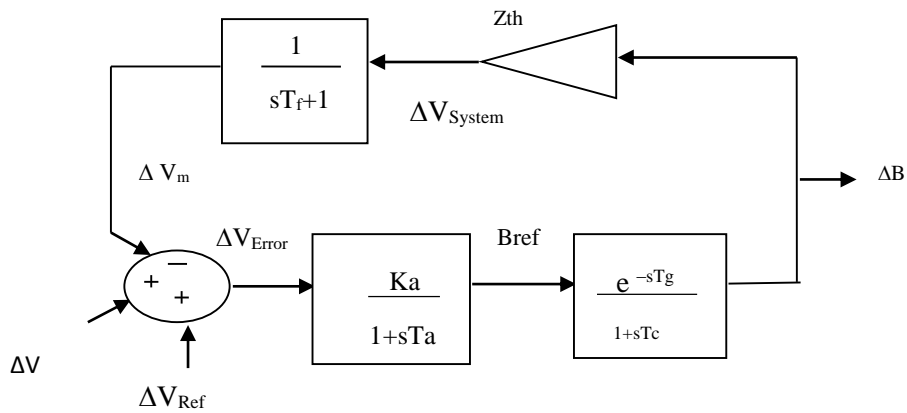


Fig. 4.15 Representation of SVC controller using different modules

### 4.3.6 Auxiliary SVC Controller

An auxiliary signal from PID fed to SVC controller introduces an additional damping in the system and damps the rotor mechanical low frequency oscillations quickly. They are placed in the supplementary control signal of SVC.

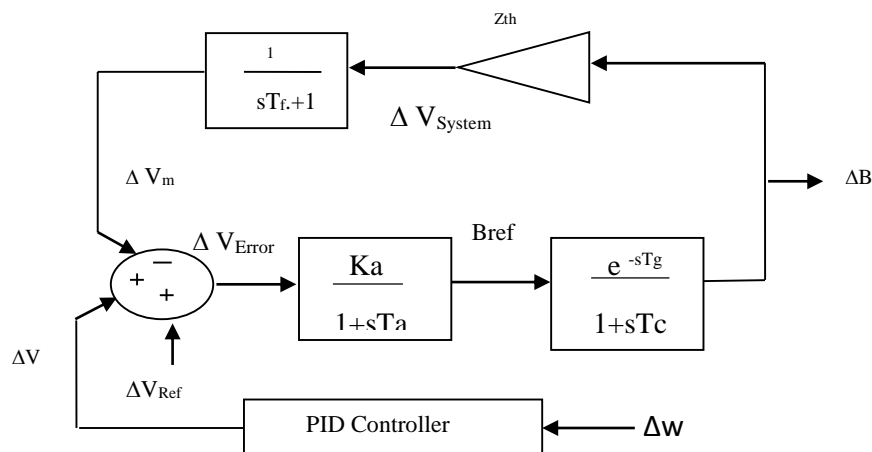


Fig. 4.16 SVC controller with auxiliary signal

### 4.3.7 Linearized Model of SMIB System with auxiliary SVC Controller

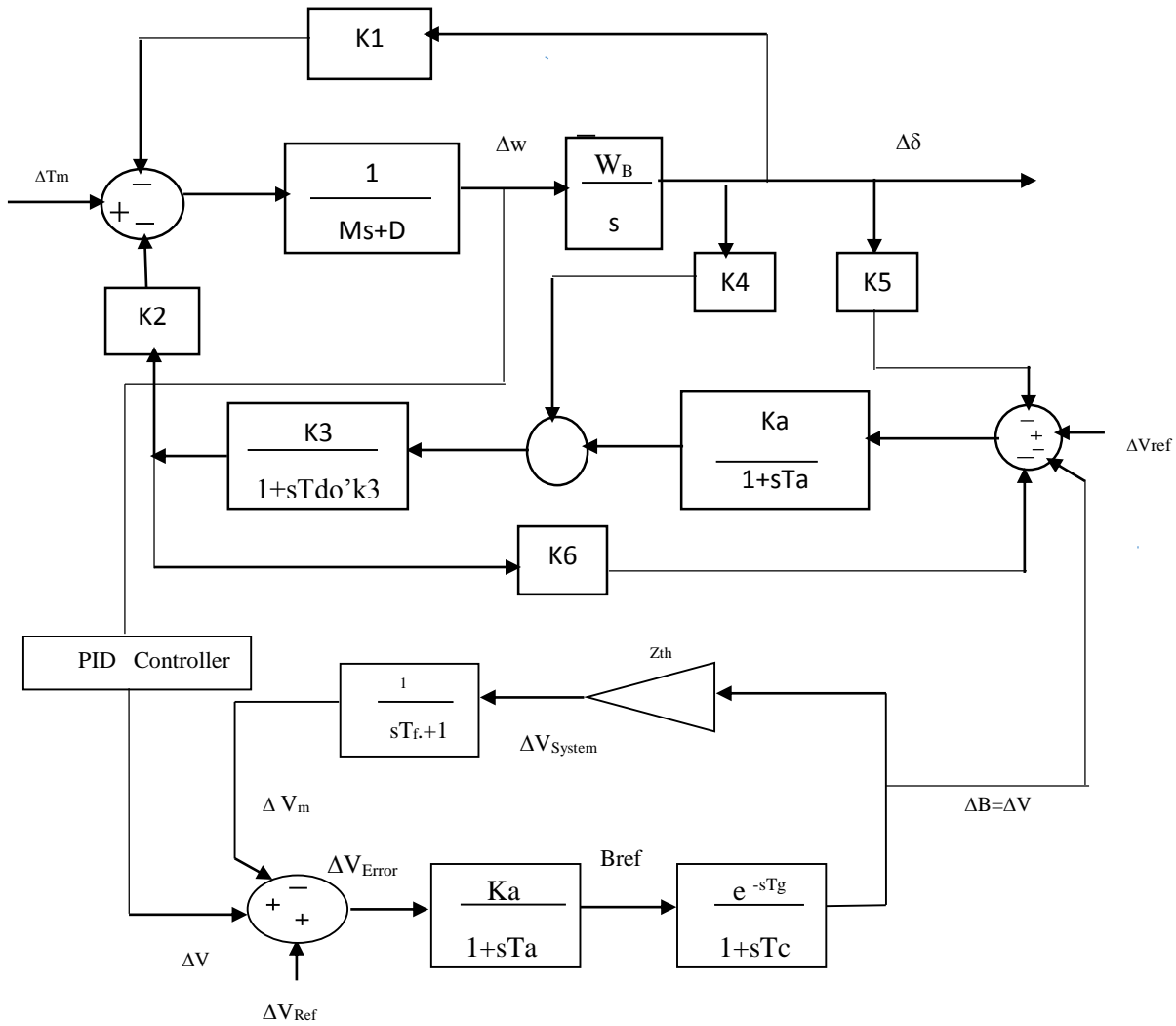


Fig. 4.17 SMIB system with auxiliary SVC controller

### 4.4 SIMULATIONS

A small perturbation of 10% in mechanical input power is then given to examine the steady state stability. Parameters of PID Controller are optimized using Ziegler Nichols method, a conventional technique for optimizing the controller parameters. But this technique has slow convergence rate and may likely to trap into local minima. Hence alternative techniques have been explored for design of controllers and for optimizing their parameters.



## 4.6 IMPLEMENTATION OF SWARM INTELLIGENCE TECHNIQUES FOR OPTIMIZATION OF PARAMETERS OF AUXILIARY SVC CONTROLLER

Various Swarm intelligence algorithms explained in chapter (3) have been investigated for managing the in-built issues of power system. Here steady state stability in power system issue has been considered. Various Swarm intelligence techniques applied are:

1. Particle Swarm Optimization and its variants.
2. Bacterial Foraging Optimization.
3. Genetic Algorithm
4. Hybrid BF-PSO optimization

Correct implementation of above algorithm leads to the global search of optimized values of SVC Controller parameters. To achieve this correct implementation, several aspects of the AI techniques have to be designed to this particular problem. First a proper objective function that evaluates the performance has to be defined to get an optimized solution. The optimized parameters obtained from conventional techniques are taken as base values for global search of the optimized values in the d-dimensional search space.

### 4.6.1 Objective Function

It is worth mentioning that the SVC controller is designed to minimize the power system oscillations after a disturbance so as to improve the stability. These oscillations are reflected in the deviations in the generator rotor speed ( $\Delta\omega$ ) and terminal voltage ( $\Delta V$ ). Most of the researchers have taken only deviation in the rotor speed ( $\Delta\omega$ ) as the error function while formulating the objective function. In the present study the objective function  $J$  is formulated as the minimization of:

$$J = \int_0^{t_{Sim}} \left[ t(\Delta\omega(t, x))^2 + t(\Delta V(t, x))^2 \right] dt \quad (4.35)$$

In the above equations,  $\Delta\omega(t, x)$  denotes the rotor speed deviation,  $\Delta V$  denotes the change in generator terminal voltage for a set of controller parameters  $x$  ( $x$  represents the parameters to be optimized;  $k_p$ ,  $k_i$  and  $k_d$  are the parameters of SVC controller), and  $t_{Sim}$  is the time range of the simulation. With the variation of the parameters  $x$ , the  $\Delta\omega(t, x)$  and  $\Delta V(t, x)$  will also be changed. For objective function calculation, the time-domain simulation of the power system model is carried out for the simulation period. It is aimed

to minimize this objective function in order to improve the system response in terms of the settling time and overshoots.

In order to verify the steady state stability analysis, the simulations are carried out using the above control strategies one by one.

#### **4.5.2 Simulation results with PSO and its variant based auxiliary SVC Controller**

Simulation is carried out both in MATLAB coding & MATLAB Simulink by giving small disturbance  $\Delta T_m = 0.1$  p.u. Seven cases have been analyzed:

1. Without SVC Controller.
2. With Conventionally tuned SVC Controller.
3. With basic PSO based SVC Controller.
4. With conventionally tuned auxiliary SVC Controller.
5. With basic PSO based auxiliary SVC Controller.
6. With PSO-Shrinkage Factor Inertia Weight Approach (SFIWA) based auxiliary SVC Controller.
7. With PSO-Time Varying Acceleration Coefficients (TVAC) based auxiliary SVC Controller.

Data of PSO and its variant parameters are given in appendix A.

**Case1:** Regulator parameters  $K_a$  and  $T_a$  of SVC controller are optimized using conventional method. Fig. 4.18.1 to 4.18.3 depict the effectiveness of SVC controller for damping the power system oscillations.

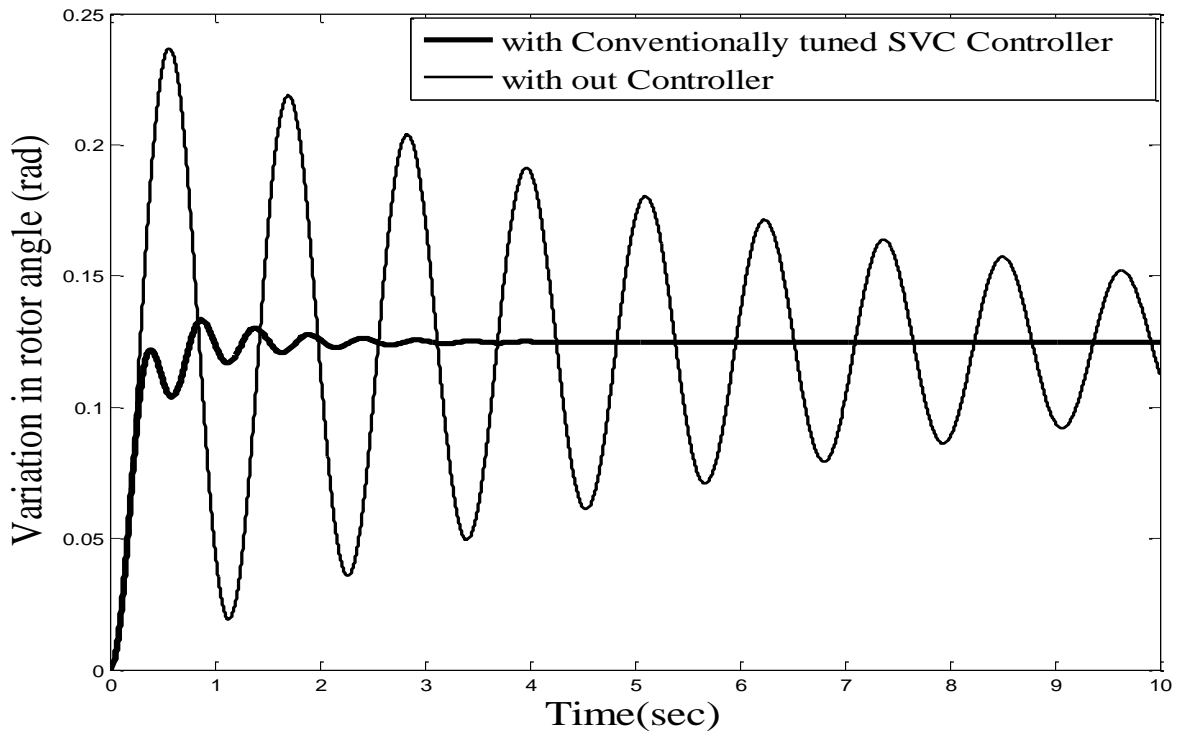


Fig.4.18.1 Time response of rotor angle without and with conventionally tuned SVC controller

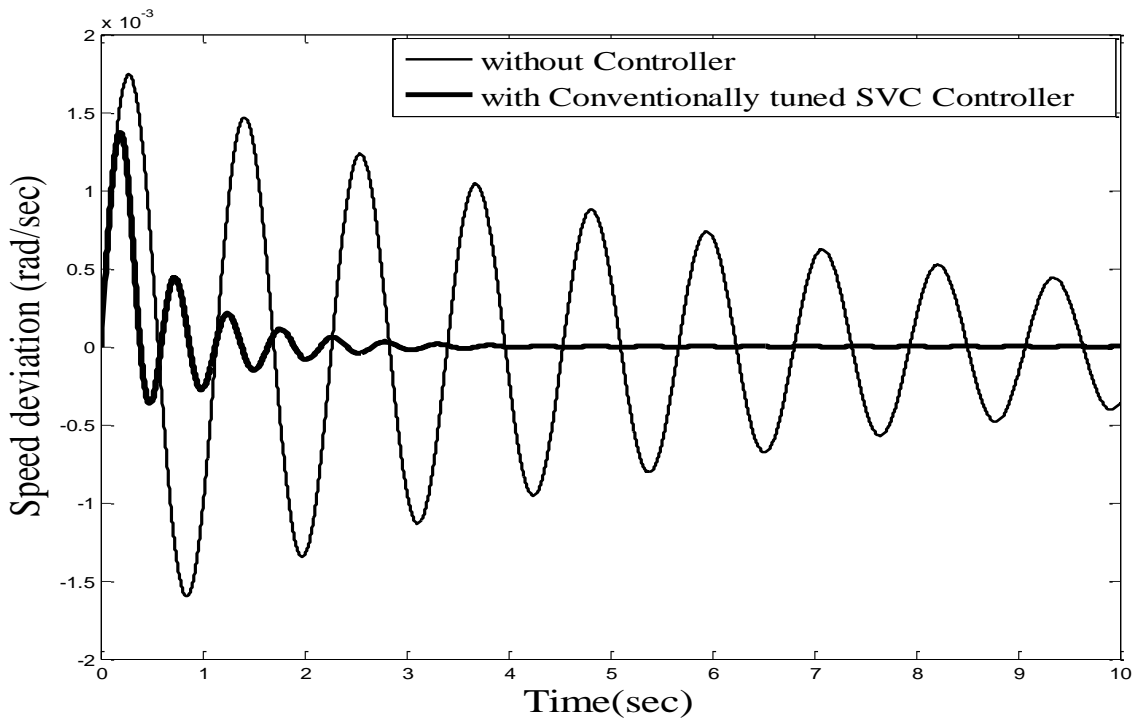


Fig.4.18.2 Time response of speed variation without and with conventionally tuned SVC controller

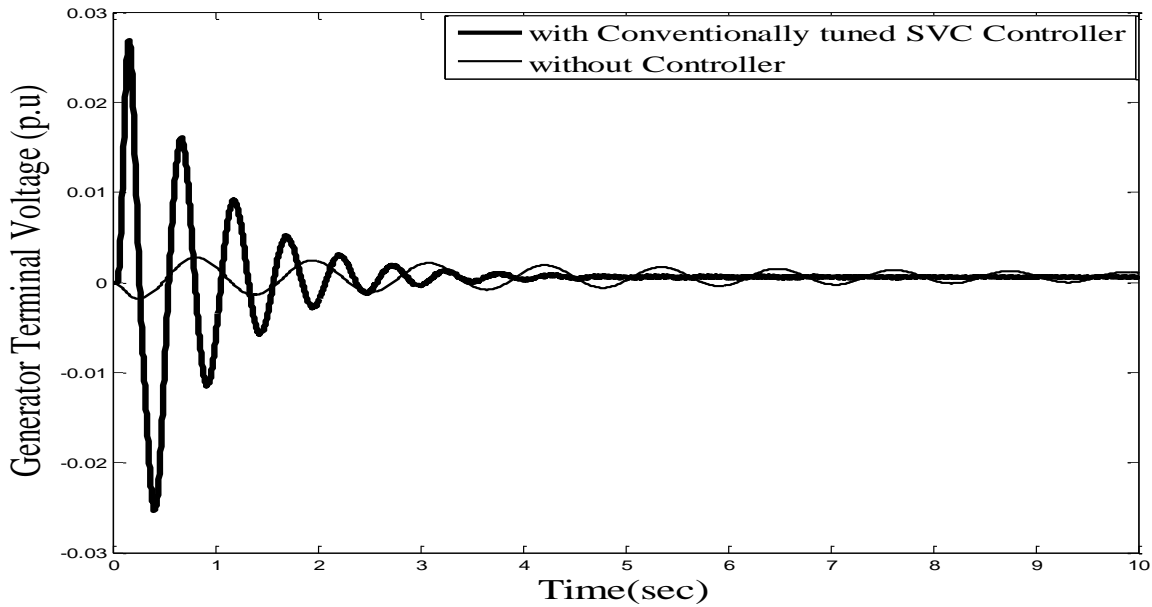


Fig.4.18.3 Time response of variation in generator terminal voltage without and with conventionally tuned SVC controller

**Case 2:** Basic Particle swarm optimization is implemented for optimizing the regulator parameters of SVC controller. The optimizing function as described in equation 4.37 is minimized to get the global minima. PSO based SVC controller is more robust as compare to conventionally tuned SVC controller as depicted in fig. 4.19.1 to 4.19.3. PSO parameters taken are given in appendix A.

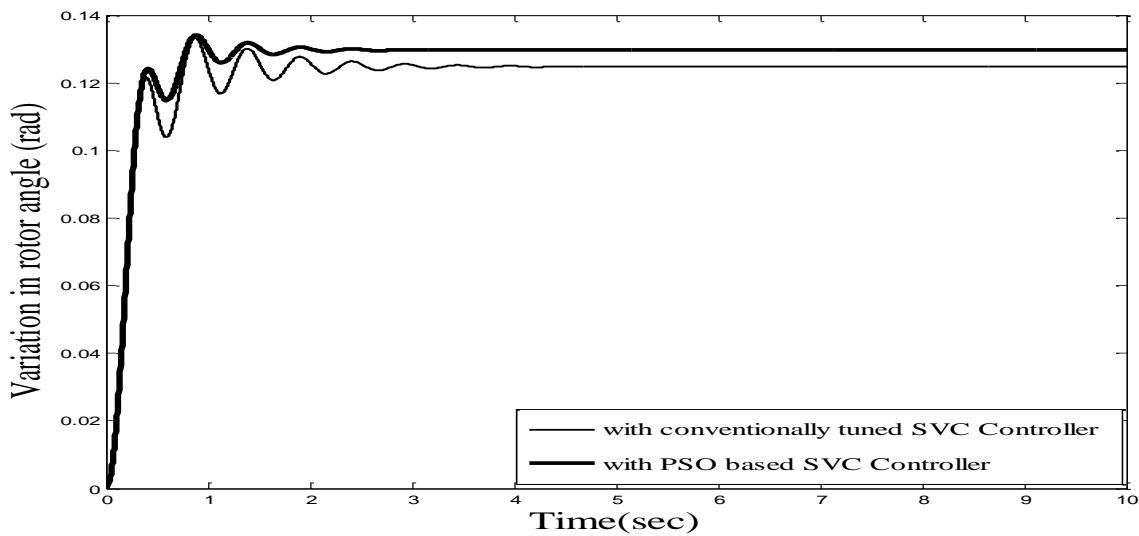


Fig. 4.19.1: Time response of variation in rotor angle with conventionally tuned SVC controller and with PSO based SVC controller

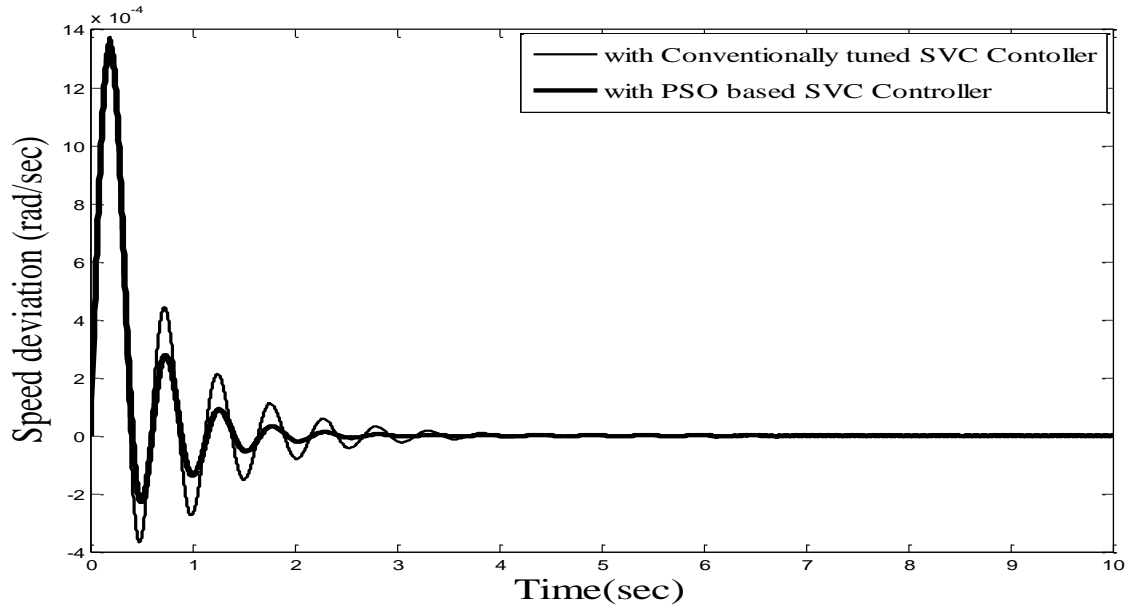


Fig. 4.19.2: Time response of speed deviation with conventionally tuned SVC controller and with PSO based SVC controller

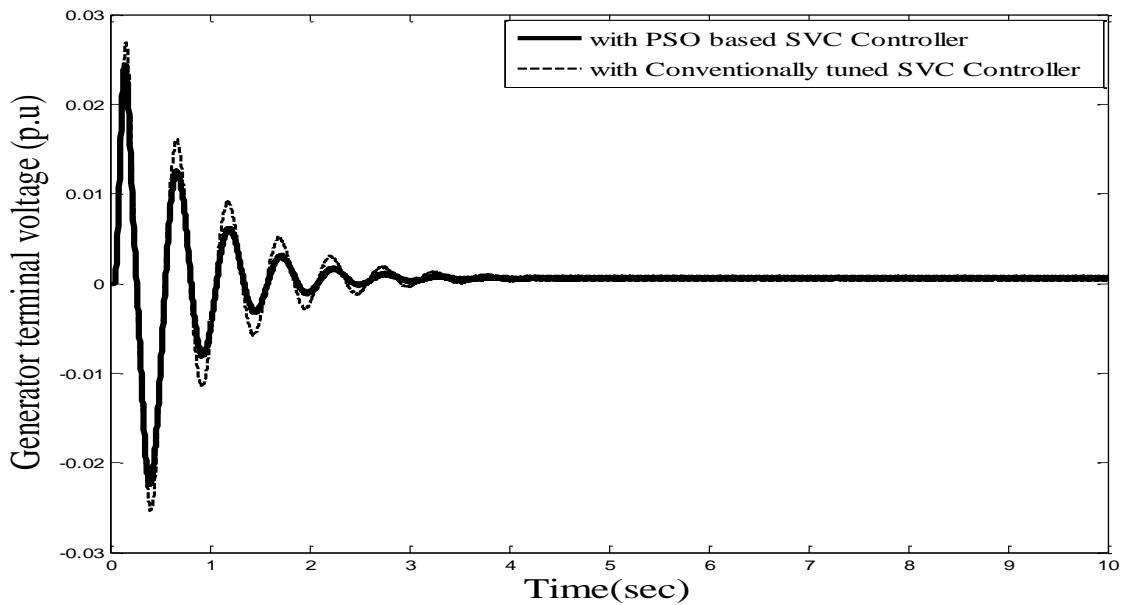


Fig. 4.19.3: Time response of variation in generator terminal voltage with conventionally tuned SVC controller and with PSO based SVC controller

**Case3:** An additional auxiliary signal from PID controller is applied to the supplementary control signal of SVC. Input to the PID controller is the speed deviation. Deviation in terminal voltage or the machine angle can also be taken as the input to the PID controller.

The parameters of this auxiliary controller are then optimized using Ziegler Nichols, a conventional method of optimization for better stability of the power system. Fig. 4.20.1 to 4.20.3 depict the effectiveness of conventionally tuned auxiliary SVC controller over the PSO based SVC controller. All parameters taken are given in appendix A.

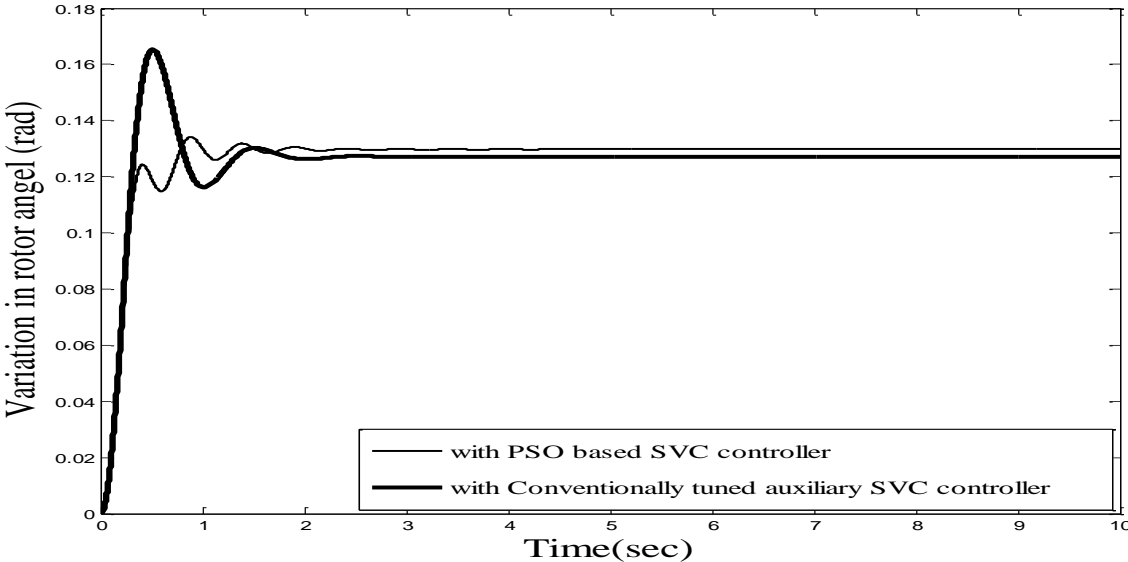


Fig. 4.20.1: Time response of variation in rotor angle with conventionally tuned auxiliary SVC controller and with PSO based SVC controller

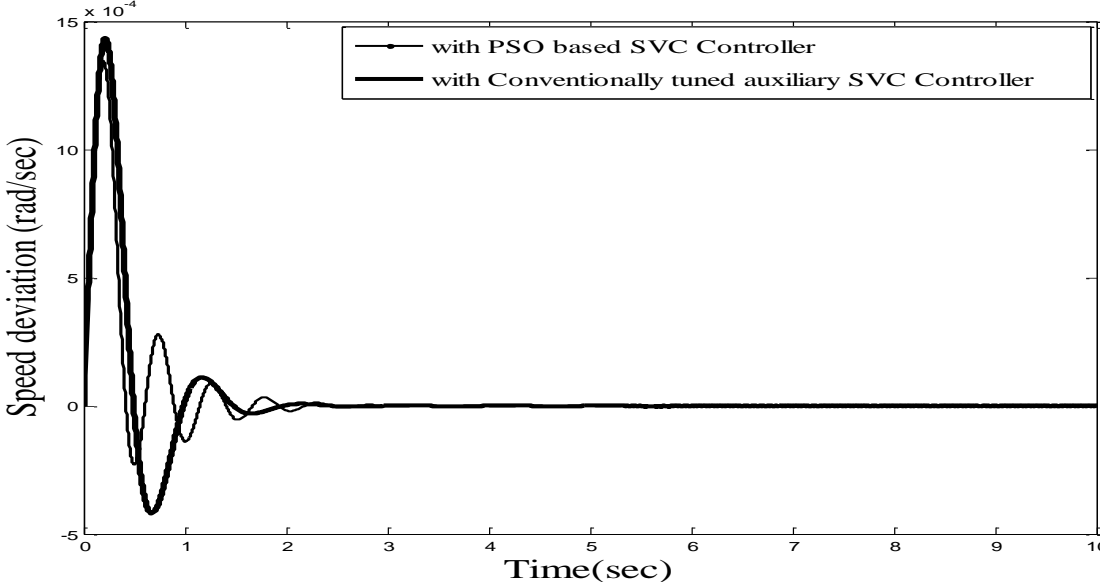


Fig. 4.20.2: Time response of speed deviation with conventionally tuned SVC controller and with PSO based SVC controller

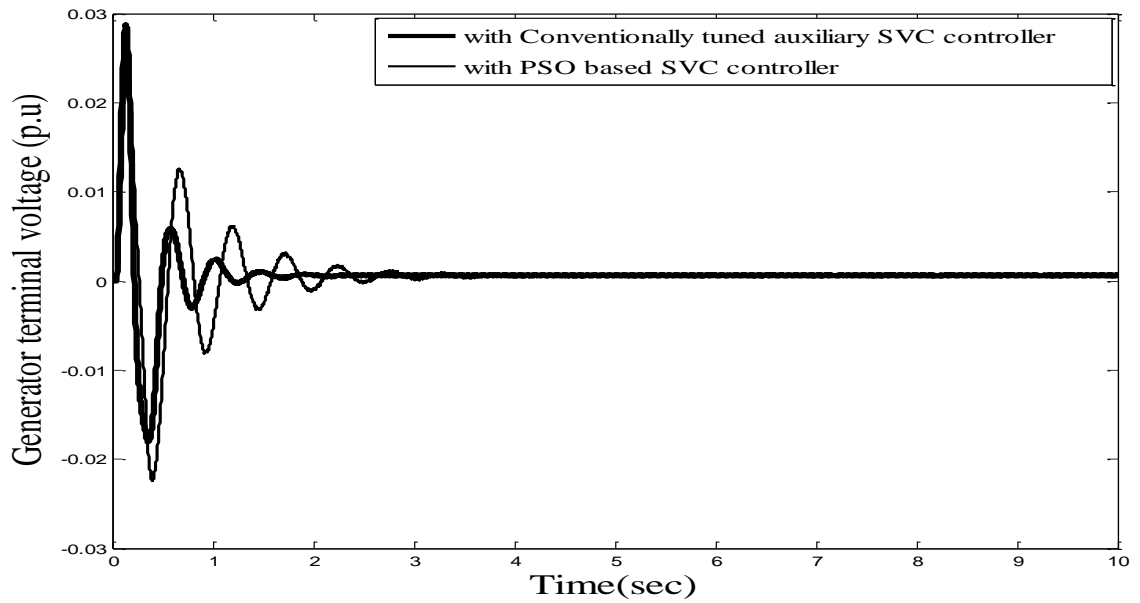


Fig. 4.20.3: Time response of variation in generator terminal voltage with conventionally tuned SVC controller and with PSO based SVC controller

**Case 4:** Basic PSO algorithm is implemented for optimizing the parameters of auxiliary SVC controller. Fig. 4.21.1 to 4.21.2 depict the robustness of AI based controllers over the conventional one.

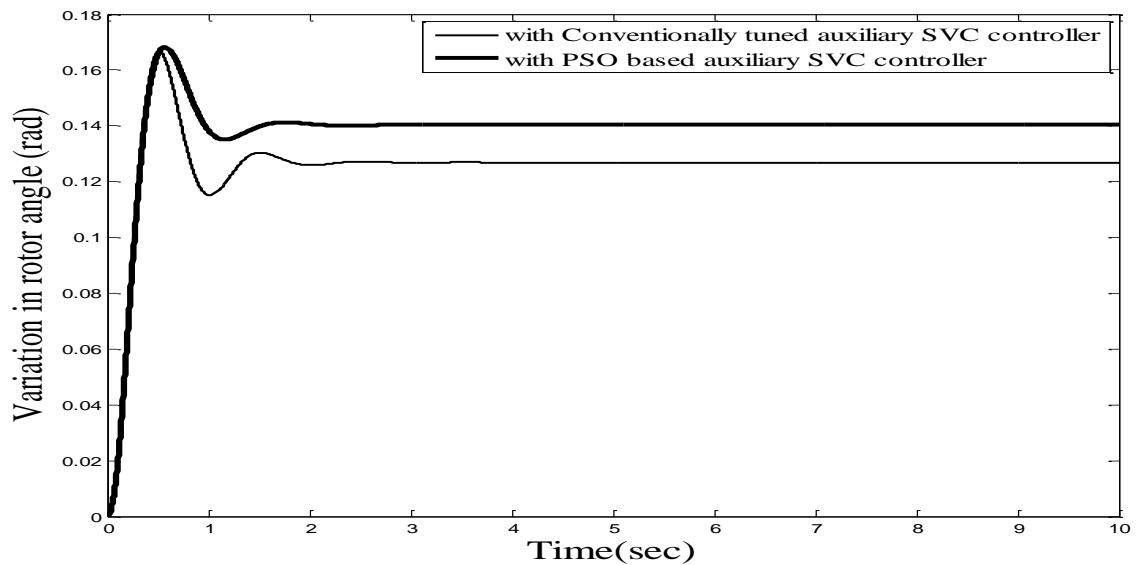


Fig. 4.21.1 Time response of variation in rotor angle with conventionally tuned auxiliary SVC controller and with PSO based auxiliary SVC controller

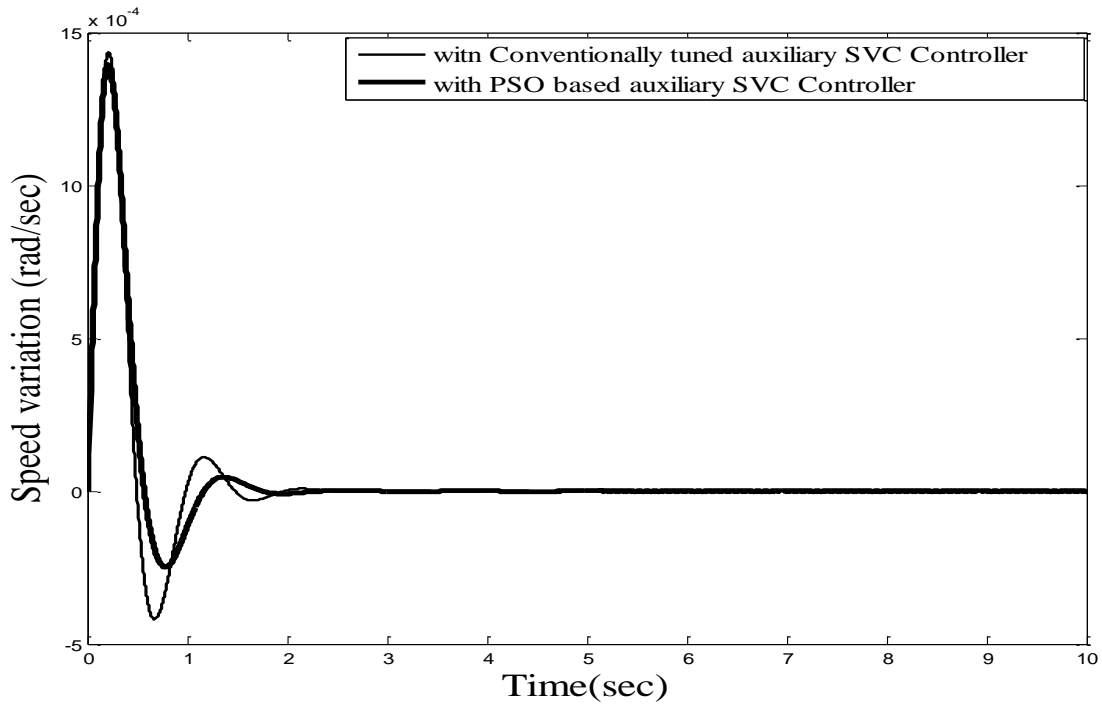


Fig. 4.21.2: Time response of speed deviation with conventionally tuned auxiliary SVC controller and with PSO based auxiliary SVC controller

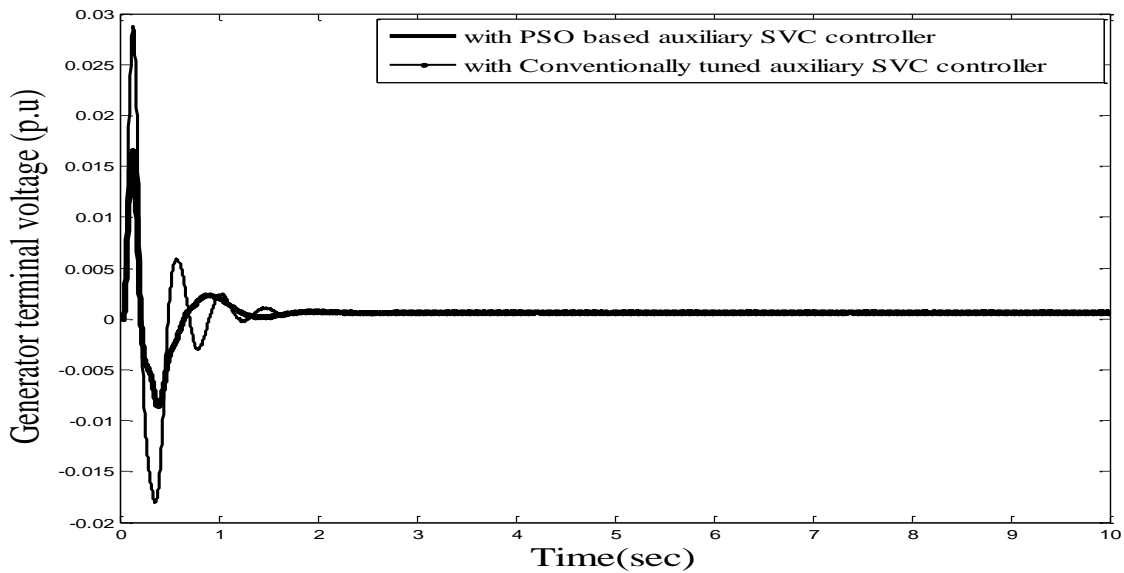


Fig. 4.21.3: Time response of variation in generator terminal voltage with conventionally tuned auxiliary SVC controller and with PSO based auxiliary SVC controller

**Case 5:** Two additional factors i.e Shrinkage factor/constriction factor and inertia weight factor varying with iteration are used in basic PSO algorithm for the search of global minima



in the m-dimensional search space. This PSO variant is implemented for optimizing the auxiliary SVC controller parameters. All PSO-SFIWA parameters chosen are given in appendix A. Fig. 4.22.1 to 4.22.3 depict the effectiveness of proposed scheme over the basic PSO algorithm.

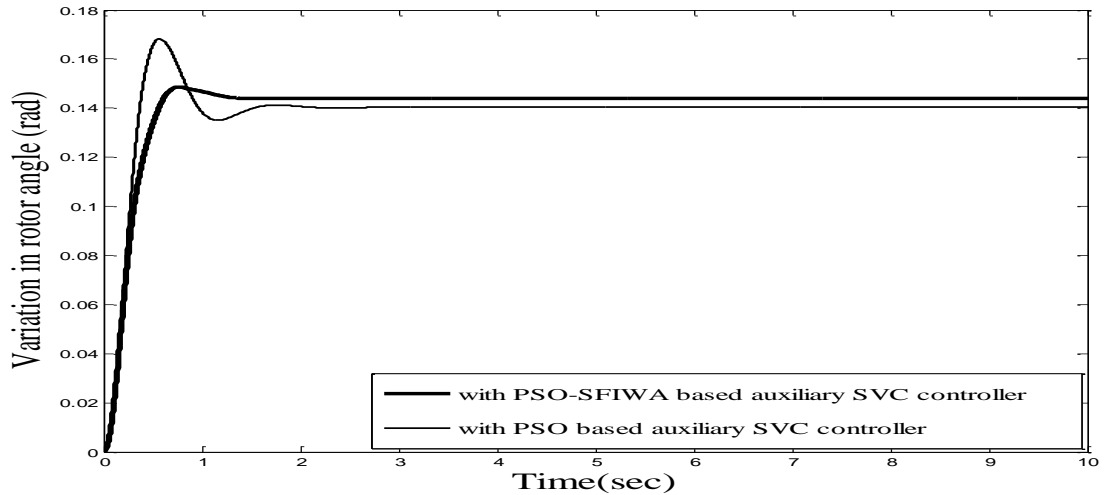


Fig. 4.22.1 Time response of variation in rotor angle with PSO based auxiliary SVC controller and with PSO-SFIWA based auxiliary SVC controller

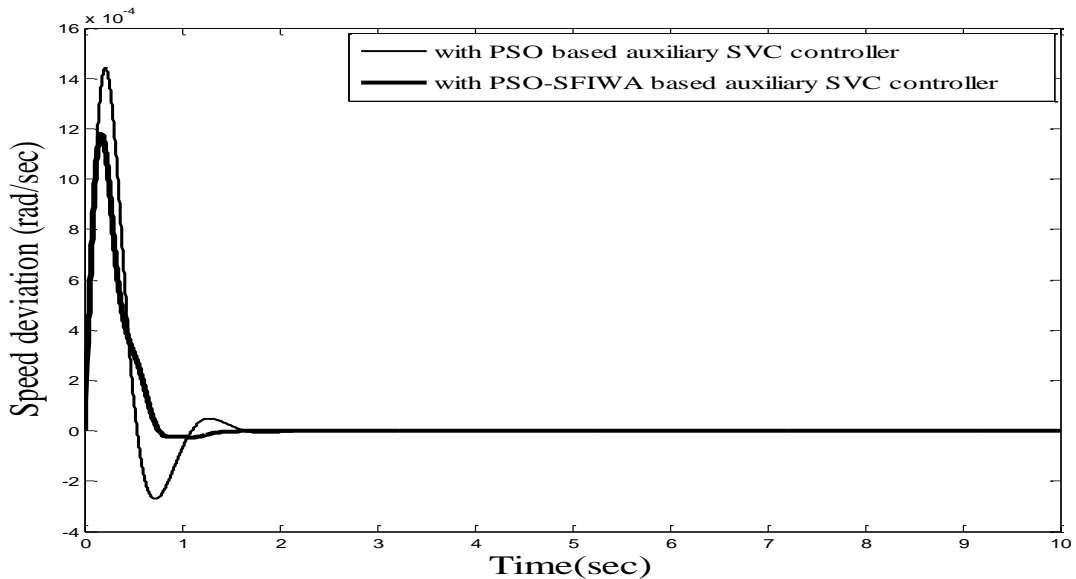


Fig. 4.22.2: Time response of speed deviation with PSO based auxiliary SVC controller and with PSO-SFIWA based auxiliary SVC controller

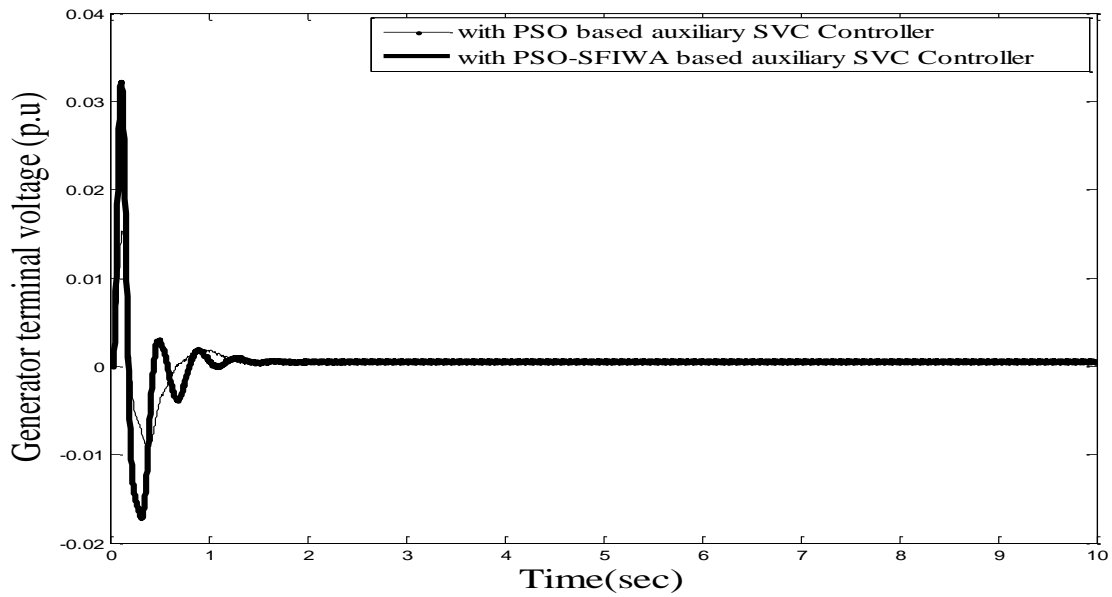


Fig. 4.22.3: Time response of variation in generator terminal voltage with PSO based auxiliary SVC controller and with PSO-SFIWA based auxiliary SVC controller

**Case 6:** Another PSO variant called PSO-time varying inertia weight approach (PSO-TVAC) is implemented for optimizing the parameters of auxiliary SVC controller. Acceleration coefficients used in basic PSO algorithm are varied with iteration in order to search the global minima in whole search area initially and later on near minima for fine tuning. This technique is used with inertia weight factor. Results depicted in fig. 4.23.1 and 4.23.3 show the effectiveness of the proposed scheme. Fig. 4.24.1 to 4.24.3 show the behavior of power system network without controller, with PSO based SVC controller and PSO-TVAC based auxiliary SVC controller when a small disturbance is applied in the form of increased input mechanical power.

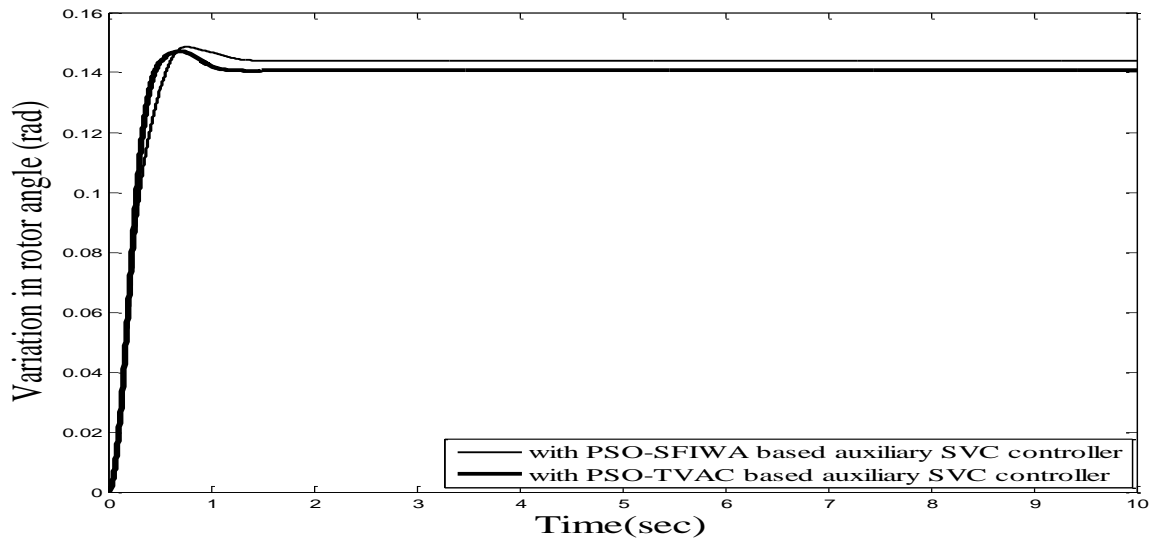


Fig. 4.23.1: Time response of variation in rotor angle with PSO--SFIWA based auxiliary SVC controller and with PSO-TVAC based auxiliary SVC controller

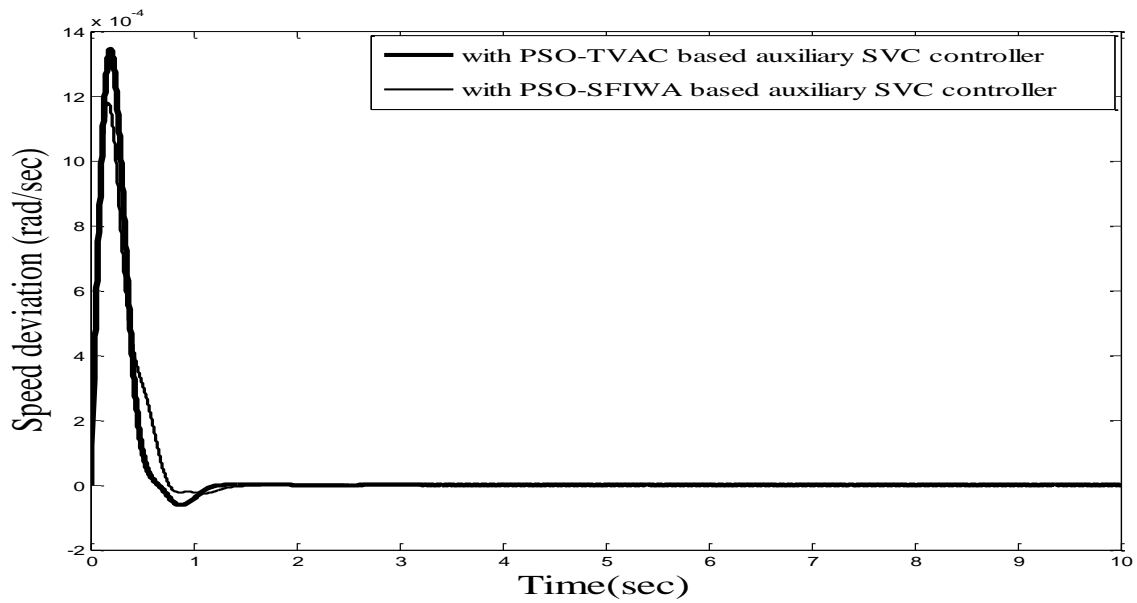


Fig. 4.23.2: Time response of speed deviation with PSO-SFIWA based auxiliary SVC controller and with PSO-TVAC based auxiliary SVC controller

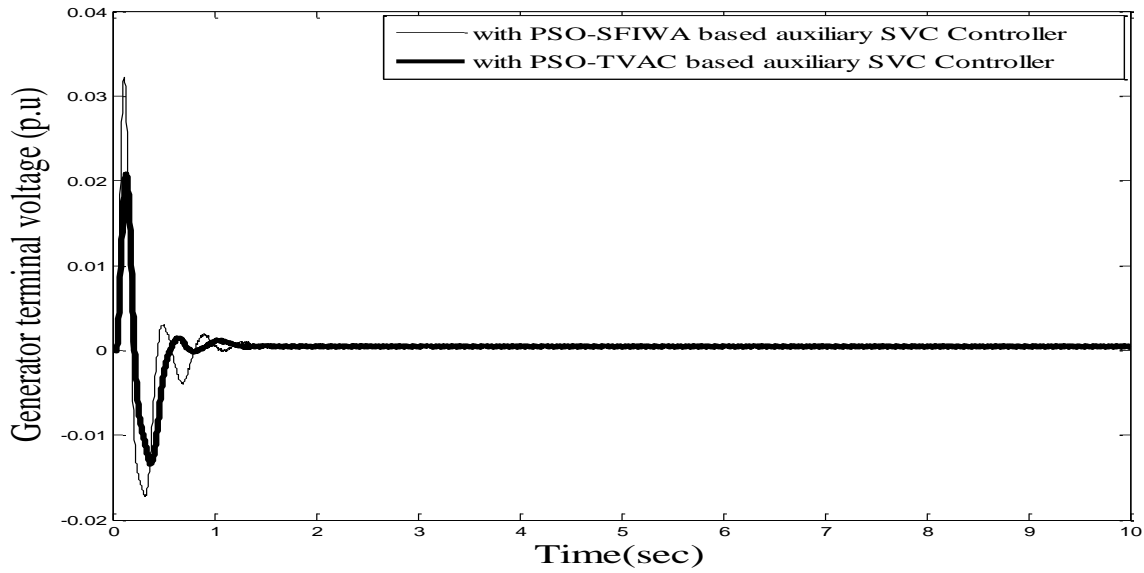


Fig. 4.23.3: Time response of variation in generator terminal voltage with PSO-SFIWA based auxiliary SVC controller and with PSO-TVAC based auxiliary SVC controller

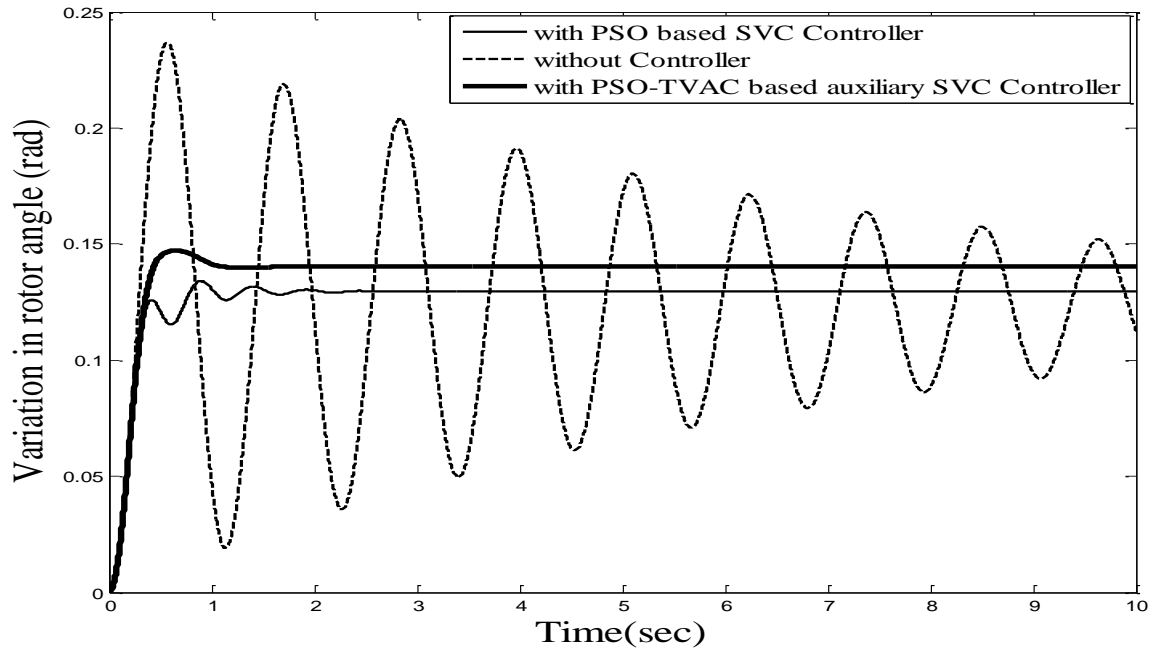


Fig. 4.24.1: Time response of variation in rotor angle without, with PSO based SVC controller and with PSO-TVAC based auxiliary SVC controller

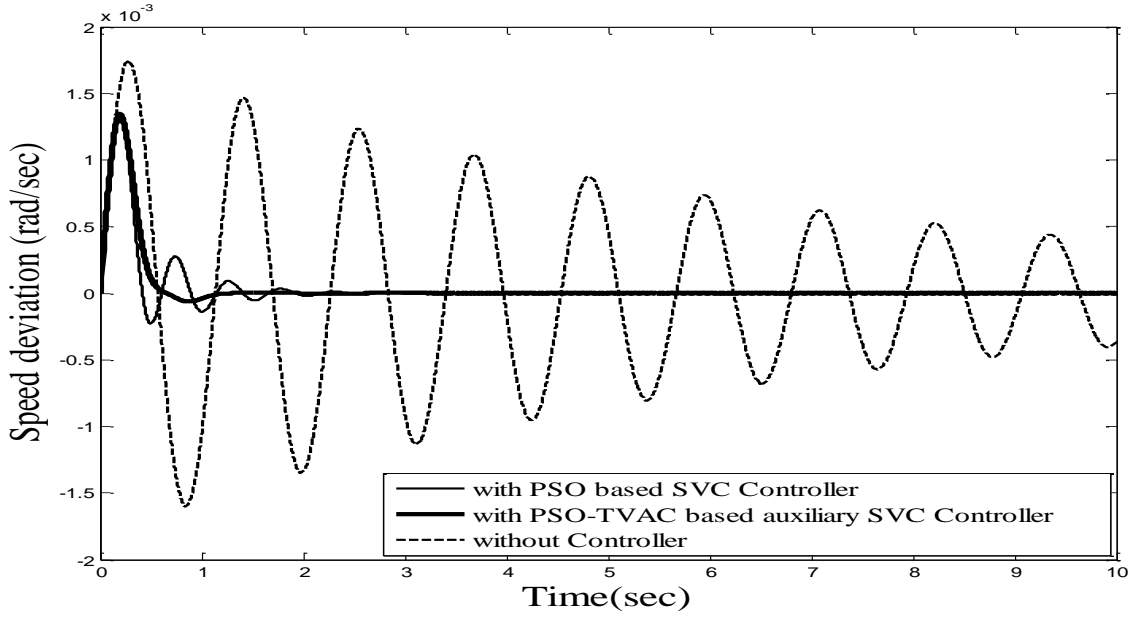


Fig. 4.24.2: Time response of speed deviation without, with PSO based SVC controller and with PSO-TVAC based auxiliary SVC controller

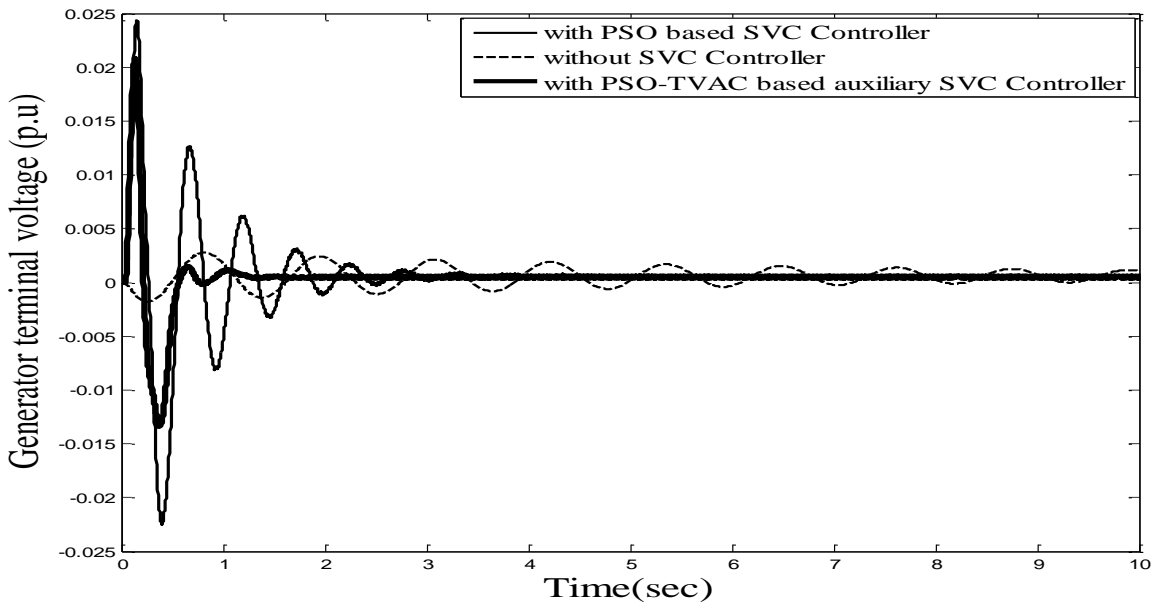


Fig. 4.24.3: Time response of variation in generator terminal voltage without, with PSO based SVC controller and with PSO-TVAC based auxiliary SVC controller

**Table3: Comparison chart with respect to settling time**

Cases	$\Delta \delta$ Settling time	$\Delta w$ Settling time	$\Delta V_t$ Settling time
Without SVC Controller	43.55 sec	45 sec	> 60 sec
With Conventionally tuned SVC Controller	4.8 sec	5.9 sec	7 sec
With PSO based SVC Controller	4 sec	3.87 sec	4.5 sec
With Conventionally tuned auxiliary SVC Controller.	3.8 sec	2.8 sec	3.0 sec
With PSO based auxiliary SVC Controller	2.4 sec	2.8 sec	2.8 sec
With PSO-SFIWA based auxiliary SVC Controller	2 sec	2.5 sec	1.8 sec
With PSO-TVAC based auxiliary SVC Controller	1.55 sec	1.7sec	1.5sec

#### 4.5.3 Simulation results with Bacterial Forging Optimization based Auxiliary SVC Controller

Bacterial Foraging algorithm presented in chapter 3 has been implemented for optimizing both regulator parameters of SVC controller and parameters of auxiliary controller of SVC. Algorithm is written in MATLAB coding. The various BFO parameters taken are given in appendix A.

**Case 1:** The simulation results shown in fig.4.25.1 to 4.25.2 depict that BFO based auxiliary controller is better than the conventionally tuned controller for enhancing the stability of the power system network by fast mitigating the power oscillations.

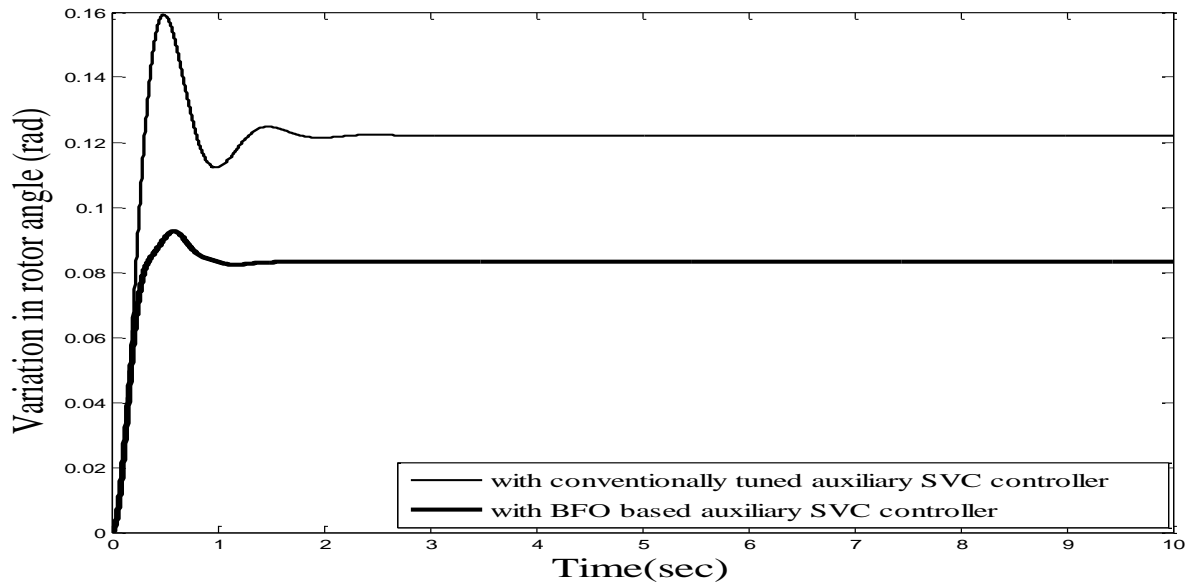


Fig. 4.25.1 Time response of variation in rotor angle with conventionally tuned auxiliary SVC controller and with BFO based auxiliary SVC controller

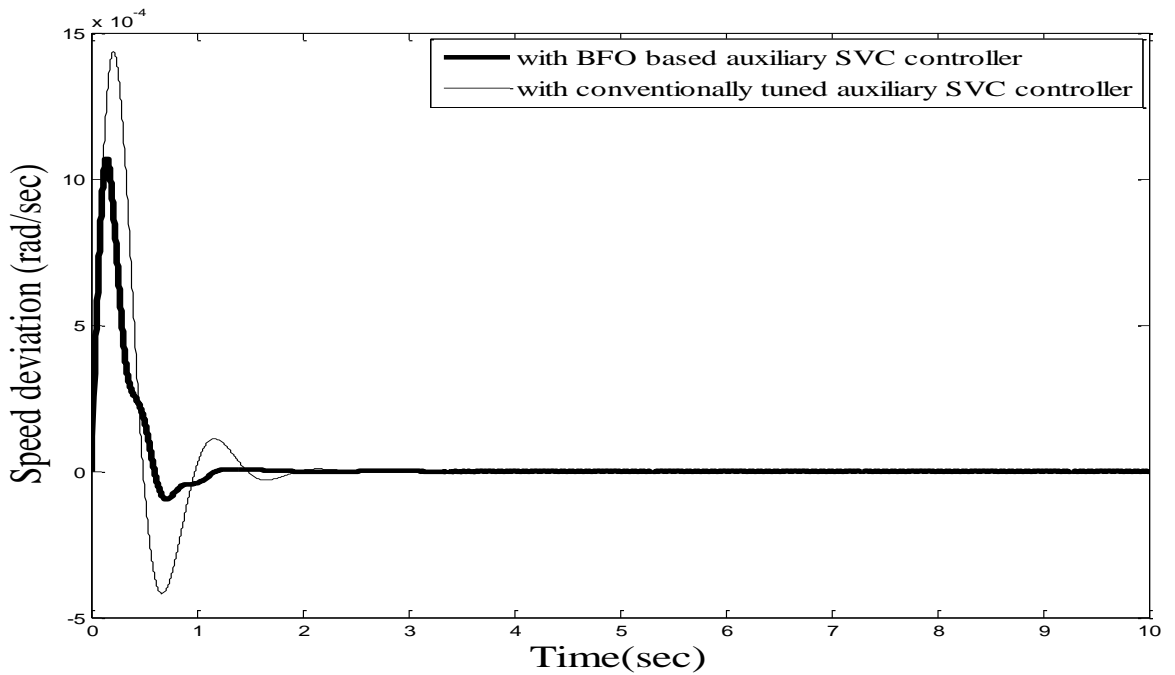


Fig. 4.25.2 Time response of speed deviation with conventionally tuned auxiliary SVC controller and with BFO based auxiliary SVC controller

**Case 2:** BFO based auxiliary SVC controller is more effective than BFO based SVC controller as depicted in fig. 4.26.1 to 4.26.3.

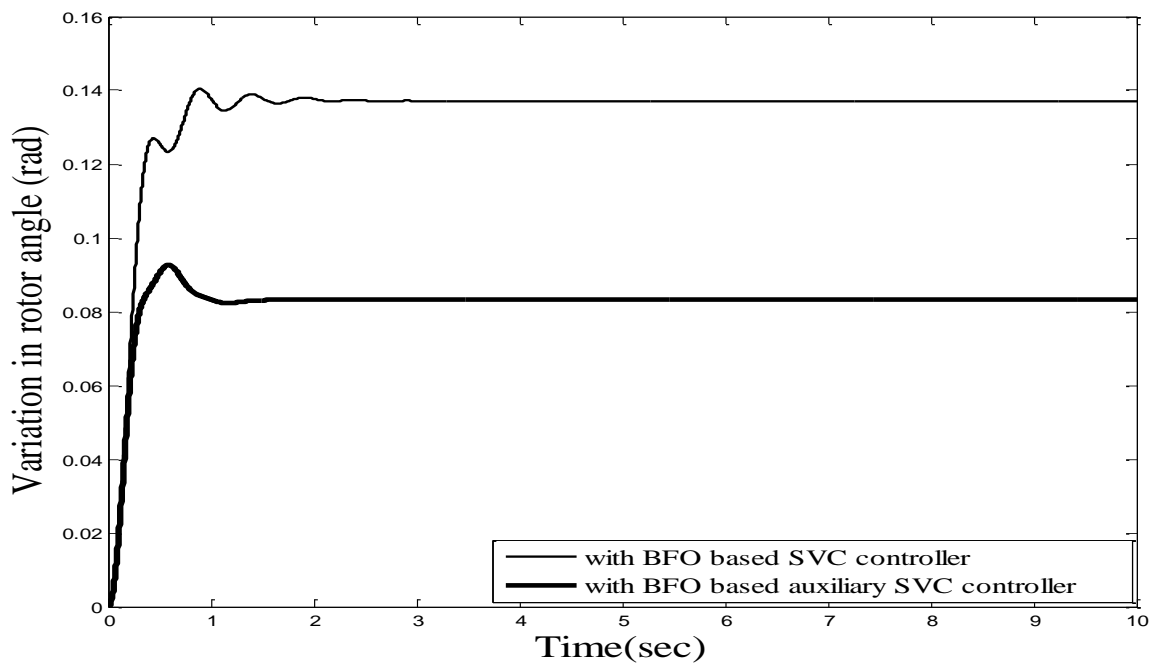


Fig. 4.26.1 Time response of variation in rotor angle with BFO based SVC controller and with BFO based auxiliary SVC controller

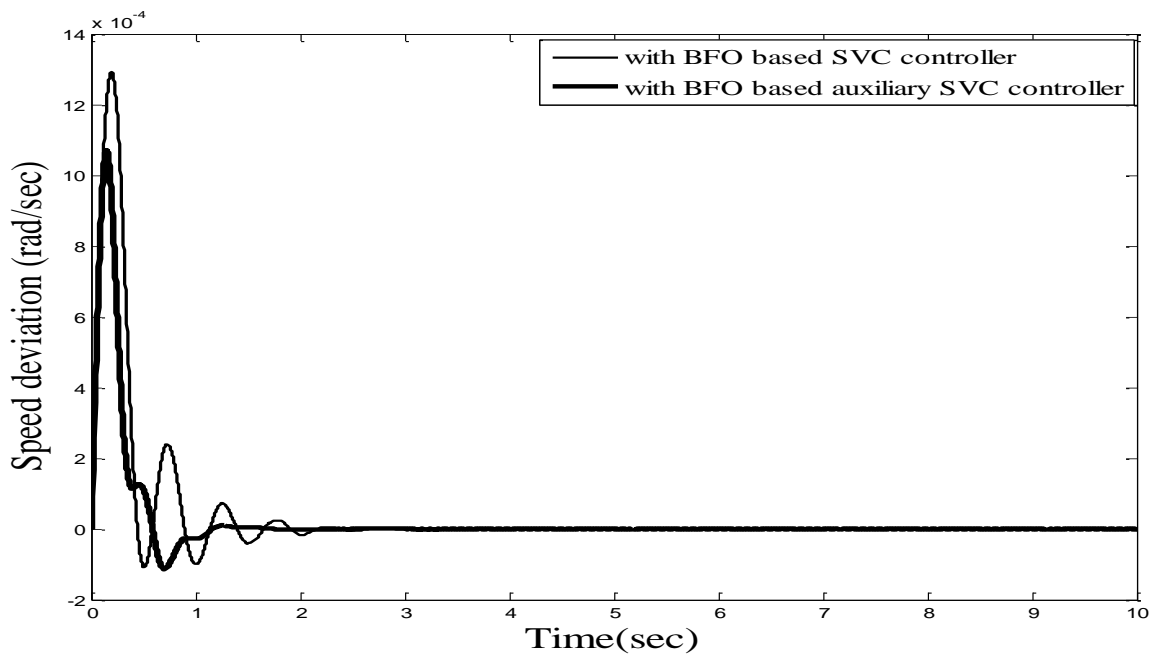


Fig. 4.26.2 Time response of speed deviation with BFO based SVC controller and with BFO based auxiliary SVC controller



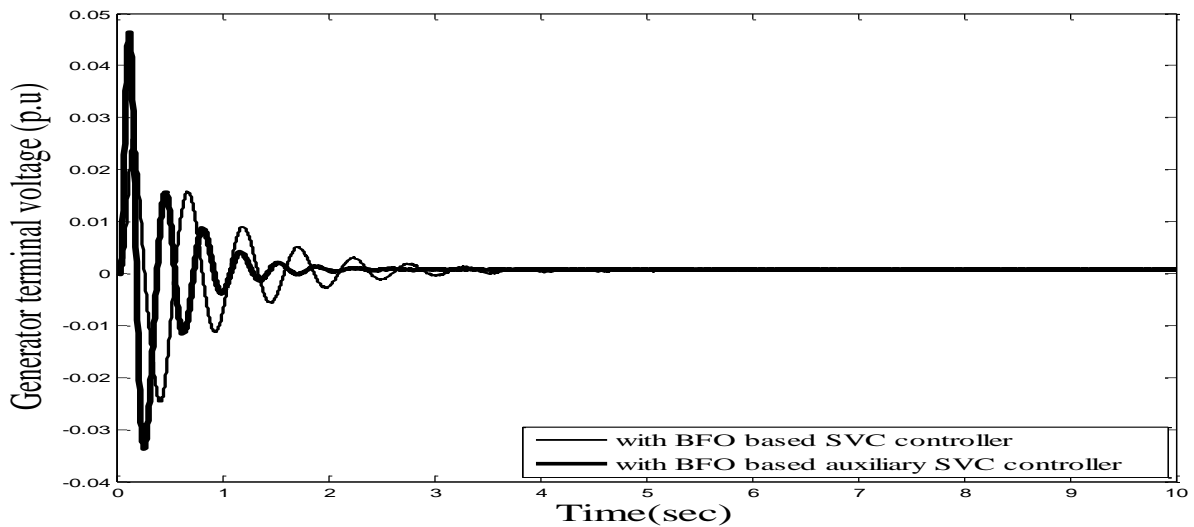


Fig 4.26.3 Time response of variation in generator terminal voltage with BFO based SVC controller and with BFO based auxiliary SVC controller

#### 4.5.4 Simulation Results with Hybrid BF-Particle Swarm Optimization based Auxiliary SVC Controller

This technique takes the advantage of both BFO as well as PSO. The global best values are achieved by incorporating the social interaction effect of PSO in BFO algorithm. The algorithm is implemented in MATLAB coding. The various parameters of Hybrid BF-PSO algorithm used are given in appendix A.

**Case 1:** Hybrid BF-PSO technique is implemented for tuning the parameters of auxiliary SVC controller for better stability enhancement and results are compared with the conventionally tuned auxiliary SVC controller.

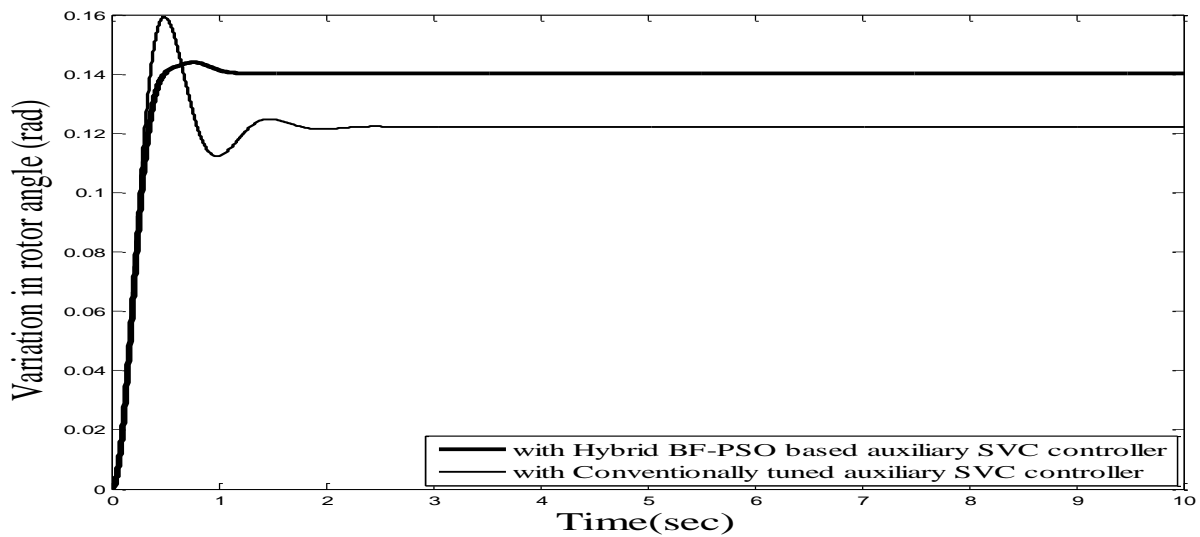


Fig. 4.27.1 Time response of variation in rotor angle with Hybrid BF-PSO based auxiliary SVC controller and with conventionally tuned auxiliary SVC controller

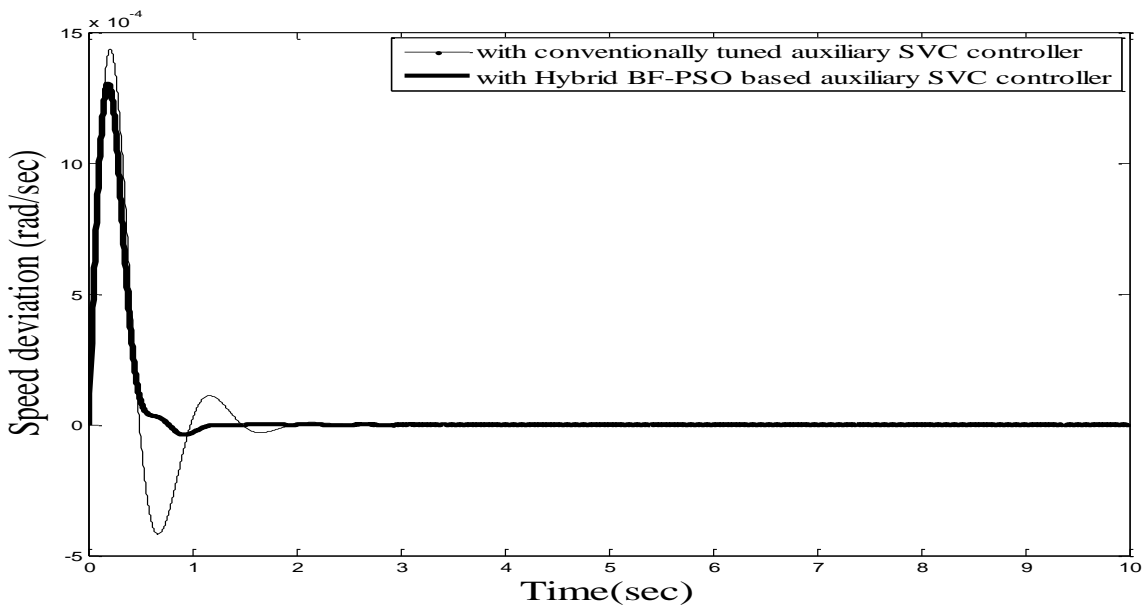


Fig. 4.27.2 Time response of speed deviation with Hybrid BF-PSO based auxiliary SVC controller and with conventionally tuned auxiliary SVC controller

**Case2:** The effectiveness of Hybrid BF-PSO based auxiliary SVC controller over the Hybrid BF-PSO based SVC controller is presented in fig. 4.28.1 and 4.28.3

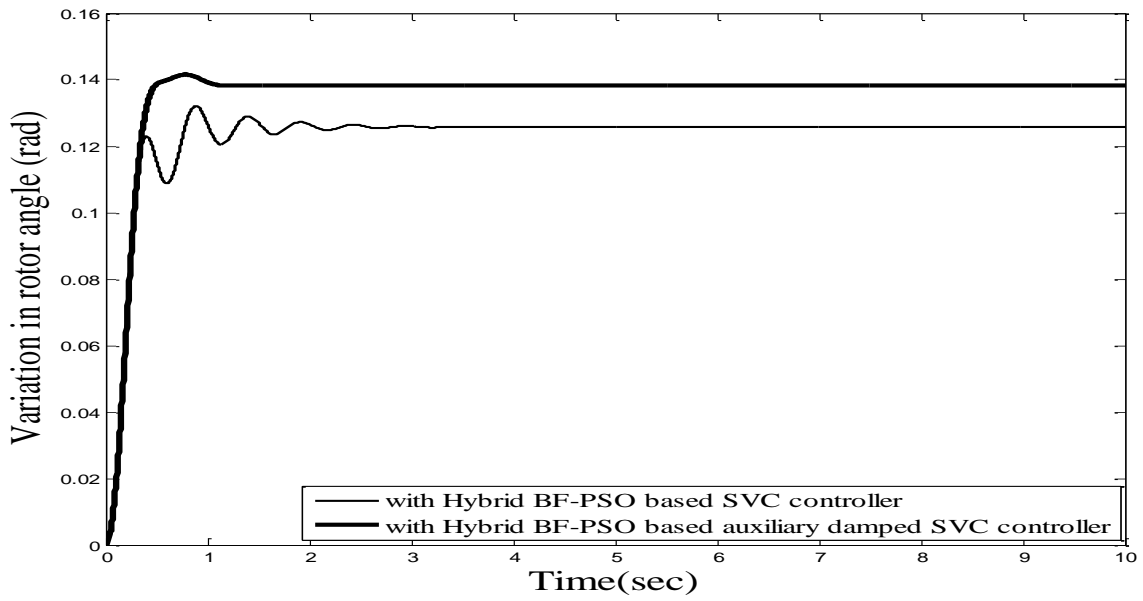


Fig. 4.28.1 Time response of variation in rotor angle with Hybrid BF-PSO based SVC controller and with Hybrid BF-PSO based auxiliary damped SVC controller

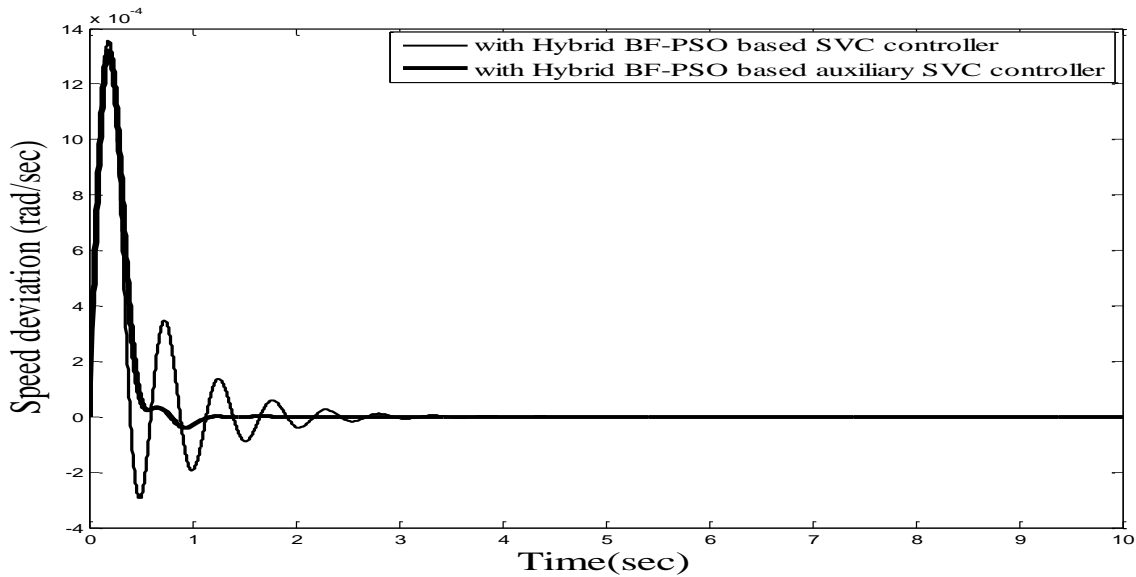


Fig. 4.28.2 Time response of speed deviation with Hybrid BF-PSO based SVC controller and with Hybrid BF-PSO based auxiliary damped SVC controller

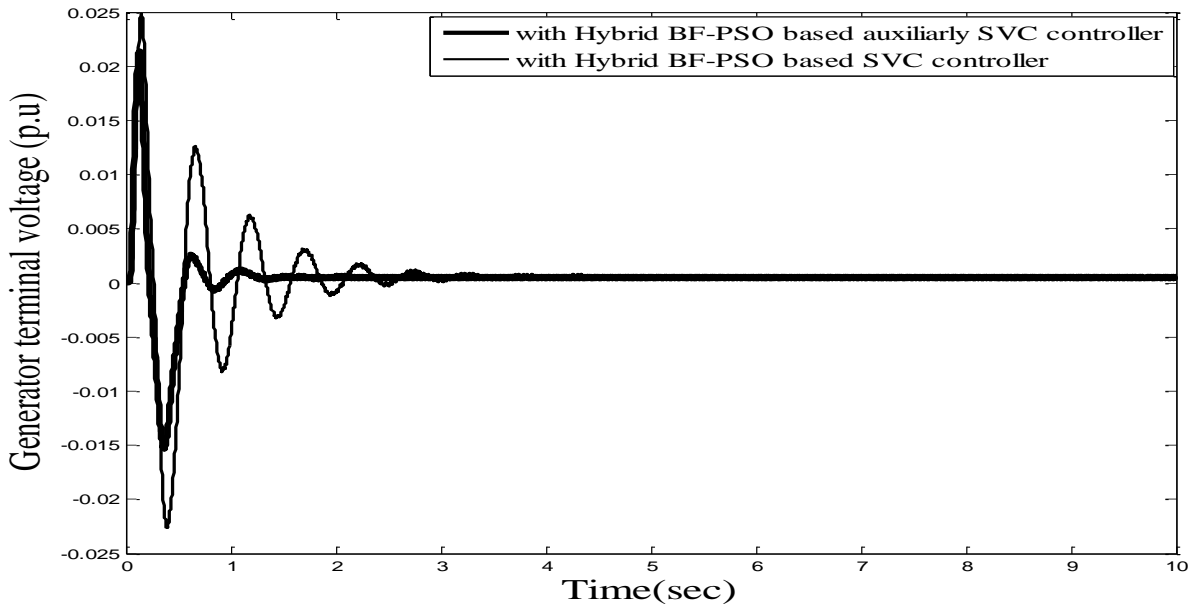


Fig. 4.28.3 Time response of variation in generator terminal voltage with Hybrid BF-PSO based SVC controller and with Hybrid BF-PSO based auxiliary damped SVC controller

#### 4.5.5 Simulation Results with Genetic Algorithm based Auxiliary SVC Controller

The evolutionary technique is implemented for optimizing the parameters of auxiliary SVC controller. GA algorithm is implemented in MATLAB programming. GA parameters used are given in appendix A.

**Case 1:** GA is implemented for tuning the parameters of auxiliary SVC controller for better stability enhancement and results are compared with the conventionally tuned SVC controller as depicted in fig. 4.29.1 and 4.29.2.

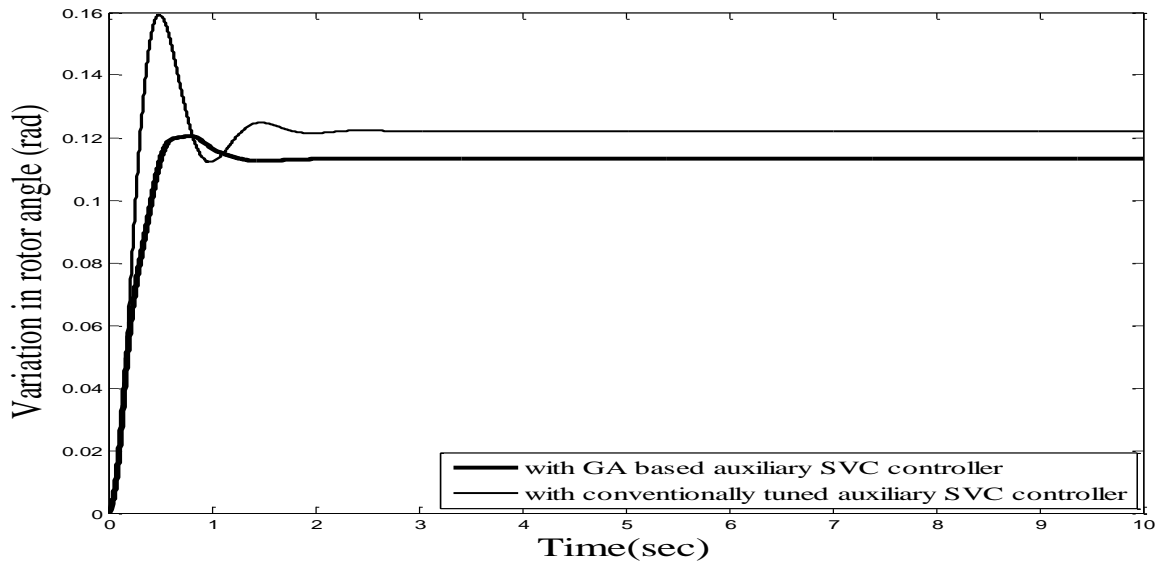


Fig. 4.29.1 Time response of variation in rotor angle with conventionally tuned auxiliary SVC controller and with GA based auxiliary SVC controller

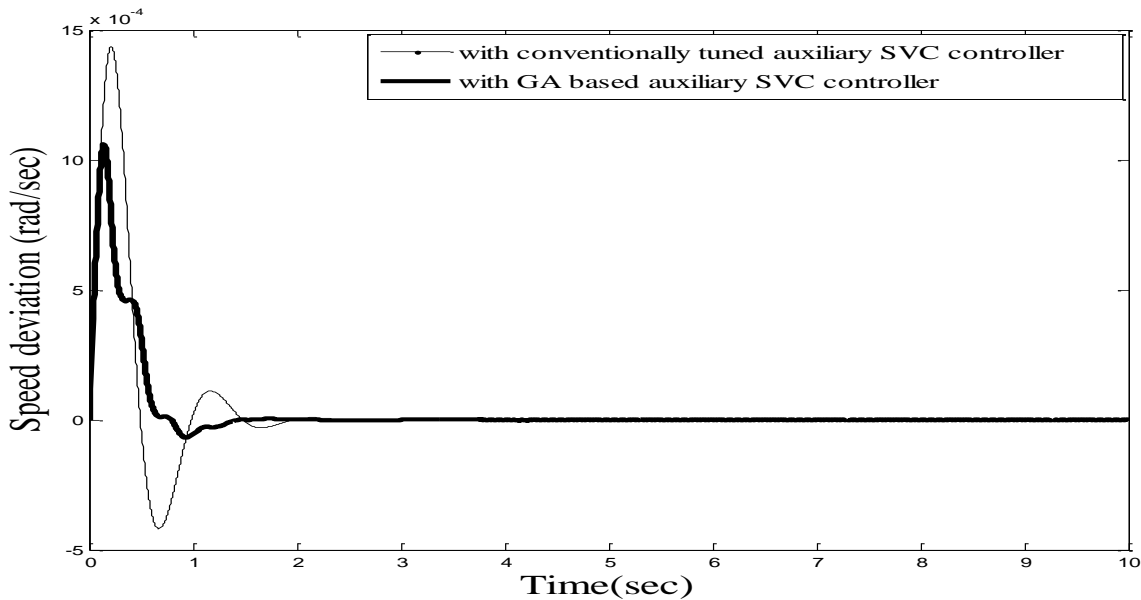


Fig. 4.29.2 Time response of speed deviation angle with conventionally tuned auxiliary SVC controller and with GA based auxiliary SVC controller

**Case 2:** The computer simulation are carried out both with GA based SVC controller and with GA based auxiliary controller and their comparison are depicted in fig. 4.30.1 to 4.30.2 and fig. 4.31.1 and 4.321.2 show the comparison of power system performance between GA based auxiliary SVC controller, with SVC controller and without controller.

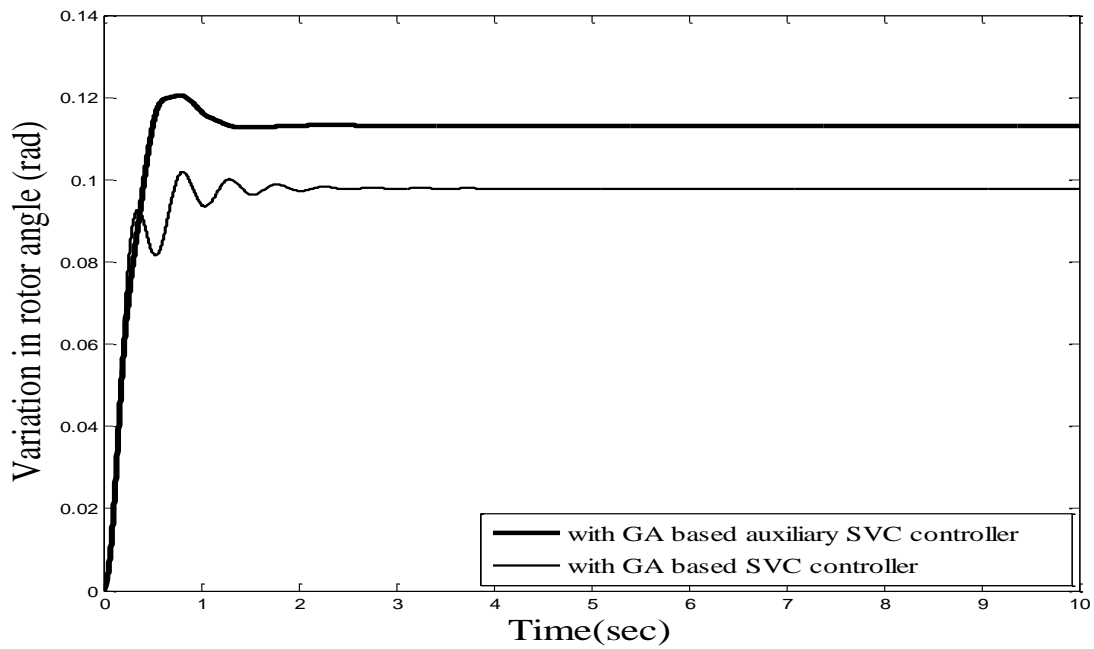


Fig. 4.30.1 Time response of variation in rotor angle with GA based auxiliary SVC controller and with GA based SVC controller

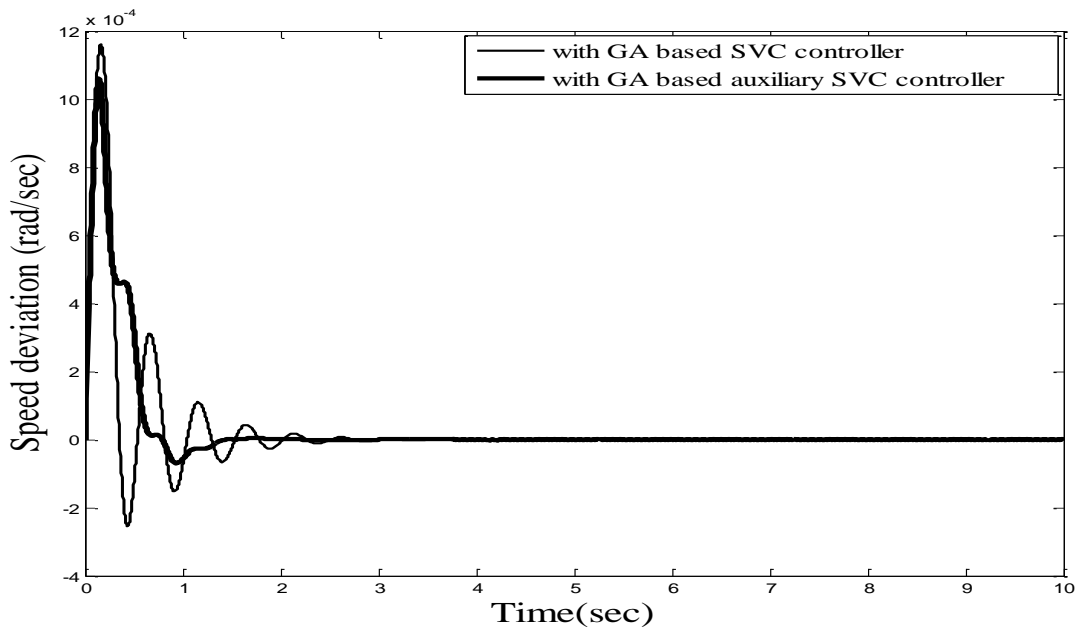


Fig. 4.30.2 Time response of speed deviation with GA based auxiliary SVC controller and with GA based SVC controller

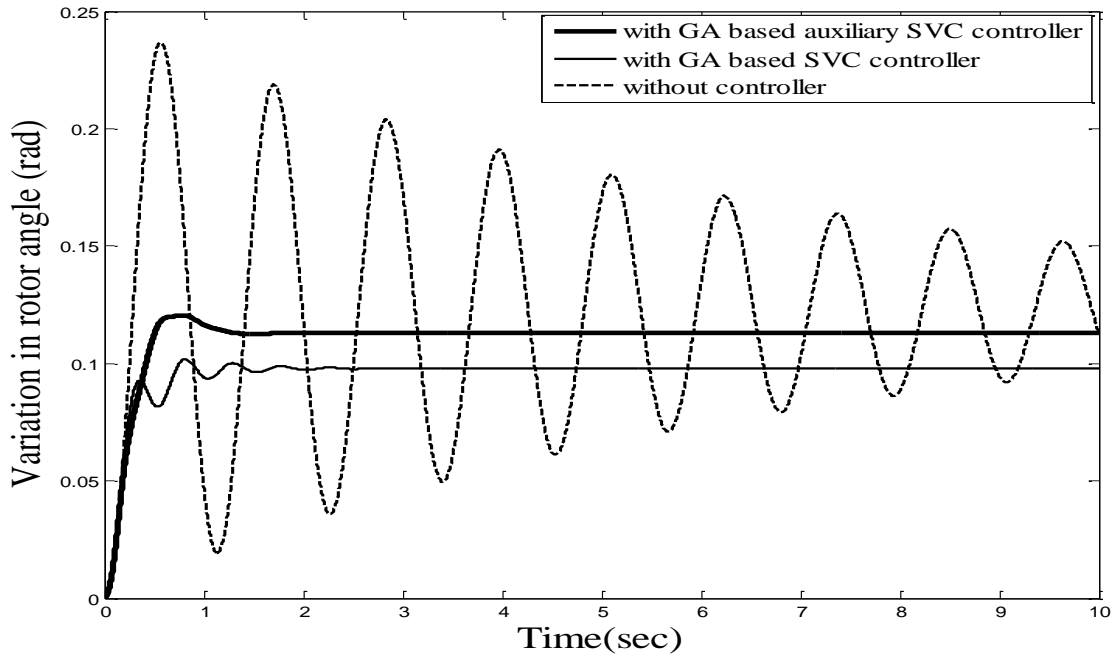


Fig. 4.31.1 Time response of variation in rotor angle with GA based SVC controller, with GA based auxiliary SVC controller and with without controller

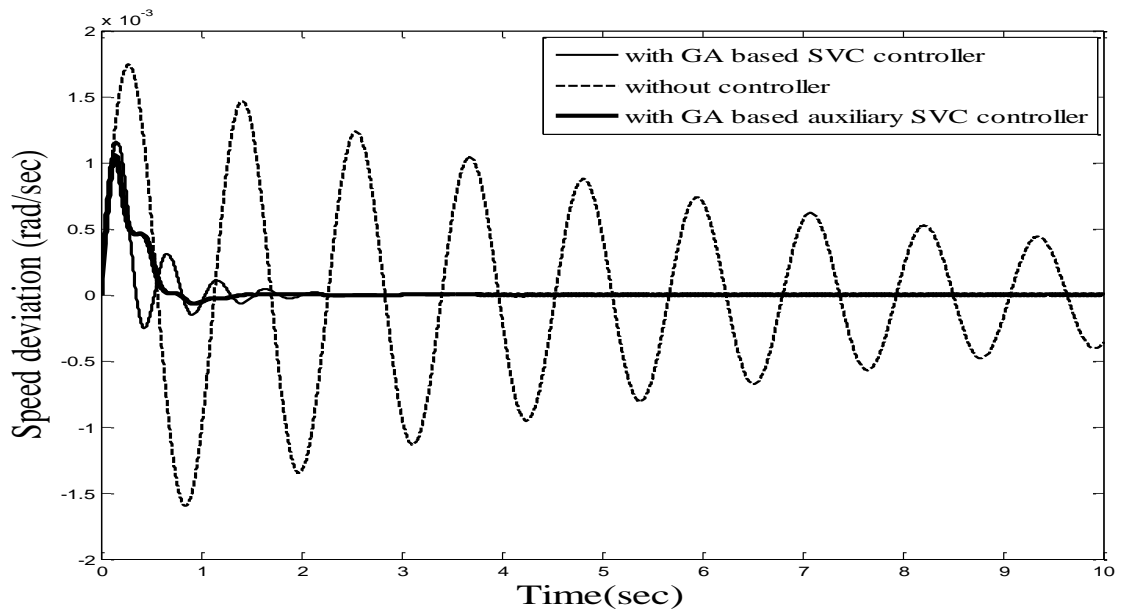


Fig. 4.31.2 Time response of speed deviation with GA based SVC controller, with GA based auxiliary SVC controller and with without controller

**Table 4: Comparison in settling time between various AI techniques based auxiliary SVC Controller**

Cases	$\Delta \delta$ Settling time	$\Delta w$ Settling time	$\Delta V_t$ Settling time
Without SVC Controller	43.55sec	45sec	>60 sec
With SVC Controller	4.8 sec	5.9 sec	7 sec
BFO based auxiliary SVC Controller	2.1 sec	2.6 sec	2.1 sec
PSO-TVAC based auxiliary SVC Controller	1.55 sec	1.7sec	1.5sec
GA based auxiliary SVC Controller	2.5 sec	2.0 sec	2.5 sec
Hybrid BF –PSO based auxiliary SVC Controller	1.15sec	1.5 sec	1.5sec

#### 4.5.6 Discussion

Simulation results show that auxiliary SVC Controller gives better power system performance enhancement in comparison to SVC Controller. AI based auxiliary SVC Controller gives further better steady state response in comparison to Conventional based method. Parameters of auxiliary PID controller are optimized by various swarm intelligent techniques and simulation results show that Hybrid BF- PSO technique proves to be the best method for optimizing the Controller parameters for enhancing the dynamic performance of the power system by taking minimum time for settling the power system oscillations. PSO-TVAC based auxiliary SVC controller is also comparable to Hybrid BF- PSO technique. The latter technique takes advantage of both elimination and dispersal events of BFO for searching the solution in m-dimensional search space and social interaction event of PSO algorithm for converging towards global minima while the former technique has the advantage that it provides randomness initially in searching for global minima in the entire m-dimensional search space in order to prevent from trapping into local minima and fine tuning when solution is near to global minima by varying the values of  $c_1$  and  $c_2$  (acceleration coefficients). Basic PSO does not give very good results. Hence modified version of PSO was



implemented for achieving better results. PSO-SFIWA based controller is also comparable to PSO-TVAC based controller, but the rotor angle stability margin has increased in PSO-TVAC based controller. Genetic algorithm, an evolutionary technique is comparable to BFO algorithm and PSO-SFIWA algorithm as can be seen from the comparison chart. Elimination and dispersal event in Bacterial Foraging, Mutation operator in GA and Shrinkage factor and Inertia weight approach in PSO algorithm provides the randomness to prevent from trapping into local minima and provide good optimized values of the controller parameters, such that auxiliary SVC controller with these parameters provides good dynamic stability to the power system network.

# **CHAPTER 5**

## **THYRISTOR CONTROLLED SERIES COMPENSATOR FOR PERFORMANCE ENHANCEMENT OF POWER SYSTEM**

### **5.1 INTRODUCTION**

Worldwide rapid industrialization and urbanization are putting utilities under pressure. This fast growing demand jeopardizes reliable and high quality power supply. Yet the global trend towards deregulated power markets means any new investment must be competitive. At the same time, environmental awareness questions the construction of additional overhead transmission lines. Due to economical reason we need to increase the loading of transmission lines. So we need some compensating devices which can solve the problem of increased power supply.

The methodology of using fixed capacitors for improvement in the transient stability is known since decades. But, connecting fixed capacitors in series with the transmission lines may lead to the problem of sub synchronous resonance that results in the instability in the system at sub-synchronous frequency. Hence the need arises for the switched series capacitors. This knowledge of varying dynamically the series compensation may only be possible by means of mechanical circuit breakers which leads to the switching in and out of capacitor banks but use of these devices for practical purposes were undesirable due to their low speed of operation. This problem was solved due to the introduction of FACTS devices, a very fast actuating power electronic devices. These are static devices used for the purpose of enhancement of power transfer capability of existing transmission lines by controlling the series compensation, provides the voltage support by supplying reactive power compensation and also provide the fast mitigation of power system oscillations. Thus by controlling any of the line parameters by these devices, the stable and secure power system can be attained. Series and shunt compensation are two types of compensation possible in transmission lines. In transmission line, there is a huge voltage drop due to large line inductance. Hence decreases the line flow and also the efficiency of the network. Thus

series FACTS controllers are employed to provide necessary compensation by reducing the line inductance as they work as controllable voltage source. Various series compensating FACTS devices available are- TCSC, SSSC, Thyristor-controlled series reactor (TCSR), Thyristor-controlled series compensator (TCSC) and Thyristor-switched series reactor (TSSR).

Vithayathil with others suggested the concept of Thyristor-Controlled Series Compensator (TCSC) first in 1986 with the idea of fast regulation of line impedance. Basic structure of this device has already been explained in chapter 2. For practical implementation, several units of TCSC's are joined in series for achieving the required operating characteristics and voltage rating.

However, the basic idea behind the TCSC scheme is to provide a continuously variable capacitor by means of partially cancelling the effective compensating capacitance by the TCR [1]. TCR has the feature to behave as a continuously variable reactive impedance at its fundamental frequency, which can be controlled by delay angle  $\alpha$ . If we take a parallel LC circuit having a fixed capacitive impedance  $X_C$  and variable inductive impedance  $X_L(\alpha)$ , then its steady state impedance is that of TCSC, where  $X_L = \omega L$  and  $\alpha$  is the delay angle measured from the crest of the capacitor (or equivalently zero crossing of the line current).

Due to which, TCSC can be seen as a tuned parallel LC circuit to AC line current. Now when the impedance of the controlled reactor  $X_L(\alpha)$  is allowed to vary from its maxima (infinity) to minima ( $\omega L$ ), the capacitive impedance of TCSC increases from its minimum value  $X_{TCSC \min} = X_C = 1/\omega C$ , till a parallel resonance at  $X_C = X_L(\alpha)$  is reached and a theoretically value of  $X_{TCSC \max}$  becomes infinite. By decrementing  $X_L(\alpha)$  further, TCSC offers an inductive impedance  $X_{TCSC}(\alpha)$  which at  $\alpha=0^\circ$ , reaches its maximum value of  $X_L X_C / (X_L - X_C)$  where the capacitor is in effect bypassed by TCR. So with TCSC arranged in its usual way, where impedance of the capacitor is more than TCR reactor  $X_L$ , the TCSC operates on two operating ranges around its internal circuit resonance, one being  $\alpha_{lim} < \alpha < \pi/2$  where  $X_{TCSC}(\alpha)$  is capacitive and the other being  $0 < \alpha < \alpha_{lim}$  where  $X_{TCSC}(\alpha)$  is inductive. However, for the performance enhancement of the power system, design of effective TCSC controller is required. To envisage the performance behavior of TCSC controller, the exact knowledge of the system and its modeling is required under any

contingencies or under abnormal conditions. Furthermore the effectiveness of AI based controllers can also be analyzed.

In the present chapter, three cases have been analyzed to show the effectiveness of TCSC controller for damping power system oscillations. SMIB system has been considered for analysis. The SMIB system of case 1 is modelled in MATLAB Simulink environment for various series compensation levels. Case 2 (SMIB system) is modelled in PSAT i.e. power system analysis toolbox. Finally a detailed linearized system model [4] as developed in chapter 4 for the study system consisting of a generator supplying power to an infinite bus over a long distance transmission line connected with TCSC controller. TCSC controller is developed and then PSO algorithm is implemented for optimizing the TCSC parameters. TCSC controller is designed for dynamically varying the series compensation level in order to study the damping effect and overall performance enhancement of power system. Comparison is made with PSO based TCSC controller with conventionally tuned TCSC controller.

## **5.2 SYSTEM MODEL -1**

### **5.2.1 System Description**

The study system consist of one 600MVA, hydraulic turbine driven synchronous generator (a four mass model) supplying bulk power to an infinite bus through long 400KV double circuit lines, out of which one is series compensated. A TCSC controller is located between bus number 2 and bus number 3 connected in series. The synchronous machines is equipped with a hydraulic turbine, governor (HTG) and excitation system.  $P=0.7$  p.u is taken as the initial system operating condition, with quantities expressed in p.u. on generator base MVA. System is analyzed for three levels of series compensation of transmission line. One at 20 percent and second at 50 percent and third at 80 percent. For analyzing the Transient stability, a three phase fault is created for 100msec at infinite bus-bar. The Simulation is carried out with and without TCSC controller. The system data and controller data are given in appendix C.

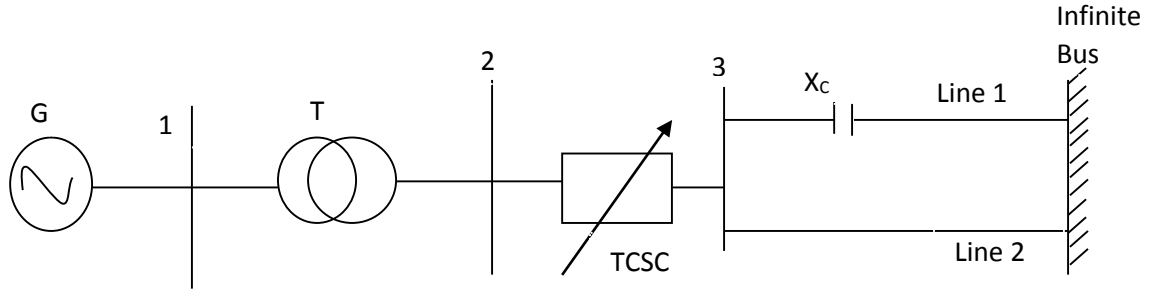


Fig. 5.1 Single line diagram of an SMIB system with TCSC connected between bus 2 and bus 3.

### 5.2.2 TCSC Controller Structure

The block diagram shown in fig. 5.2 represents the control algorithm for TCSC for controlling the firing angle  $\alpha$ , so that required series voltage is injected to mitigate the power oscillations and increase the power transfer in the line. The parameters of controller are given in appendix B.

The firing angle of the thyristors are controlled to adjust the TCSC reactance in accordance with the system control algorithm, normally in response to some system parameter variations. The relationship between  $X_{TCSC}$  and  $\alpha$  is represented as:

$$X_{TCSC} = A - 1 + \left( \frac{W_o}{W_e} \right)^2 \left( \frac{1}{2\pi f C} \left( 1 - \left( \frac{W_o}{W_e} \right) \right) \right)^2$$

$$\text{Where } A = \frac{\pi - (\pi - 2\alpha - \sin(\pi - 2\alpha))}{(\pi - 2\alpha)^2}$$

$$W_o = \frac{1}{\sqrt{LC}} \quad \text{and} \quad W_e = \frac{\pi - 2\alpha}{\pi\sqrt{LC}}$$

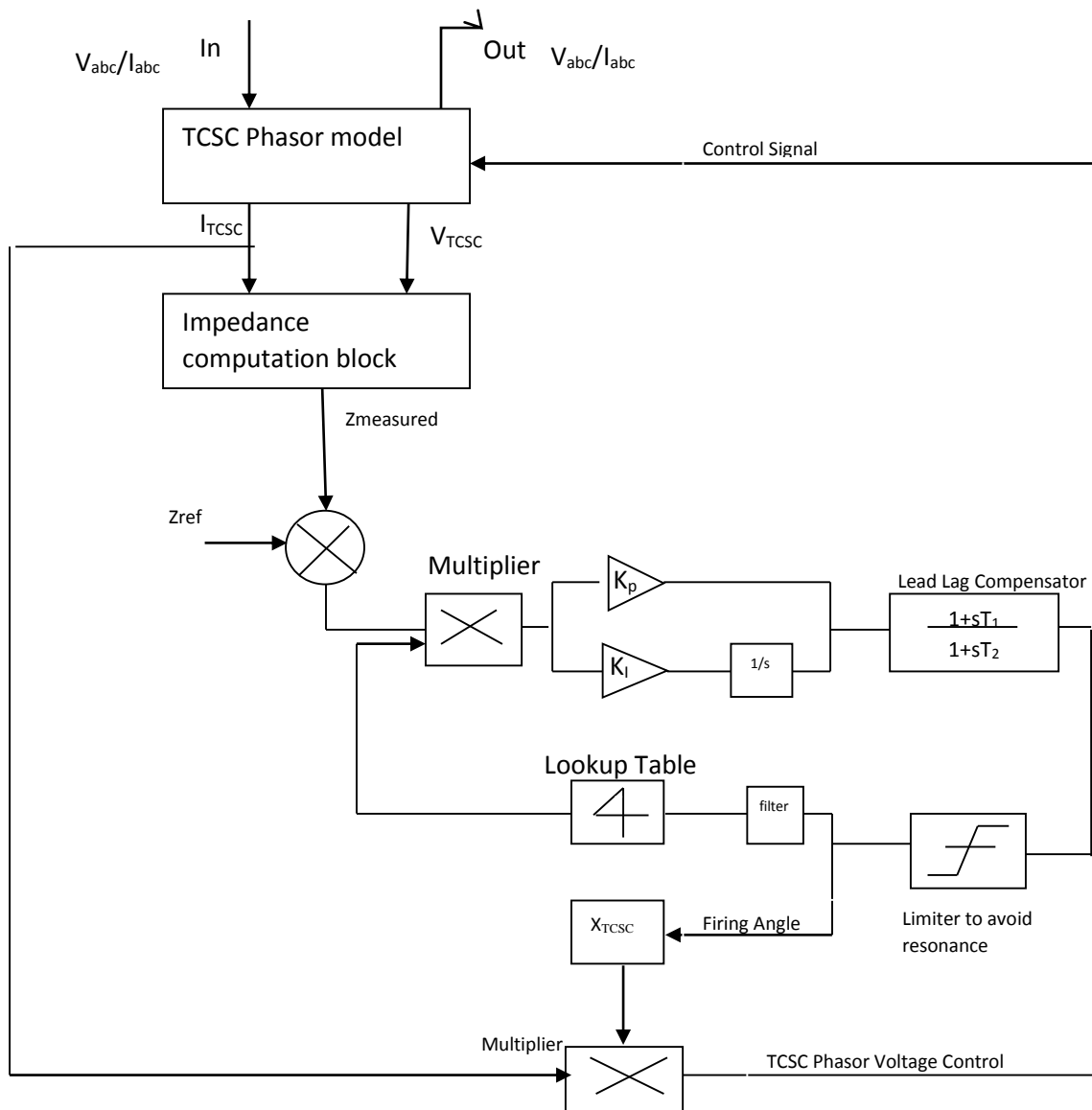


Fig. 5.2 Representation of TCSC controller.

### 5.2.3 Simulation Results with 20 percent series compensation

The simulations are carried out with and without TCSC controller connected between bus number 3 and 4 for analyzing the transient stability analysis under three phase fault conditions. Fig. 5.1.1 to 5.1.5 are shown for 20 percent series compensation level.

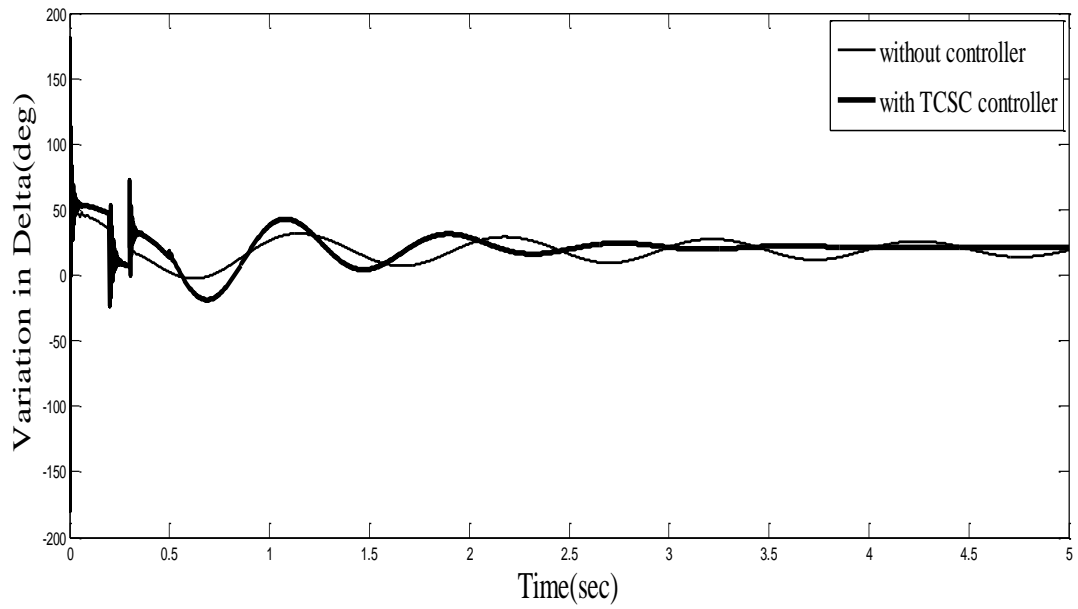


Fig. 5.1.1 Time response of power angle with and without TCSC controller for 20% series compensation

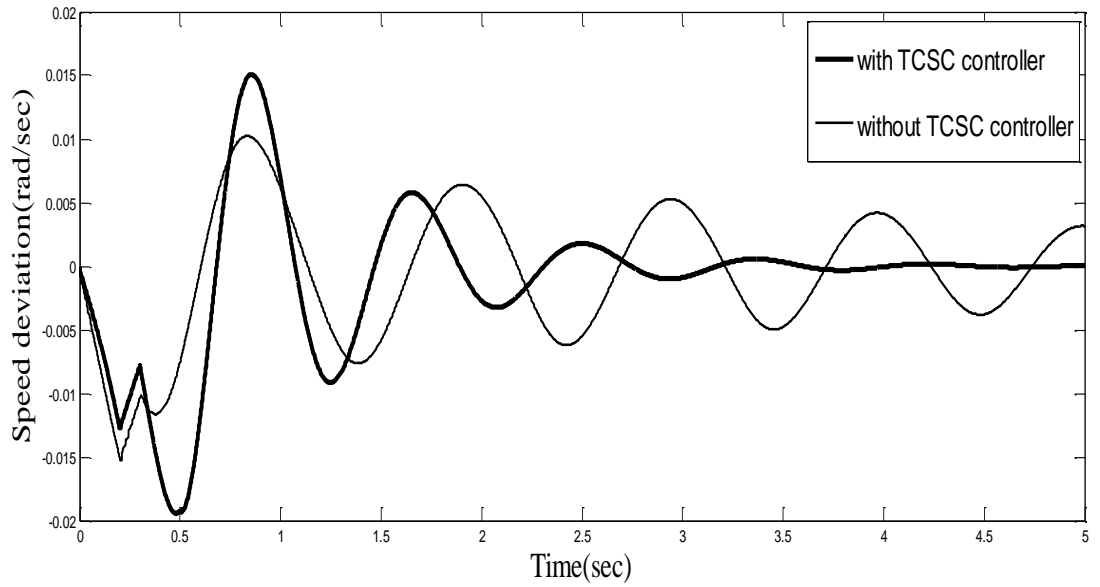


Fig. 5.1.2 Time response of speed variation with and without TCSC controller for 20% series compensation

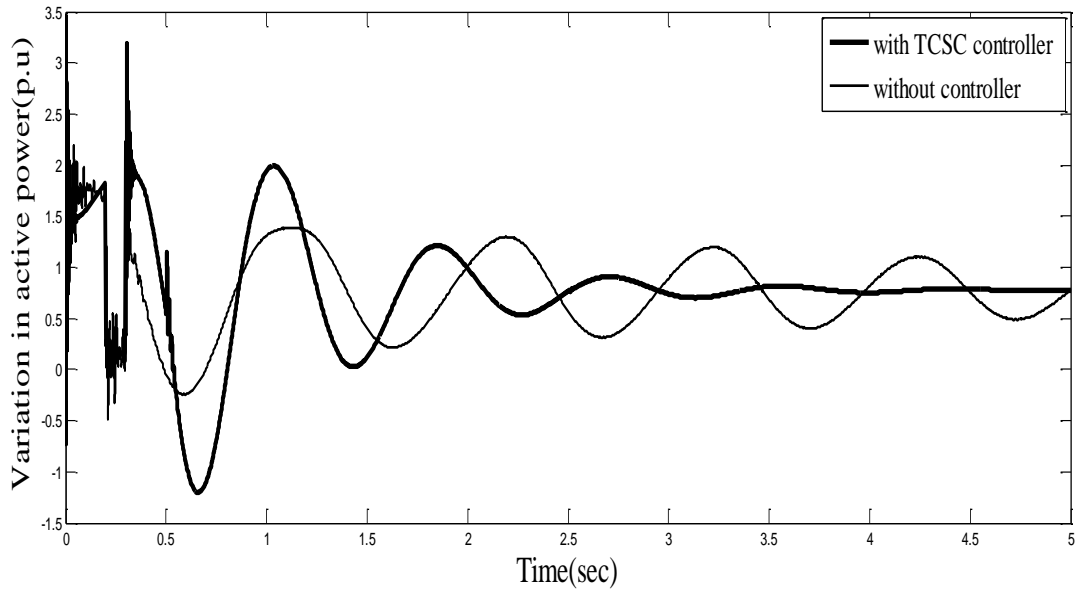


Fig. 5.1.3 Time response of variation in active power with and without TCSC controller for 20% series compensation

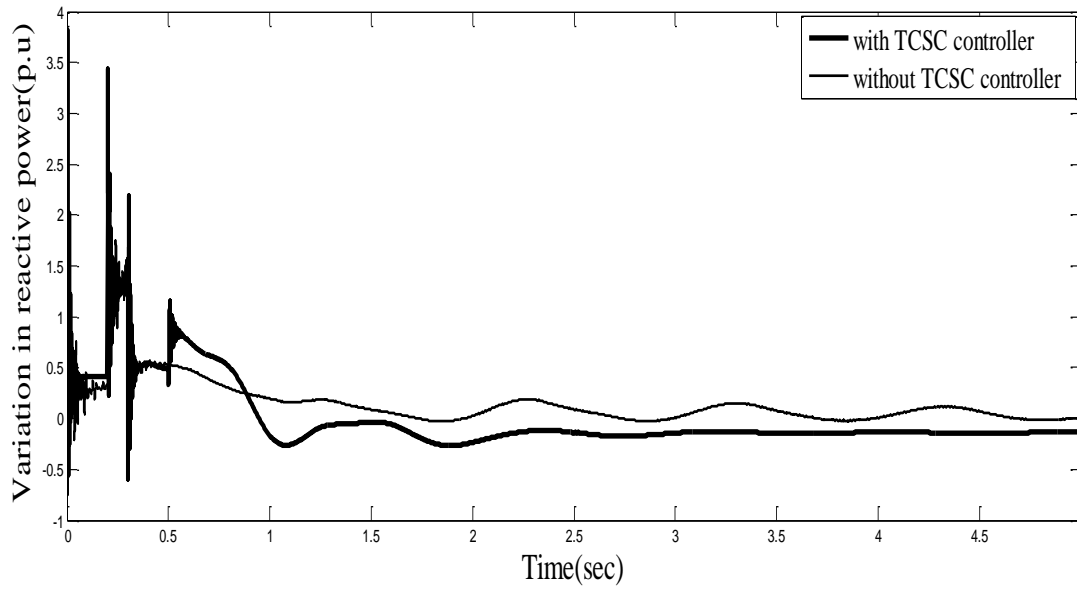


Fig. 5.1.4 Time response of variation in reactive power with and without TCSC controller for 20% series compensation



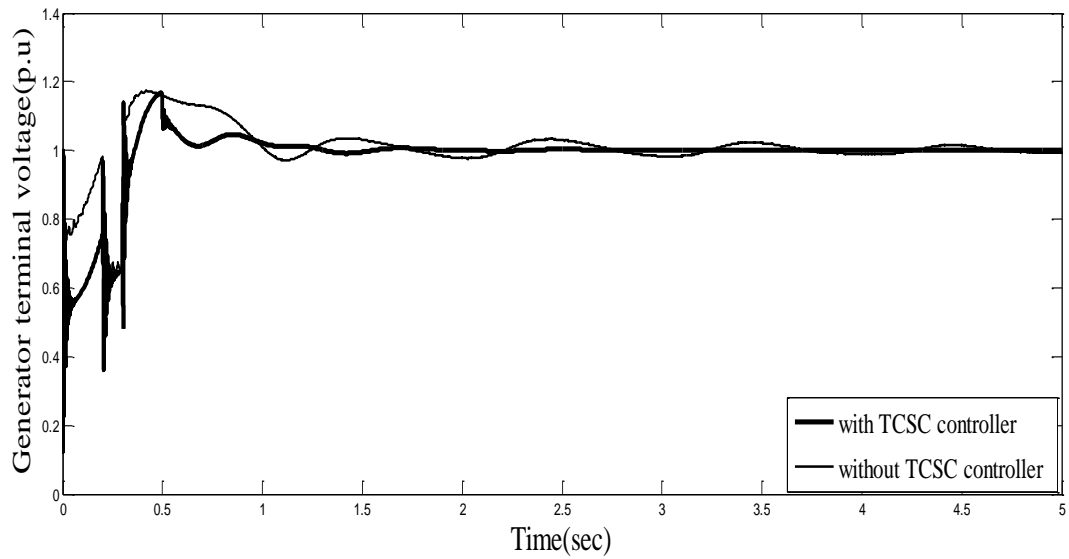


Fig. 5.1.5 Time response of Generator terminal voltage with and without TCSC controller for 20% series compensation

#### 5.2.4 Simulation Results with 50 percent series compensation

The simulations are carried out with and without TCSC controller connected between bus number 3 and 4 for analyzing the transient stability analysis under three phase fault conditions. Fig. 5.2.1 to

5.2.2 are shown for 50 percent series compensation level.

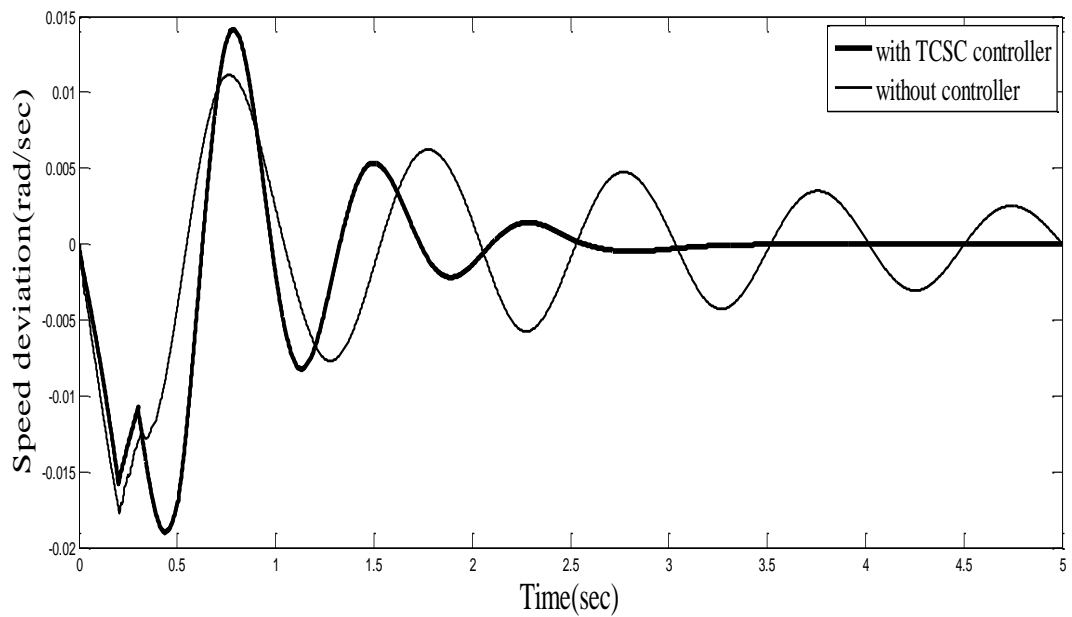


Fig. 5.2.1 Time response of speed deviation with and without TCSC controller for

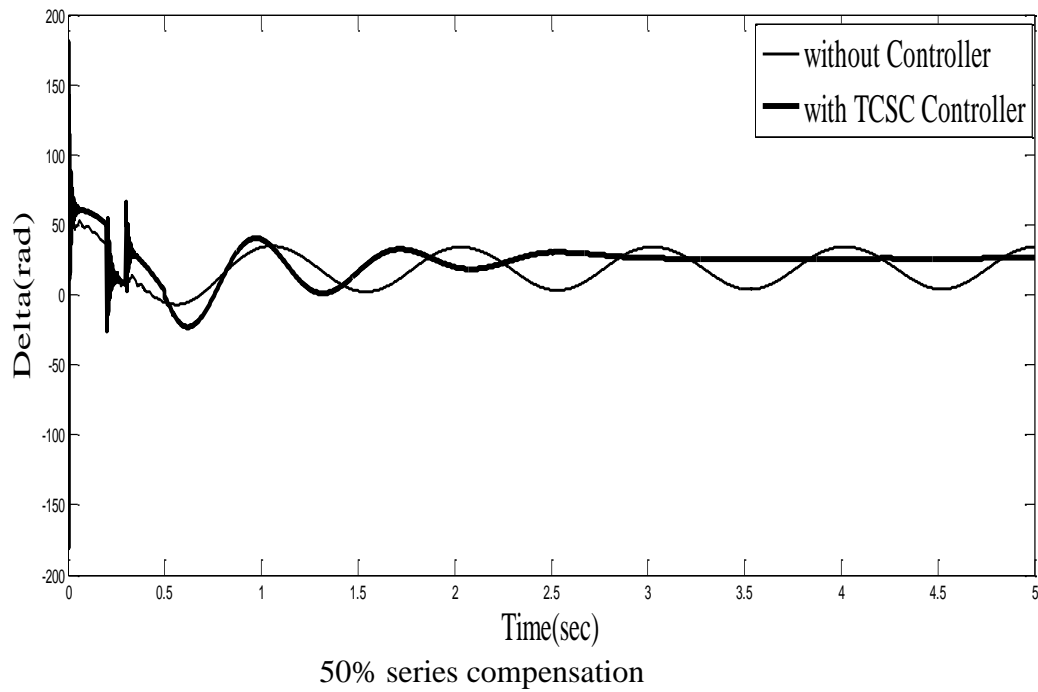


Fig. 5.2.2 Time response of speed deviation with and without TCSC controller for 50% series compensation

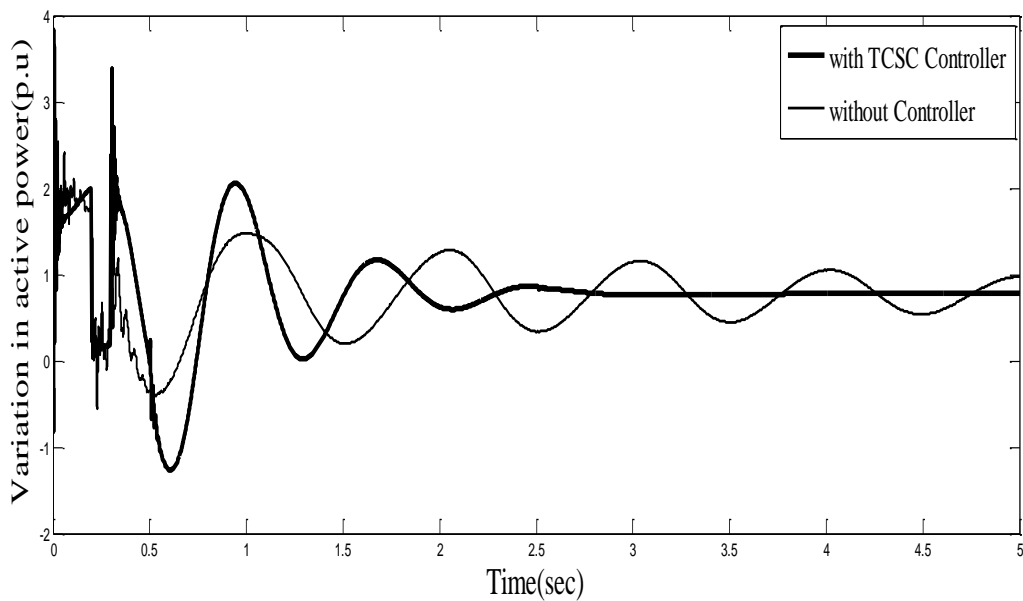


Fig. 5.2.3 Time response of active power variation with and without TCSC controller for 50% series compensation

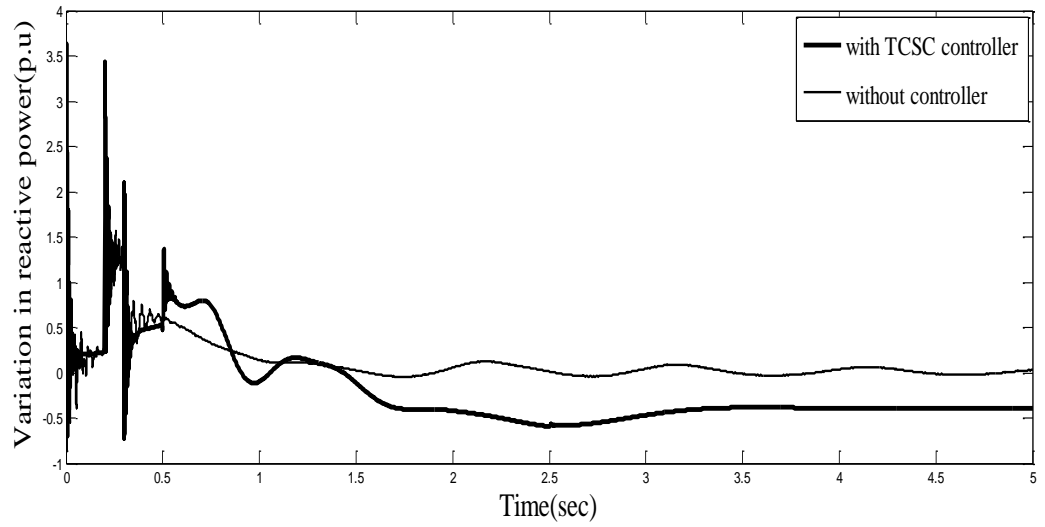


Fig. 5.2.4 Time response of variation in Reactive power with and without TCSC controller for 50% series compensation

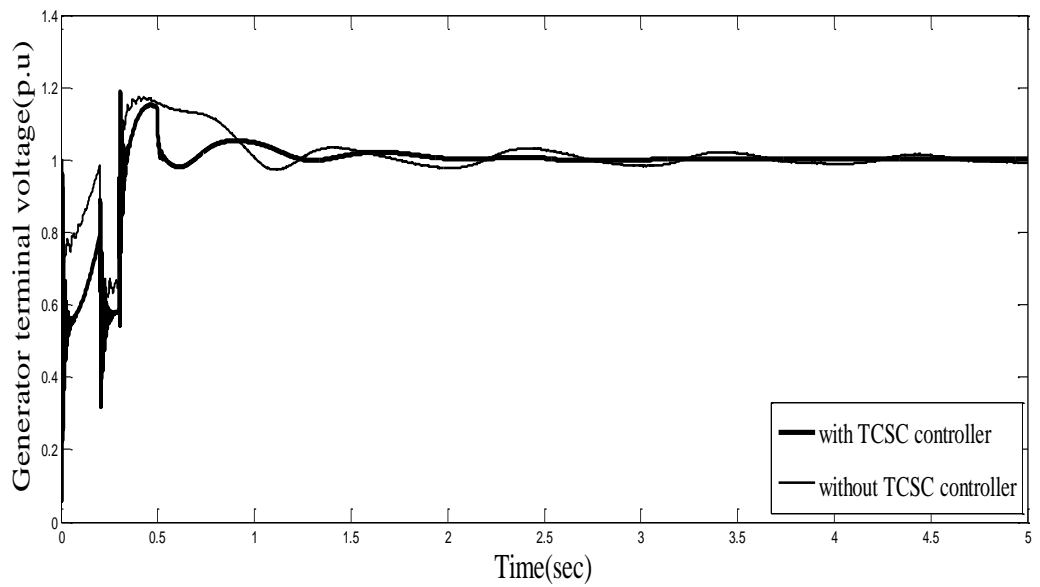


Fig. 5.2.5 Time response of variation in Generator terminal voltage with and without TCSC controller for 50% series compensation

### 5.2.5 Simulation Results with 80 percent series compensation

The simulations are carried out with and without TCSC controller connected between bus number 3 and 4 for analyzing the transient stability analysis under three phase fault conditions. Fig. 5.3.1 to 5.3.5 are shown for 80 percent series compensation level.

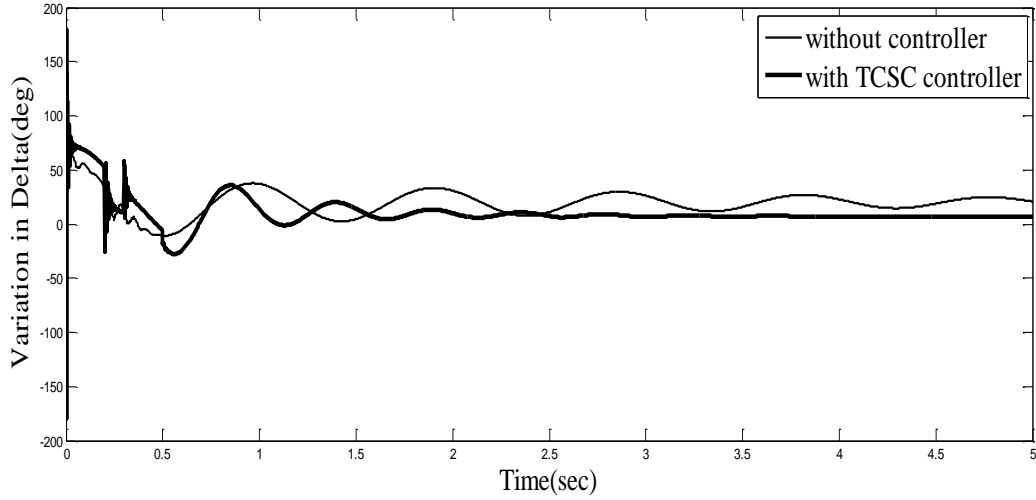


Fig. 5.3.1 Time response of power angle with and without TCSC controller for 80% series compensation

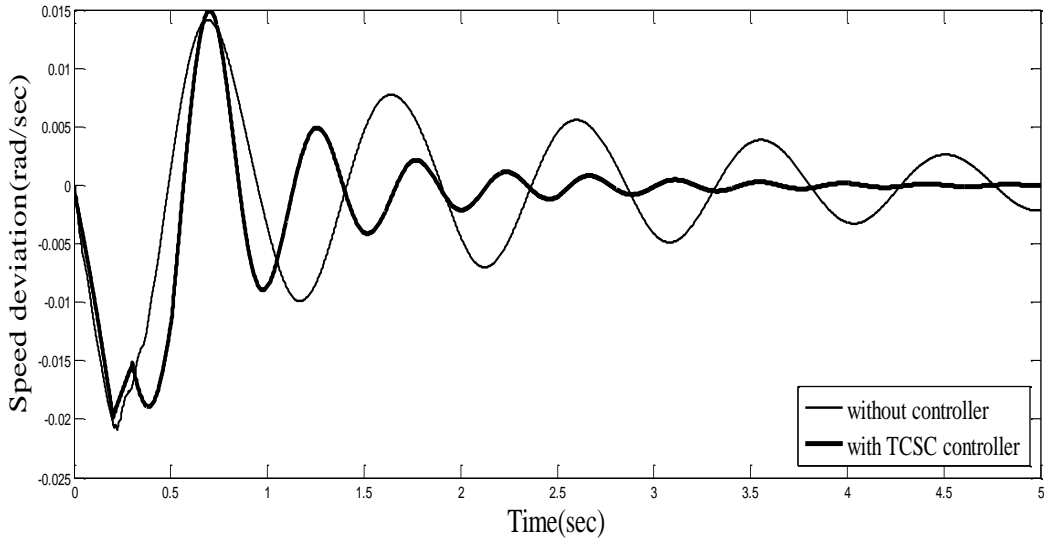


Fig. 5.3.2 Time response of speed deviation with and without TCSC controller for 80% series compensation

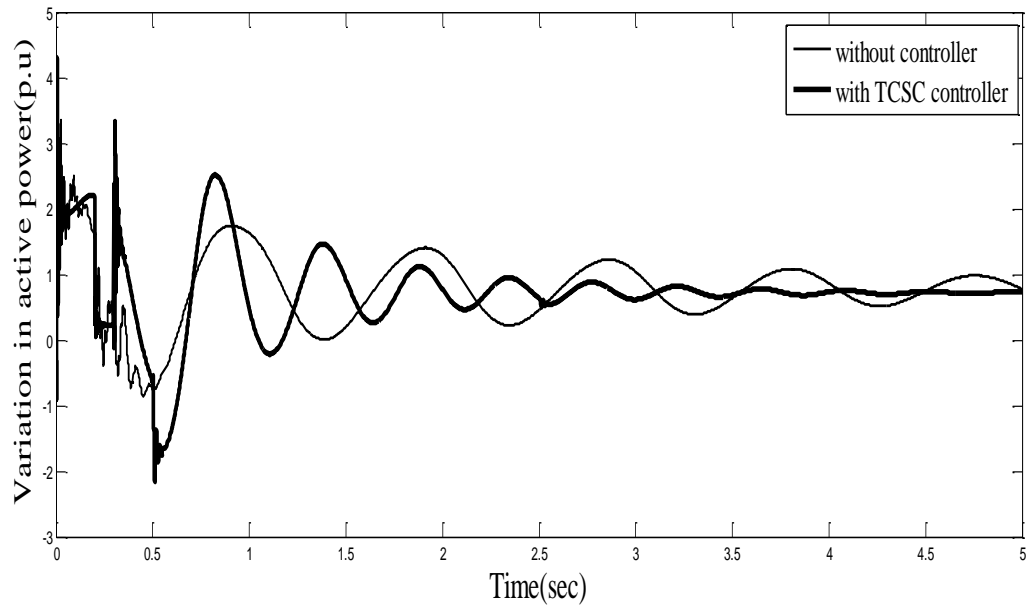


Fig. 5.3.3 Time response of variation in active power with and without TCSC controller for 80% series compensation

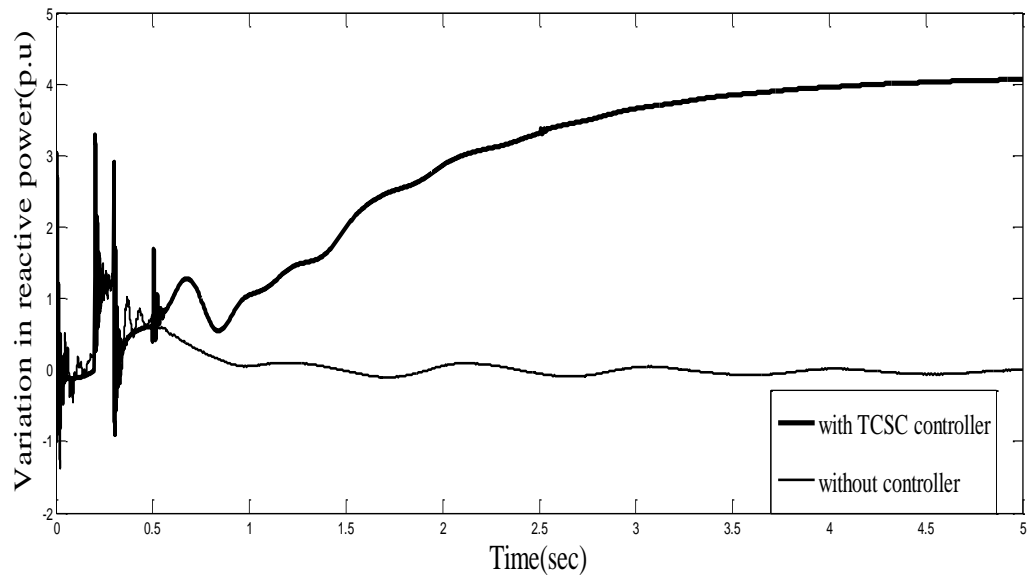


Fig. 5.3.4 Time response of variation in reactive power with and without TCSC controller for 80% series compensation

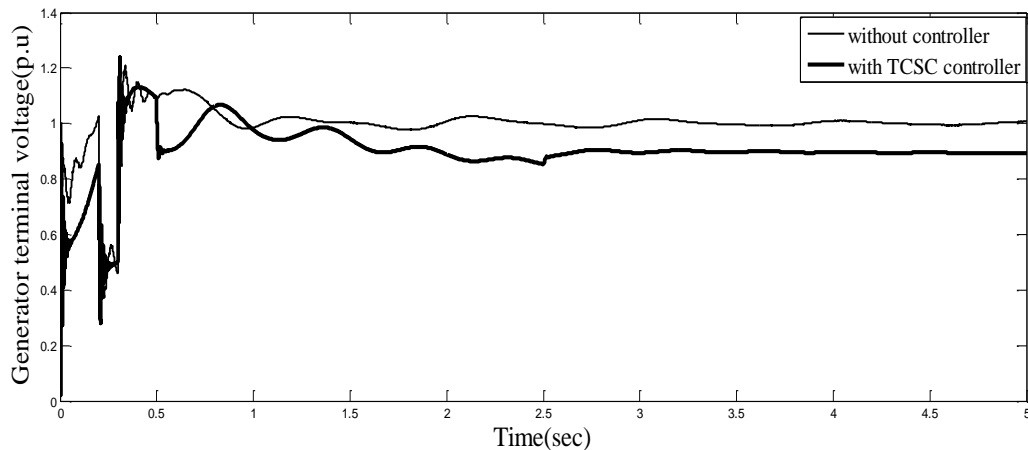


Fig. 5.3.5 Time response of variation in generator terminal voltage with and without TCSC controller for 80% series compensation

### 5.2.6 Discussion

TCSC controller designed has given the satisfactory results for various levels of series compensation, ranging from a value of 20 percent to very high value i.e 80 percent. Present TCSC controller is highly effective for transient stability enhancement for medium level of series compensation as seen from the simulation results for 50 percent compensation level. It has been observed from fig 5.3(iv) that TCSC has to provide large reactive power compensation to maintain the system stability for high level of series compensation.

### 5.3 SYSTEM MODEL-2

One generating unit of 2200 MVA, 24kv and 60 Hz respectively, is connected via long double circuit transmission line to the infinite bus-bar. A TCSC controller is located in series with the transmission line and is connected between bus number 2 and bus number 3. Six order machine system is considered.  $P=0.4$  p.u is taken as the initial system operating condition, with quantities expressed in p.u. on generator base MVA. For analyzing the Transient stability, a three phase fault is created for 0.2 sec at third bus. The Simulation for transient stability is carried out with and without TCSC controller. The system data and controller data are given in appendix C. Eigenvalue analysis is carried out for analyzing the dynamic behavior of the system. Enhancement of power transfer capability of the system is also analyzed.

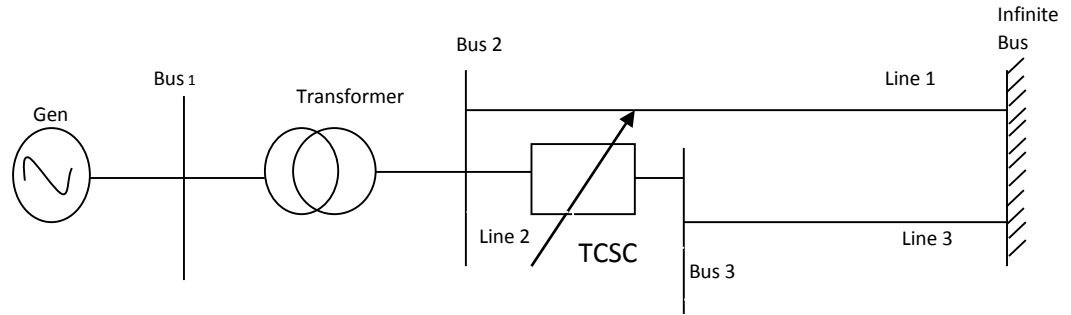


Fig 5.4 Single line diagram of SMIB system connected with TCSC Controller.

### 5.3.1 TCSC Controller Structure

The following structure of TCSC controller is implemented for performance enhancement of the power system network shown in fig. 5.5.  $k_r$  and  $T_r$  are the regulator gains and time constant respectively and  $K_p$  and  $K_i$  are parameters of PI controller. Values of which are optimized to achieve system stability. The controller parameters are given in appendix C.

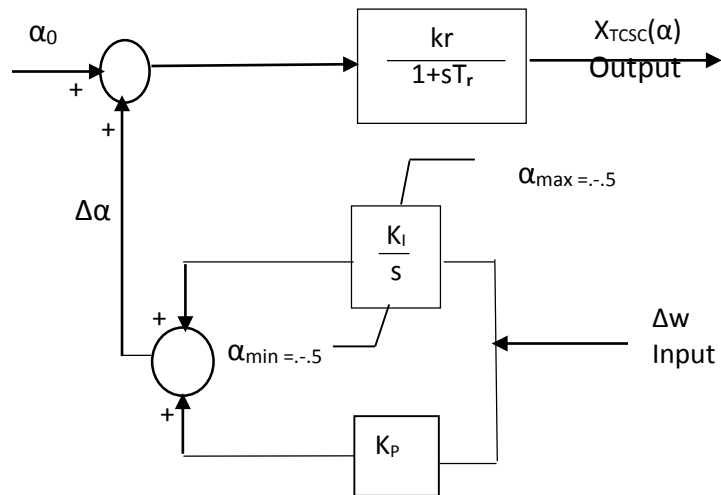


Fig. 5.5 Single line diagram of representation of TCSC controller

### 5.3.2 Simulation Results

The three phase fault is created for 0.2 sec and transient stability analysis is carried out without and with TCSC controller. The simulation is carried out in PSAT software.

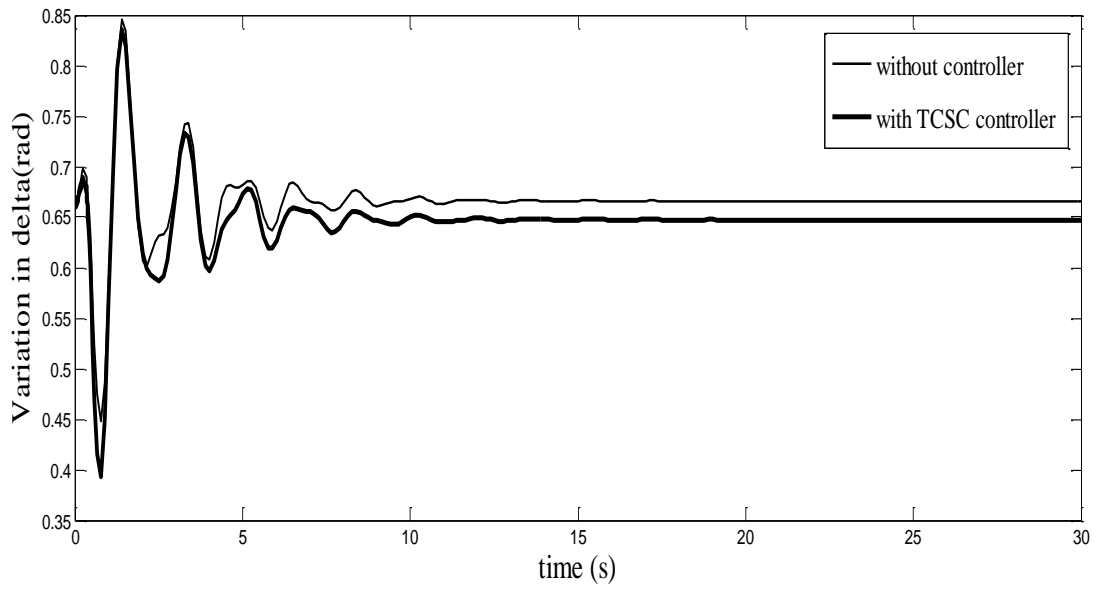


Fig. 5.6.1 Time response of variation in delta with and without TCSC controller.

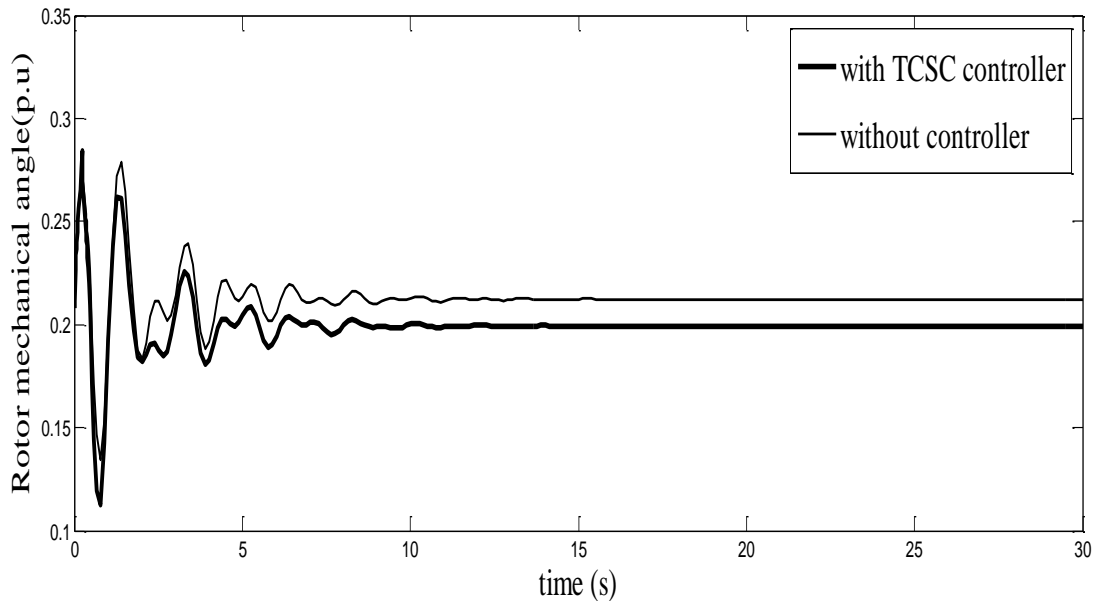


Fig. 5.6.2 Time response of variation in rotor mechanical angle with and without TCSC controller



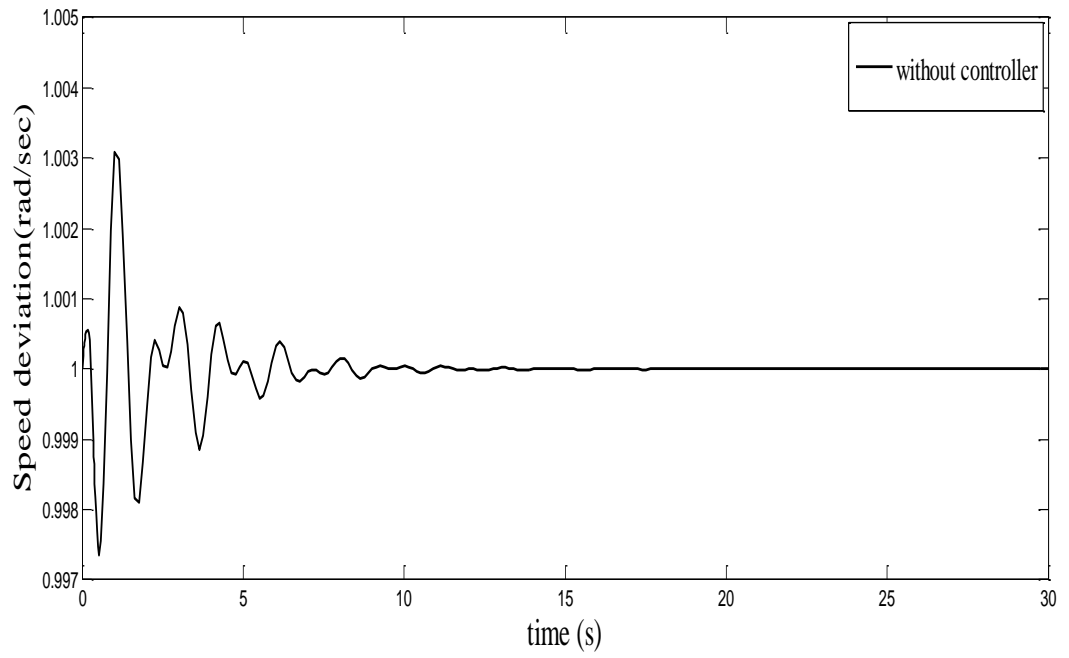


Fig. 5.6.3 Time response of speed deviation without TCSC controller

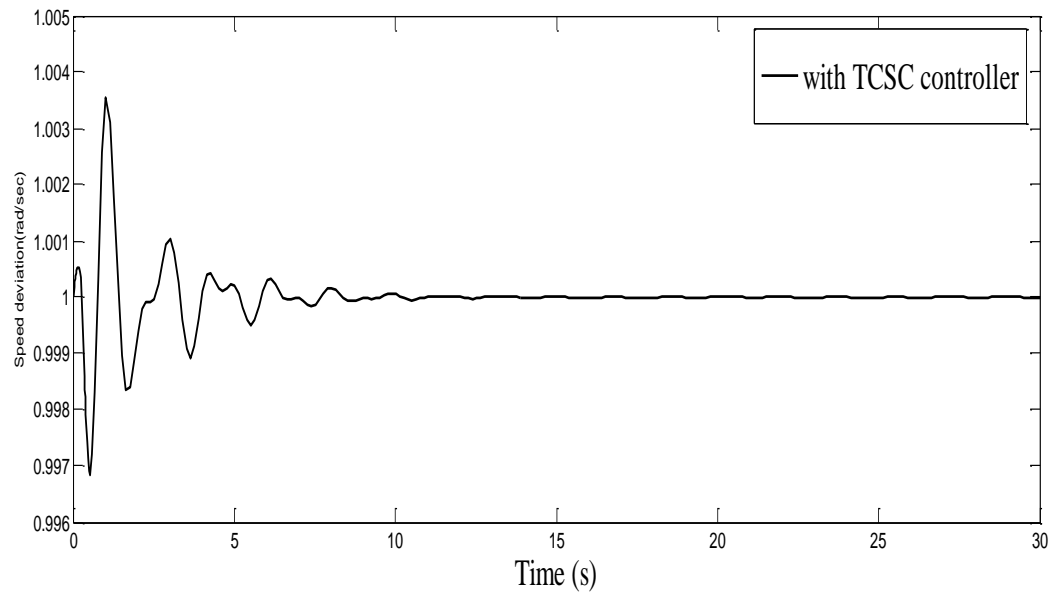


Fig. 5.6(iv) Time response of speed deviation with TCSC controller

**Table 5: Active and Reactive Power Flow in Line with and without TCSC controller**

<b>Without TCSC</b>		
<b>Line</b>	<b>P Flow (p.u)</b>	<b>Q Flow (p.u)</b>
1	5.7634	3.1526
2	3.1165	1.6615
3	3.1104	1.1781
4	8.8799	5.5554

<b>With TCSC controller</b>		
<b>Line</b>	<b>P Flow(p.u)</b>	<b>Q Flow(p.u)</b>
1	3.5306	2.4413
2	5.3494	3.6989
3	5.3494	3.2807
4	8.88	7.0046

**Table 6: Comparison of Eigenvalue Report with and without TCSC Controller.**

<b>Statics</b>	<b>With TCSC controller</b>	<b>Without controller</b>
Dynamic Order	11	9
Negative Eigen	10	9
Positive Eigen	0	0
Complex pair	2	2
Zero Eigen	1	0

**Table 7: Eigenvalues of the system with or without TCSC controller**

<b>. With TCSC controller</b>	<b>Without controller</b>
-66.4095 +j 0	-66.4058 +j 0
-37.5354 +j 0	-37.4111 +j 0
-21.5161+j 0	-21.2286 +j 0
-0.53107 +j 6.7858	-0.49843 +j6.6579
-0.53107-j6.7858	-0.49843 -j 6.6579
-0.44784 +j3.6672	-1.437-j 0
-0.44784-j3.6672	-0.4373+j3.7157
-1.4441+j 0	-0.4373 -j3.7157
-1+j0	-1+j 0
-2+j0	-----
0+j0	-----

### 5.3.3 Discussion

The results reveal that TCSC controller does not only enhance the power transmission in the line to which it is connected but also damp the power system oscillations effectively under severe contingency. By connecting TCSC in line 2 which is connected in series with line 3, the line flow has increased from 3.1165p.u in line 2 to 5.3494p.u and from 3.1104 p.u to 5.3494 p.u in line 3. Thus enhances the power transfer capability of the line. Dynamic performance is also enhanced as seen from the Eigen value analysis table. Almost all Eigenvalues have become more negative by connecting TCSC controller in the power system network. The Transient analysis is also carried out and as seen from fig. (5.6(i) to 5.6(iv)) that power oscillations have been damped effectively with TCSC controller in comparison to without controller.

### 5.4 SYSTEM MODEL-3

The study system consists of a generating unit of 2200 MVA, 24kV and 50 Hz respectively, is connected via long transmission line to the infinite bus-bar. A TCSC controller is installed in series with the long transmission line.  $R_T$  and  $X_T$  are the resistance and reactance of the transmission line.  $R_T$  is neglected in comparison to  $X_T$ .  $V_T$  and  $E_B$  are generator terminal voltage and the infinite bus-bar voltage. For analyzing the steady state stability, disturbance of 10% in mechanical input power is given for a duration of 100msec. All the parameters are expressed in p.u. on generator base MVA. A synchronous machine is represented by model 1.1, considering field winding in the d-axis and only one damper winding in the q axes. Also, the armature resistance of the machine is neglected and the excitation system is represented by a single time-constant system. The single line diagram of the study system is shown in fig 5.12. TCSC is represented by variable reactance model. All system parameters are given in appendix B.

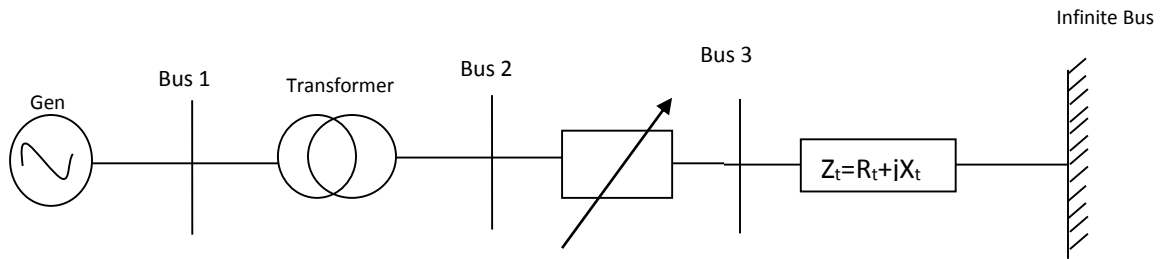


Fig. 5.7 Single line representation of study system

#### 5.4.1 Linearized Model of SMIB

The same linearized model of SMIB system as developed in chapter 4 is used. The nonlinear equations and algebraic equations are linearized around an operating point. In the current model, the linearized constants are dynamically varying and not fixed as in the case described in chapter 4. They change according to the continuous variation in the reactance of TCSC controller which alters the line reactance, in turn regulate the power flow and subsequently mitigate the electromechanical power system oscillations. The controller parameters are optimized by trial and error method to reduce the oscillations quickly and thereby enhance the stability of the SMIB system.

SMIB system is represented by the following Nonlinear differential equations:

$$p\delta = w_B(w-1) \quad (5.1)$$

$$pw = \frac{1}{M} [T_m - T_e - Dw]$$

(5.2)

$$pE'_q = \frac{1}{T'_{do}} [E_{fd} - E'_q + (x_d - x'_d) i_d]$$

(5.3)

$$pE_{fd} = \frac{(K_E (V_{Ref} - V_T)) - E_{fd}}{T_E}$$

(5.4)

Where,  $p=d/dt$ ,  $w$ =rotor speed,  $E_{fd}$ =excitation voltage,  $E_q$  = internal generator voltage,  $K_E$  and  $T_E$  are voltage regulator gain and time constant respectively,  $T_m$  and  $T_e$  are mechanical and electrical torque respectively and  $D$  is damping factor which is taken as zero.

$$V_T = v_q + jv_d$$

(5.5)

$$v_d = E'_d - x_q i_q \text{ and } v_q = E'_q + x'_d i_d$$

(5.6)

On Linearizing the above 8 equations around an operating point, we have the following linearized equations:

$$p\Delta\delta = w_B \Delta w$$

(5.7)

$$p\Delta w = \frac{1}{M} [-D\Delta w + \Delta T_m - \Delta T_e]$$

(5.8)

$$p\Delta E'_q = \frac{1}{T'_{do}} [\Delta E_{fd} + (x_d - x'_d) \Delta i_d - \Delta E'_q]$$

(5.9)

$$\Delta p E_{fd} = \frac{(K_E (\Delta V_{Ref} - \Delta V_T)) - \Delta E_{fd}}{T_E}$$

(5.10)

$$\Delta T_e = [\Delta E'_{q0} - (x'_q - x'_d) i_{d0}] \Delta i_q - (x'_q - x'_d) i_{q0} \Delta i_d + i_{q0} \Delta E'_q$$

$$\Delta T_e = K_2 \Delta E'_q + K_1 \Delta \delta$$

(5.11)

where..... $K_1 = \{E'_{q0} a_4 + i_{q0} - (x'_q - x'_d) i_{q0} a_2\} a_3 - ((x'_q - x'_d) i_{q0} a_1$

$$\Delta v_T = K_5 \Delta \delta + K_6 \Delta E'_q \quad (5.12)$$

### 5.4.2 TCSC Controller

Reactance model of TCSC has been developed. TCSC controller is represented by the gain block  $K_G$ , wash out block which act as a as a high-pass filter having  $T_w$  as time constant sufficiently large to permit the oscillations present in the input signal to pass unchanged. It is followed by a lead lag compensator and PI controller. The parameters of controller are given in appendix B. The input signal of the proposed controller is the speed deviation ( $\Delta \omega$ ), and the output signal is the reactance offered by the TCSC.

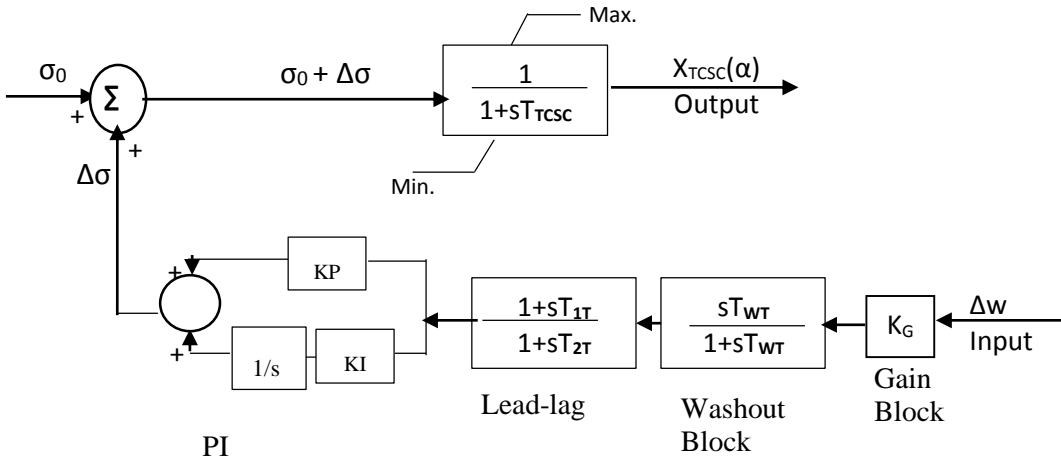


Fig 5.8 Representation of TCSC controller structure

The net reactance of TCSC controller is given by the parallel combination of capacitive reactance and inductive reactance which is a function of firing angle  $\alpha$ .

$$X_{TCSC}(\alpha) = \frac{X_C X_L(\alpha)}{X_L(\alpha) - X_C} \quad (5.13)$$

$$X_L(\alpha) = X_L \frac{\pi}{\pi - 2\alpha - \sin \alpha}$$

Where  $X_L \leq X_L(\alpha) \leq \infty$

During steady state conditions, value of  $\sigma_0$  is constant and value of  $\Delta \sigma$  is zero. While during dynamic conditions, conduction angle  $\sigma$  and hence  $X_{TCSC}(\alpha)$  is modulated to improve the power

system stability. The desired value of compensation is obtained through the change in the conduction angle  $\Delta\sigma$ , according to the speed deviation ( $\Delta w$ ). The effective value of conduction angle  $\sigma$  during dynamic conditions is given as :

$$\sigma = \sigma_0 + \Delta\sigma$$

Effective line reactance =  $X_e - X_{TCSC}(\alpha)$ , where  $X_e$  is the fixed reactance of the network. TCSC is operated in capacitive mode only as modelling is difficult for stability studies due to large harmonics produced when operating in inductive mode.

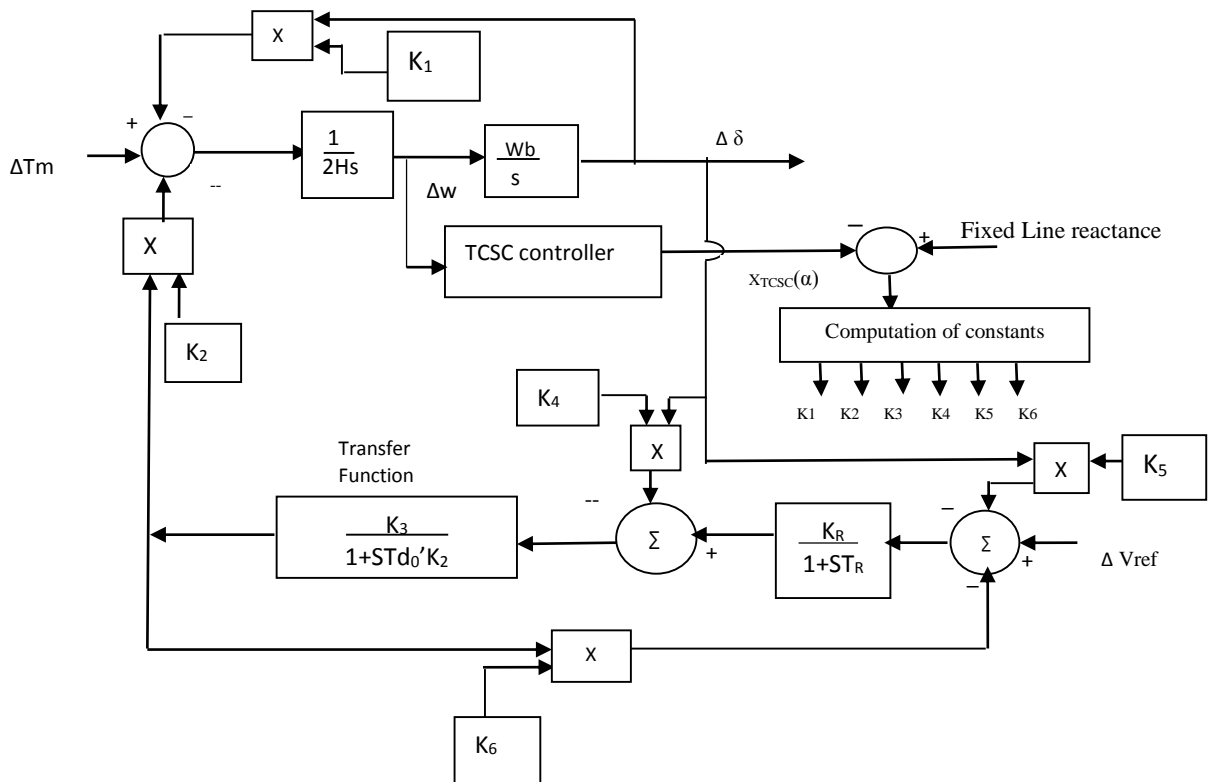


Fig. 5.9 Single line diagram of linearized model of SMIB with TCSC Controller

### 5.4.3 Simulation Results

Computer simulation is carried by considering three cases and the TCSC controller parameters and excitation parameters are tuned by hit and trial method for performance enhancement of the power system network. In the first case, the disturbance of 10% is given in mechanical input power. The variation in rotor angle, rotor speed, generator terminal voltage and active power are plotted. In second case the system is resumed back by removing the disturbance after 100msec

and all the variations are again noted down and finally in the third case, severe fault is created by one line outage.

### Case 1

Disturbance of 10% is given in input mechanical power. The simulation results are shown in fig 5.10 .1 to 5.10.4.

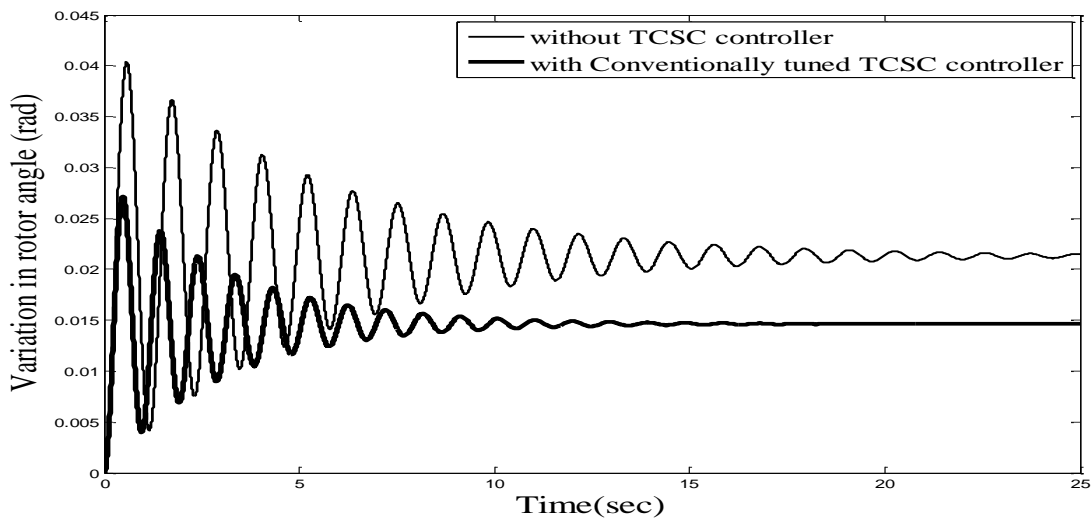
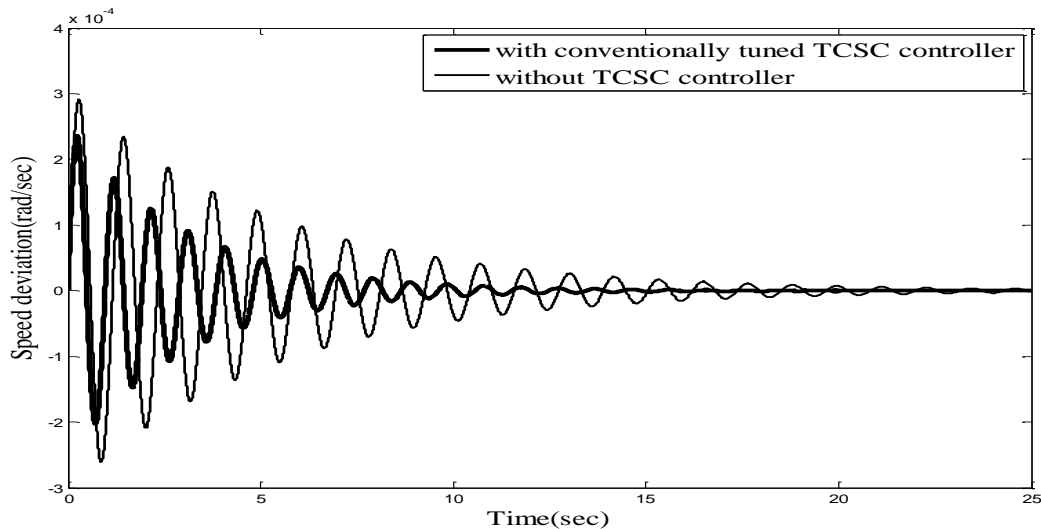
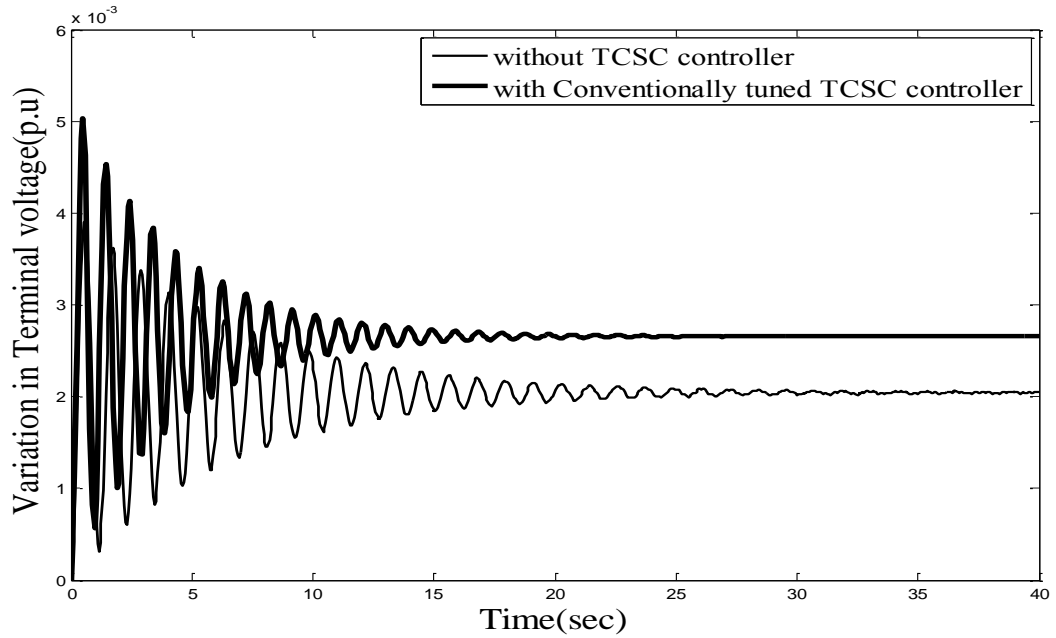


Fig. 5.10.1 Time response of rotor angle variation without and with conventionally tuned TCSC controller

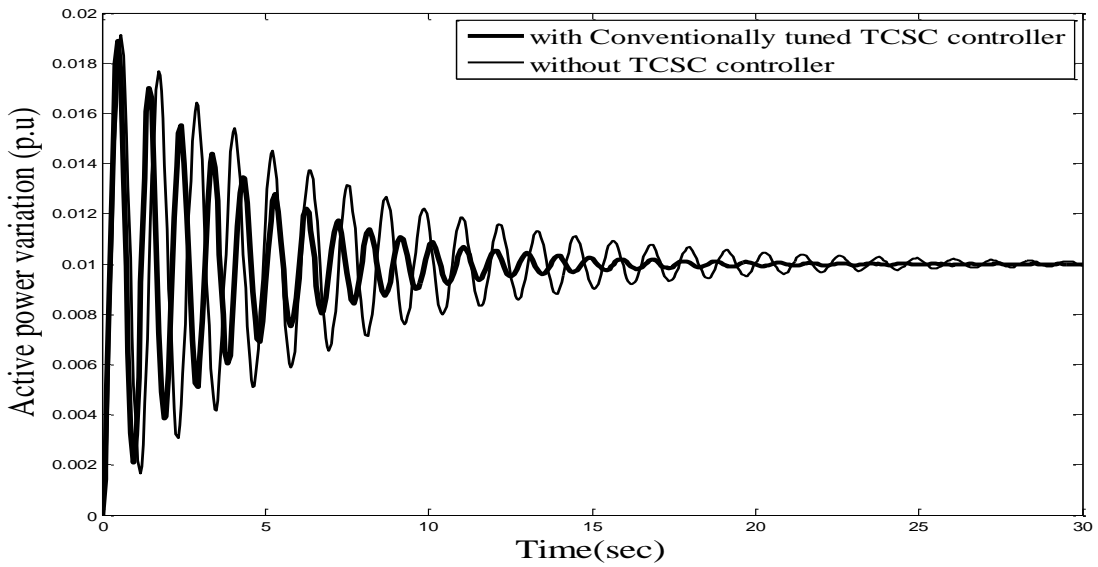


5.10.2 Time response of speed deviation without and with conventionally tuned TCSC controller





5.10.3 Time response of variation in generator terminal voltage without and with conventionally tuned TCSC controller



5.10.4 Time response of variation in active power without and with conventionally tuned TCSC controller

## Case 2

System is resumed after giving disturbance of 10% in 100msec in input mechanical power. The simulation results are shown in fig 5.11.1 to 5.11.4.

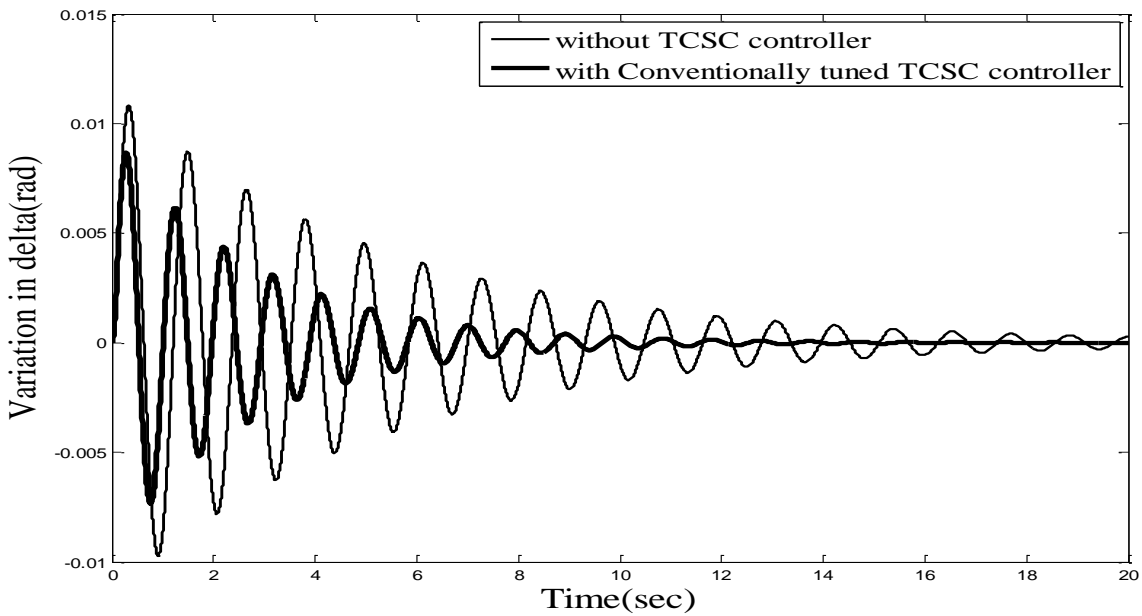
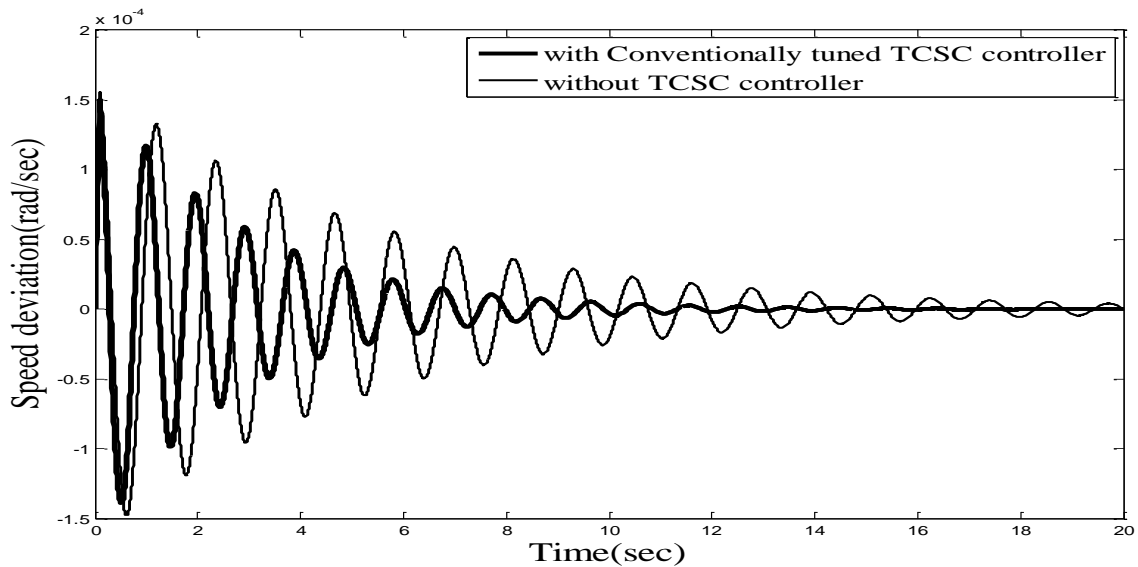
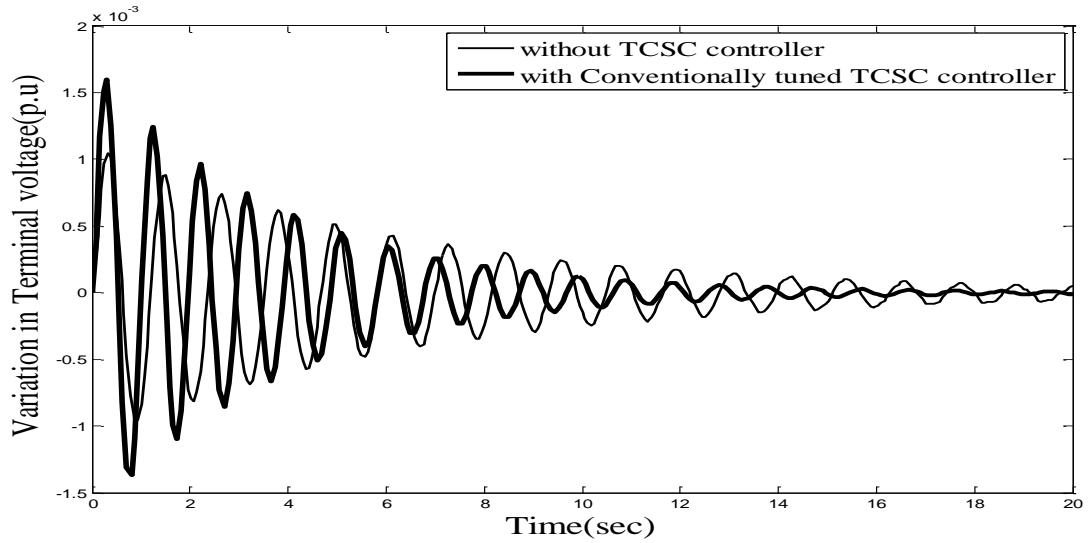


Fig. 5.11.1 Time response of rotor angle variation without and with conventionally tuned TCSC controller



5.11.2 Time response of speed deviation without and with conventionally tuned TCSC controller



5.11.3 Time response of variation in generator terminal voltage without and with conventionally tuned TCSC controller

**Case 3**

Severe fault is created by simulating the model with one line outage. Figure 5.12.1 to 5.12.3 shows the variation in rotor angle, speed deviation and terminal voltage. The first transient swing has considerably reduced and the machine has stabilized to a lower power angle, thereby increased the stability margin as depicted from the response.

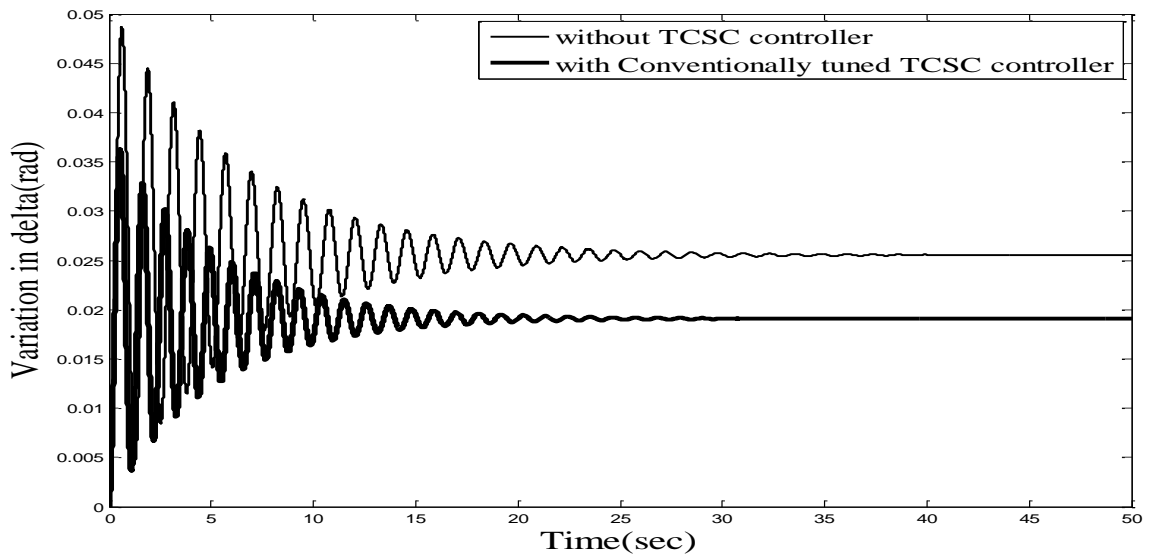
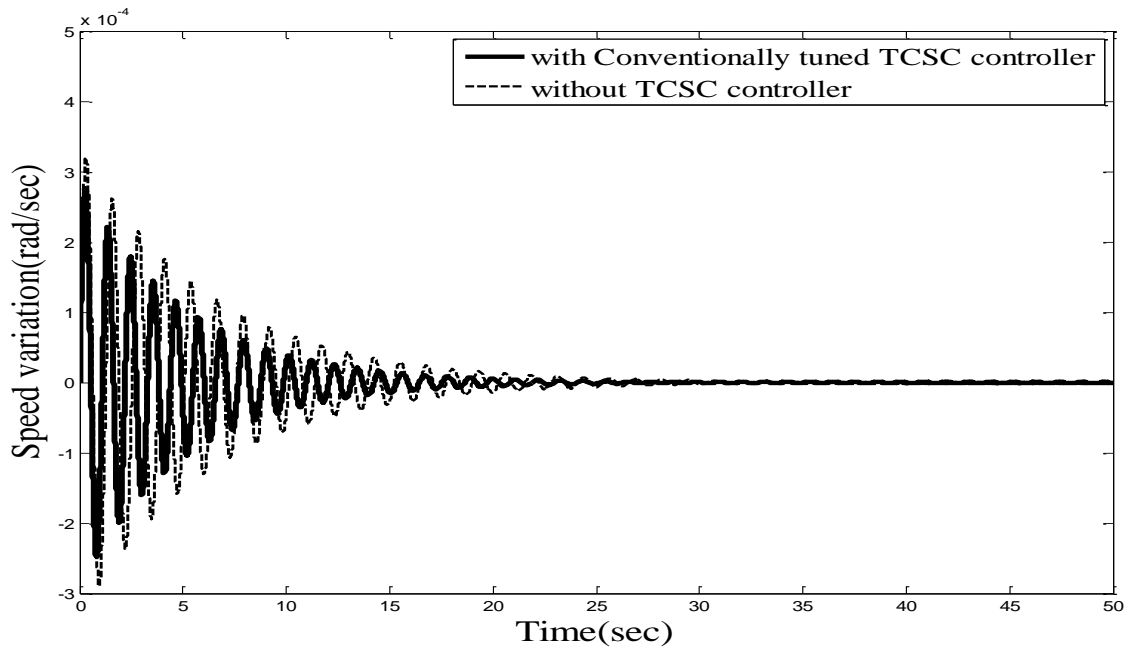


Fig. 5.12.1 Time response of rotor angle variation without and with conventionally tuned TCSC controller (with one line outage)



5.12.2 Time response of speed deviation without and with conventionally tuned TCSC controller (with one line outage)

#### 5.4.4 Optimizing the parameters of TCSC Controller using Particle swarm optimization for small signal stability enhancement

Particle swarm optimization technique as described in chapter 3 has been implemented using Mat lab coding for optimizing the TCSC controller parameters. Appropriate number of particles, inertia weight and acceleration coefficients are chosen and the following Objective function is formulated

$$J = \int_0^t \left[ (\Delta\omega(t, x))^2 + (\Delta v_t(t, x))^2 \right] dt \quad (5.14)$$

Main objective of optimization is to reduce the change in rotor speed, rotor angle and generator terminal voltage. In this case, speed deviation and terminal voltage variation are taken as error signal in an ITSE function. The parameters of PSO used are given in appendix B. PSO algorithm is implemented for optimizing both excitation and TCSC controller parameters. The simulation results depicting the comparison between conventionally tuned TCSC controller and PSO based TCSC controller are given in fig. 5.13.1 to 5.13.4 for case 1 and fig. 5.14.1 to 5.14.3) for case 2.

**Case 1**

Disturbance of 10% deviation in mechanical input is given for 100msec. Simulation results are shown in the figures given below.

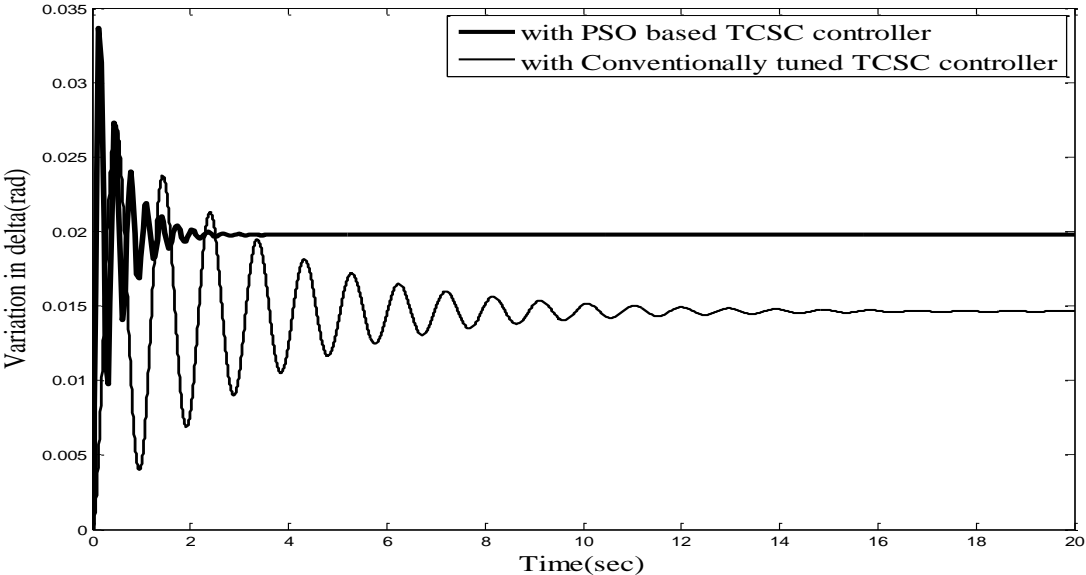


Fig. 5.13.1 Time response of rotor angle variation with conventionally tuned and PSO based TCSC controller

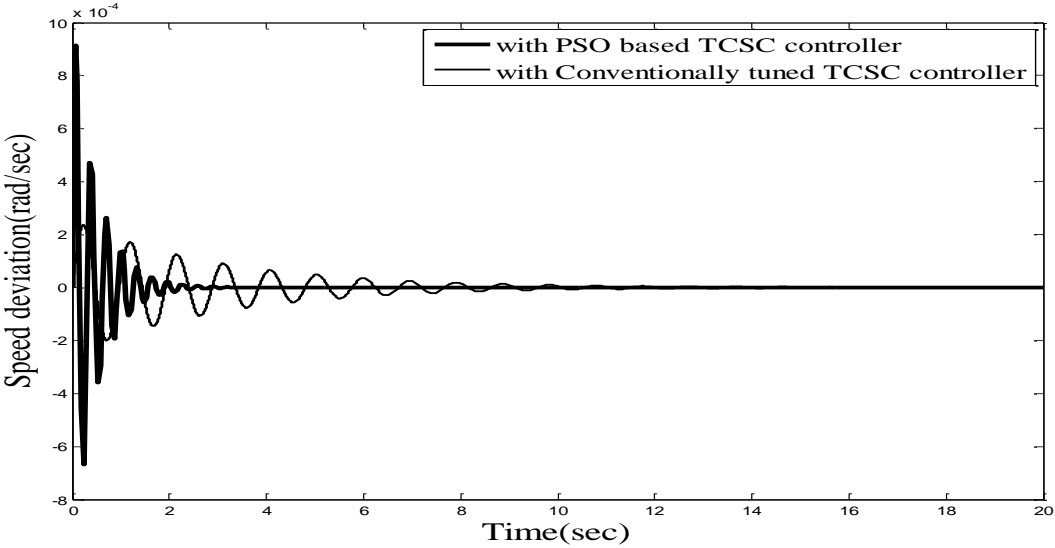


Fig. 5.13.2 Time response of speed deviation with conventionally tuned and PSO based TCSC controller

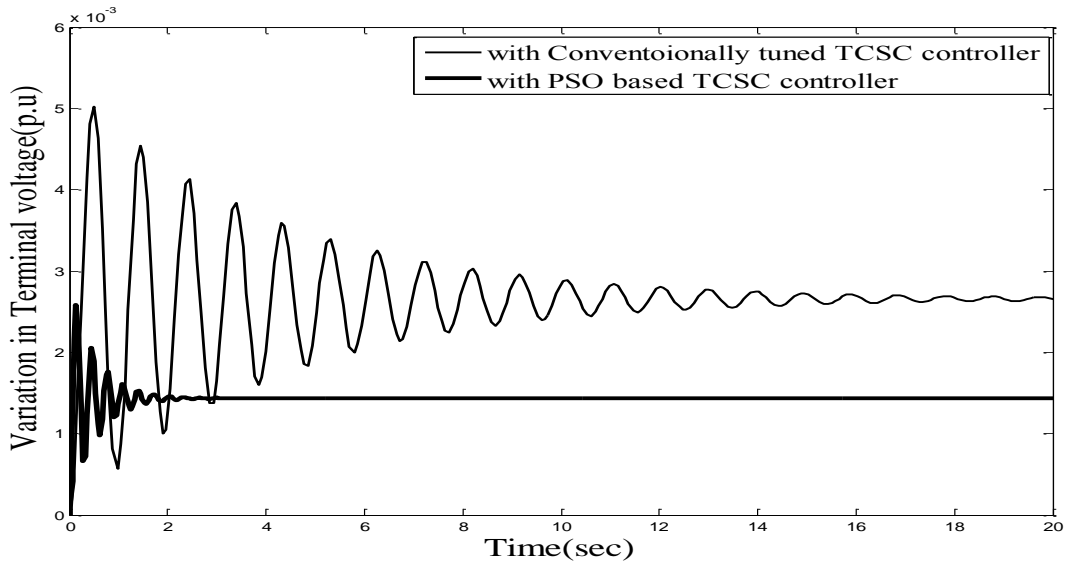
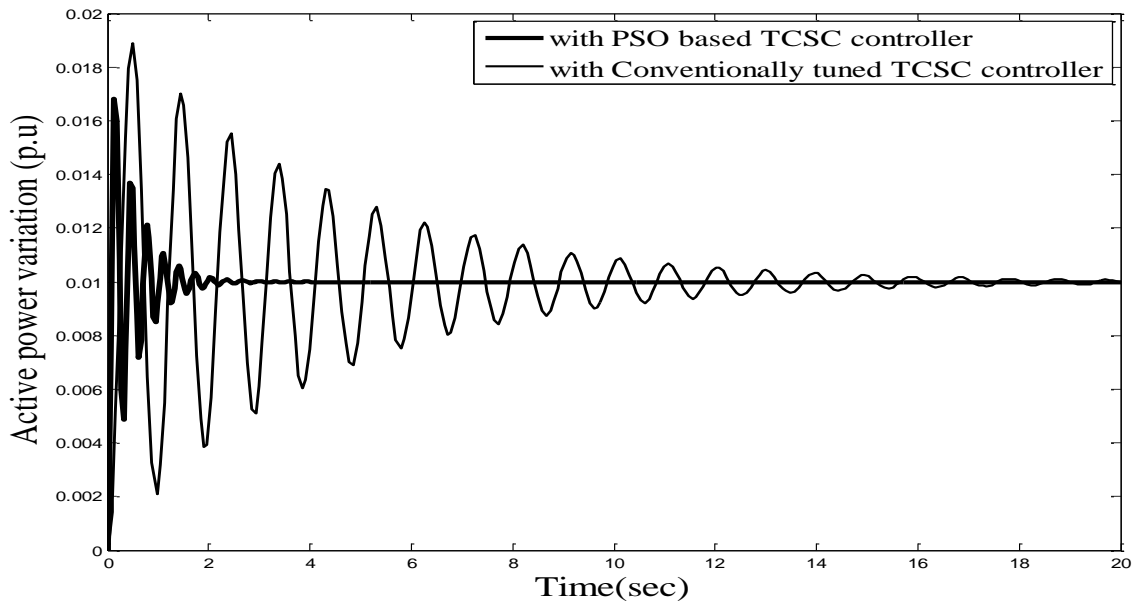


Fig. 5.13.3 Time response of generator terminal voltage with conventioionally tuned and PSO based TCSC controller



5.13.4 Time response of variation in active power with conventioionally tuned and PSO based TCSC controller

## Case 2

System is resumed after giving disturbance of 10% in 100msec in input mechanical power. The simulation results depicting the comparison of PSO based TCSC controller with that of the conventional one incorporated in an SMIB system are shown in fig 5.14.1 to 5.14.4.

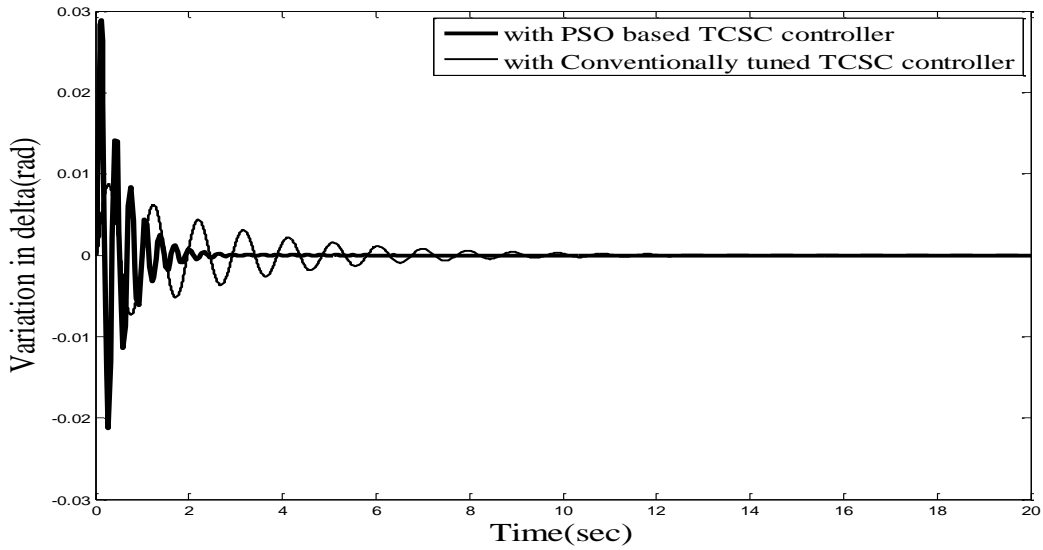


Fig. 5.14.1 Time response of rotor angle variation with conventionally tuned and PSO based TCSC controller

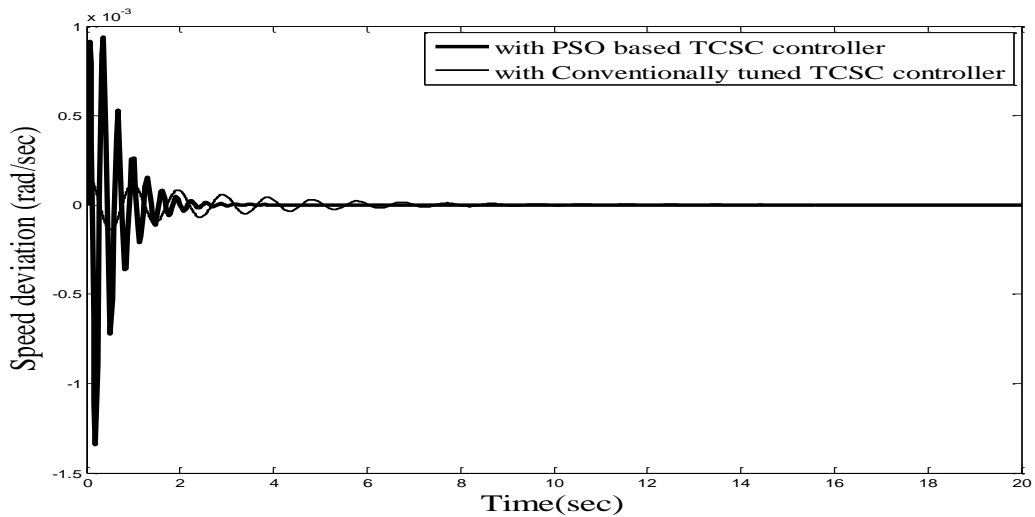


Fig. 5.14.2 Time response of speed deviation with conventionally tuned and PSO based TCSC controller

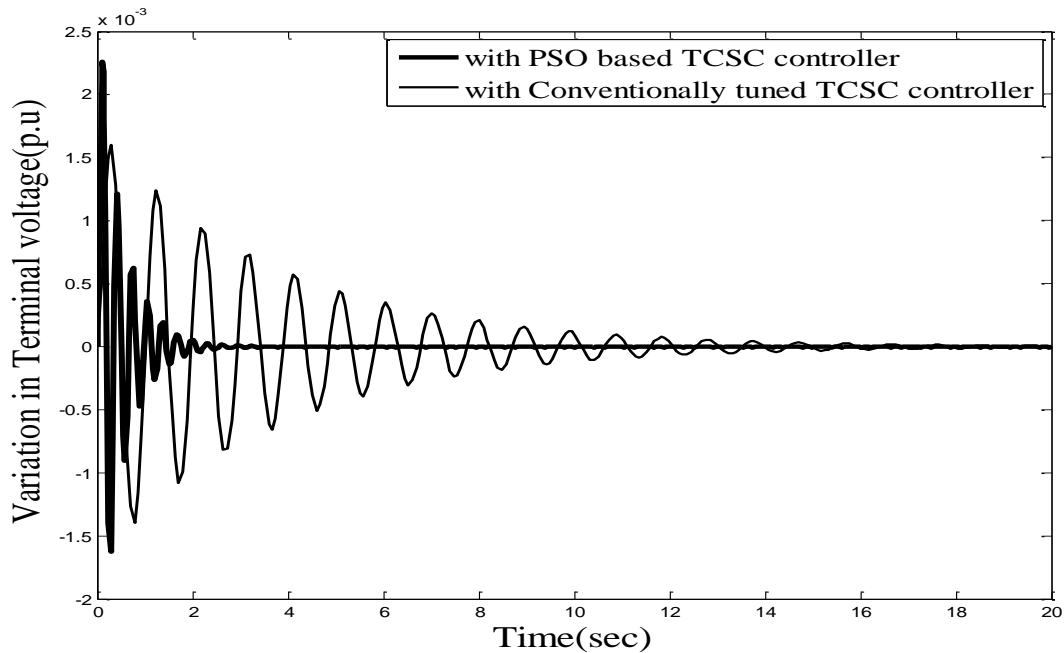


Fig. 5.14.3 Time response of generator terminal voltage with conventionally tuned and PSO based TCSC controller

#### 5.4.5 Discussion

Simulation results show that PSO based TCSC controller is more effective than the conventionally tuned TCSC controller in damping the power system oscillations. Fig 5.10.1 shows that after the disturbance, the machine stabilizes to a new machine angle with TCSC controller. Moreover the use of TCSC controller has increased the rotor stability margin as the rotor angle settles down to a smaller angle. Since the conventional method of optimizing the controller parameters is time consuming and sometimes the solution may not converge, hence AI technique (PSO) is implemented to develop the Controller for stability enhancement. PSO algorithm is very simple and easy to implement using Mat-lab coding for the global search of optimized parameters in m-dimensional search space and the same has been proved from the simulation graphs shown in fig. 5.13.1 to 5.13.4. In case 2, when disturbance of 10% in mechanical input power is removed at 100 msec after the initiation of the perturbation, SMIB system with TCSC controller is highly effective in bringing the system to the steady state condition as seen in figures from 5.14.1 to 5.14.3 and thus enhances the performance of the SMIB system.



# CHAPTER 6

## PERFORMANCE ENHANCEMENT OF POWER SYSTEM USING UNIFIED POWER FLOW CONTROLLER

### 6.1 INTRODUCTION

The Unified power flow controller (UPFC) was firstly suggested by L. Gyugyi in 1991 [80], [81] and [82]. The most Versatile FACTS device is UPFC. It has the advantage of regulating real and reactive power independently for reliable and flexible operation of existing modern power system. Before UPFC, a few mechanical or other FACTS devices such as a Thyristor Controlled Series Compensator (TCSC), Static Var Compensator (SVC), a phase shifter, etc. were used to control independently various network parameters like impedance of the line, power angle or voltage magnitudes that vary active and reactive power flow on the transmission line. But these shortcomings were overcome after UPFC came into existence due to its application of independent and simultaneous control of the above said system parameters by using various control structures and strategies in real time. This device has many applications like provides voltage support, damps low frequency power system oscillations and thus improves the transient stability. Due to the above smart features, modeling and controlling an UPFC has become the recent research areas. Several references are there where researchers have developed a linearized, dynamic and steady state models of UPFC. Steady state model of UPFC, which is also termed as power injection model as explained in [83] where UPFC is represented by as a series reactance along with the dependent loads which are injected at the sending end and receiving end buses of UPFC controller. The model is easy and useful in understanding its effect on the system network. In order to get the required load flow solution, manual control of amplitude modulation and phase angle and of the series voltage source converter has been carried out.

Fundamental frequency model, another name for the dynamic model of UPFC has been implemented in [51], [70] and [83]. It comprises of two equivalent voltage sources. Out of two, one is connected in series and other is connected in shunt. The series connected voltage source forms the series converter while the shunt connected forms the shunt

converter. The function of both converters in the model is to add voltage at the fundamental frequency. The researchers, in their papers [88, 89] have not used the dynamics of dc link capacitor which might not give accurate results. However researchers in [49], [83] have done the UPFC modeling that includes the dynamics of dc capacitor that gives better and accurate responses and the same has been implemented for studying the impact of UPFC in real time operation of power system.

For analyzing the steady state stability, Phillips Heffron model [85] of SMIB system connected with UPFC is used. [56], [57] have proposed the linearized model of UPFC. While developing the UPFC model, paper [88] has neglected the dynamics of dc link capacitor, whereas, model in [63], [81], [83] and [84], a different approach has been adopted. Instead of using the linearized model of UPFC, the author has considered the two buses between which the UPFC is connected as the generator buses and accordingly analysis is being carried out. This approach allows UPFC to be connected anywhere in the network.

Basic control design of UPFC includes reactive and active power flow control in transmission network, dc voltage control and bus voltage control. Schauder and Mehta in 1991 [87] proposed Vector-control scheme, the commonly used control strategy which provide independent control of reactive and active power and the same is suitable for UPFC application.

Both SMIB and Multi-machine system are used to exhibit the performance of controller under dynamic conditions. Simulation outcomes reveal that the UPFC can meaningfully improve the power system operation on applying large disturbances. It is achieved by changing the 3-phase balanced system into a synchronously rotating orthogonal system.

The proposed control scheme used here incorporates the control of real and reactive power flow by the converter connected in series with the line automatically. The control is accomplished by injecting the voltage by the series converter in series with the line. The in-phase component of this voltage with the line current influences the flow of reactive power and the quadrature component of leads to the control of flow of real power in the line. The various Swarm intelligent techniques are also implemented to optimize the UPFC controller parameters for transient stability enhancement. In this chapter, UPFC controller is also used in multi-machine power system network for the transient stability

enhancement. PSO algorithm is implemented for the optimization of controller parameters. Power Injection model of UPFC is integrated in the multi-machine system.

## 6.2 UPFC BASIC OPERATION AND CHARACTERISTICS

UPFC comprises of 2 switching converters that are treated as voltage source inverters. These inverters employ Gate-turn Off (GTO) thyristor valves as shown in fig 6.1. A d.c link capacitor is connected between the two inverters. AC to ac power conversion is possible with this configuration of UPFC. This arrangement allows the active power to flow freely in both the directions between the two inverters. Apart from this, independent generation and absorption of reactive power is also possible by each inverter at the bus to which it is connected.

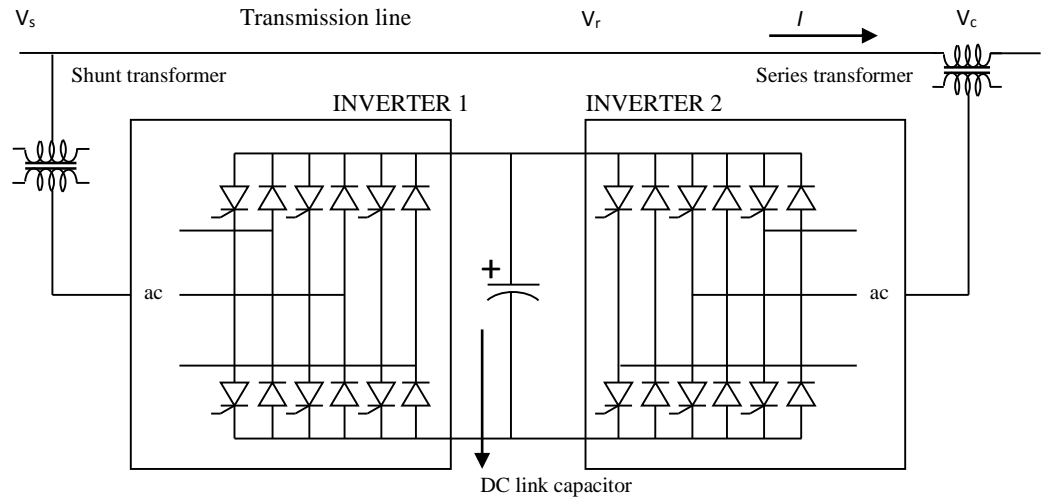


Fig. 6.1 Circuit diagram of unified power flow controller

The main objective of the UPFC is carried out by inverter 2 by providing a controllable ac voltage  $V_c$  ( $0 \leq |V_c| \leq |V_c|_{max}$ ) and its phase angle ( $0 \leq \alpha \leq 2\pi$ ), in series with the transmission line through series transformer. This injected voltage at power frequency can be treated as a synchronous ac voltage source. Exchange of real and reactive power between the converter and the ac network is possible due to the current produced by the equivalent voltage sources. The inverter converts the active power that has been exchanged from ac terminals into dc power which appeared across the dc link capacitor either as positive or negative active power demand. For any real power demand in the line, inverter

I has to provide this real power demand. Inverter I exchanges the real power from the ac network terminal to which it is connected and this power then appears across the dc link capacitor. This dc power is then converted into ac power and is then injected into the transmission line through the series transformer. The vice versa is also possible. Thus for real power compensation, both the converters have to participate. One has to operate as a converter and other as an inverter, whereas each inverter can also generate and absorb the reactive power locally at the ac terminal independently and thereby provide shunt reactive power compensation. If inverter I is operated at unity power factor then only inverter II can be able to provide reactive power exchange as per the requirement.

From the standpoint of conventional power transmission based on reactive series compensation, shunt compensation, and phase shifting, the UPFC can meet all these functions and thereby fulfills multiple control objectives by adding the injected voltage  $V_c$ , with appropriate amplitude and phase angle, to the terminal voltage  $V_0$ . The basic UPFC power flow control functions are illustrated in Fig 6.2 using phasor representation.

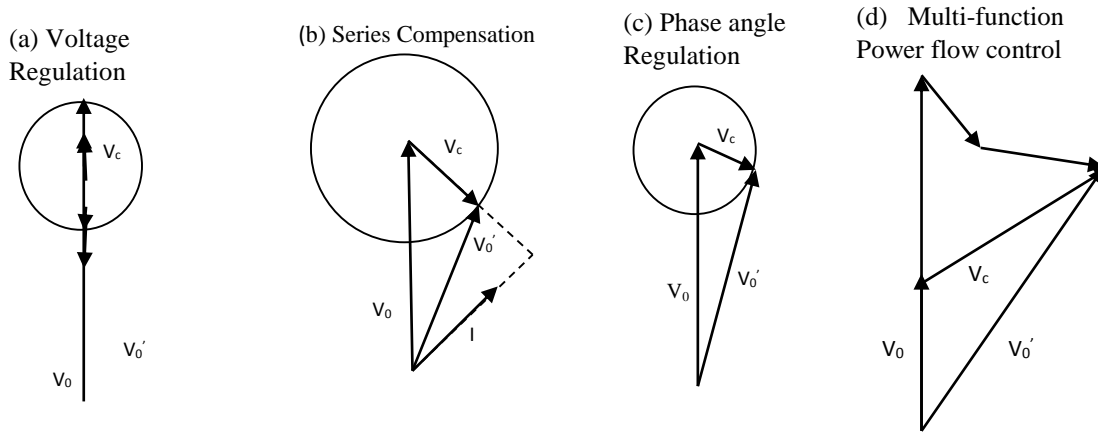


Fig 6.2 Elementary control functions of UPFC: (a) Voltage Regulation, (b) Series compensation, (c) Angle regulation and (d) Multi function power flow control  
 In Fig.6.2 (a) where  $V_c$  is injected in phase with the  $V_0$ , terminal voltage regulations similar to transformer tap-changer having infinitesimally steps is obtained. Capacitive compensation is shown in Fig.6.2 (b) where  $V_c$  is injected in quadrature with the line current. Phase shifting is shown in Fig 6.2 (c) where  $V_c$  is injected with an angular relationship with respect to  $V_0$  that achieve the desired phase shift without any magnitude change. Multi-function power flow control, executed by simultaneous terminal voltage regulation, series capacitive line compensation, and phase shifting is shown at Fig.6.2 (d).

The powerful competences of the UPFC as described in terms of basic transmission control theories, very basic terms of phase shifting and series compensation, etc has been unified into a comprehensive uncontrollable, reactive and active power in the line. UPFC has the advantage of controlling the active and reactive power flow in the transmission line in order to meet the increased demands by controlling the magnitude and phase angle of the added voltage by series converter of the UPFC in the line in real time.

### 6.3 CASE STUDY

For analyzing the UPFC in mitigation of power oscillations, parameters of the system like terminal voltage, theta, and generator rotor angle, real and reactive power are considered. The case study comprises of – A 200MVA, 13.8KV, 50Hz generator supplying power to an infinite bus via double circuit transmission lines as depicted in fig 6.3. All the values are taken on 100MVA, 13.8 KV base. Line resistances are assumed to be negligible. System is operated and analyzed at different operating conditions like light loads, normal loads and heavy loads. All the system parameters in p.u. are given in appendix C. System is subjected to two kinds of faults for analyzing the effectiveness of UPFC controller for the transient stability of the power system network to which it is installed. For simulating the first case, the 3- phase line to ground fault is made at infinite bus-bar for 100msec duration & simulation is done for 10sec. to examine the damping of power oscillations after the transient disturbance in the study system. In the second case, one transmission line is removed and restored back after 0.1 sec. Simulation is carried out for 10 sec.

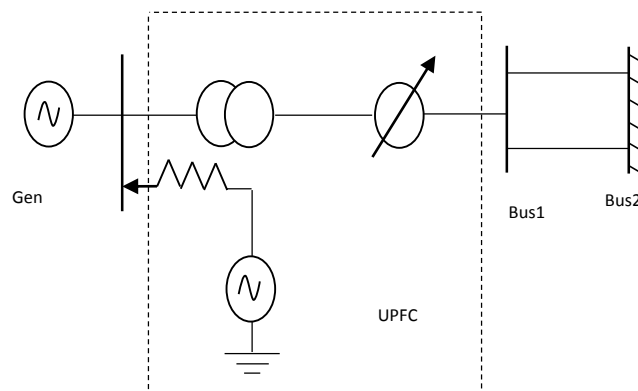


Fig. 6.3. Representation of Single Machine connected to an Infinite Bus system.

### 6.3.1 Modeling of SMIB System Connected with UPFC Controller

#### a. Synchronous Machine Model

Several researchers have formulated many mathematical models of Generator varies from basic model to the more explanatory one. In this paper, third order machine model [2] has been used to represent the generator. All damper windings are neglected. Only field winding is considered in the d-axis.

Stator Winding Equation:

$$v_q = E'_q - r_s i_q - x'_d \dot{i}_d \quad (6.1)$$

$$v_d = E'_d - r_s i_d - x'_q \dot{i}_q \quad (6.2)$$

$$V_1 = v_d + jv_q \quad I = i_d + ji_q \quad (6.3)$$

$$S = V_1 I^*$$

$$p = v_d \dot{i}_d + v_q \dot{i}_q \quad (6.5)$$

$$q = v_q \dot{i}_d - v_d \dot{i}_q \quad (6.6)$$

$$\frac{\delta\omega}{dt} = \frac{T_m - T_e}{M} \quad (6.7)$$

$$\omega = \omega_o + \frac{d\delta}{dt} \quad (6.8)$$

Damping and spring constant are taken as zero

$r_s$  is rotor winding resistance

$x'_q$  is q-axis transient resistance

$x'_d$  is d-axis transient resistance

$E'_q$  is q-axis transient voltage

$E'_d$  is d-axis transient voltage

Rotor Winding Equation:

$$T'_{do} \frac{dE'_q}{dt} = E_f - (x_d - x'_d) i_d - E'_q \quad (6.8)$$

$$\frac{dE'_q}{dt} = \frac{E_f - (x_d - x'_d) i_d - E'_q}{T'_{do}} \quad (6.9)$$

where,  $T_{qo}'$  is q-axis open-circuit transient time constant,  $T_{do}'$  is d-axis open-circuit transient time constant and  $E_f$  is the field voltage.

Electrical Torque Equation:

$$T_e = E'_d i_d + E'_q i_q + (x'_q - x'_d) i_q i_d \quad (6.10)$$

Excitation System Equation

$$\frac{d(\Delta E_{fd})}{dt} = \frac{K_e (V_{ref} - V_t)}{T_e} - \frac{\Delta E_{fd}}{T_e} \quad (6.11)$$

Where  $-0.6 \leq E_{fd} \leq 0.6$

## b. Modeling of UPFC Controller

UPFC operates in two modes. One is the PQ mode and the other is the Voltage Regulation Mode. In the latter case, the shunt voltage source converter regulates the bus voltage besides controlling the d.c capacitor voltage constant [49]. It can be realized by regulating the quadrature components and the in phase components of the shunt current with respect to the system bus voltage.

In first case, the shunt converter of the UPFC may be controlled to provide the d.c capacitor voltage constant along with the bus voltage regulation. This is achieved by controlling the in phase & quadrature components of the shunt current [49] with respect to the system bus voltage to which the UPFC is installed. It is accomplished by using PI regulators. The reactive power component of shunt converter is regulated to control the voltage magnitude at the UPFC bus as proposed for STATCOM by Schauder & Mehta [87]. The proposed controller can be operated in both PQ mode and voltage regulation

mode. In this paper, the proposed controller is made to operate in PQ mode only. By regulating the series voltage injection, active and reactive power demand is met on the load side. After the initiation of the fault at infinite bus, it is necessary to control the quadrature and in phase component of the series injected voltage for attaining the system stability. This control is achieved by proper optimization of UPFC controller parameters.

### Series Controller of UPFC

Let  $V_{se}$  be the voltage injected by the series voltage source converter.  $V_{se}$  can be represented in d-q frame of reference as

$$V_{seq} = V_{se} \cos(\theta - \varphi) \quad \text{and} \quad V_{sed} = V_{se} \sin(\theta - \varphi) \quad (6.12)$$

$$V_{se} = \sqrt{(V_{sed})^2 + (V_{seq})^2} \quad (6.13)$$

Where,  $\theta = \tan^{-1} \frac{V_d}{V_q}$

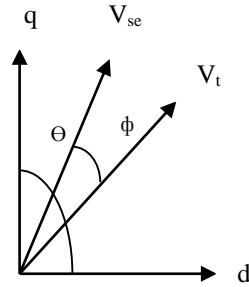


Fig. 6.4 d-q representation of series converter

Both quadrature and phase components of series injected voltage,  $V_{se}$  are responsible for real and reactive power flow in transmission line.

The quadrature and in phase component of  $V_{se}$  are represented by the summation of their change to the initial values and mathematically represented as:

$$V_{seq} = V_{seq0} + \Delta V_q \quad (6.14)$$

$$V_{sed} = V_{sed0} + \Delta V_p \quad (6.15)$$

d-q components of infinite bus voltage  $V_b$  are computed as

$$V_{bd} = V_{sed} + (X'_d + X_1) i_q - X_1 i_{sq} \quad (6.16)$$



$$V_{bq} = V_{seq} + e'_q - (X'_d + X_1)i_d - X_1 i_{sd} \quad (6.17)$$

$$V_b = \sqrt{V_{bd}^2 + V_{bq}^2} \quad (6.18)$$

Where  $X_d'$  is the machine transient reactance,  $X_1$  is the line reactance and  $i_{sd}$  and  $i_{sq}$  are d-q component of shunt current injected by shunt converter and  $E_q'$  is the voltage of generator behind the transient reactance.

Reference values of active and reactive powers are computed mathematically as:

$$\begin{aligned} p_{ref} &= (V_d + V_{sed})(i_d - i_{sd}) + (V_q + V_{seq})(i_q - i_{sq}) \\ q_{ref} &= (V_q + V_{seq})(i_d - i_{sd}) - (V_d + V_{sed})(i_q - i_{sq}) \end{aligned} \quad (6.19)$$

Where,

$$V_{sepo} = V_{sed} \sin\left(\tan^{-1} \frac{i_d - i_{sd}}{i_q - i_{sq}}\right) + V_{seq} \cos\left(\tan^{-1} \frac{i_d - i_{sd}}{i_q - i_{sq}}\right) \quad (6.20)$$

$$\Delta V_p = k_{p1} \Delta P + k_{i1} \int_0^T \Delta P \quad \Delta V_q = k_{p2} \Delta Q + k_{i2} \int_0^T \Delta Q \quad (6.21)$$

$$\Delta P = p_{ref} - p \quad \Delta Q = q_{ref} - q \quad (6.22)$$

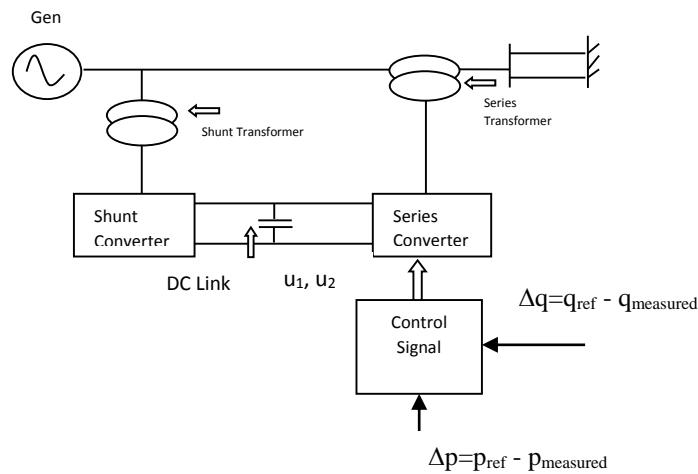


Fig. 6.5 UPFC Controller with SMIB System in PQ Mode

## Shunt Converter

The shunt voltage source converter injects the current  $i_s$  which is considered to be in same phase as that of generator terminal voltage. Thus it will not absorb or supply the reactive power & its objective is to provide the active power demand of series power voltage source converter.

For a lossless UPFC device,

$$R(S_{CONV1} - S_{CON2}) = 0$$

And when losses are considered then shunt power should be equal to sum of series power and capacitor power in order to maintain the voltage across the d.c capacitor connected between shunt and series converters. Mathematically

$$V_t i_s = V_{sed} (i_d - i_{sd}) + V_{seq} (i_q - i_{sq}) + V_{dc} C \frac{dV_{dc}}{dt} \quad (6.23)$$

Thus  $i_s$  can be computed from the above equation.

d-q components of current  $i_s$  are computed by the following relation

$$i_{sd} = i_s \sin \theta, \quad i_{sq} = i_s \cos \theta \quad (6.24)$$

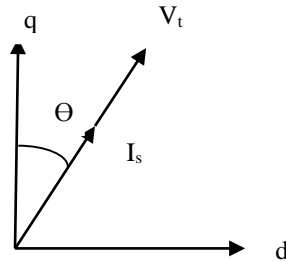


Fig.6.6. d-q representation of shunt converter

### A. Transmission Line currents

Let  $i_L$  be the transmission line current.  $i_{Ld}$  and  $i_{Lq}$  are its d-q components which are computed in terms of machine currents and shunt current.

$$i_{Ld} = i_d - i_{sd}, \quad i_{Lq} = i_q - i_{sq}$$

(6.25)

### B. Capacitor Dynamics

Capacitor power is given by the difference between the shunt power and series power.

Mathematically it can be represented as,

Capacitor power=Shunt power– Series power

$$\left( C \frac{dV_{dc}}{dt} \right) V_{dc} = P_{sh} - P_{se} \quad (6.26)$$

$$P_{sh} = V_t i_s \quad (6.27)$$

$$P_{se} = V_{sed} i_{td} + V_{seq} i_{tq} \quad (6.28)$$

$$\left( C_{eq} \frac{dV_{dc}}{dt} \right) V_{dc} = V_t i_s - (V_{sep} i_{td} + V_{seq} i_{tq}) \quad (6.29)$$

From equation (6.29), the shunt current injected by shunt converter is computed as

$$i_s = \frac{(V_{sep} (i_d - i_{sd}) + V_{seq} (i_q - i_{sq}) + CV_{dc} \tanh \sigma)}{V_1} \quad (6.30)$$

Where,

$$\sigma = V_{dcref} - V_{dc}$$

#### 6.4 CONTROL SCHEMES FOR PI CONTROLLER OF UPFC

Many techniques have been suggested by many researchers which are based on experimental or approximation of system with one order system with delay such as Cohen-Coon, Ziegler Nichols Apart from these, there are some general methods available like adaptive control, predictive control, neural control and fuzzy control. Some disadvantages of these control techniques for tuning PI controllers are:

- Excessive number of rules to set the gains
- Inadequate dynamics of closed loop responses
- Difficulty in dealing with nonlinear processes
- Mathematical complexity of the control design

Moreover the real time implementation of Artificial Neural Networks (ANN), and Fuzzy Logic (FL) which have developed over the last ten years, is quite difficult. Hence optimization problem has become the major concern for the researchers. In recent years, extensive research on heuristic stochastic search techniques like GA [94], PSO [61, 90, 91], BFO [92, 93], Hybrid BF-PSO [69] and many more have been carried out to optimize PI gains to solve complex problems.

In this chapter, PI Controller parameters of UPFC are computed using conventional technique & then using these parameters as base, Heuristic search techniques are applied for computing better optimal values of PI controller, so that transient stability can be enhanced further for the power system network.

## **6.5 IMPLEMENTATION OF SWARM INTELLIGENCE TECHNIQUES FOR OPTIMIZATION OF UPFC CONTROLLER PARAMETERS**

In this chapter, various Swarm intelligence algorithms explained in chapter (3) have been explored for the control of various concerns of power system. Here the issue of transient stability in power system has been considered. Various Swarm intelligence techniques implemented are:

1. Particle Swarm Optimization
2. Bacterial Foraging Optimization
3. Advanced Adaptive BFO-Particle Swarm optimization.
4. Genetic Algorithm

The correct choice of various parameters involved in the above algorithms is very important for the global search of optimized values of UPFC Controller parameters. A very important aspect is to formulate a proper objective function that evaluates the performance of the system to get an optimized solution.

## **6.6 OBJECTIVE FUNCTION**

UPFC controller is so designed that it minimizes the power system oscillations after a disturbance and thus the power system stability can be improved. In this paper, the objective function defined is such that it includes all those parameters in which the oscillations are reflected like, deviations in the generator rotor speed ( $\Delta\omega$ ), active power ( $\Delta P$ ) & reactive power ( $\Delta Q$ ). In the present study the objective function  $J$  is formulated as the minimization of:

$$J = \int_0^t \left[ t(\Delta\omega(t, x))^2 + t(\Delta P(t, x))^2 + t(\Delta Q(t, x))^2 \right] dt \quad (6.31)$$

Subject to the conditions,

$$k_{p1 \min} < k_{p1} < k_{p1 \max}$$

$$k_{i1 \min} < k_{i1} < k_{i1 \max}$$

$$k_{p2 \min} < k_{p2} < k_{p2 \max}$$

$$k_{i2 \min} < k_{i2} < k_{i2 \max}$$

In the above equations,  $\Delta w(t, x)$  denotes the rotor speed deviation,  $\Delta P$  denotes the change in Real Power flow &  $\Delta Q$  denotes the change in Reactive Power flow for a set of controller parameters  $x$  (where  $x$  represents the parameters to be optimized;  $k_{p1}$ ,  $k_{i1}$ ,  $k_{p2}$ ,  $k_{i2}$  are the parameters of UPFC controller), and  $t$  is the time range of the simulation. With the variation of the parameters  $x$ , the  $\Delta w(t, x)$ ,  $\Delta P(t, x)$ ,  $\Delta Q(t, x)$ , will also be changed. For objective function calculation, the time-domain simulation of the power system model is carried out for the simulation period. It is aimed to minimize this objective function in order to improve the system response in terms of the settling time and overshoots.

## 6.7 SIMULATION RESULTS

For investigating the transient stability analysis, the simulations are carried out using the above control strategies one by one. A single machine infinite bus system (SMIB) as shown in figure (6.3) is taken for simulation.

C. Using hit and trial method, PI controller parameters of UPFC are tuned. Two cases of faults have been analyzed i) A three phase fault near infinite busbar for 100ms ii) One line outage for 100 msec.

**Case 1:** Three phase fault near infinite busbar is created near infinite bus bar for 100ms.

- a. The synchronous generator is made to operate at light load of  $P=40\text{MW}$  before the disturbance. The robustness of the UPFC controller is established. Oscillations in machine angle, speed, active power, reactive power, terminal voltage, dc capacitor voltage and d-q axis series injected voltage are shown respectively in fig. 6.7.1 to 6.7.10.

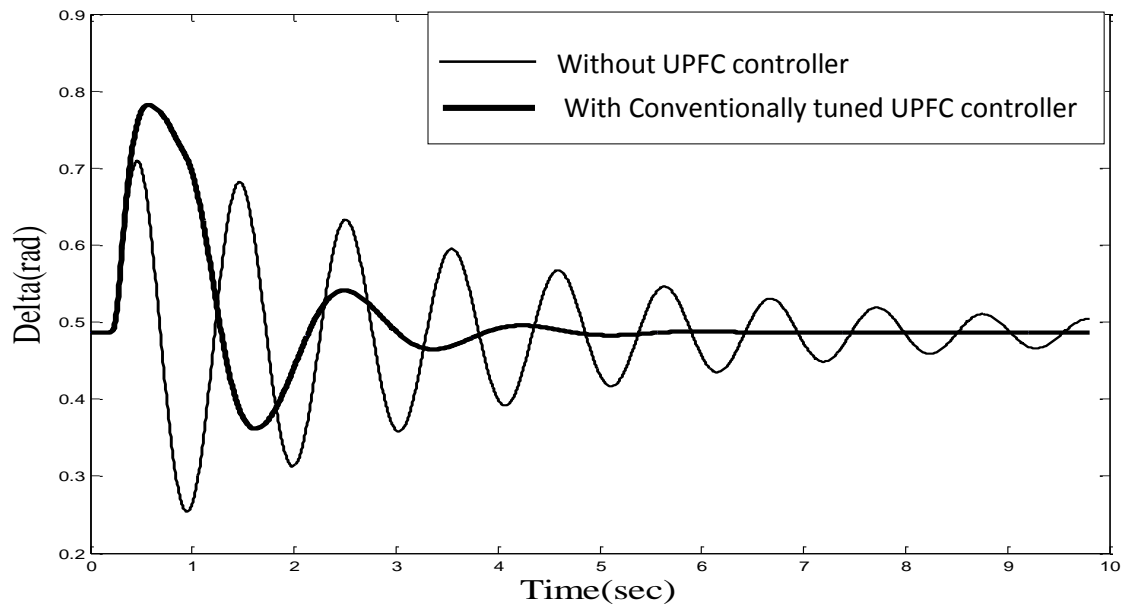


Fig. 6.7.1 Time response of Power angle without and with conventionally tuned UPFC controller (for 40 MW load with 3-Phase fault)

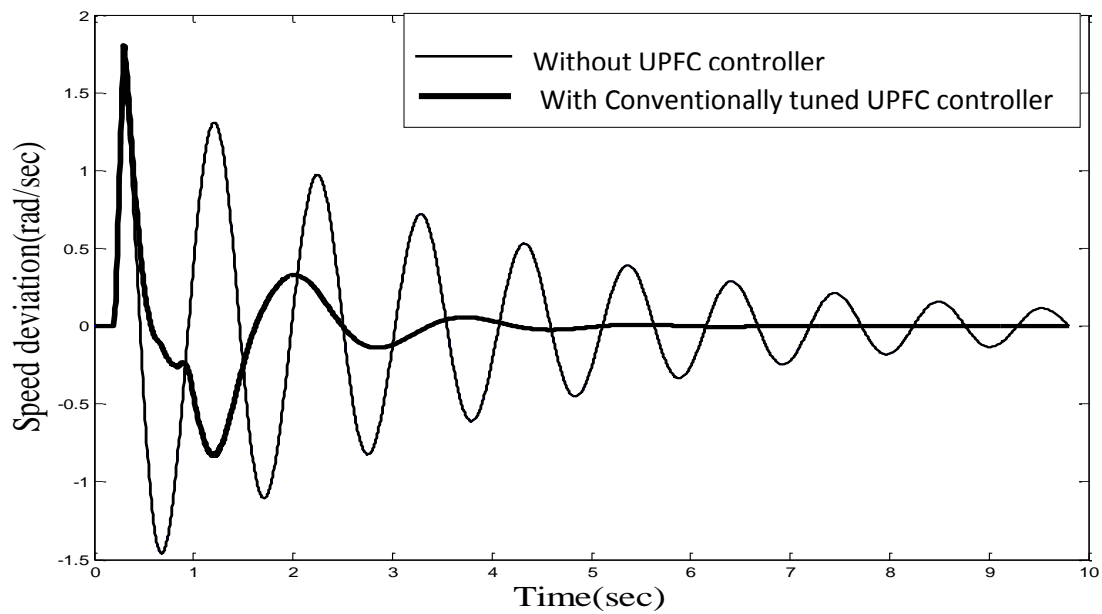


Fig. 6.7.2 Time response of speed deviation without and with conventionally tuned UPFC controller (for 40 MW load with 3-Phase fault)

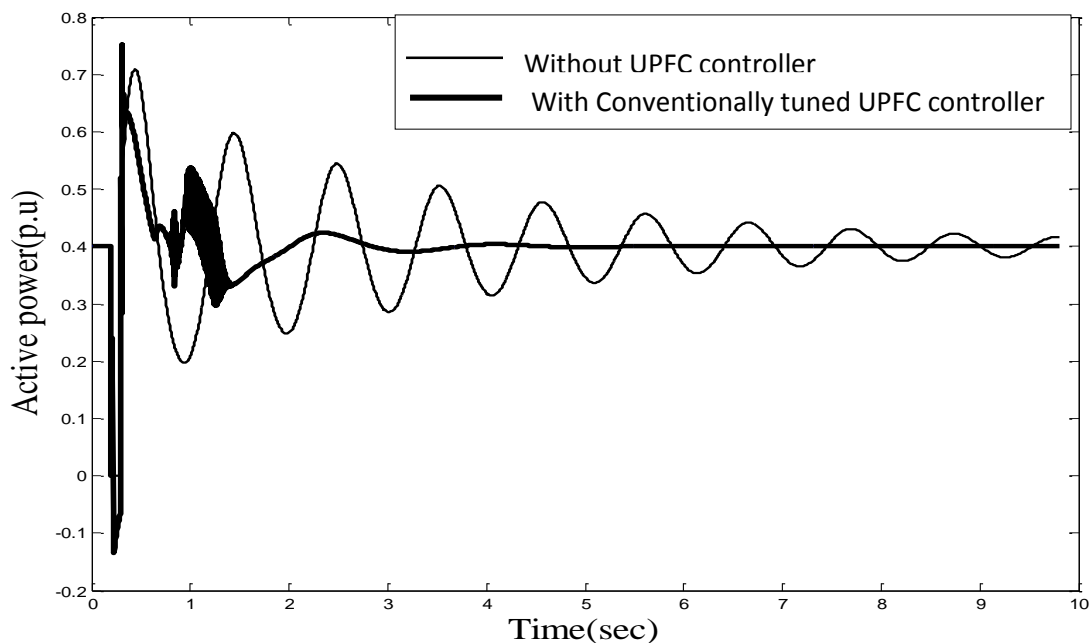


Fig. 6.7.3 Time response of active power without and with conventionally tuned UPFC controller (for 40 MW load with 3-Phase fault)

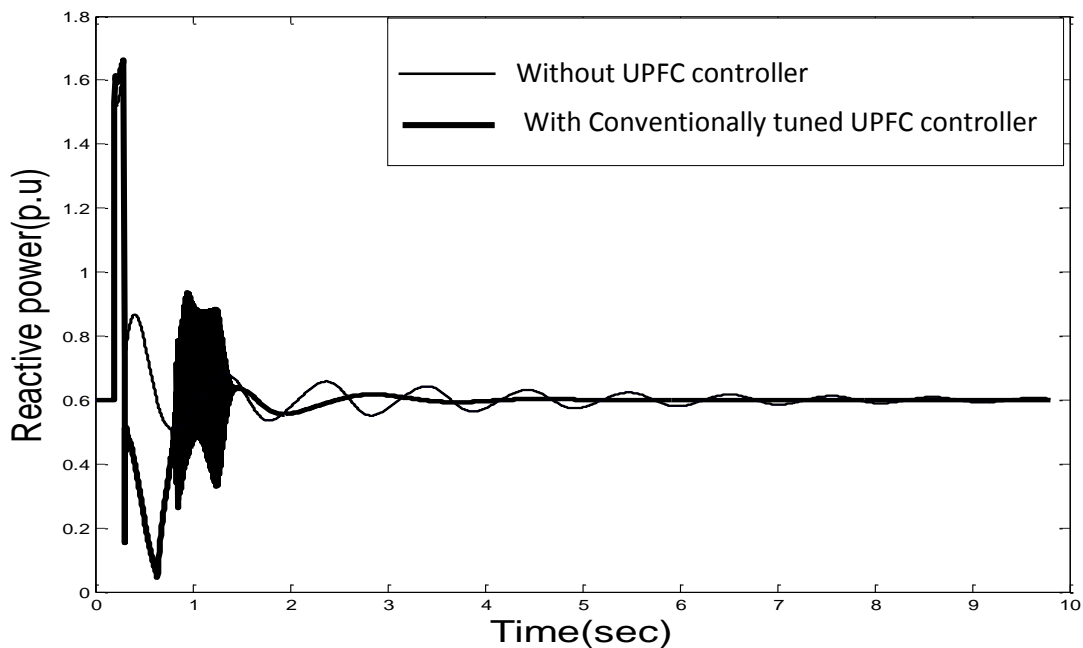


Fig. 6.7.4 Time response of reactive power without and with conventionally tuned UPFC controller (for 40 MW load with 3-Phase fault)

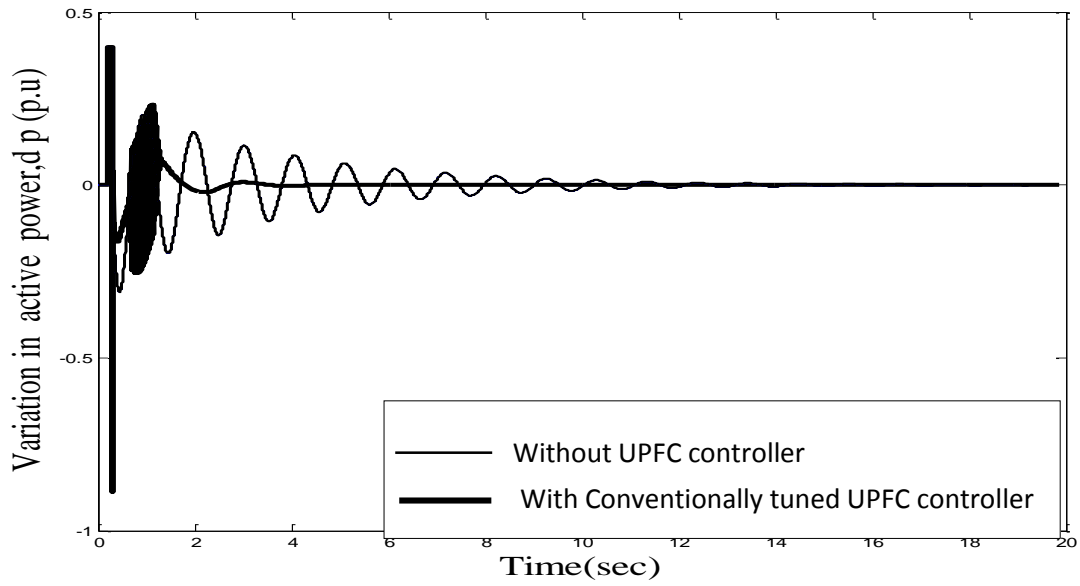


Fig. 6.7.5 Time response of variation in active power without and with conventionally tuned UPFC controller (for 40 MW load with 3-Phase fault)

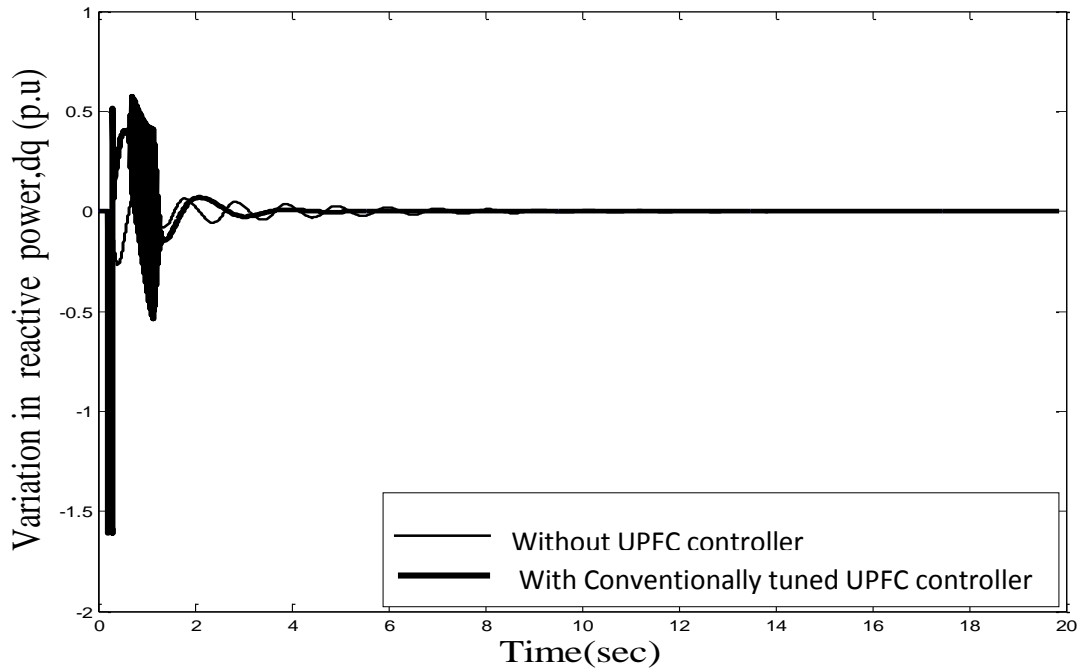


Fig. 6.7.6 Time response of variation in reactive power without and with conventionally tuned UPFC controller (for 40 MW load with 3-Phase fault)



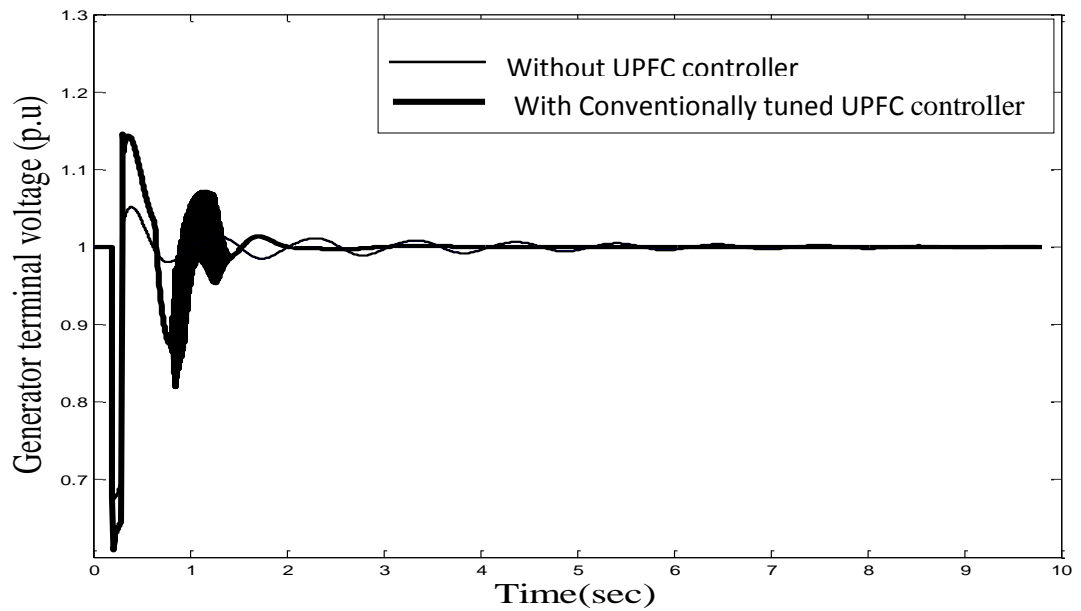


Fig. 6.7.7 Time response of variation in Generator terminal voltage without and with conventionally tuned UPFC controller (for 40 MW load with 3-Phase fault)

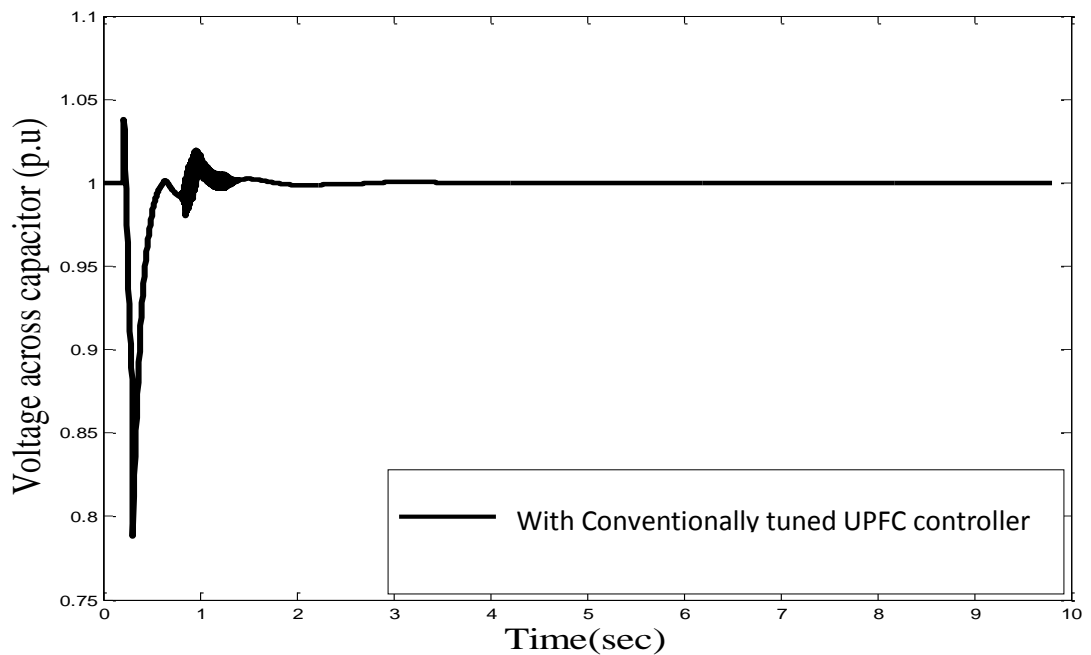


Fig. 6.7.8 Time response of variation in dc capacitor voltage with conventionally tuned UPFC controller (for 40 MW load with 3-Phase fault)

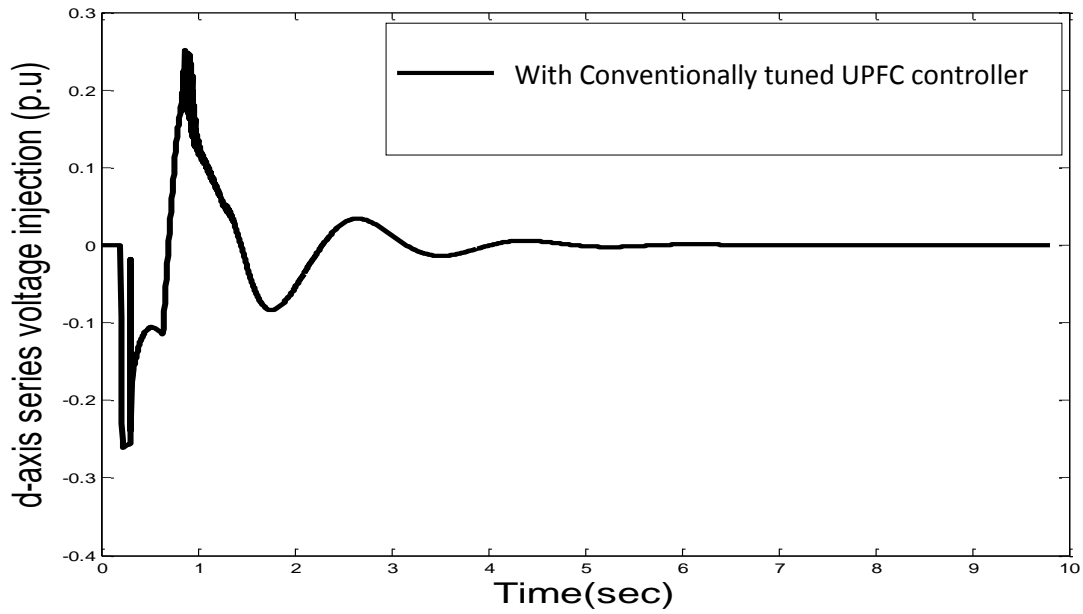


Fig. 6.7.9 Time response of variation in d-axis series voltage injection with conventionally tuned UPFC controller (for 40 MW load with 3-Phase fault)

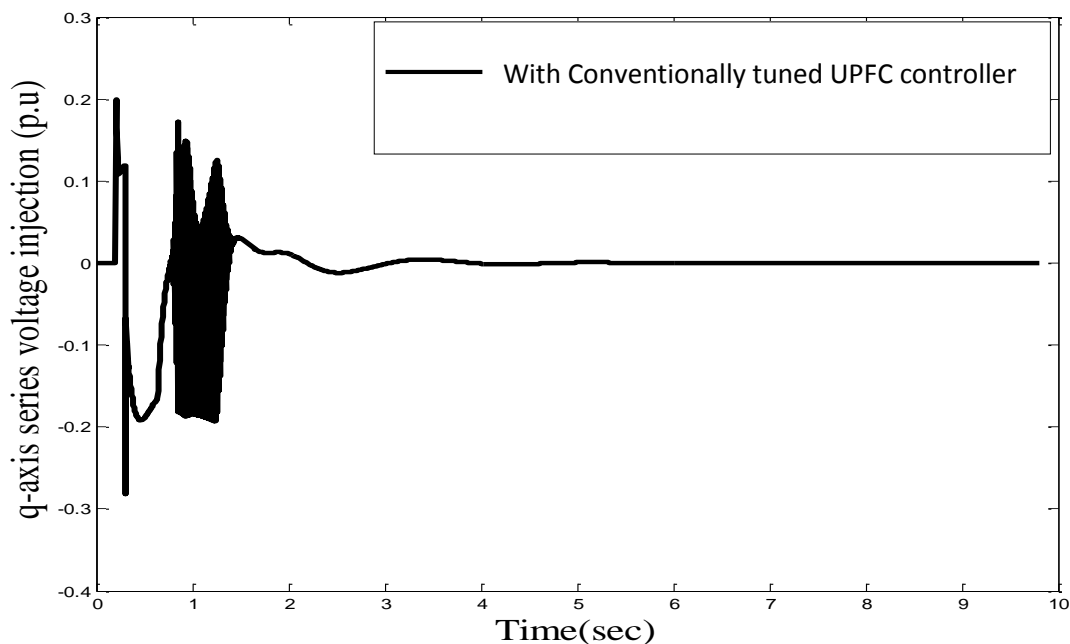


Fig. 6.7.10 Time response of variation in q-axis series voltage injection with conventionally tuned UPFC controller (for 40 MW load with 3-Phase fault)

- b. The operating conditions of the SMIB system are changed by loading the generator at 80 MW and the robustness of the proposed UPFC controller is established for the same fault condition as the earlier case. Fig. 6.8.1 to 6.8.2 depicts the variation in delta and speed of the generator.

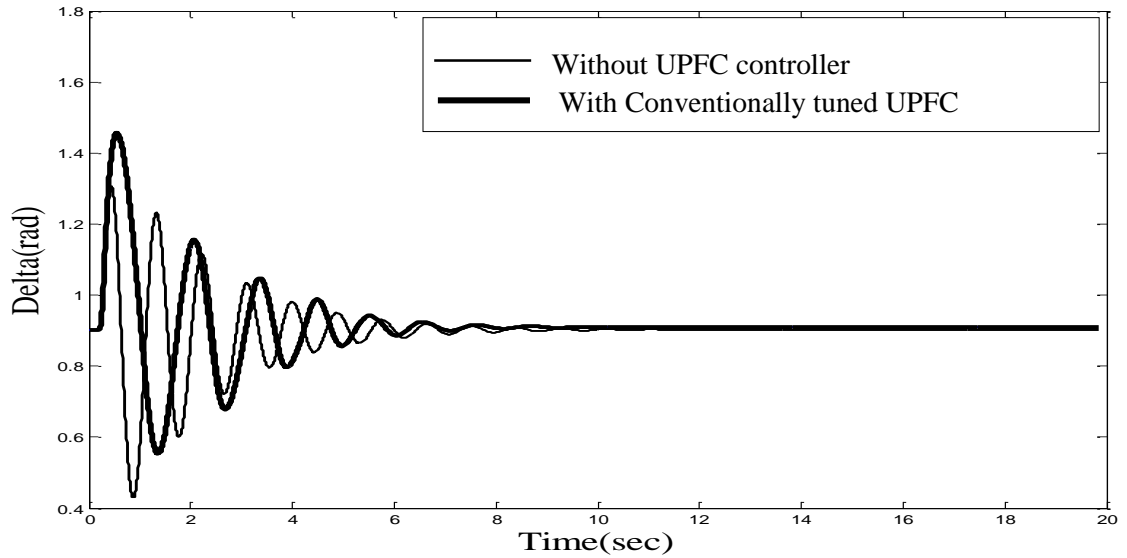


Fig. 6.8.1 Time response of Power angle without and with conventionally tuned UPFC controller (for 80 MW load with 3-Phase fault)

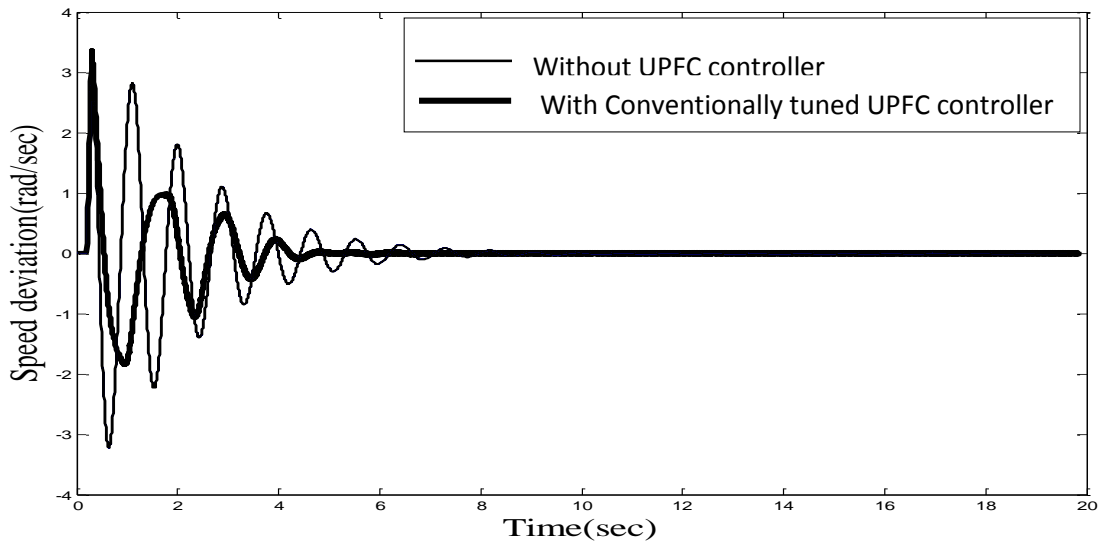


Fig. 6.8.2 Time response of speed deviation without and with conventionally tuned UPFC controller (for 80 MW load with 3-Phase fault)

- c. The operating condition of the generator is then further changed by loading the generator at a higher load of 100MW before the disturbance. The same fault as applied in above two cases is then created for the same time period. The robustness of the UPFC controller is depicted in fig. 6.9.1 and 6.9.2 respectively. Beyond this loading conventionally tuned controller is not effective in mitigation of power oscillations.

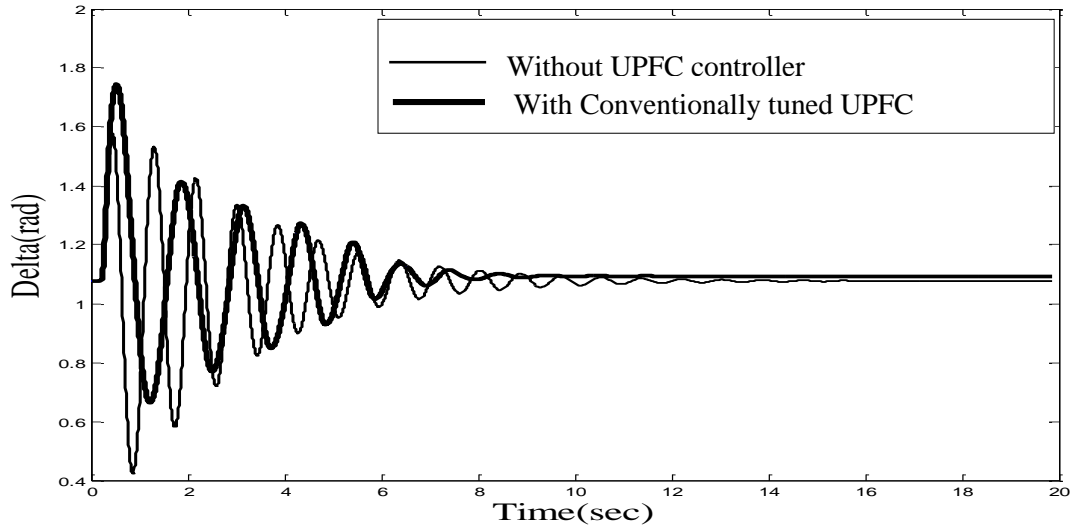


Fig. 6.9.1 Time response of Power angle without and with conventionally tuned UPFC controller (for 100 MW load with 3-Phase fault)

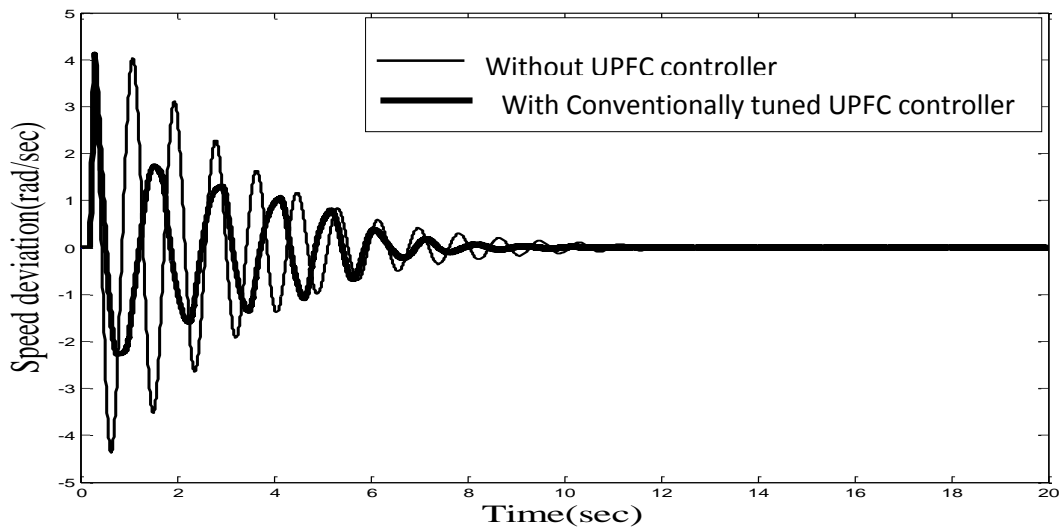


Fig. 6.9.2 Time response of speed deviation without and with conventionally tuned UPFC controller (for 100 MW load with 3-Phase fault)

**Case2:** A severe fault is created by tripping of one line out of two parallel transmission lines. The line is restored back to normal condition after 100 msec.

- a. The synchronous generator is made to operate at light load of 40MW before the disturbance. The proposed UPFC controller is found to be robust even under severe fault conditions as depicted in fig.6.10.1 and 6.10.2 respectively. Simulation is carried out for 20 sec.

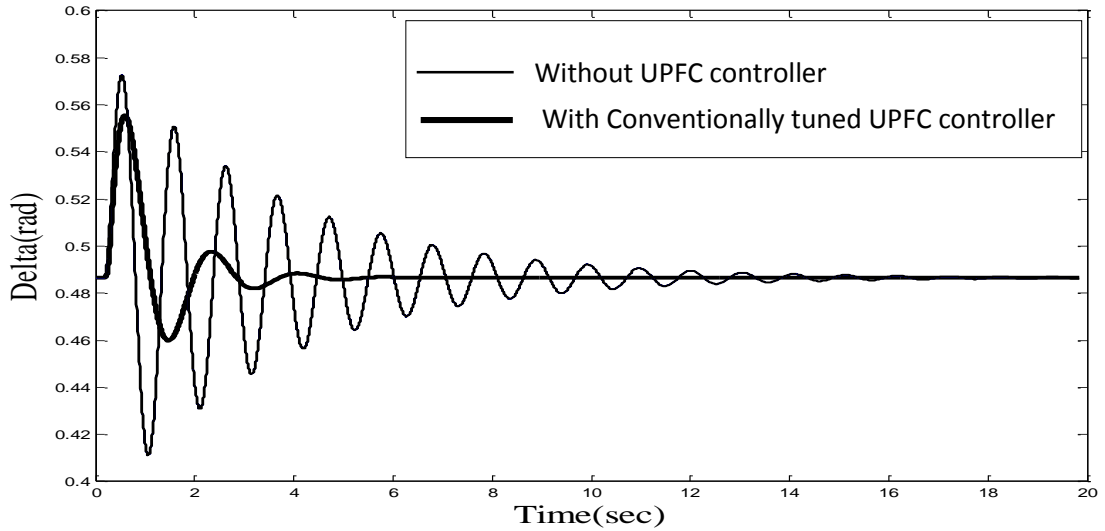


Fig. 6.10.1 Time response of Power angle without and with conventionally tuned UPFC controller (for 40 MW with line outage)

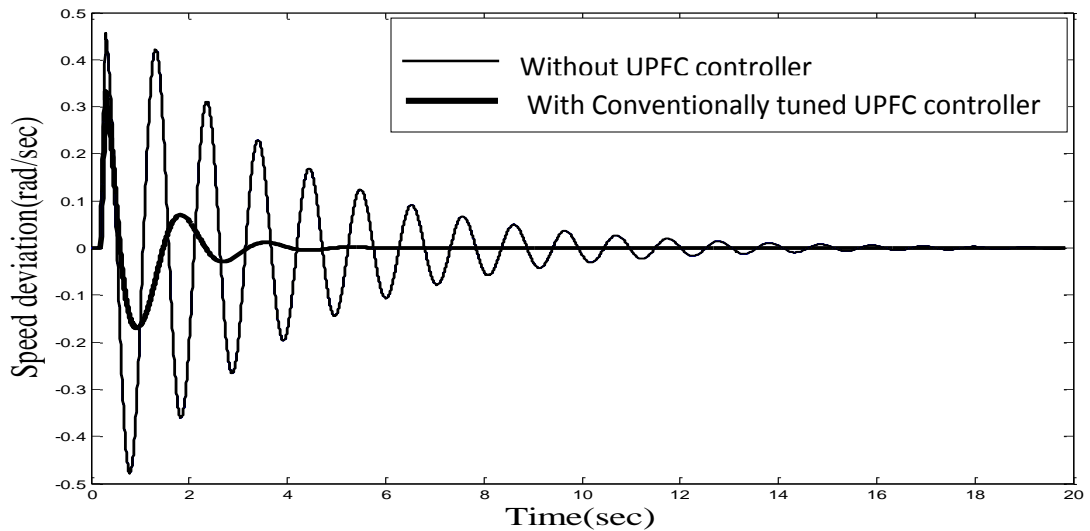


Fig. 6.10.2 Time response of speed deviation without and with conventionally tuned UPFC controller (for 40 MW with line outage)

b. The operating condition of the synchronous machine is changed by loading it to a heavy load of 120 MW before the disturbance. Fig 6.11.1 and 6.11.2 shows the robustness of the controller for the transient stability enhancement for the same severe fault of one line outage.

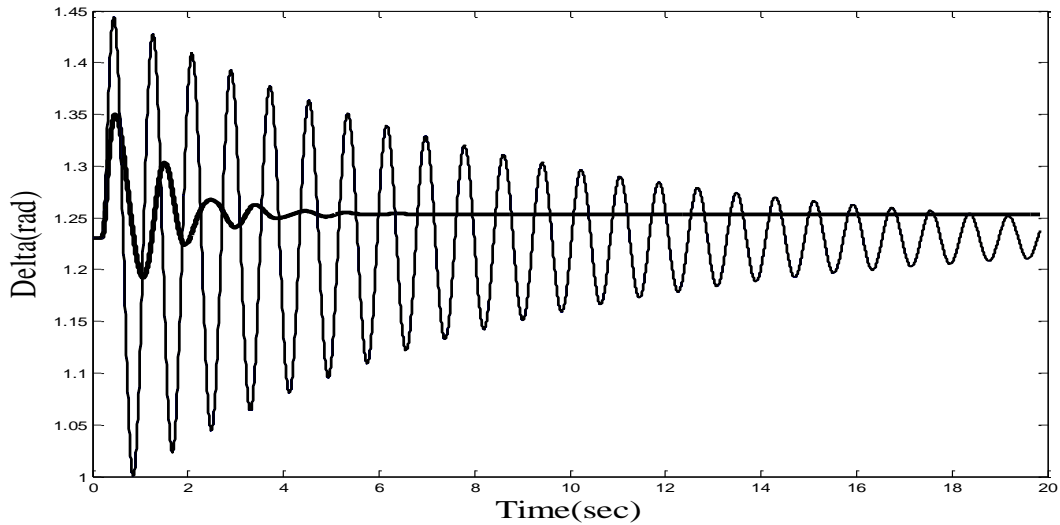


Fig. 6.11.1 Time response of Power angle without and with conventionally tuned UPFC controller (for 120 MW load with line outage)

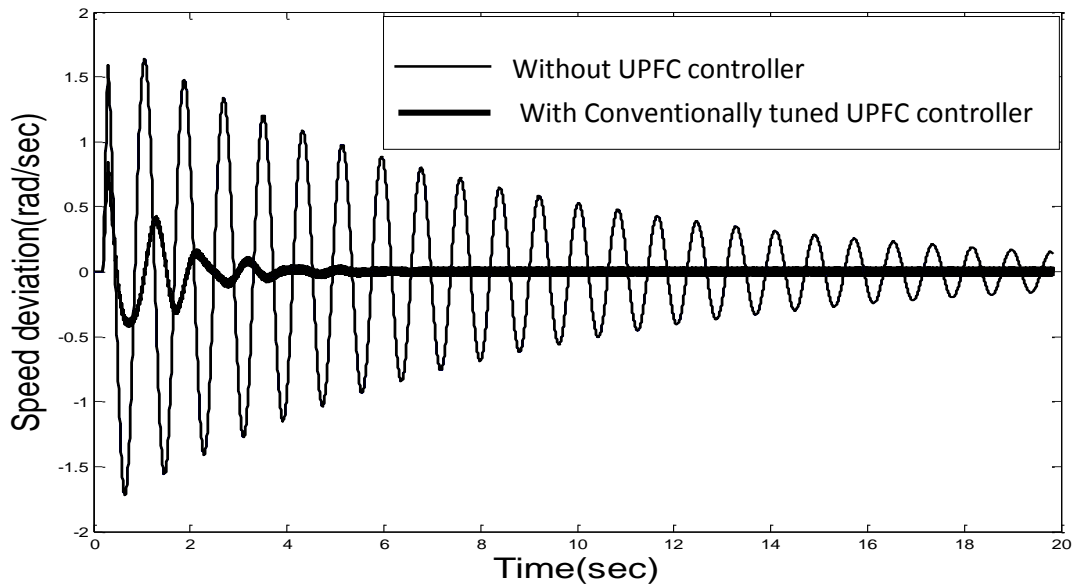


Fig. 6.11.2 Time response of speed deviation without and with conventionally tuned UPFC controller (for 120 MW load with line outage)

- c. The operating conditions are further changed by loading the generator to much higher load of 150MW before the disturbance. Fig. 6.12.1 and 6.12.2 depicts that the conventionally tuned UPFC controller is still making the system stable to some extent, whereas the system becomes unstable without controller as shown in fig.6.12.3.

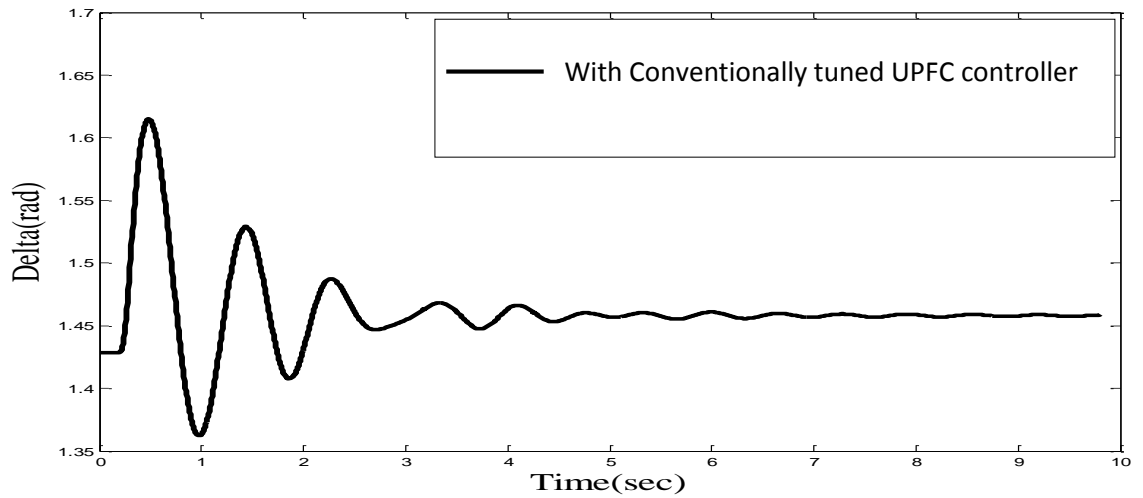


Fig. 6.12.1 Time response of Power angle with conventionally tuned UPFC controller  
(with line outage for 150 MW load)

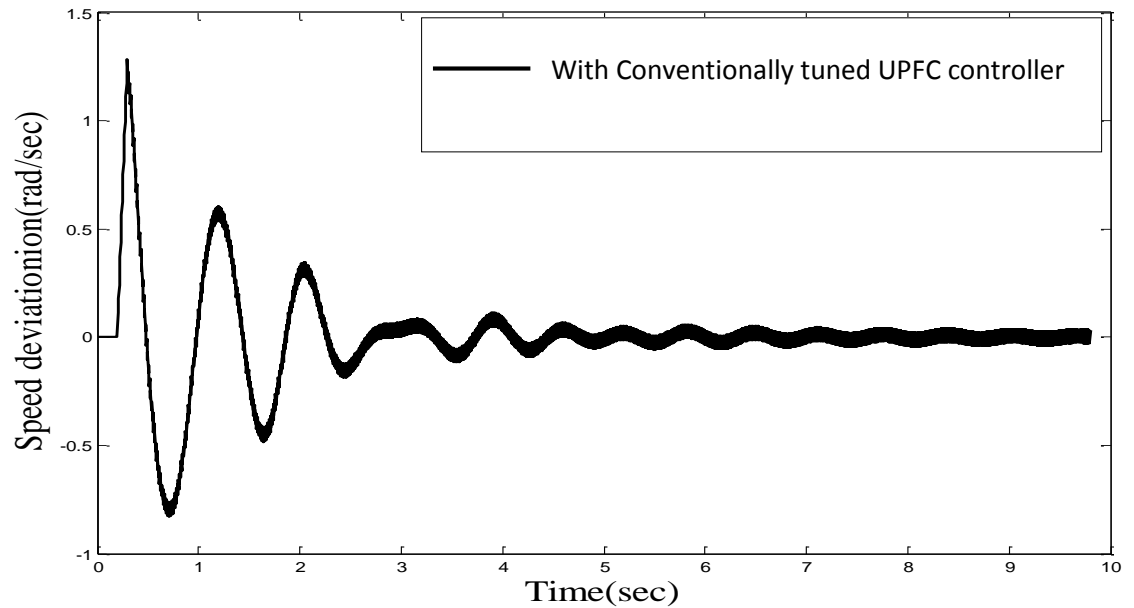


Fig. 6.12.2 Time response of speed deviation with conventionally tuned UPFC controller  
(with line outage for 150 MW load)

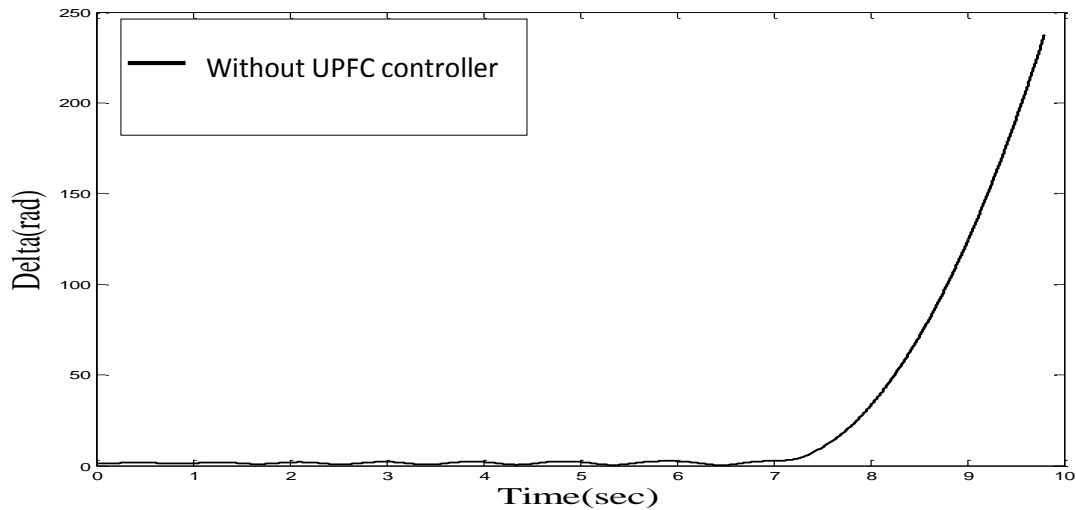


Fig. 6.12.3 Time response of Machine angle without UPFC controller (with line outage for 150 MW load)

D. Bacterial Foraging technique is implemented for optimizing the PI controller parameters of UPFC. The ITSE function as given in equation 6.31 is used to optimize the four controller parameters i.e  $k_{p1}$ ,  $k_{p2}$ ,  $k_{i1}$  &  $k_{i2}$ . Parameters of BFO are listed in Appendix C. Two cases of faults have been analyzed i) A three phase fault near infinite busbar for 100ms ii) One line outage for 100 msec

**Case 1:** The simulation is carried out with three phase fault near infinite bus-bar for 100msec & system is simulated for 10 seconds. The simulation result have been shown with PI controller parameters tuned by conventional method & PI controller parameters tuned by BFO (each bacterium is assigned with a set of 4 variables to be optimized and assigned with random value within the universe of disclosure).

- a. The synchronous generator is made to operate at light load of 40 MW before the disturbance. Three phase fault is created near the infinite busbar for 100ms. Fig. 6.13.1 to fig. 6.13.4 shows the effectiveness of BFO based UPFC controller over the conventional one.



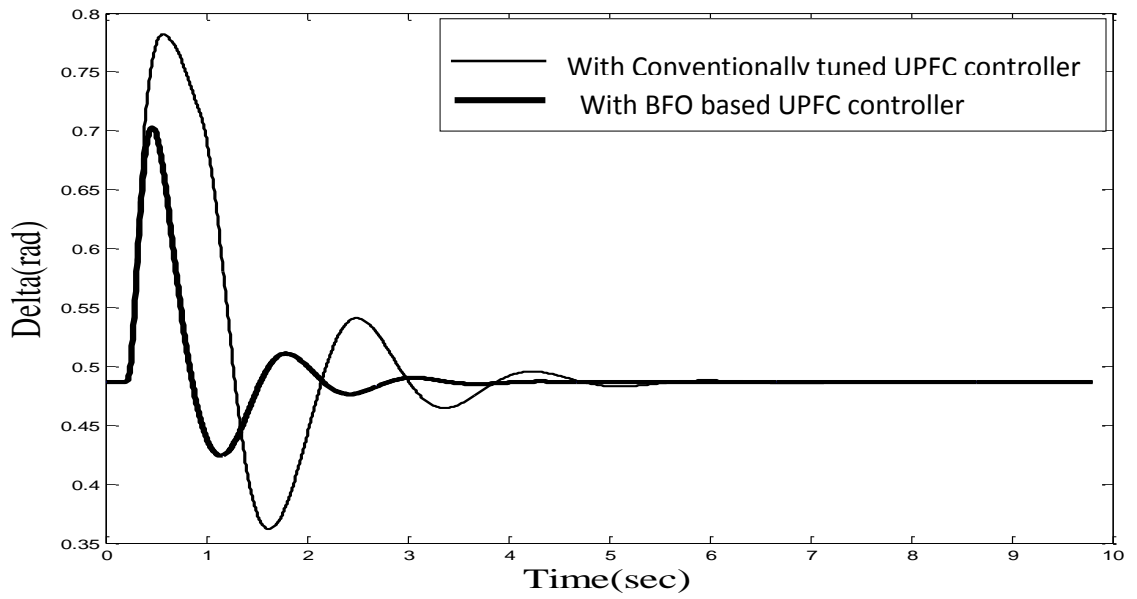


Fig 6.13.1 Time response of Power angle with conventionally tuned and BFO based UPFC controller (for 40 MW load with 3-Phase fault)

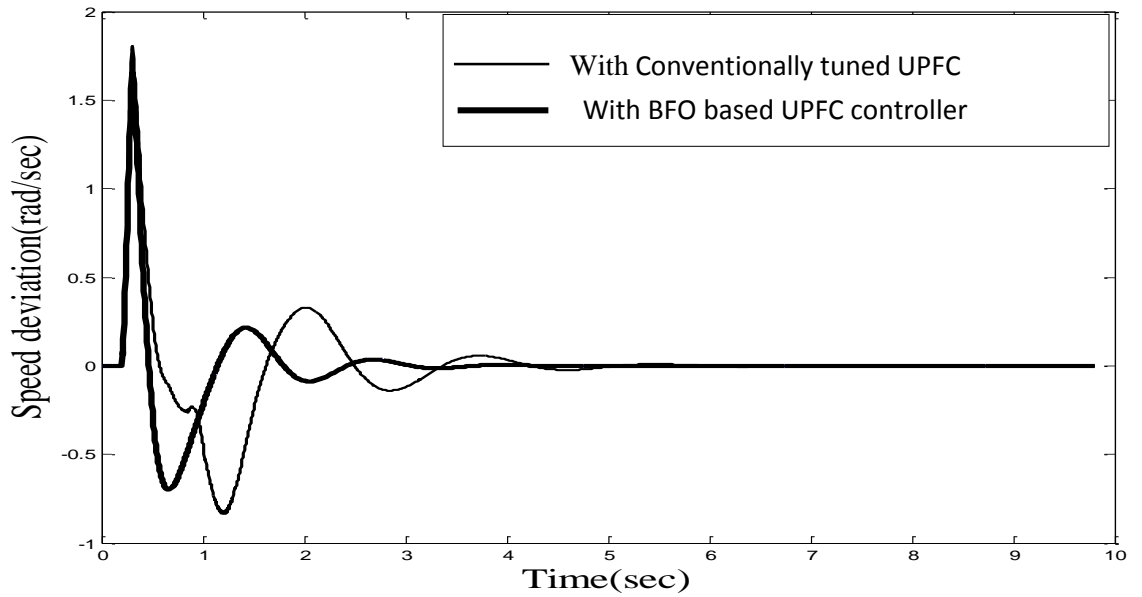


Fig 6.13.2 Time response of speed deviation with conventionally tuned and BFO based UPFC controller (for 40 MW load with 3-Phase fault)

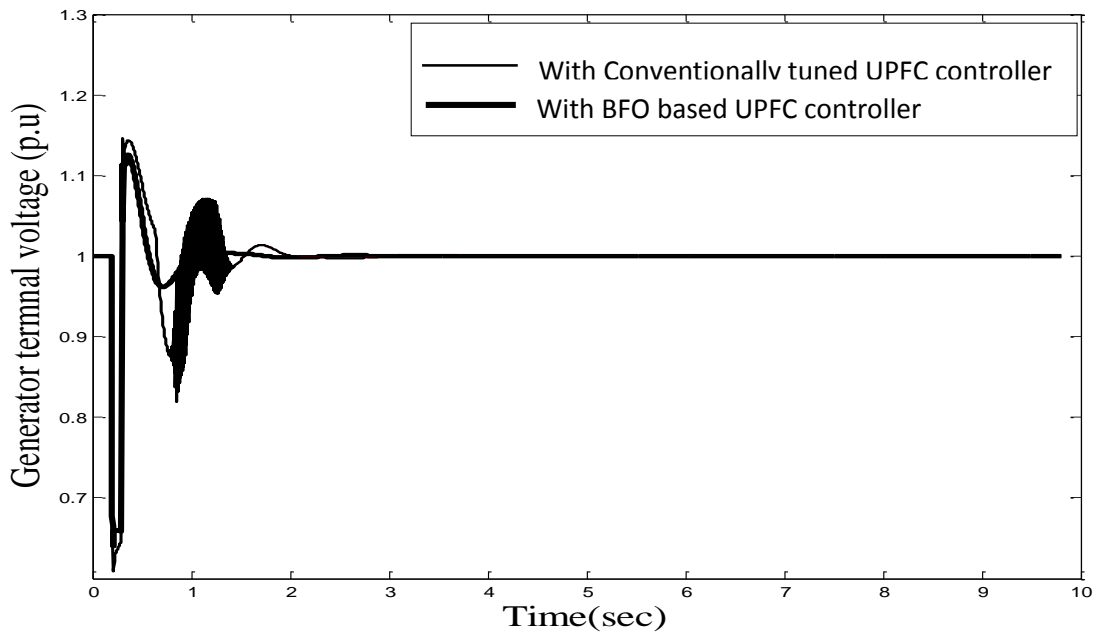


Fig 6.13.3 Time response of generator terminal voltage with conventionally tuned and BFO based UPFC controller (for 40 MW load with 3-Phase fault)

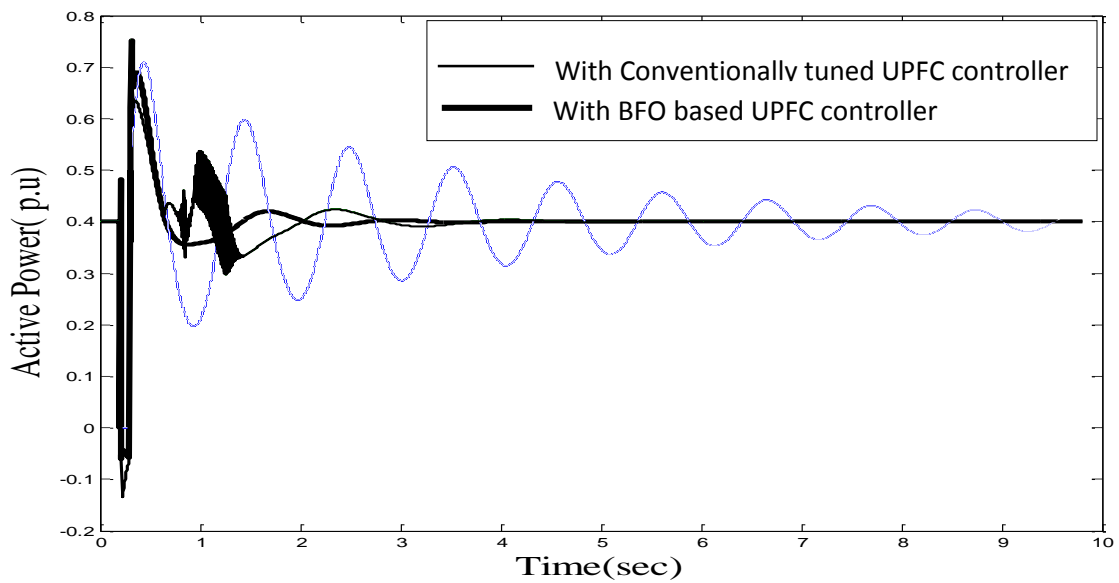


Fig 6.13.4 Time response of active power with conventionally tuned and BFO based UPFC controller (for 40 MW load with 3-Phase fault)

- b. The synchronous generator is now loaded at normal load of  $P=80$  MW before the disturbance. The simulations are carried out with the same three phase fault near infinite bus-bar for 100msec.

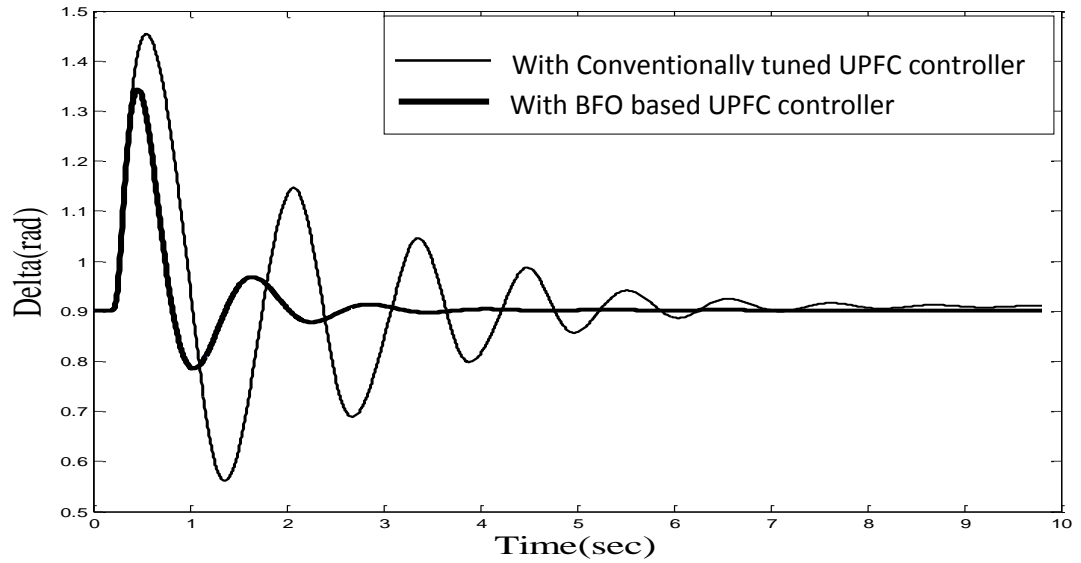


Fig 6.14.1 Time response of Power angle with conventionally tuned and BFO based UPFC controller (for 80 MW load with 3-Phase fault)

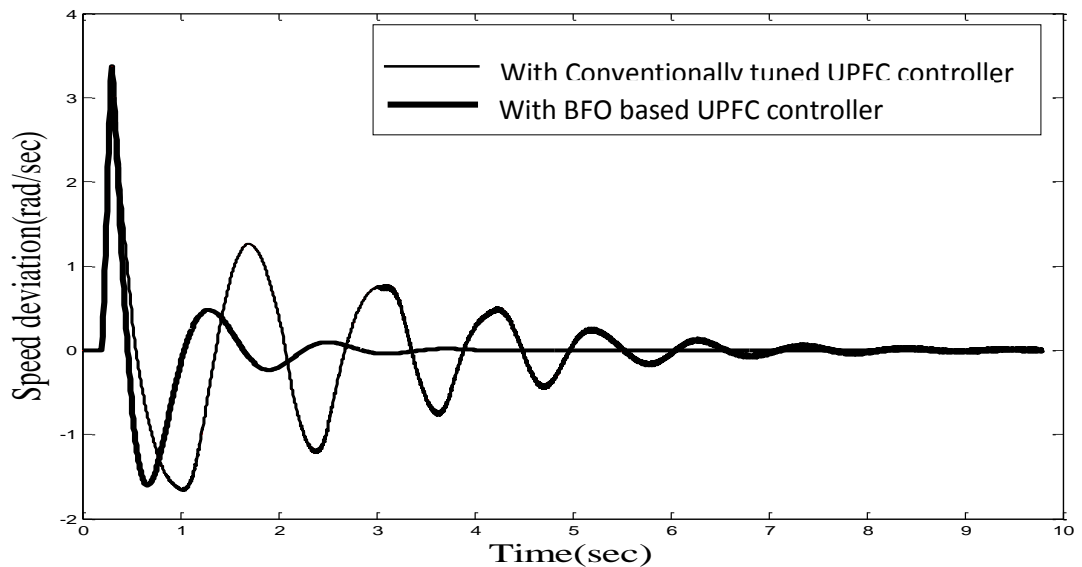


Fig 6.14.2 Time response of speed deviation with conventionally tuned and BFO based UPFC controller (for 80 MW load with 3-Phase fault)

- c. The operating condition of the generator is now changed. It is heavily loaded to 120 MW load and simulation results depict the effectiveness of BFO based UPFC controller for damping the power system oscillations.

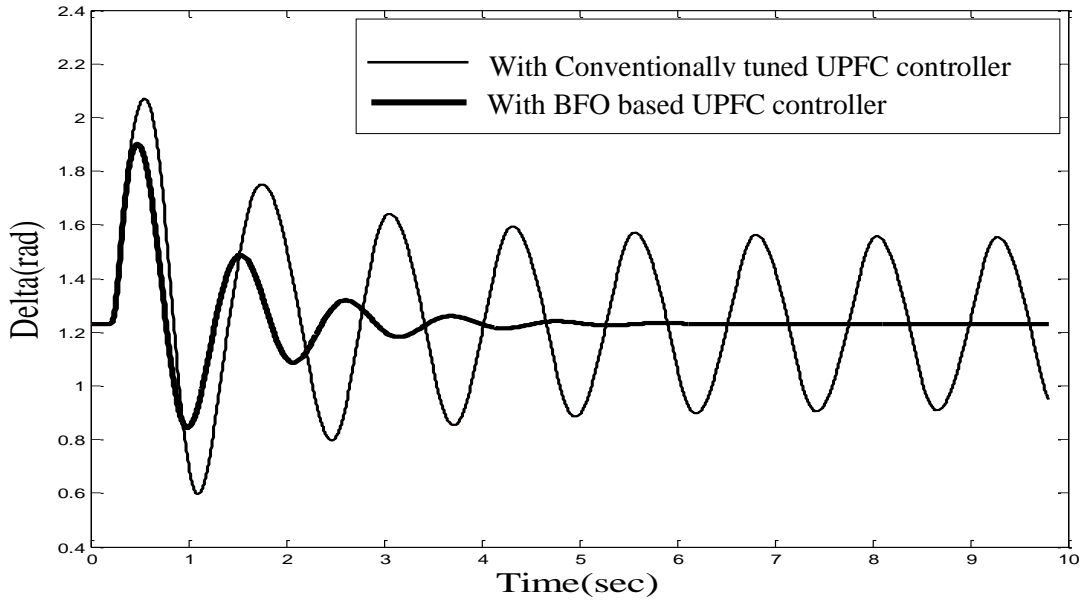


Fig 6.15.1 Time response of Power angle with conventionally tuned and BFO based UPFC controller (for 120 MW load with 3-Phase fault)

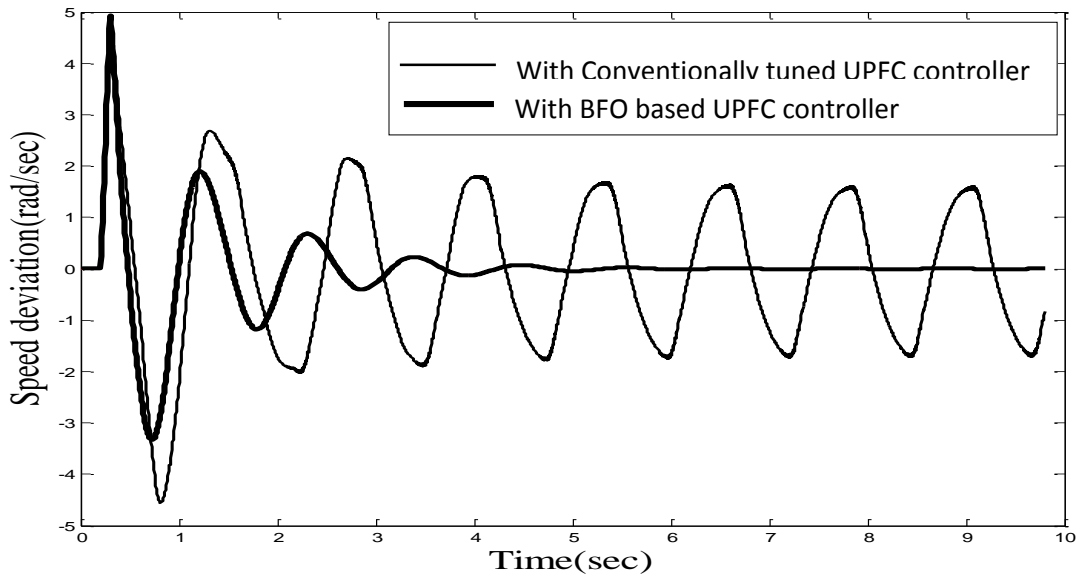


Fig 6.15.2 Time response of speed deviation with conventionally tuned and BFO based UPFC controller (for 120 MW load with 3-Phase fault)

- d. The operating conditions are further changed and the synchronous generator is now loaded to 150 MW load before the disturbance. BFO based UPFC controller is still effective as depicted in fig. 6.16.1 and 6.16.2.

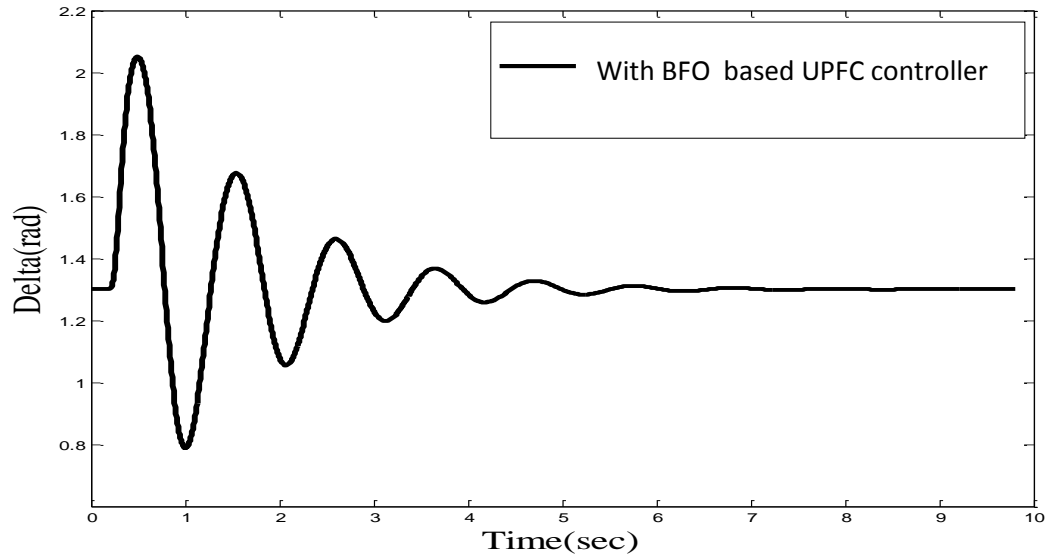


Fig 6.16.1 Time response of Power angle with BFO based UPFC controller (for 150 MW load with 3-Phase fault)

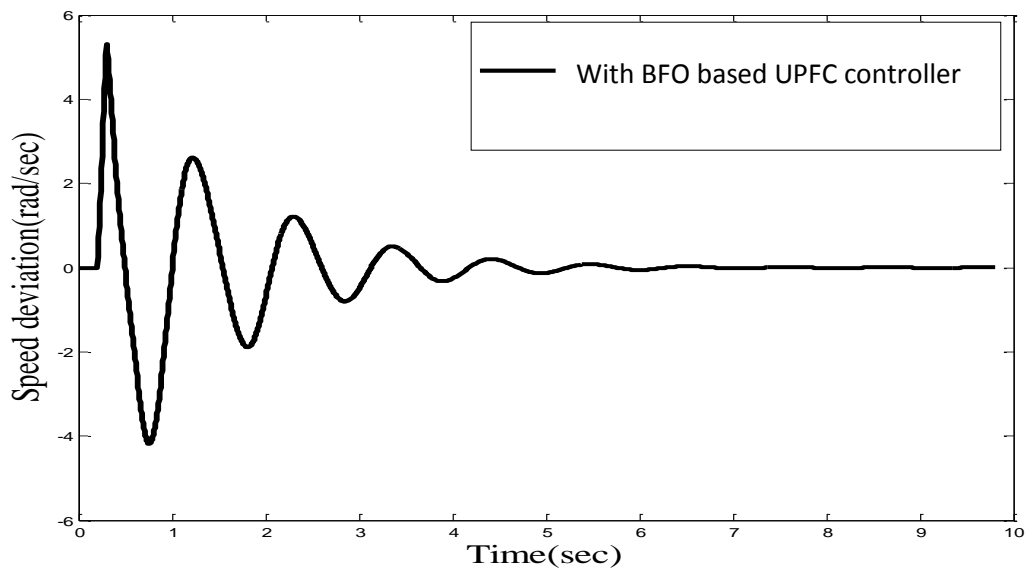


Fig 6.16.2 Time response of speed deviation with BFO based UPFC controller (for 150 MW load with 3-Phase fault)

**Case 2:** The simulations are carried out with one line outage. Generator is loaded with 160MW before the disturbance. Fig.6.17.2 and 6.17.4 depict the robustness of BFO based UPFC controller over the conventionally tuned UPFC controller as depicted in fig 6.17.1 and 6.17.3. On further loading of generator to 170 MW, the proposed BFO based UPFC controller is able to mitigate the oscillations but takes very long time to settle down these oscillations as depicted in fig. 6.18.1 and 6.18.2.

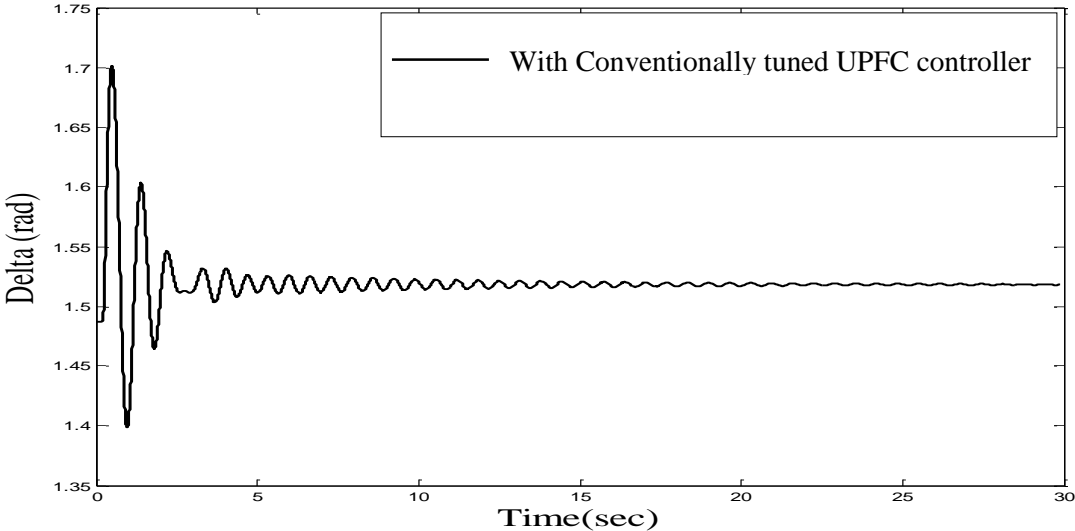


Fig 6.17(i) Time response of Power angle with conventionally tuned UPFC controller (for 160 MW with line outage)

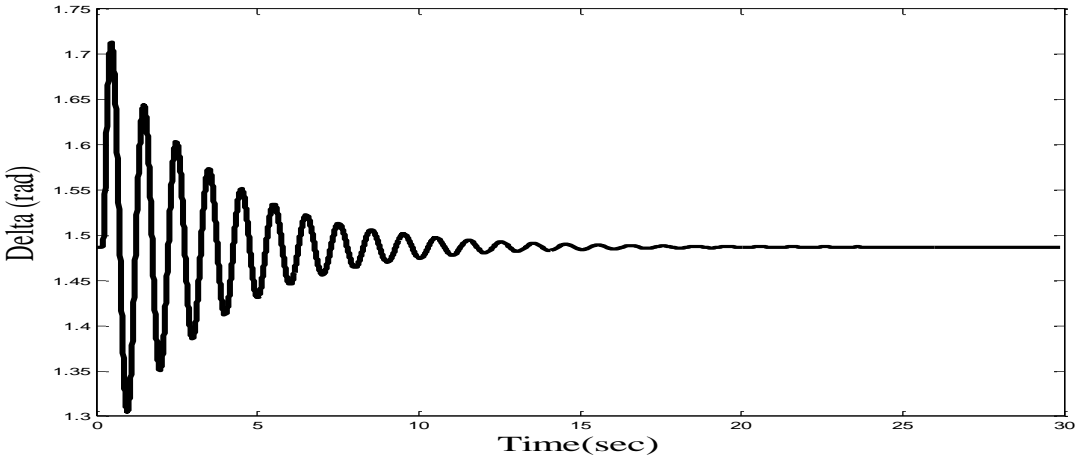


Fig 6.17.2 Time response of Power angle with BFO based UPFC controller for 160 MW with line outage)

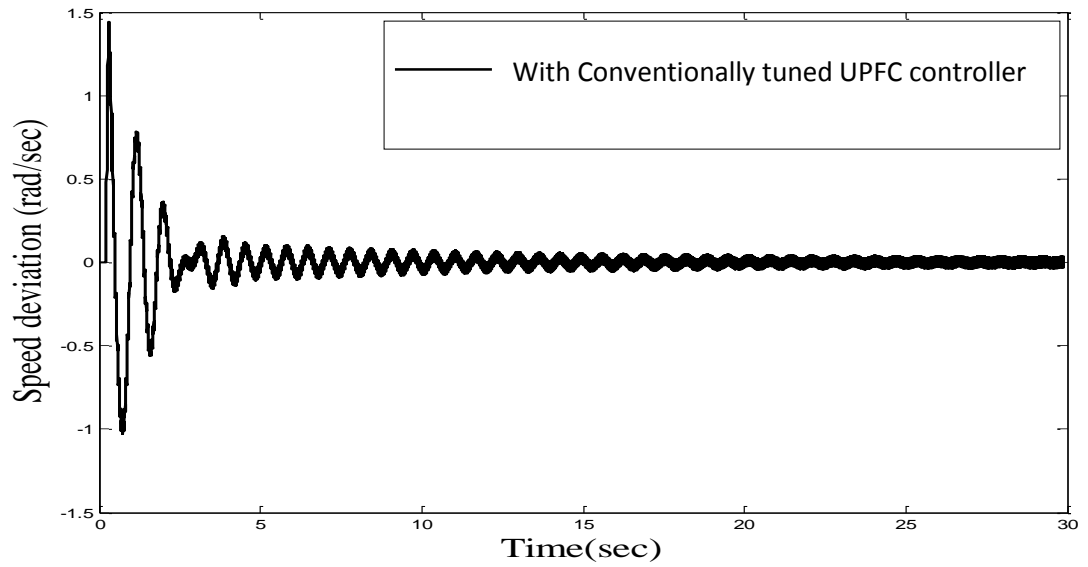


Fig 6.17.3 Time response of speed deviation with conventionally tuned UPFC controller (for 160 MW with line outage)

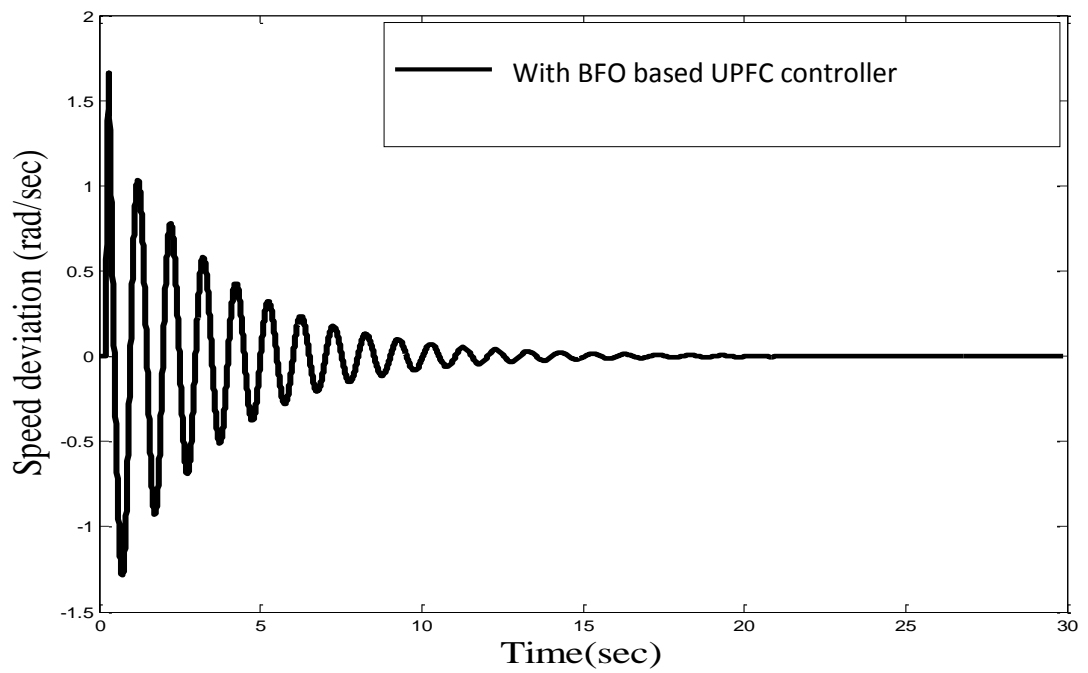


Fig 6.17.4 Time response of speed deviation with BFO based UPFC controller (for 160 MW with line outage)

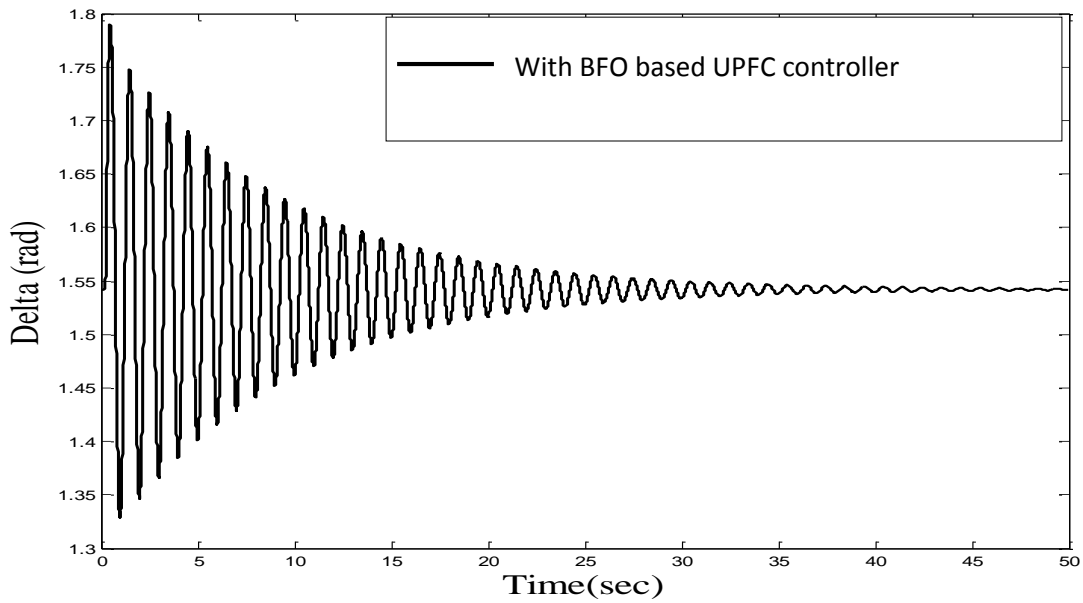


Fig 6.18.1 Time response of Power angle with BFO based UPFC (for 170 MW with line outage)

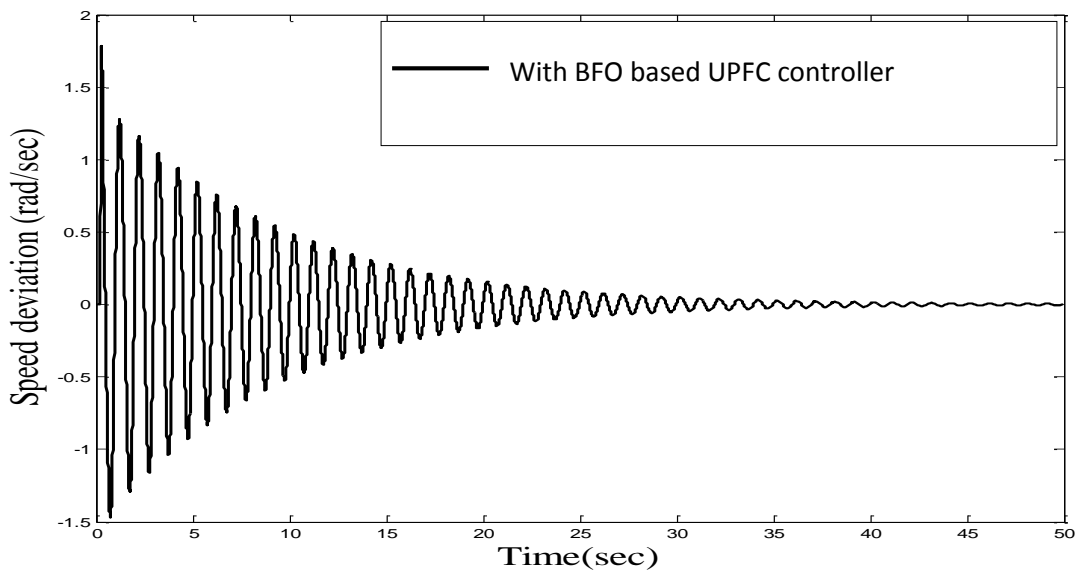


Fig 6.18.2 Time response of speed deviation with BFO based UPFC (for 170 MW with line outage)

E. Particle Swarm Optimization technique is implemented in matlab coding for optimizing the parameters of PI controller of UPFC to see the robustness of PSO based Controller for transient stability enhancement of the SMIB system. All the parameters



of PSO taken are given in appendix C. System stability is analyzed under same kinds of faults as for earlier cases. Three phase fault near infinite bus-bar and a severe fault of one line outage.

**Case 1:** The analysis is carried out with three phase fault near infinite bus-bar for 100msec & system is simulated for 10 seconds. The simulation result have been shown with PI controller parameters tuned by conventional method & PI controller parameters tuned by PSO (each particle is assigned with a set of 4 variables to be optimized and assigned with random values within the search bounds).

- a. The synchronous generator is operating at light load of  $P= 40\text{MW}$  before the disturbance. The robustness of PSO based UPFC controller is depicted in fig.6.19.1 and 6.19.2 for three phase fault near infinite bus-bar.

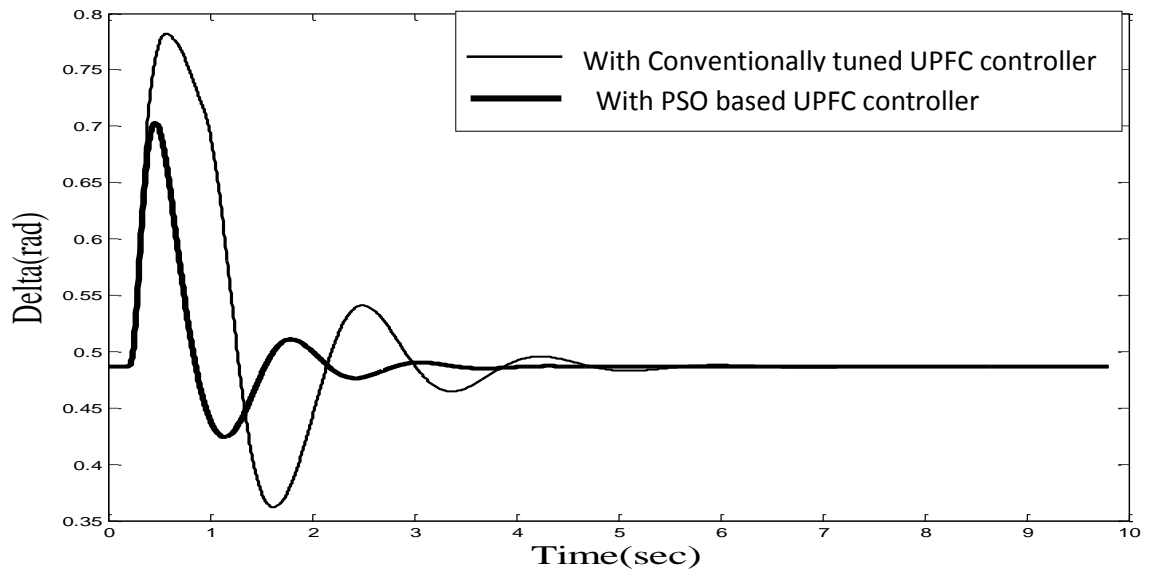


Fig. 6.19.1 Time response of Power angle with conventionally tuned and PSO based UPFC controller (for 40 MW load with 3-Phase fault)

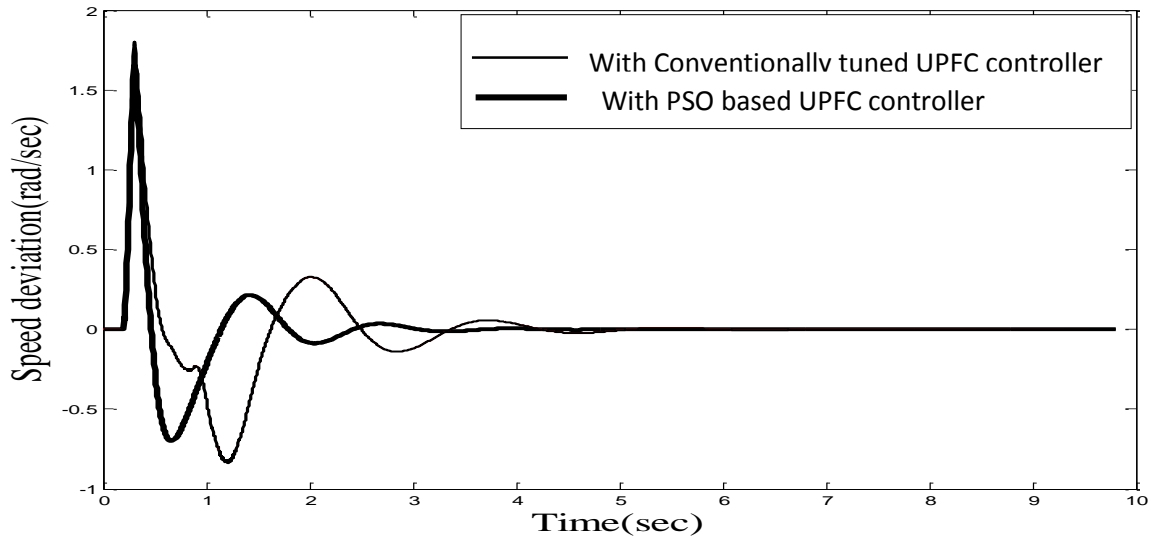


Fig. 6.19.2 Time response of speed deviation with conventionally tuned and PSO based UPFC controller (for 40 MW load with 3-Phase fault)

b. The generator operating conditions are changed. The normal load of 80 MW is considered and simulations are carried out to see the effect of PSO based controller on the damping of power oscillations. Fig 6.20.1 To fig.6.20.2 depict the variation in machine/power angle and generator speed.

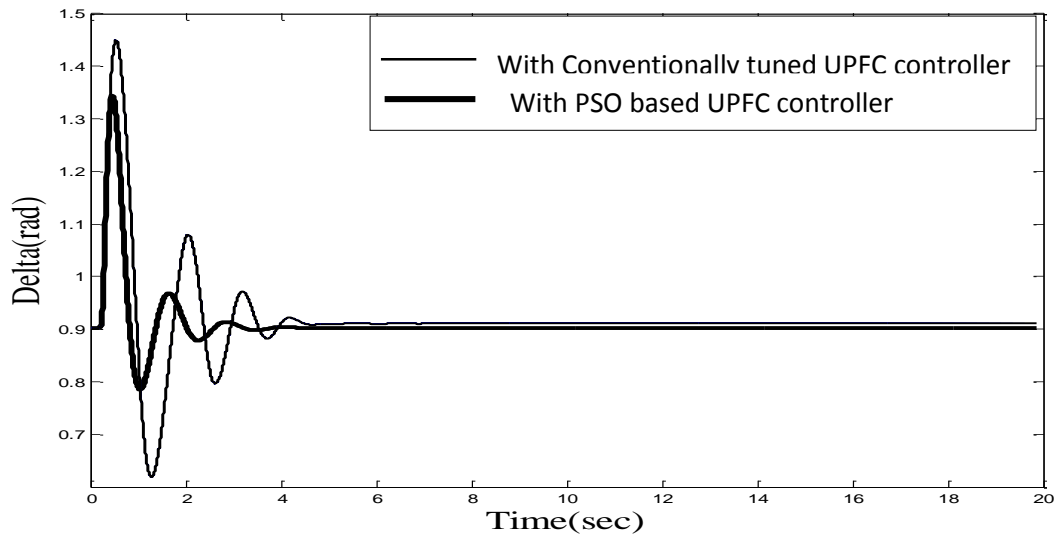


Fig. 6.20.1 Time response of Power angle with conventionally tuned and PSO based UPFC controller (for 80 MW load with 3-Phase fault)

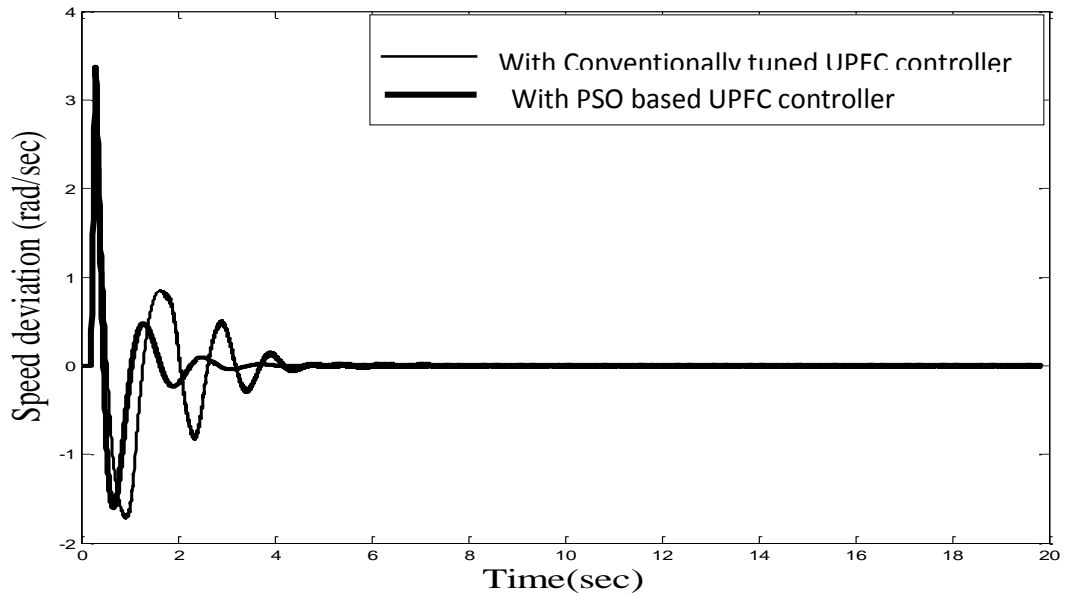


Fig. 6.20.2 Time response of speed deviation with conventionally tuned and PSO based UPFC controller (for 80 MW load with 3-Phase fault)

- c. Synchronous generator is provided with a heavy load of 120 MW. The simulation results depicted in fig.6.21.1 and fig.6.21.2 show that PSO based UPFC controller is highly effective in damping out the power oscillations under heavy load conditions subjected to three phase fault near infinite bus-bar whereas conventionally tuned UPFC controller is unable to damp out the oscillations..

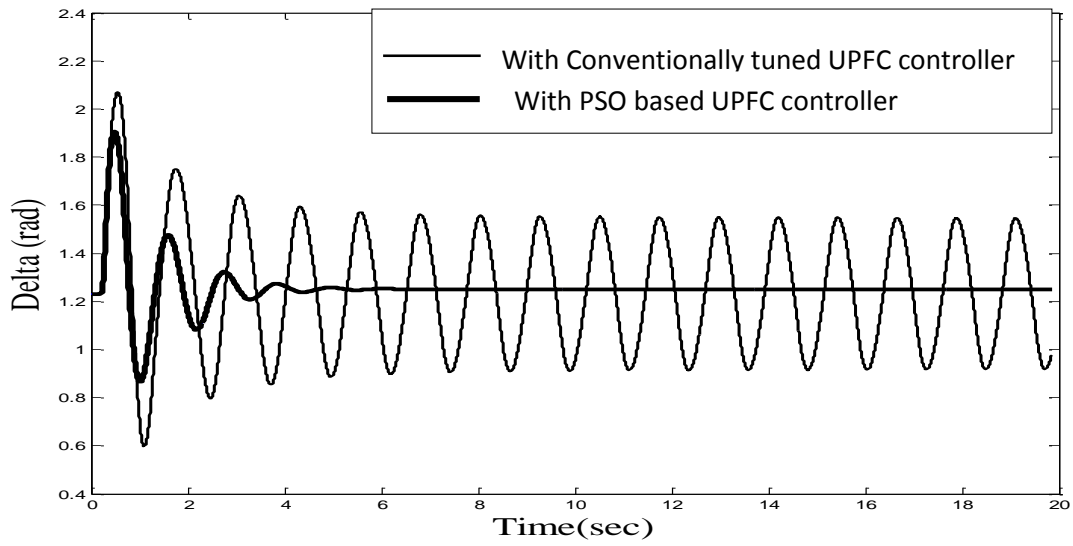


Fig. 6.21.1 Time response of Machine angle with conventionally tuned and PSO based UPFC controller (for 120 MW load with 3-Phase fault)

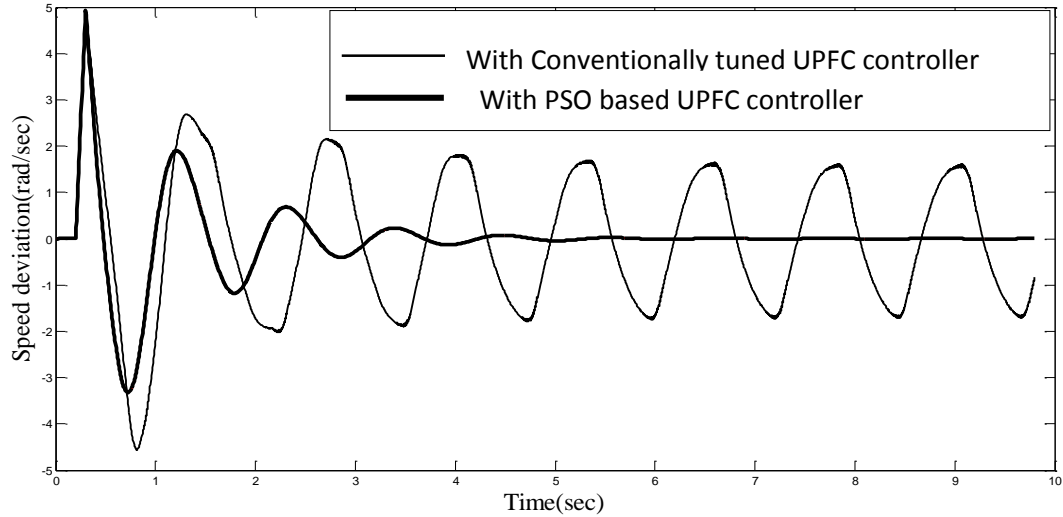


Fig. 6.21.2 Time response of speed deviation with conventionally tuned and PSO based UPFC controller (for 120 MW load with 3-Phase fault)

- d. The operating conditions are further changed by enhancing the load on generator to 140 MW. The simulation results show the effectiveness of PSO based UPFC Controller even at higher loadings when conventionally tuned controller fails.

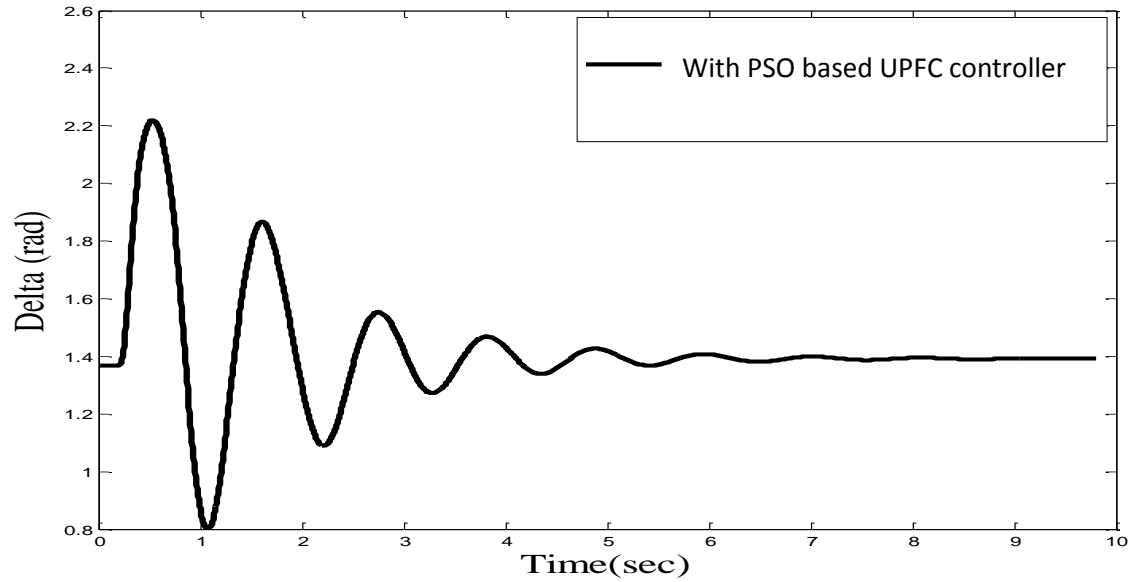


Fig. 6.22.1 Time response of Machine angle with PSO based UPFC controller (for 140 MW load with 3-Phase fault)

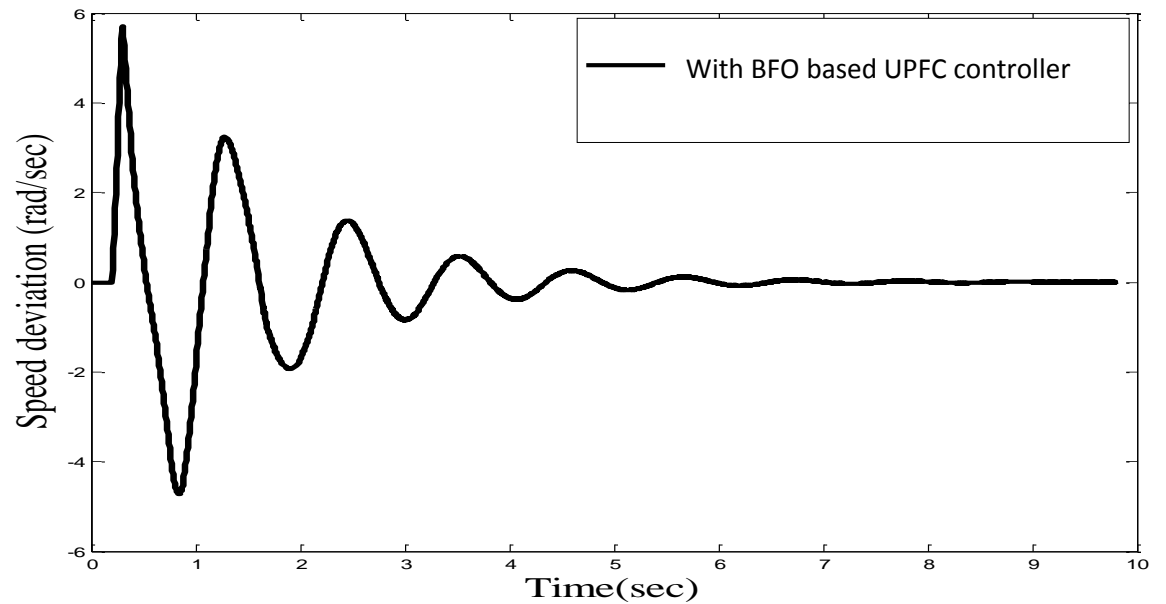


Fig. 6.22.2 Time response of speed deviation with PSO based UPFC controller (for 140 MW load with 3-Phase fault)

**Case 2:** Severe fault is created by tripping of one line for 100 msec. Fig.6.23.1 and 6.23.2 show the robustness of PSO based UPFC controller even at heavy loading conditions of 160MW and170 MW before the disturbance.

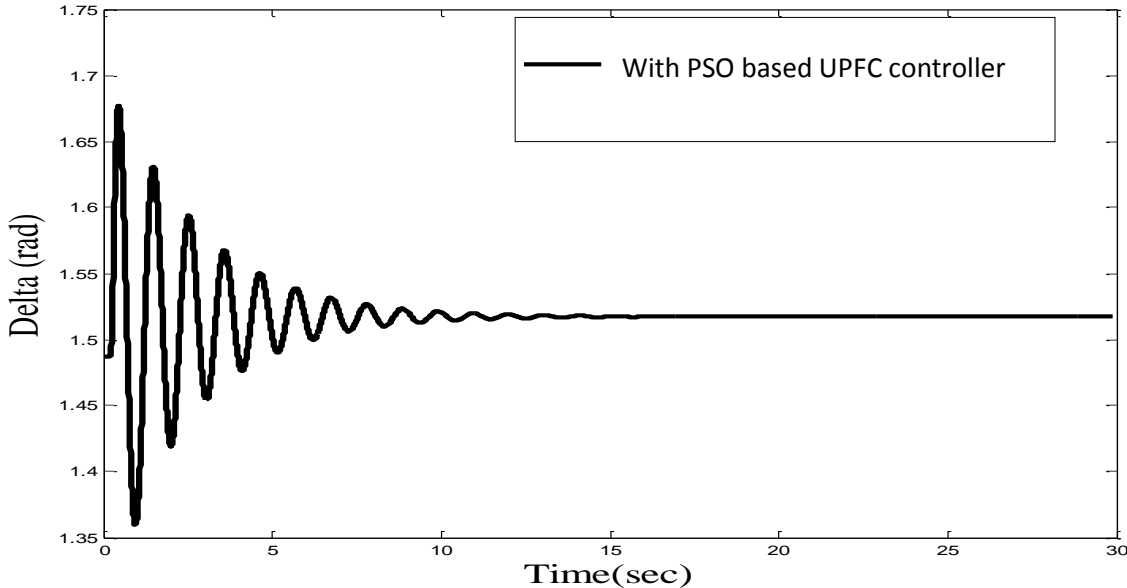


Fig. 6.23.1 Time response of Power angle with PSO based UPFC controller (for 160 MW load with line outage)

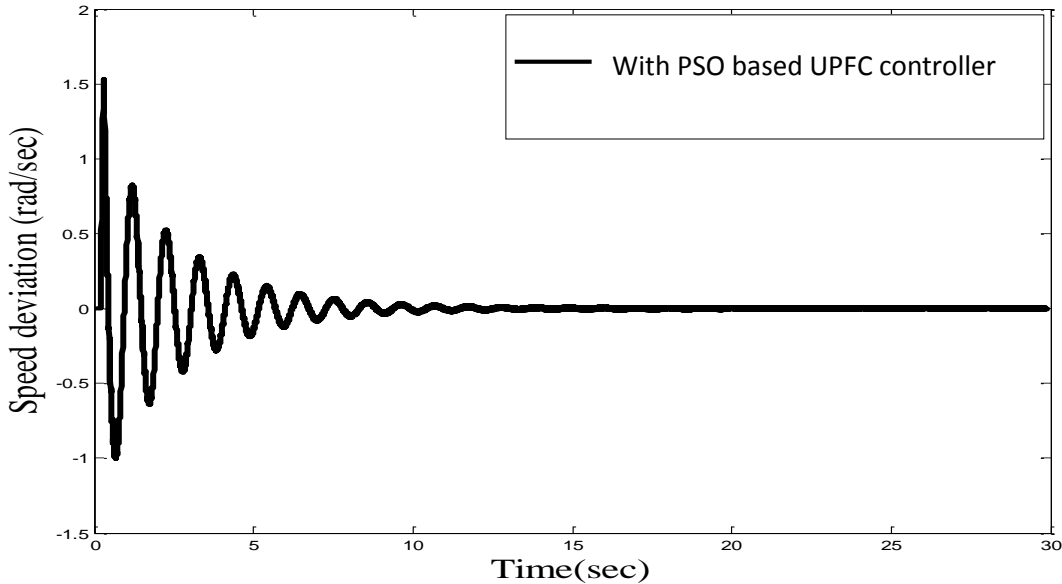


Fig. 6.23.2 Time response of speed deviation with PSO based UPFC controller (for 160 MW load with line outage)

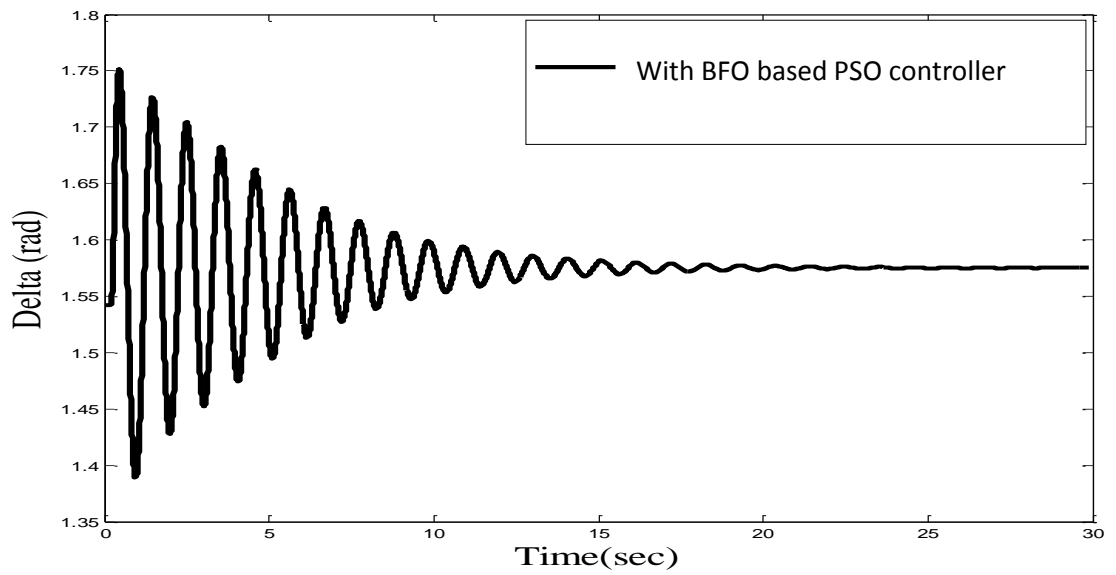


Fig. 6.23.1 Time response of Power angle with PSO based UPFC controller (for 170 MW load with line outage)

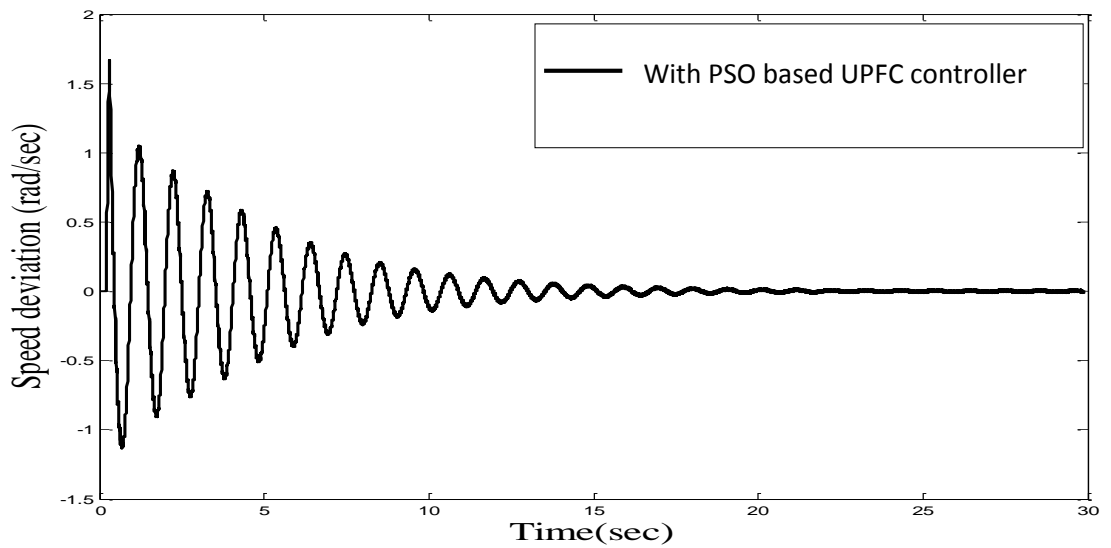


Fig. 6.23.2 Time response of speed deviation with PSO based UPFC controller (for 170 MW load with line outage)

F. Another swarm intelligent technique called Hybrid BF-PSO with time varying acceleration coefficients algorithm, also called as Advanced Adaptive BF-Particle Swarm Optimization technique as discussed in chapter 3 is applied for optimizing the parameters of PI Controller of UPFC. ITSE function used includes the variation in speed, active power and reactive power. Simulations are carried out for both three phase fault near infinite bus and with one line outage.

**Case 1:** The simulation is carried out with three phase fault near infinite bus-bar for 100msec. The simulation result have been shown with PI controller parameters tuned by conventional method & PI controller parameters tuned by hybrid BF-PSO with time varying acceleration coefficients.

a. The synchronous generator is operating with  $P=40$  MW before the disturbance. UPFC controller based on synergy of two algorithm is highly effective in damping out the power oscillations. The robustness of BF-PSO-TVAC based UPFC controller can be seen in fig.6.24.1 and 6.24.2.

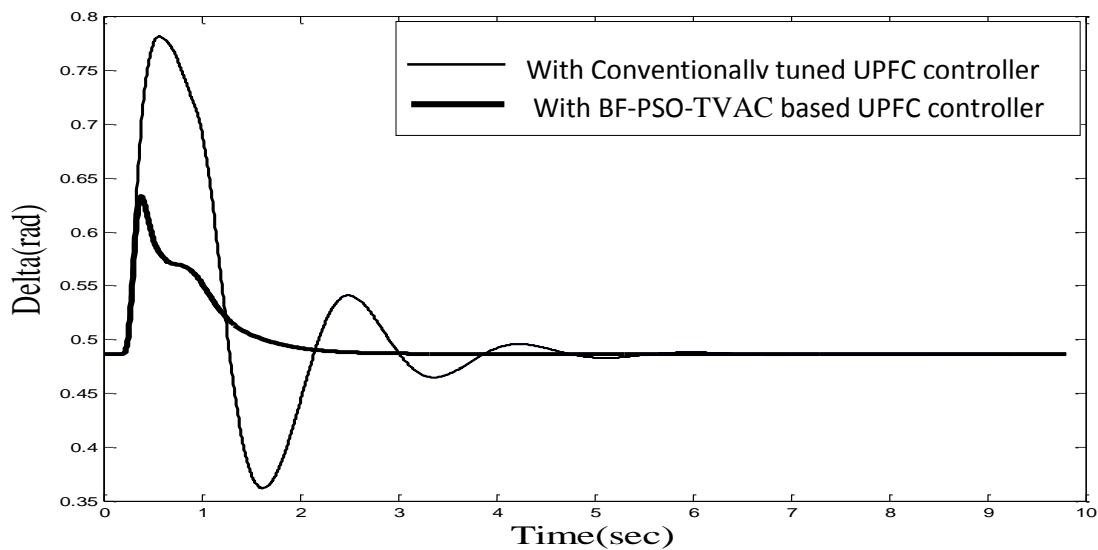


Fig. 6.24.1 Time response of Power angle with conventionally tuned and Hybrid BF-PSO based UPFC controller (for 40 MW load with 3-Phase fault)



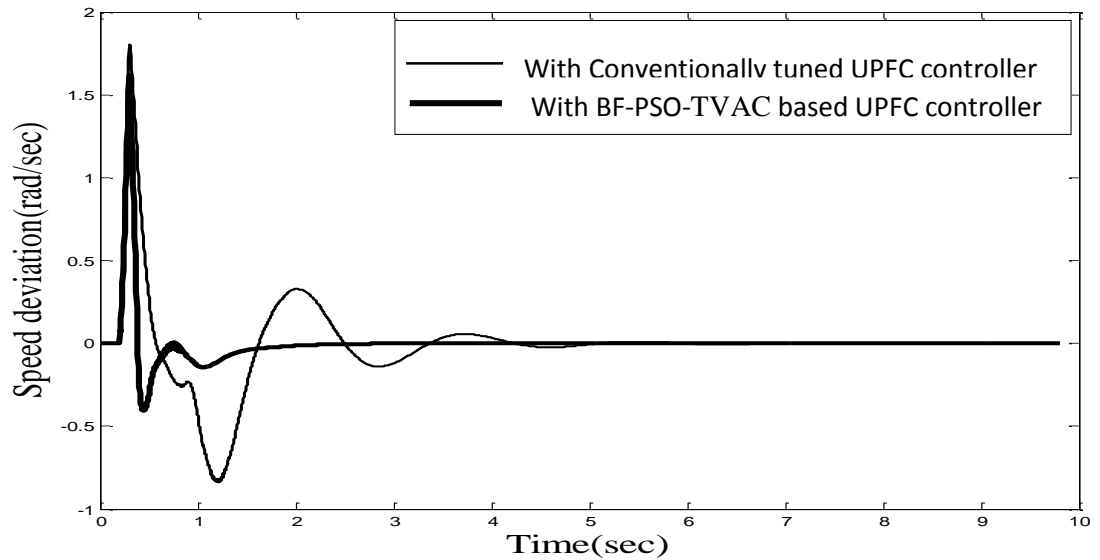


Fig. 6.24.2 Time response of speed deviation with conventionally tuned and Hybrid BF-PSO based UPFC controller (for 40 MW load with 3-Phase fault)

- b. The operating condition of synchronous generator is changed. 80 MW of load is connected on the machine. Simulation results show the effectiveness of proposed controller.

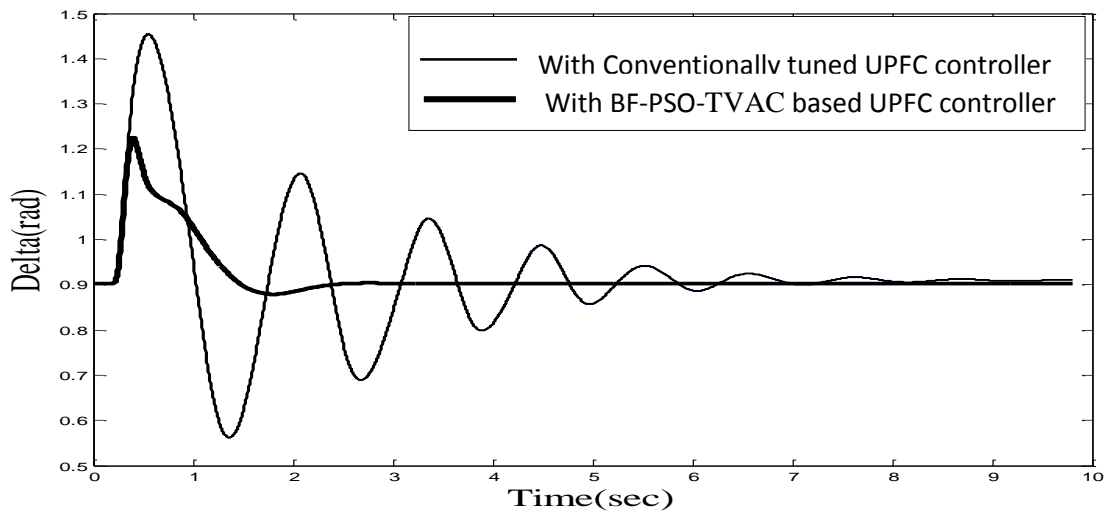


Fig. 6.25.1 Time response of Power angle with conventionally tuned and Hybrid BF-PSO based UPFC controller (for 80 MW load with 3-Phase fault)

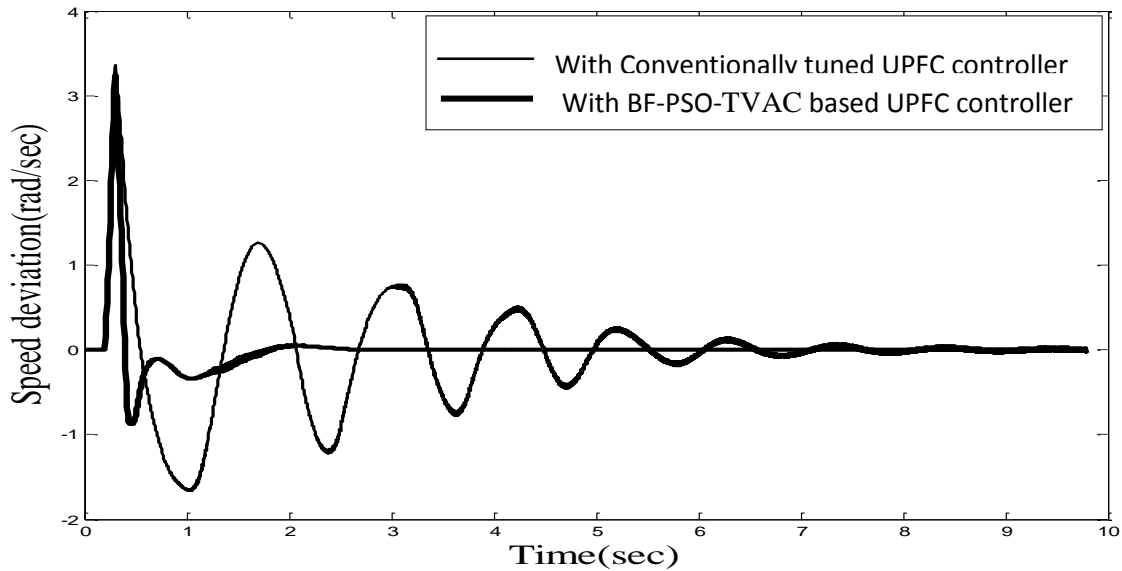


Fig. 6.25.2 Time response of speed deviation with conventionally tuned and Hybrid BF-PSO based UPFC controller (for 80 MW load with 3-Phase fault)

The synchronous generator is connected with heavy load of 120 MW. Fig. 6.26.1 and 6.26.2 depicts that proposed controller is highly effective in mitigating the oscillations during three phase fault. Thereby enhances the system transient stability.

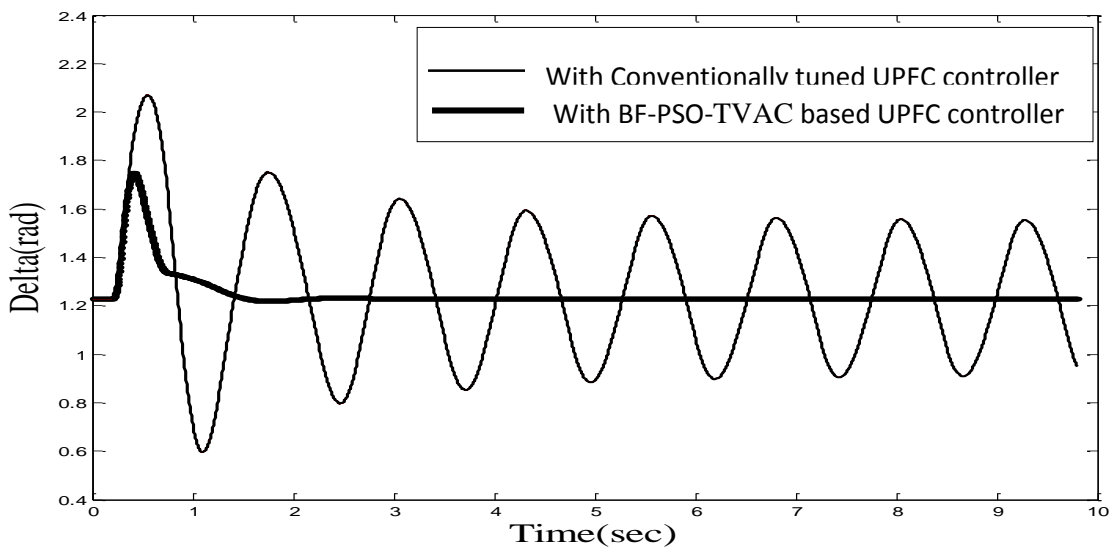


Fig. 6.26.1 Time response of Power angle with conventionally tuned and Hybrid BF-PSO based UPFC controller (for 120 MW load with 3-Phase fault)

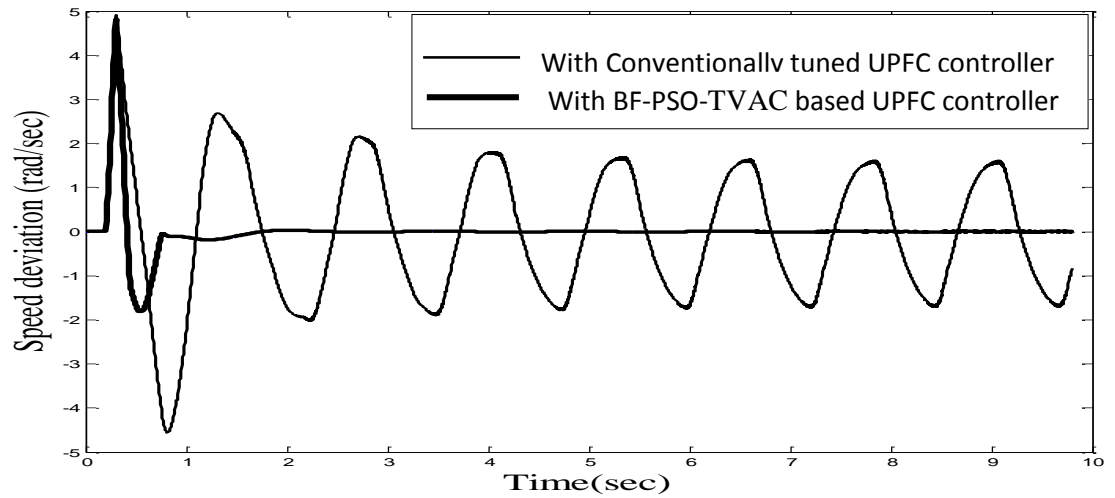


Fig. 6.26.2 Time response of speed deviation with conventionally tuned and Hybrid BF-PSO based UPFC controller (for 120 MW load with 3-Phase fault)

- c. The synchronous generator is made to operate at much heavier load of 160MW. The controller provides stability as shown in fig. 6.27.1 and 6.27.2 under three phase fault near infinite bus-bar beyond which the proposed controller do not provide control.

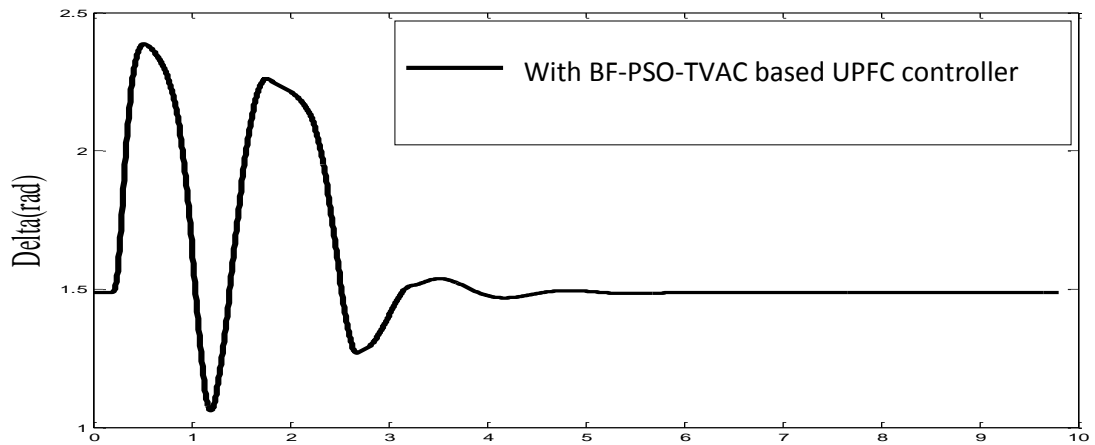


Fig. 6.27.1 Time response of Power angle with Hybrid BF-PSO based UPFC controller (for 160 MW load with 3-Phase fault)

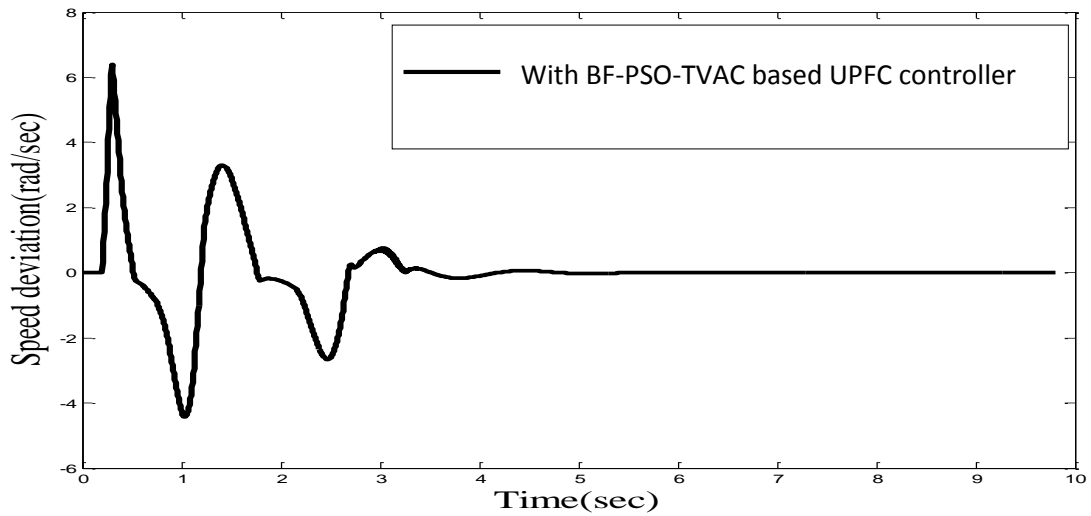


Fig. 6.27.2 Time response of speed deviation with Hybrid BF-PSO based UPFC controller (for 160 MW load with 3-Phase fault)

**Case 2:** The simulation is carried out with one line outage for the same time period of 100msec. The generator is loaded with a load of 170MW. Hybrid technique based UPFC controller proved to be highly effective in mitigating the oscillations as depicted in fig.6.29.1 and 6.29.2.

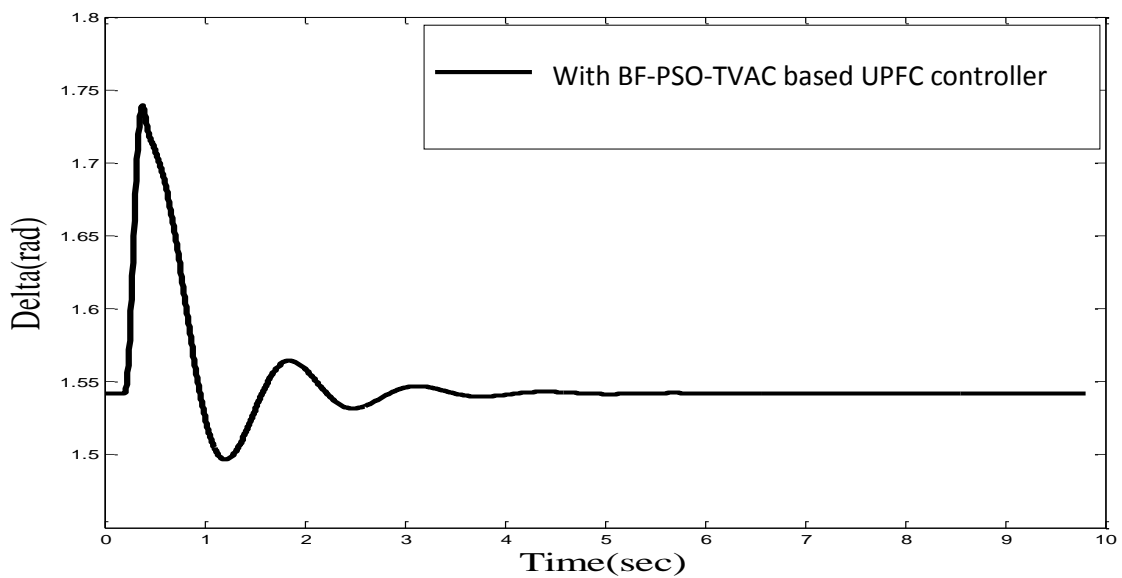


Fig. 6.29.1 Time response of Power angle with Hybrid BF-PSO based UPFC controller (for 170 MW load with line outage)

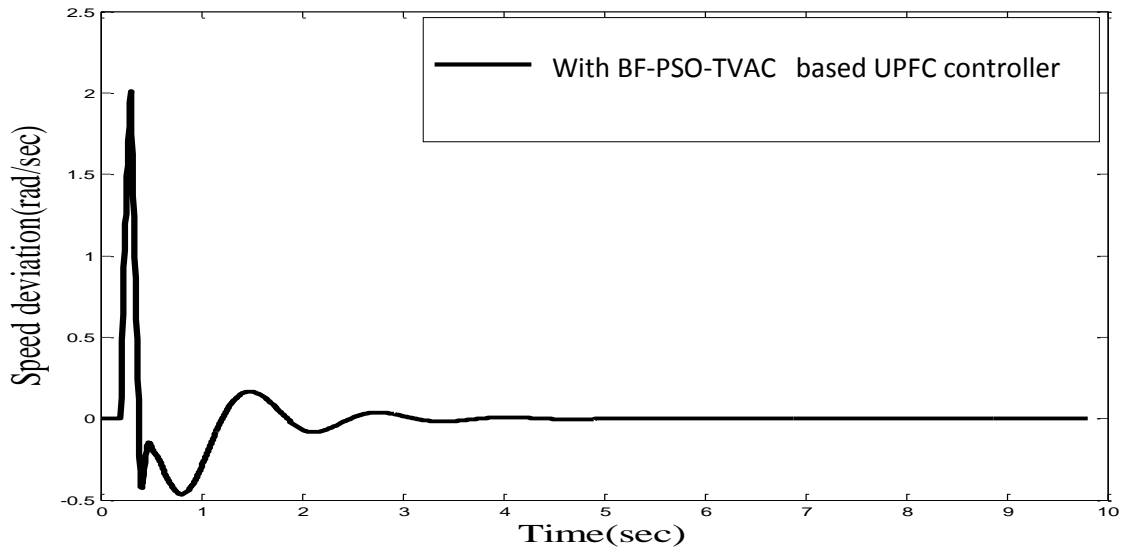


Fig. 6.29.2 Time response of speed deviation with Hybrid BF-PSO based UPFC controller (for 170 MW load with line outage)

G. The Genetic Algorithm, an evolutionary technique is now implemented in optimizing the controller parameters for transient stability enhancement. The technique used is already discussed in chapter 4. Simulations are carried out for both three phase fault near infinite bus and with one line outage.

**Case 1:** The simulation is carried out with three phase fault near infinite bus-bar for 100msec. The simulation result have been shown with both conventionally controlled and GA based PI controller parameters of UPFC controller. The parameters of GA are listed in appendix C.

- a. The synchronous generator is operating with  $P=40$  MW before the disturbance. Simulation results can be seen in fig.6.30.1 and 6.30.2.

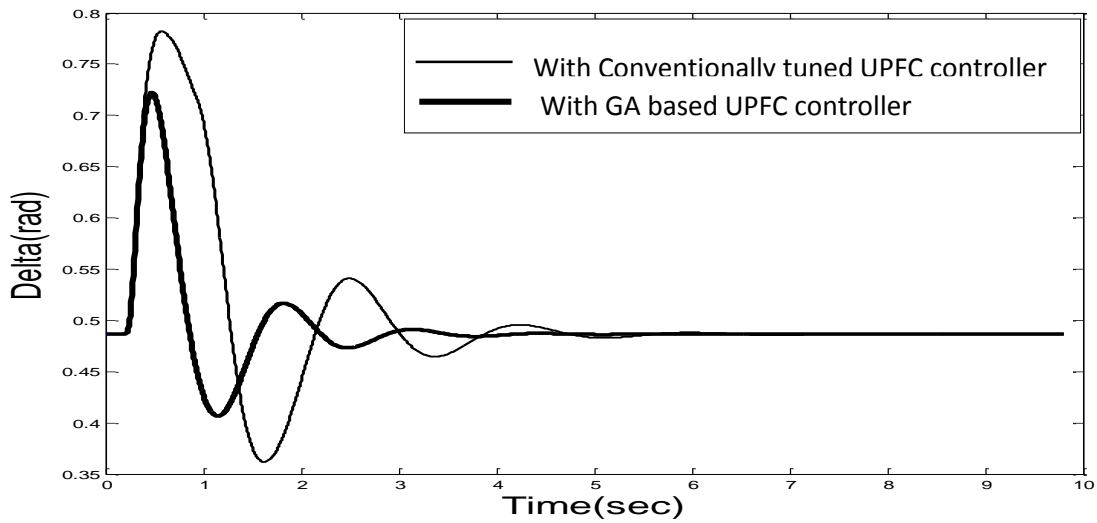


Fig. 6.30.1 Time response of Power angle with conventionally tuned and GA based UPFC controller (for 40 MW load with 3-Phase fault)

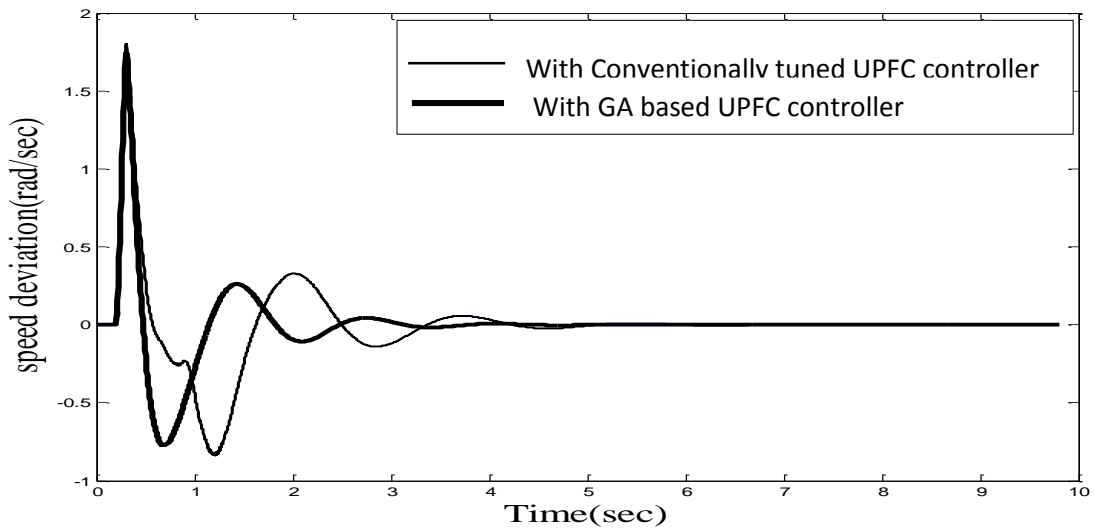


Fig. 6.30.2 Time response of speed deviation with conventionally tuned and GA based UPFC controller (for 40 MW load with 3-Phase fault)

- b. The operating level of the generator is then changed by heavily loading the generator to 120 MW. The simulation results show the robustness of GA based UPFC controller for the transient stability enhancement of the power system network.

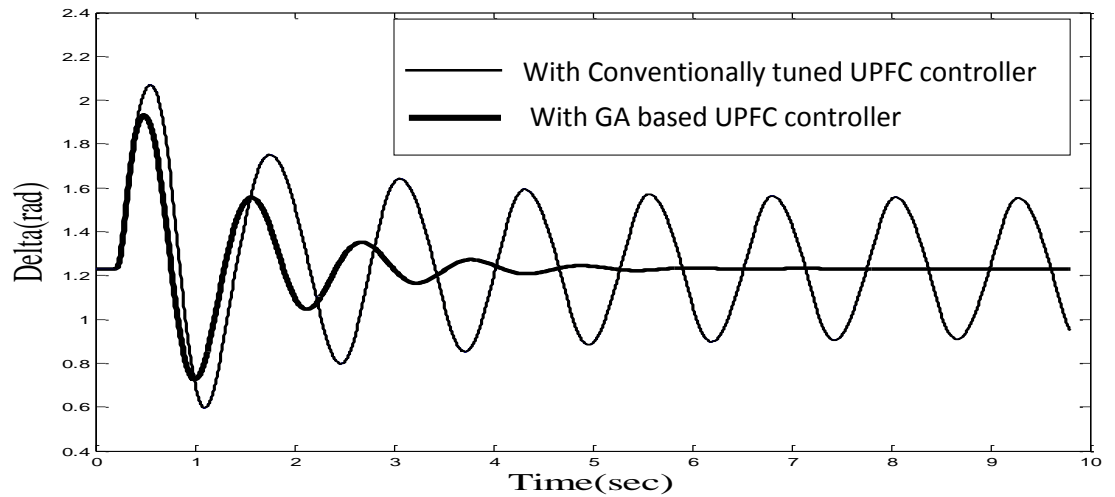


Fig. 6.31.1 Time response of Power angle with conventionally tuned and GA based UPFC controller (for 120 MW load with 3-Phase fault)

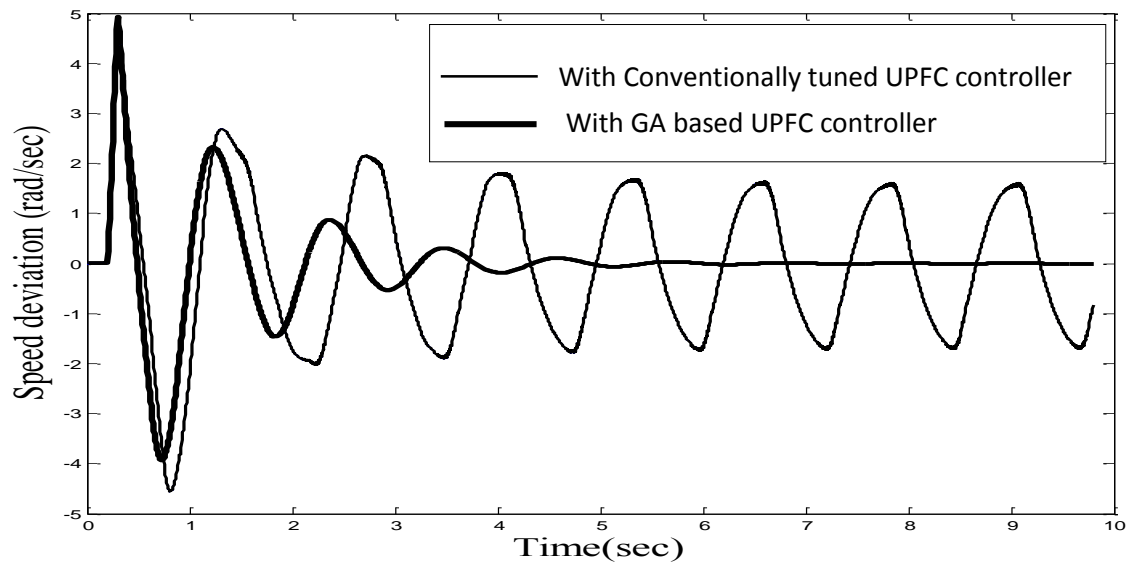


Fig. 6.32.2 Time response of speed deviation with conventionally tuned and GA based UPFC controller (for 120 MW load with 3-Phase fault)

**Case 2:** The simulation is carried out with one line outage for the same time period of 100msec. Fig. 6.32.1 and 6.32.2 show the simulation results with 160 MW load on generator and fig. 6.33.1 and 6.33.2 are for 170 MW generator loading. GA based UPFC controller proved to be equally effective in mitigating the oscillations as BFO and PSO

based UPFC controller. In contrast conventionally tuned UPFC controller are ineffective even for 160MW as depicted in fig. 6.17.1 and 6.27.3.

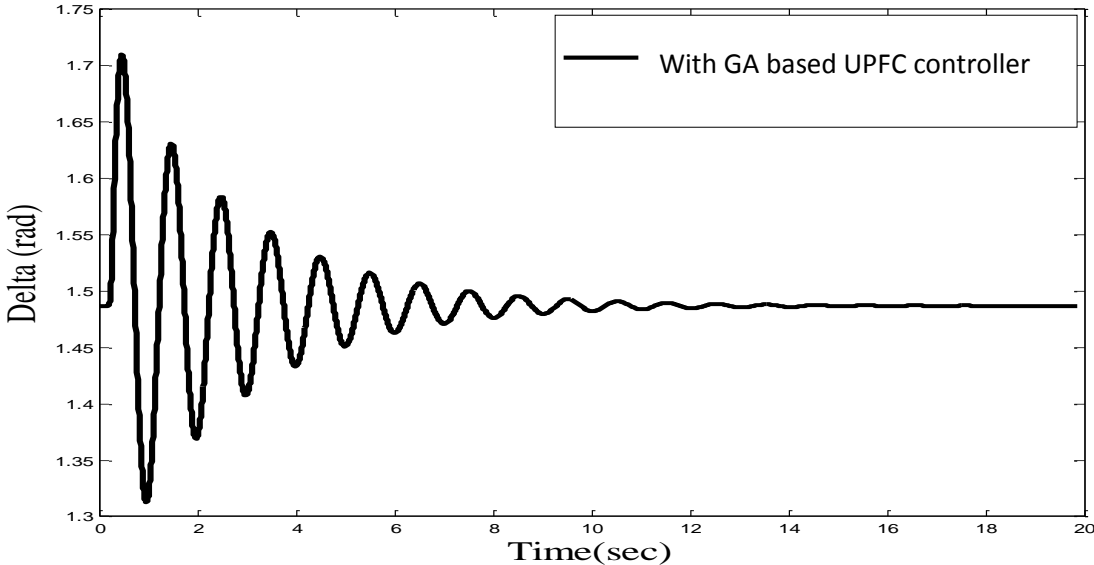


Fig. 6.32.1 Time response of power angle with GA based UPFC controller (for 160 MW load with line outage)

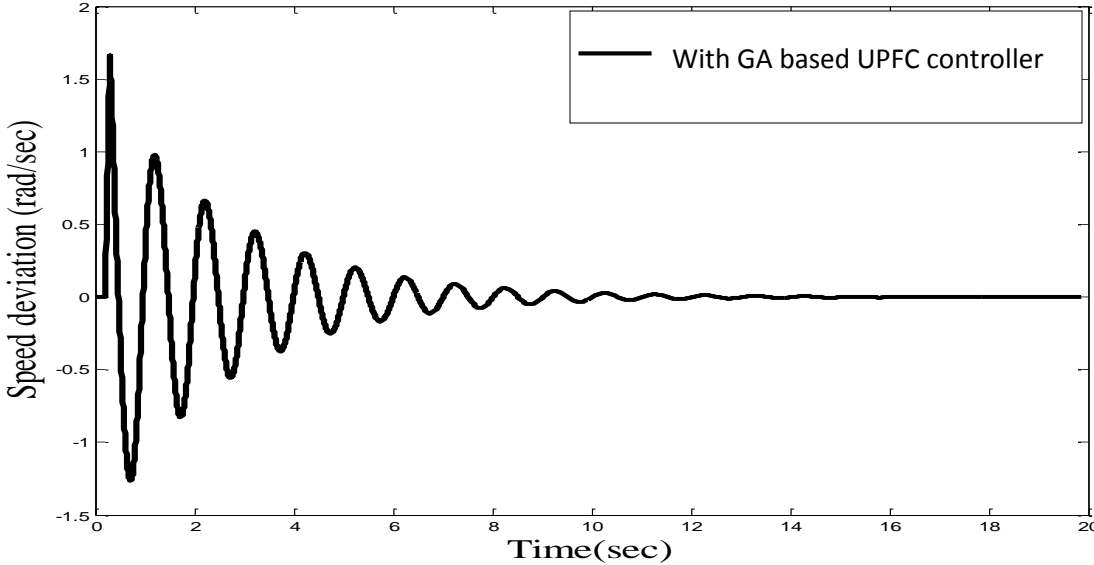


Fig. 6.32.2 Time response of speed deviation with GA based UPFC controller (for 160 MW load with line outage)



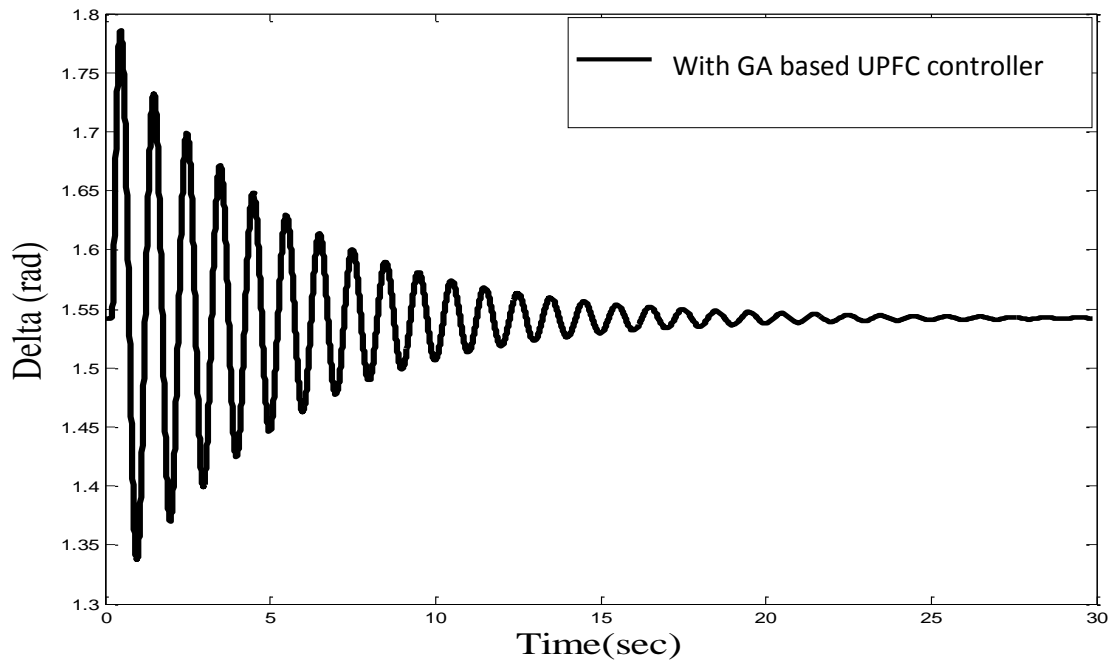


Fig. 6.33.1 Time response of power angle with GA based UPFC controller (for 170 MW load with line outage)

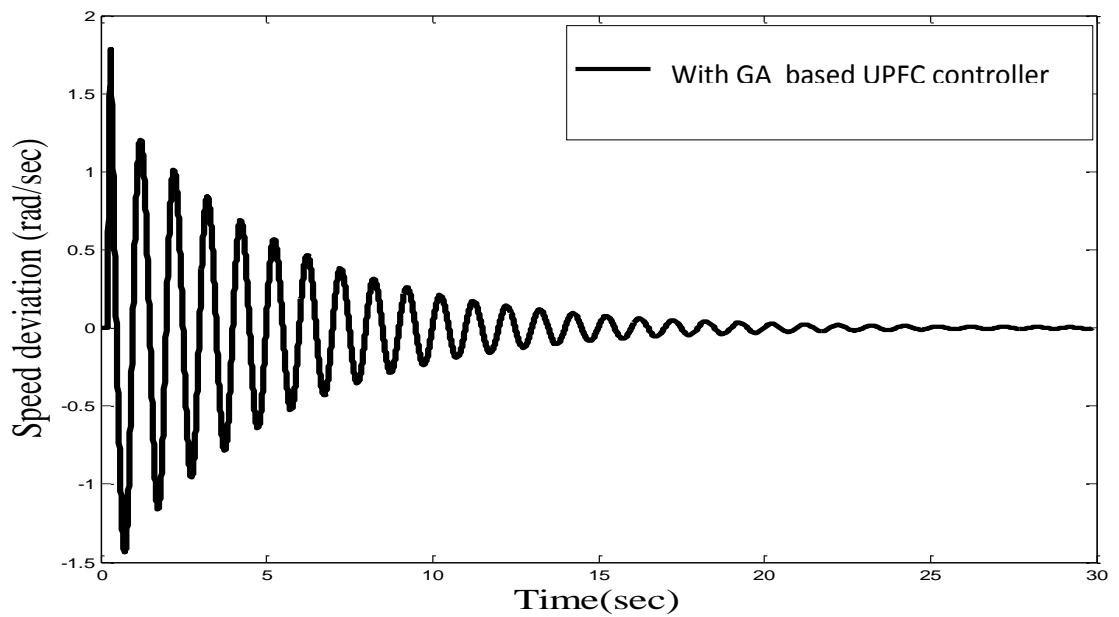


Fig. 6.33.2 Time response of speed deviation with GA based UPFC controller (for 170 MW load with line outage)

**Table 8: Comparison in settling time between various AI techniques based UPFC Controller in an SMIB system for 40MW generator loading under 3-phase fault condition.**

Cases	$\Delta \delta$ Settling time	$\Delta w$ Settling time	ITSE
Without UPFC Controller	24 sec	21 sec	$1.0217 \times 10^3$
Conventionally tuned UPFC Controller	6.5 sec	5.2 sec	111.2392
BFO based UPFC Controller	4.0 sec	3.8 sec	44.3734
PSO based UPFC Controller	4.2 sec	3.8 sec	44.0037
Hybrid BF –PSO – TVAC based UPFC Controller	2.5 sec	2.8 sec	15.8306
GA based UPFC Controller	4.0 sec	3.8 sec	56.4697

## 6.8 DISCUSSION

From the simulation results, it can be seen that Transient stability enhancement is achieved effectively by using UPFC Controller and this is a very important criterion for successful operation of series & shunt voltage source inverters. UPFC Controller is designed by optimizing its parameters using various soft computing techniques are much better than conventional based. Among all soft computing techniques mentioned above, Advanced Adaptive BFO-Particle Swarm Optimization based UPFC Controller has the advantage of both fast convergence as well as fine tuning to global minima. ITSE value is the lowest in this case as seen in table I. In this algorithm, both cognitive part and social part of velocity plays an important role in optimising to global minima. In order to increase the randomness at the initial stage, value of  $c1$  is made larger than

c2. This allows particle to search the optima in the whole m-dimensional search space. Lower value of c1 can lead to trapping into local minima due to premature convergence. Whereas, higher value of c2 than c1 is desired at later stage to enhance the social interaction and hence converges efficiently to global minima. It is mentioned here that this algorithm is used with time varying inertia weight factor. This Controller is highly effective in damping power oscillations even at much higher operating active power than others. From the responses, it is observed that there is a reduction of first swing in machine angle in all soft computing based UPFC Controller. BFO, PSO and GA based UPFC controller are comparable in mitigating the power system oscillations. Although, simulation results reveal that BFO based controller is able to mitigate power oscillations under contingency at higher generator loading as compare to PSO based UPFC controller.

## **6.9 MODELING OF MULTI-MACHINE SYSTEM**

### **Case Study**

A multi-machine power system (8 bus system) with two UPFC's connected are considered as shown in fig 2. Three generators are connected at buses 1, 2 and 3. Generator 1 is hydro & G2 & G3 are Thermal generators. The parameters of all the generators are given in appendix. Bus number 1 is taken as slack bus. The transmission line parameters are also given in appendix. UPFC1 is connected between bus number 4 and 5, while UPFC2 is connected between bus number 7 and 8. Loads are connected at bus number 1, 2 and 3. They are represented in terms of admittances  $Y_{L1}$ ,  $Y_{L2}$ ,  $Y_{L3}$  and  $Y_{L4}$  & are computed from load bus data. Using power Injection model [63], [81] and [83] of UPFC1 and UPFC2, they are represented by equivalent admittances and the admittance matrix of the power network is then modified. Simple AVR are connected to each generator. The operating conditions taken are:  $p1=4.5$ ,  $q1=1.5$ ,  $p2=1.3$ ,  $q2=0.6$ ,  $p3= 1.0$ ,  $q3=0.5$ . Fault is created at the Centre of line 3-4 at 0.5 sec & cleared at 0.6 sec which results in power deviation in the transmission line. The real power deviation in the transmission line generates the component  $V_{SEQ}$  of series voltage injection in quadrature with line current and the reactive power deviation in line generates the in phase component  $V_{SEP}$ .  $k_p$  and  $k_i$  relates these components to power deviations. These PI controller parameters are then tuned by PSO

technique to damp the inter area and local area oscillations effectively. The synchronous generator is represented by third order machine model. The differential equations governing the dynamics of each machine are already described in SMIB system.

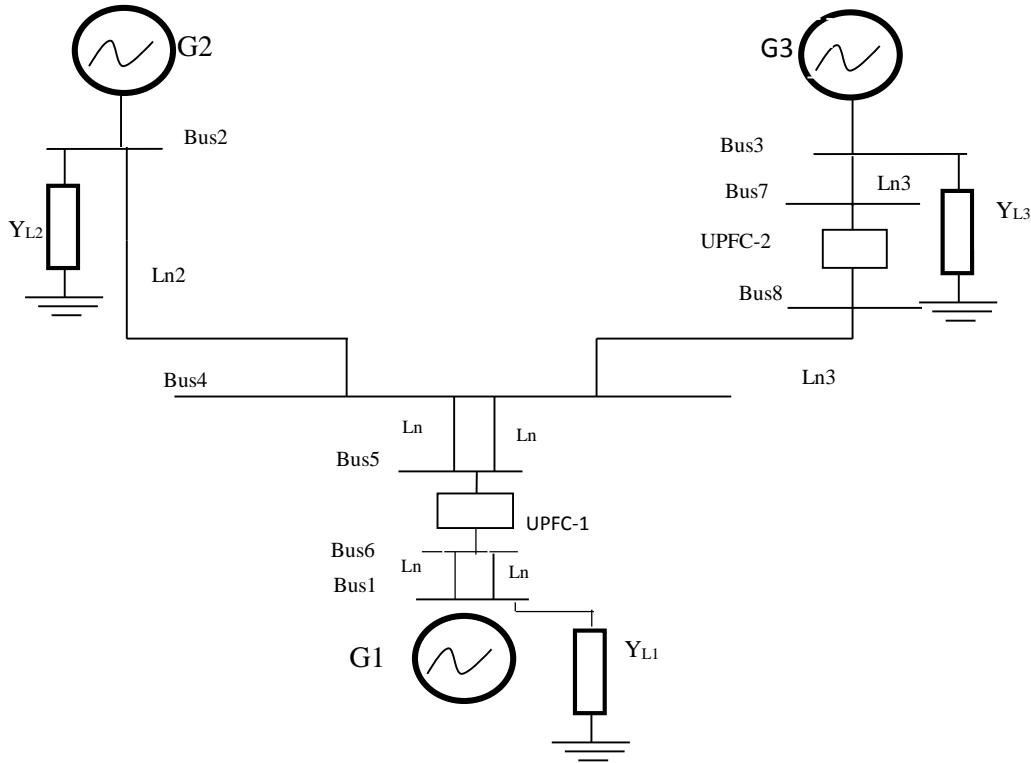


Fig. 6.34 Single line diagram of Multi-machine power system with UPFC Controllers

### 6.10 POWER INJECTION MODEL OF UPFC

The automatic power control mode cannot be achieved with conventional compensators. In order to show how line power flow can be affected by the UPFC operated in the automatic power flow mode, UPFC is placed at the beginning of the transmission line connecting buses  $i$  and  $j$  as shown in Fig. 6.35. Line conductance is neglected. UPFC is represented by two ideal voltage sources of controllable magnitude and phase angle.

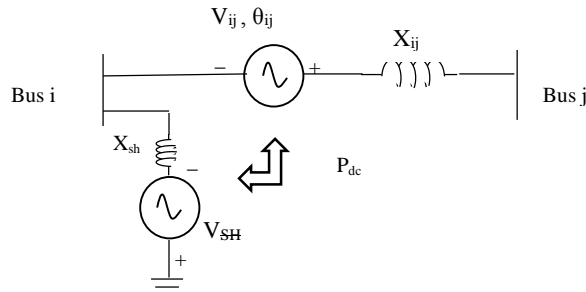


Fig 6.35 Two voltage source model of UPFC

### Shunt Converter

Let the current injected by the shunt converter is  $I_{SH}$  & voltage source is  $V_{SH}$  shown in fig.6.35. The shunt side of UPFC is converted into power injection at bus bar i only.

$$S_{i0} = P_{i0} + jQ_{i0} = V_i \left( \frac{V_i - V_{SH}}{Z_{i0}} \right)^* \quad (6.32)$$

Where,  $Z_{i0} = R_{i0} + jX_{i0}$

Since the shunt reactive compensation capability of UPFC is not utilized that is the UPFC shunt converter is assumed to be operating at unity power factor [49]. Its main function is to transfer the real power demand of series converter through the dc link, so

$$P_{i0} = V_i I_{SH} \text{ and } Q_{i0} = 0 \quad (6.33)$$

### H. Series Converter

Let the ideal voltage injected by the series converter is  $V_{se}$  and reactance  $X_{ij}$  be present between two buses (i, j) in the power system shown below [boo]. The series side of UPFC is then converted into two power injections at buses i & j.

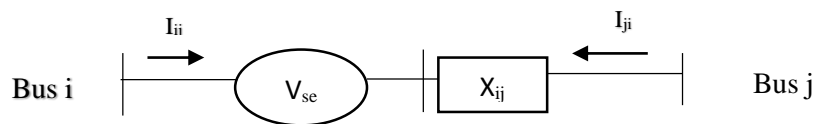


Fig.6.36 Voltage source representation of series converter

The Norton equivalent of the above circuit is shown as:

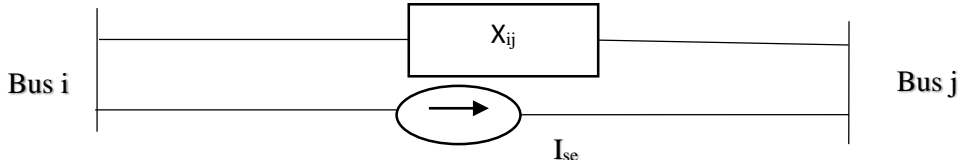


Fig.6.37 Current source representation of series converter

$$I_{SE} = \frac{-V_{SE}}{X_{ij}} \text{ in parallel with the line } B_{ij} = 1/X_{ij}$$

The current source  $I_{se}$  leads to injection powers namely,  $S_i$  and  $S_j$  and can be computed as follows:

$$S_i = P_i + jQ_i = V_i \left( \frac{-V_{SE}}{X_{ij}} \right)^* = V_i (-V_{SE} B_{ij}) \quad (6.34)$$

Since  $V_{SE} = \rho V_i e^{j\beta}$  and

$$\beta = \tan^{-1} \left( \frac{V_{SEQ}}{V_{SEP}} \right) + \tan^{-1} \left( \frac{I_{ijd}}{I_{ijq}} \right) - \tan^{-1} \left( \frac{V_{id}}{V_{iq}} \right) \quad (6.35)$$

$$S_i = V_i \left( jB_{ij} \rho V_i e^{j\beta} \right)^* = -B_{ij} \rho |V_i|^2 \sin(\beta) - jB_{ij} \rho |V_i|^2 \cos(\beta) \quad (6.36)$$

$$P_i(inj) = -B_{ij} \rho |V_i|^2 \sin(\beta) \text{ and } Q_i(inj) = -B_{ij} \rho |V_i|^2 \cos(\beta) \quad (6.37)$$

Similarly,

$$S_j = V_j (I_{SE})^* = V_j (V_{SE} B_{ij})^* \quad (6.38)$$

$$S_j = V_j \left( -jB_{ij} \rho V_i e^{j\beta} \right)^* = B_{ij} \rho |V_i| |V_j| \sin(\theta_{ij} + \beta) + jB_{ij} \rho |V_i| |V_j| \cos(\theta_{ij} + \beta) \quad (6.39)$$

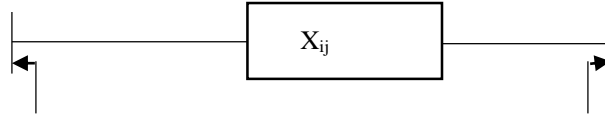
$$P_j(inj) = B_{ij} \rho |V_i| |V_j| \sin(\theta_{ij} + \beta) \quad (6.40)$$

$$Q_j(inj) = B_{ij} \rho |V_i| |V_j| \cos(\theta_{ij} + \beta) \quad (6.41)$$

Where

$$\theta_{ij} = \theta_i - \theta_j$$

Based on the explanation above the injection model of a series connected voltage source can be represented by two independent loads as shown in fig 6.38.



$$\begin{aligned} \text{Bus i} \quad P_i &= -B_{ij}\rho|V_i|^2 \sin(\beta) & \text{Bus j} \quad P_j &= B_{ij}\rho|V_i||V_j| \sin(\theta_{ij} + \beta) \\ Q_i &= -B_{ij}\rho|V_i|^2 \cos(\beta) & Q_j &= B_{ij}\rho|V_i||V_j| \cos(\theta_{ij} + \beta) \end{aligned}$$

Fig. 6.38 Representation of series converter with equivalent load form

Further the real power associated with converter-1 can be written as

$$P_{io} = |V_i| I_{SH}$$

Where  $I_{SH}$  is in phase current with the bus voltage  $V_i$

$P_{dc}$  is the power transfer from shunt side to series side.

$$P_{dc} = \text{Re} \left[ V_{SE} \left( \frac{V_i + V_{SE} - V_j}{X_{ij}} \right) \right]^* = \text{Re} \left[ \rho V_i e^{j\beta} \left( \frac{V_i + V_{se} - V_j}{X_{ij}} \right) \right]^* \quad (6.42)$$

On solving,

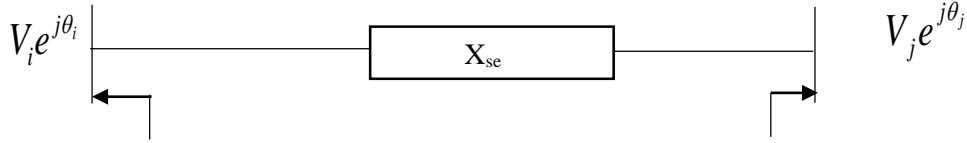
$$P_{dc} = B_{ij}\rho|V_i||V_j| \sin(\theta_{ij} + \beta) - B_{ij}\rho|V_i|^2 \sin(\beta) \quad (6.43)$$

When power loss inside the UPFC is neglected, than

$P_{io} = P_{dc}$  and modified injection model is formulated as shown in fig.(6.39).

$$S_i(inj) = S_i - S_{io} = P_i - P_{io} + jQ_i \quad (6.44)$$

$$S_j(inj) = S_j = P_j + jQ_j \quad (6.45)$$



$$\begin{aligned}
 P_i &= -B_{ij}\rho|V_i|^2 \sin(\beta) - |V_i|I_{SH} & P_j &= B_{ij}\rho|V_i||V_j| \sin(\theta_{ij} + \beta) \\
 Q_i &= -B_{ij}\rho|V_i|^2 \cos(\beta) & Q_j &= B_{ij}\rho|V_i||V_j| \cos(\theta_{ij} + \beta)
 \end{aligned}$$

Fig. 6.39 Power Injection model of UPFC

Where  $I_{ijd}$  and  $I_{ijq}$  are d-q axis transmission line currents and  $V_{id}$  and  $V_{iq}$  are d-q axis voltage of  $i^{\text{th}}$  bus of UPFC.

The component in phase and quadrature component of  $V_{se}$  is responsible for real and reactive power flow in line & hence finally mitigate the power oscillations.

### 6.11 UPFC DYNAMIC MODEL

For transient stability studies, the DC link dynamics have to be taken into account. The DC link capacitor will exchange energy with the system and its voltage will vary.

The power frequency dynamic model can be described by the following equation [49]. The dynamics of the D.C voltage neglecting losses can be represented by

$$CV_{dc} \frac{dV_{dc}}{dt} = [P_{io} - P_{dc}] \quad (6.46)$$

By putting the values of  $P_{io}$  and  $P_{dc}$ , in above equation, the dynamics of the D.C link is represented as:

$$\frac{dV_{dc}}{dt} = \frac{1}{C V_{dc}} \left[ |V_i|I_{SH} - B_{ij}\rho|V_i||V_j| \sin(\theta_{ij} + \beta) + B_{ij}\rho|V_i|^2 \sin(\beta) \right] \quad (6.47)$$



## 6.12 PROCEDURE FOR MULTI-MACHINE POWER SYSTEM SIMULATION

The digital simulation reads the initial nodes specifications and generates the steady state load flow solution assuming the reference bus voltage in p.u as 1 angle  $0^0$ , corresponding to a common reference frame rotating at synchronous speed thus representing Q axis. The common reference frame & the reference frame of the  $i^{\text{th}}$  machine are related by the transformation [3].

$$\begin{bmatrix} V_{Di} \\ V_{Qi} \end{bmatrix} = \begin{bmatrix} a & \dots & \dots & b \\ c & \dots & \dots & d \end{bmatrix} \begin{bmatrix} V_{di} \\ V_{qi} \end{bmatrix}$$

$$\begin{bmatrix} I_{Di} \\ I_{Qi} \end{bmatrix} = \begin{bmatrix} a & \dots & \dots & b \\ c & \dots & \dots & d \end{bmatrix} \begin{bmatrix} I_{di} \\ I_{qi} \end{bmatrix} \quad (6.48)$$

Where

$$a=d=\cos(\delta_i), \quad b=-\sin(\delta_i) \quad \text{and} \quad c=-b$$

Where  $\delta_i$  is the angle between the machine reference axes ( $d_i, q_i$ ) and the common reference axes (D,Q) as shown:

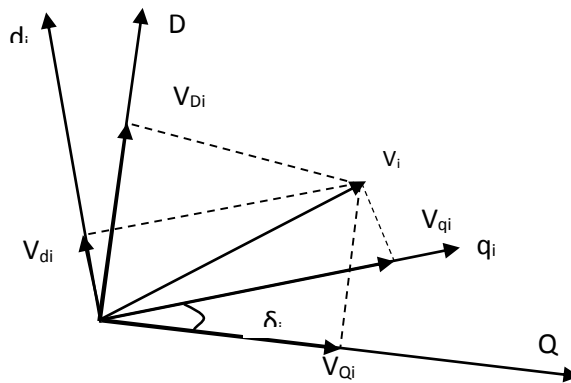


Fig. 6.40 Phasor representation

Further the voltage behind the transient reactance ( $E_q'$ ), transient reactance ( $x_{di}$ ), quadrature axis reactance ( $x_{qi}$ ) of the  $i^{\text{th}}$  machine are related to its terminal voltage components in the common reference frame as

$$\begin{bmatrix} 0 \\ E'_{qi} \end{bmatrix} = \begin{bmatrix} 0 & x_{qi} \\ -x'_{di} & 0 \end{bmatrix} \begin{bmatrix} a \dots\dots\dots b \\ c \dots\dots d \end{bmatrix} \begin{bmatrix} I_{Di} \\ I_{Qi} \end{bmatrix} = \begin{bmatrix} a \dots\dots\dots b \\ c \dots\dots\dots d \end{bmatrix} \begin{bmatrix} V_{Di} \\ V_{Qi} \end{bmatrix} \quad (6.49)$$

$a = d = \cos(\delta_i)$ ,  $b = \sin(\delta_i)$  and  $c = -\sin(\delta_i)$

Hence machine angle  $\delta_i$  can be computed as

$$\tan(\delta_i) = \frac{x_{qi} I_{Qi} - V_{Di}}{x_{qi} I_{Di} - V_{Qi}} \quad (6.50)$$

This voltage is then utilized in the 3<sup>rd</sup> order machine model and the differential equations are solved.

Using this machine angle, the voltage behind the transient reactance of machine are solved.

Moreover for an 'n' number of machines & 'm' number of load buses in a power network, the algebraic equations are written in compact form:

$$E_m + x_m T_{mn}^{-1} I = T_{mn}^{-1} V \quad (6.51)$$

$$I = Y_m V \quad (6.52)$$

$$E_m + x_m T_{mn}^{-1} Y_m V = T_{mn}^{-1} V \quad (6.53)$$

Hence the generator terminal voltage components in the common reference frame and the machine internal voltages are related by

$$V = \left[ U - T_{mn}^{-1} x_m T_{mn}^{-1} Y_m \right]^{-1} T_{mn}^{-1} E_m \quad (6.54)$$

Where U is the unity matrix.

Both UPFC's are represented by an equivalent admittances derived from their power injection models :

$$\begin{aligned} Y_{Li} &= \frac{P_i - jQ_i}{V_i^2} \\ Y_{Lj} &= \frac{P_j - jQ_j}{V_j^2} \end{aligned} \quad (6.55)$$

Where

$$P_i = B_{ij}\rho|V_i|^2 \sin(\beta) + |V_i| I_{SH} \quad \text{and} \quad P_j = B_{ij}\rho|V_i||V_j| \sin(\theta_{ij} + \beta) \quad (6.56)$$

$$Q_i = B_{ij}\rho|V_i|^2 \cos(\beta) \quad \text{and} \quad Q_j = -B_{ij}\rho|V_i||V_j| \cos(\theta_{ij} + \beta) \quad (6.57)$$

When fault is created in any line, the admittance matrix is then modified according to position of fault & taking into account of UPFC admittances. All system equations are converted into common frame of reference which is rotating at synchronous speed.

### 6.13 Implementation of Particle Swarm Optimization for optimization

Correct implementation of PSO algorithm leads to the global search of optimized values of UPFC Controller parameters. To achieve this correct implementation, several aspects of the PSO have to be designed to this particular problem. First a proper objective function that evaluates the performance of each particle has to be defined. Then, taking in account the definition of the objective function, the particle's position vector has to be defined, i.e., how many dimensions does the problem have and how should this dimensions be defined, followed by the characterization of unfeasible solutions.

### 6.14 FORMULATION OF AN OBJECTIVE FUNCTION

The objective function J is formulated as the minimization of

$$J = \int_0^t \left[ (\Delta\omega_1(t, x))^2 + (\Delta\omega_2(t, x))^2 + (\Delta\omega_3(t, x))^2 \right] dt \quad (6.58)$$

In the above equations,  $\Delta\omega_1(t, x)$ ,  $\Delta\omega_2(t, x)$  and  $\Delta\omega_3(t, x)$  denotes the rotor speed deviations of generator 1,2 & 3 for a set of controller parameters x and (note that, here x represents the parameters to be optimized i.e  $k_p$  &  $k_i$ , the parameters of PI controller) and t is the time range of the simulation. For objective function calculation, the time-domain simulation of the power system model is carried out for the simulation period. It is aimed to minimize this objective function in order to improve the system response in terms of the settling time and overshoots.

## 6.15 SIMULATIONS

Bus 1 is taken as a slack bus. A fault is created at the centre of the transmission line connecting bus numbers 3 and 7 & simulation is carried out for operating conditions  $P_1=4.6325$ ,  $Q_1=1.2760$ ,  $P_2=1.5$ ,  $Q_2=0.4$ ,  $P_3=1.1$ ,  $Q_3=0.3$  and  $P_{ref}=0.9919$ . All values are in p.u. Both inter area & local mode of oscillations are investigated.

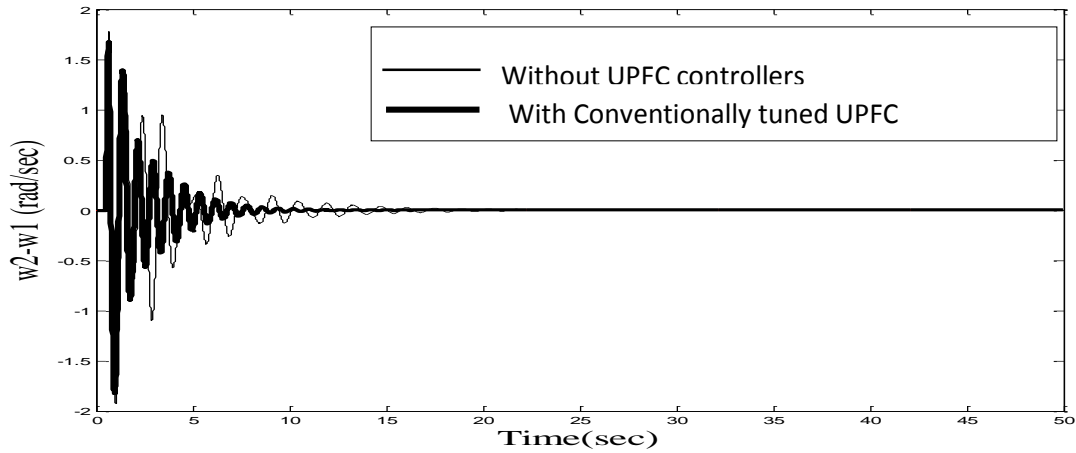


Fig. 6.41 Time response of speed deviation ( $w_2-w_1$ ) (Inter area mode oscillations without and with conventionally tuned UPFC controllers)

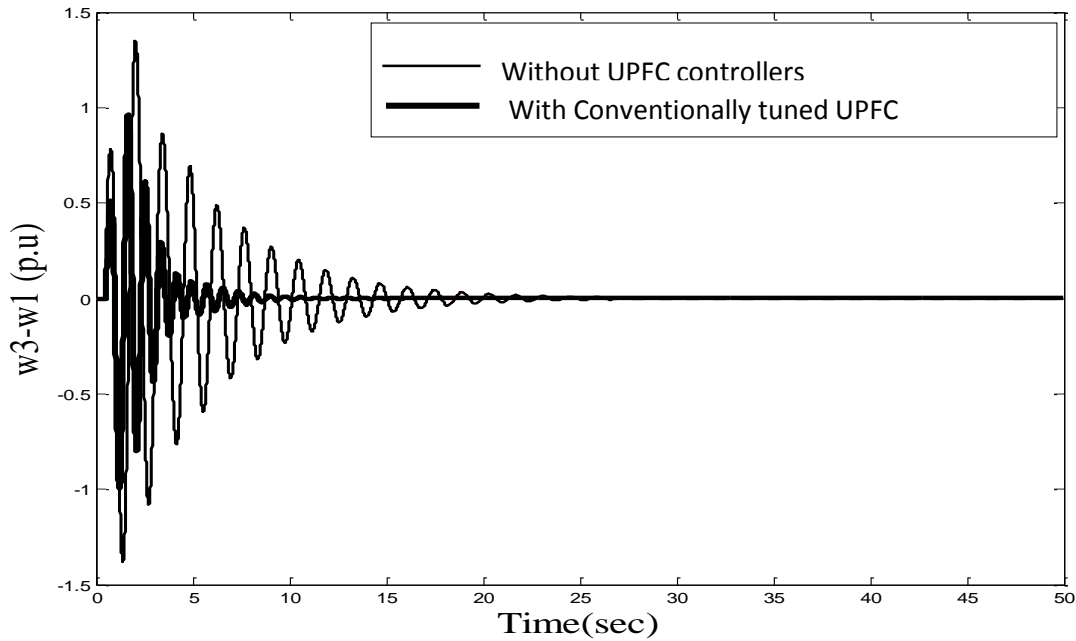


Fig. 6.42 Time response of speed deviation ( $w_3-w_1$ ) (Inter area mode oscillations without and with conventionally tuned UPFC controllers)

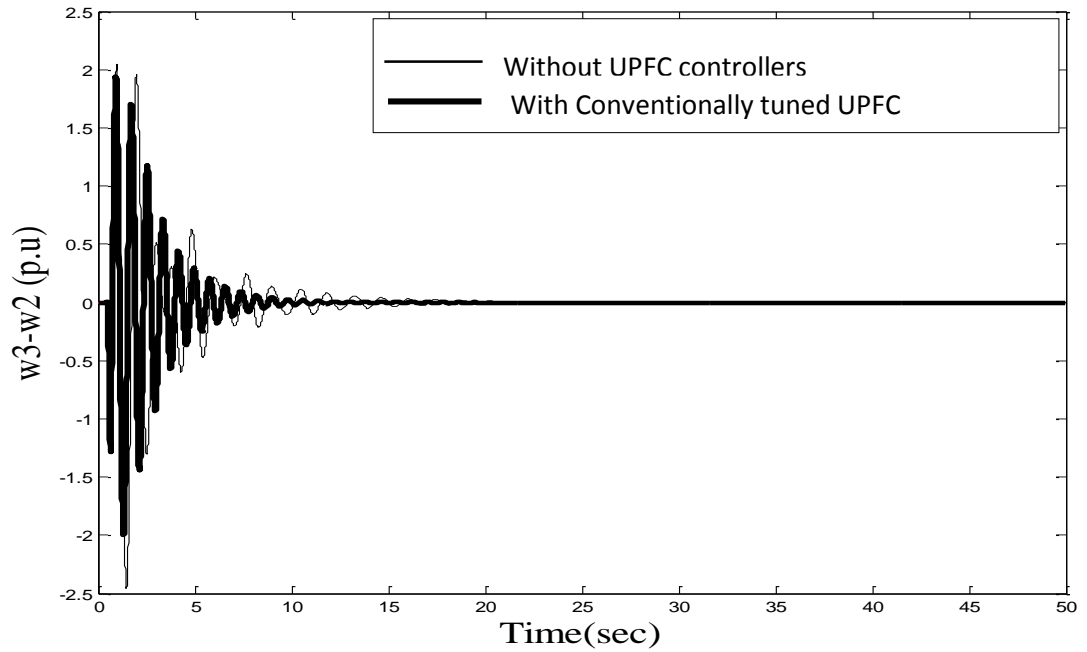


Fig.6.43 Time response of speed deviation ( $w_3-w_2$ ) (Intra area mode oscillations without and with conventionally tuned UPFC controllers))

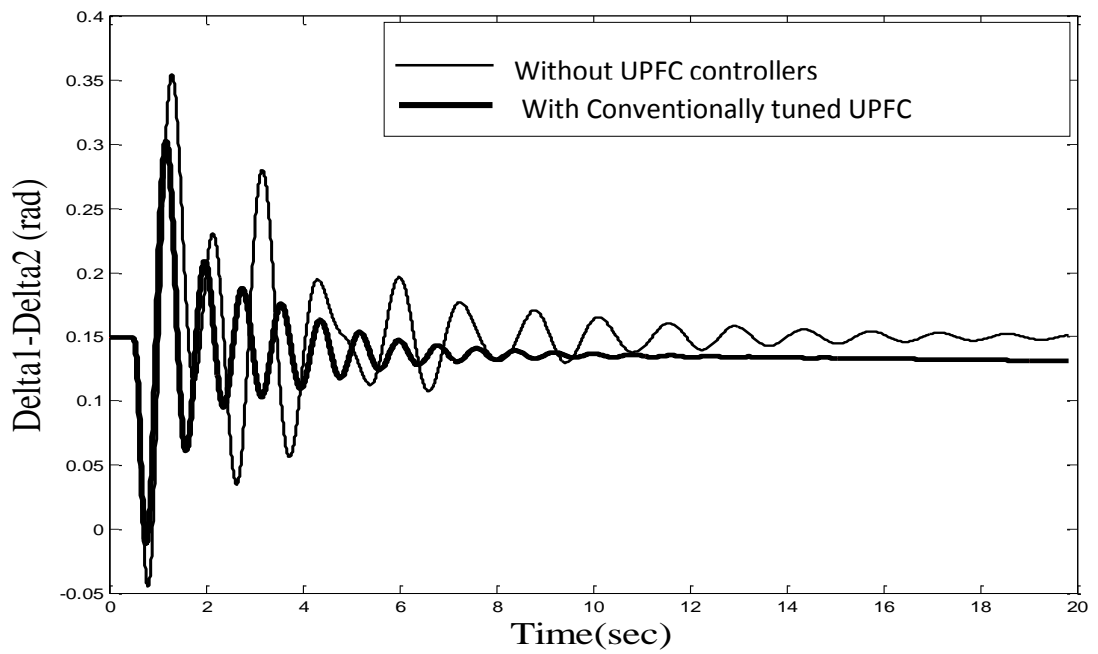


Fig. 6.44 Time response of power angle ( $\delta_1 - \delta_2$ ) without and with conventionally tuned UPFC controllers

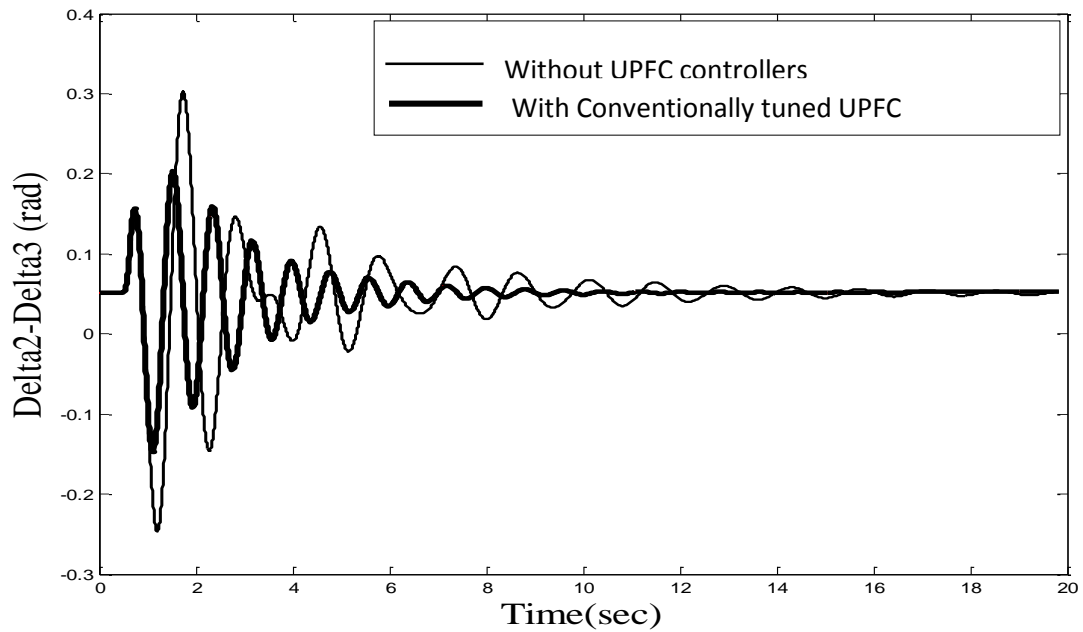


Fig. 6.45 Time response of power angle ( $\delta_2 - \delta_3$ ) (without and with conventionally tuned UPFC controllers)

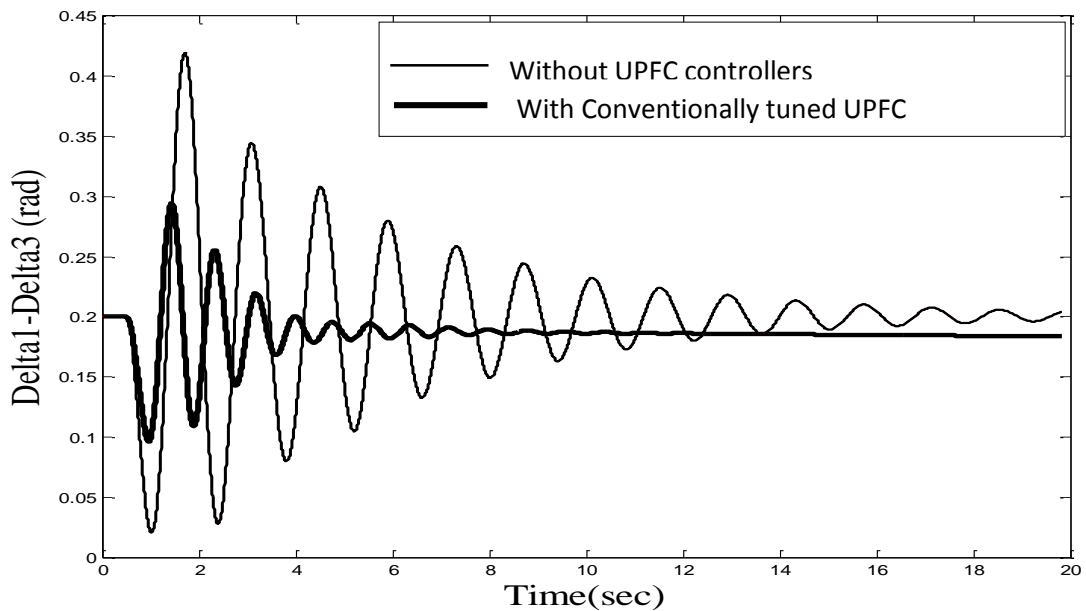


Fig. 6.46 Time response of machine angle deviation ( $\delta_1 - \delta_3$ ) (without and with conventionally tuned UPFC controllers)

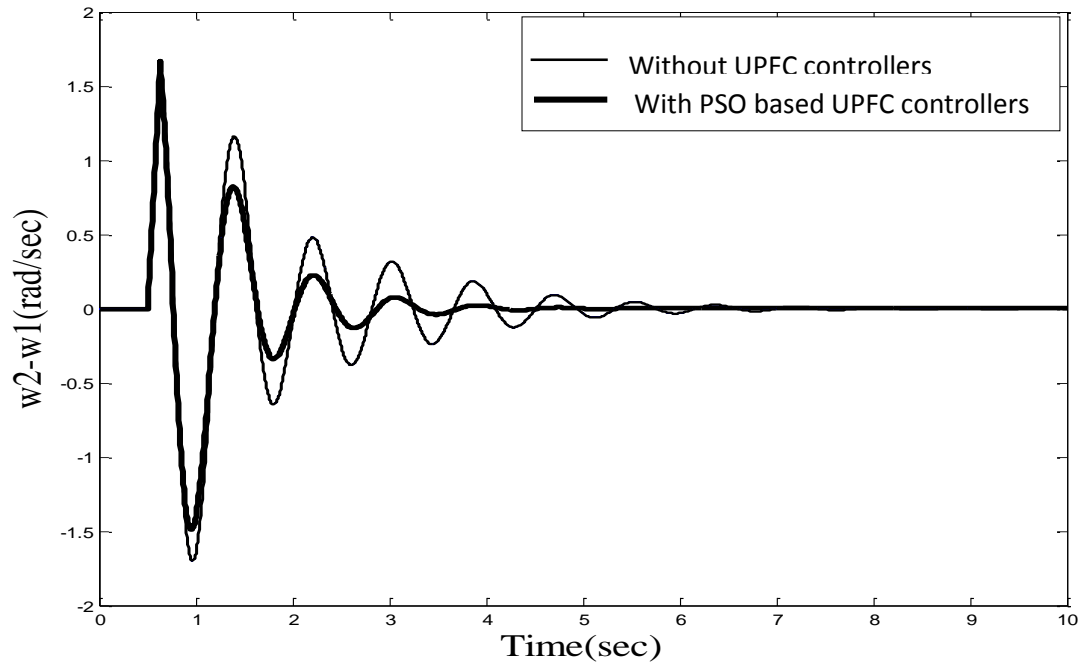


Fig. 6.47 Time response of speed deviation ( $w_2 - w_1$ ) (with conventionally tuned and with PSO based UPFC controllers)

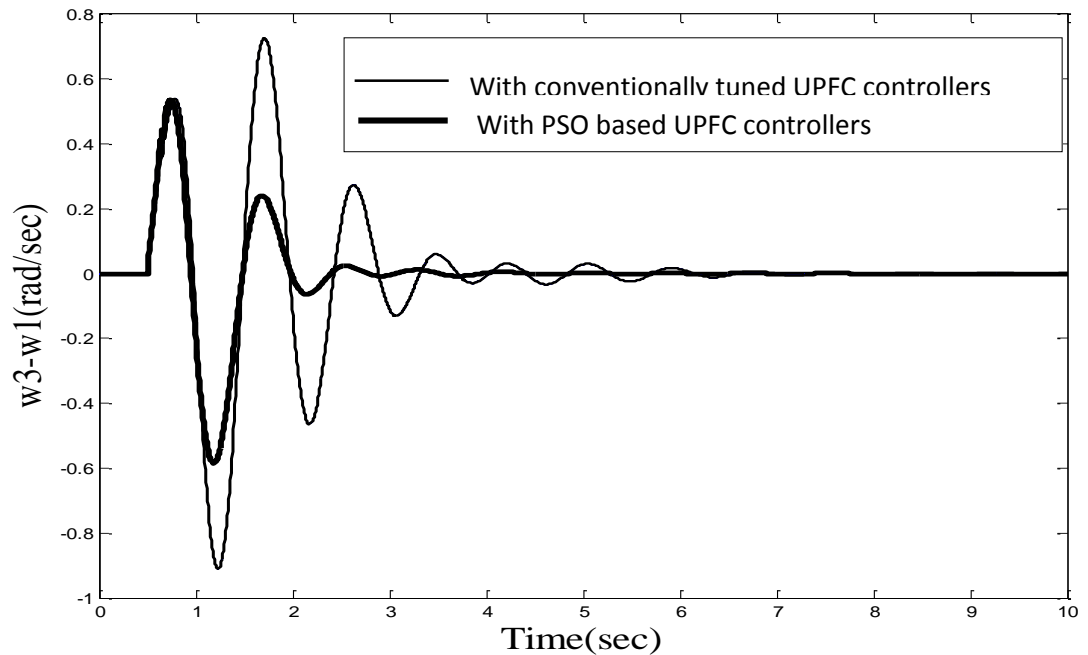


Fig. 6.48 Time response of speed deviation ( $w_3 - w_1$ ) (with conventionally tuned and with PSO based UPFC controllers)

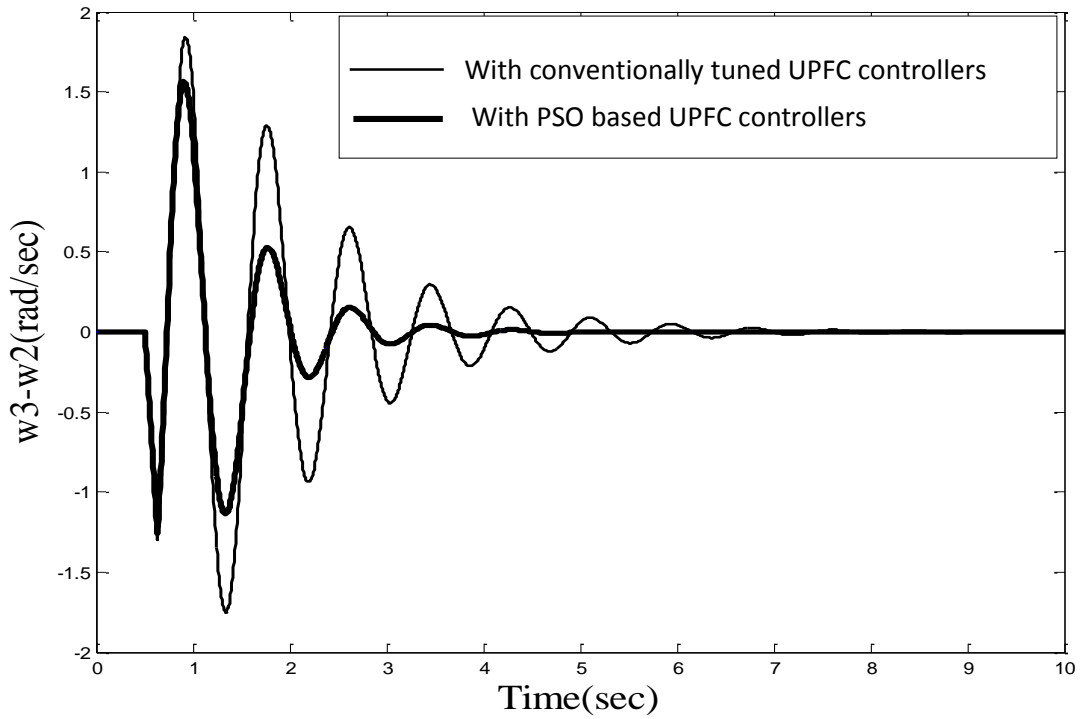


Fig. 6.49 Time response of speed deviation ( $w_3-w_2$ ) (with conventionally tuned and with PSO based UPFC controllers)

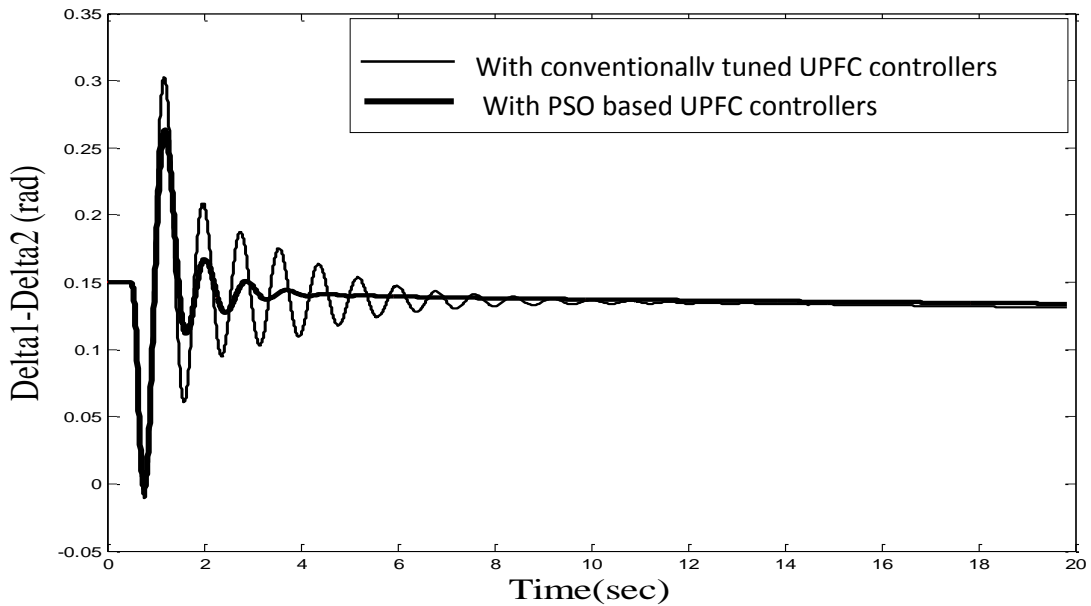


Fig 6.50 Time response of power angle ( $\delta_1-\delta_2$ ) (with conventionally tuned and with PSO based UPFC controllers)



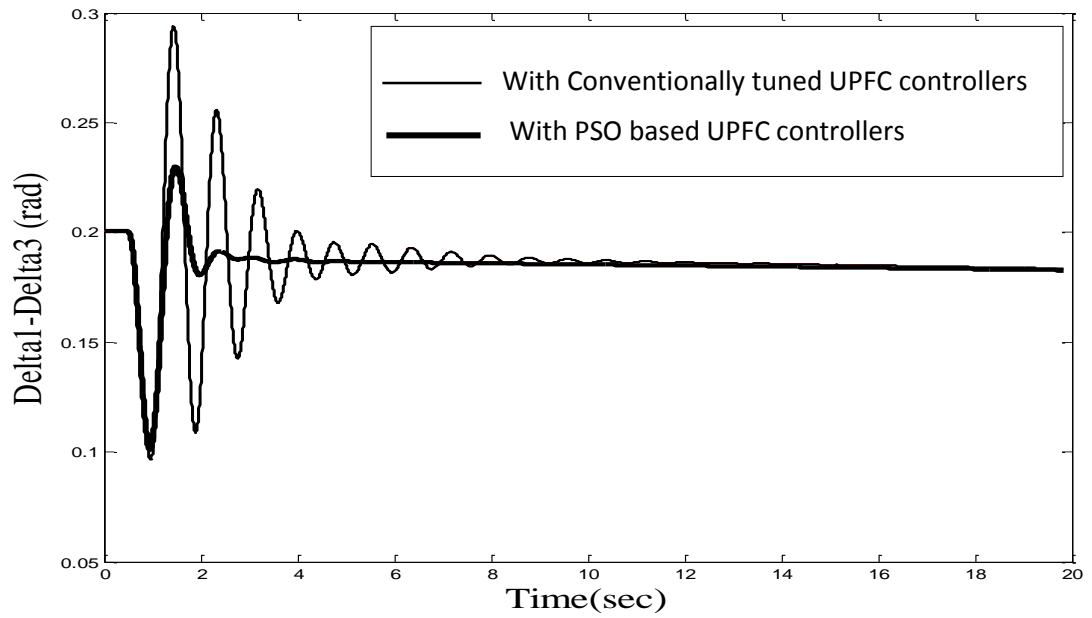


Fig. 6.51 Time response of power angle ( $\delta_1 - \delta_3$ ) (with conventionally tuned and with PSO based UPFC controllers)

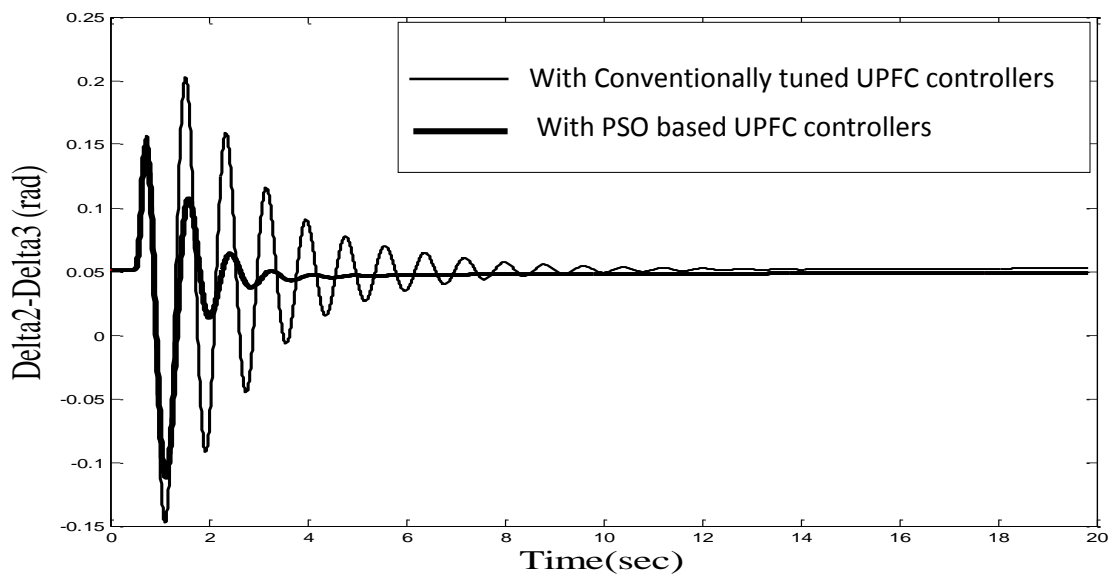


Fig.6.52 Time response of power angle ( $\delta_2 - \delta_3$ ) (with conventionally tuned and with PSO based UPFC controllers)

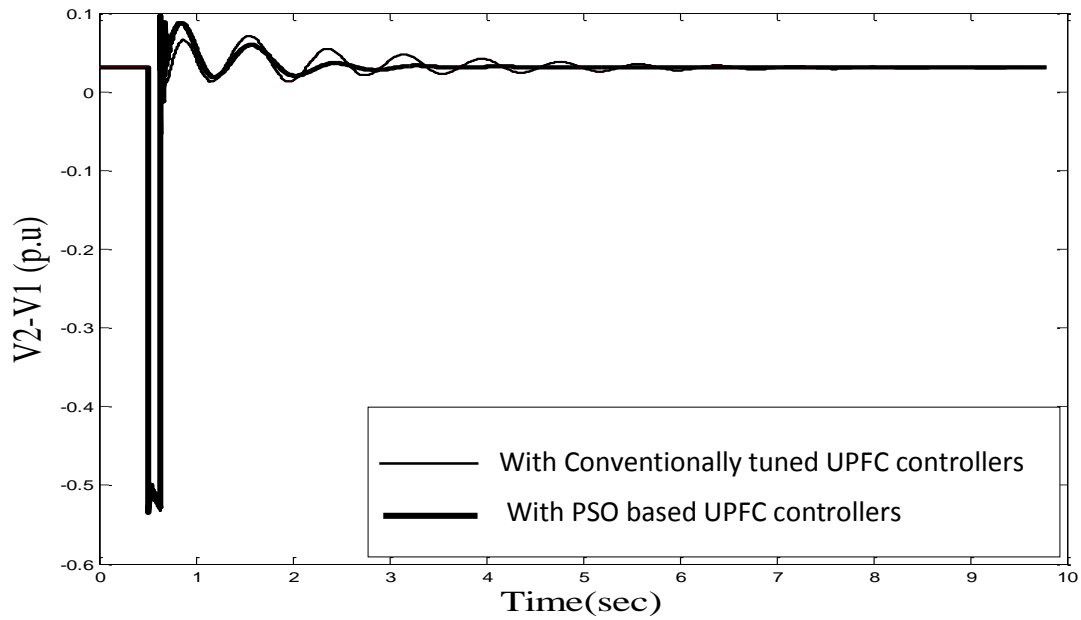


Fig. 6.53 Time response of Generator terminal voltage deviation ( $v_2-v_1$ ) (with conventionally tuned and with PSO based UPFC controllers)

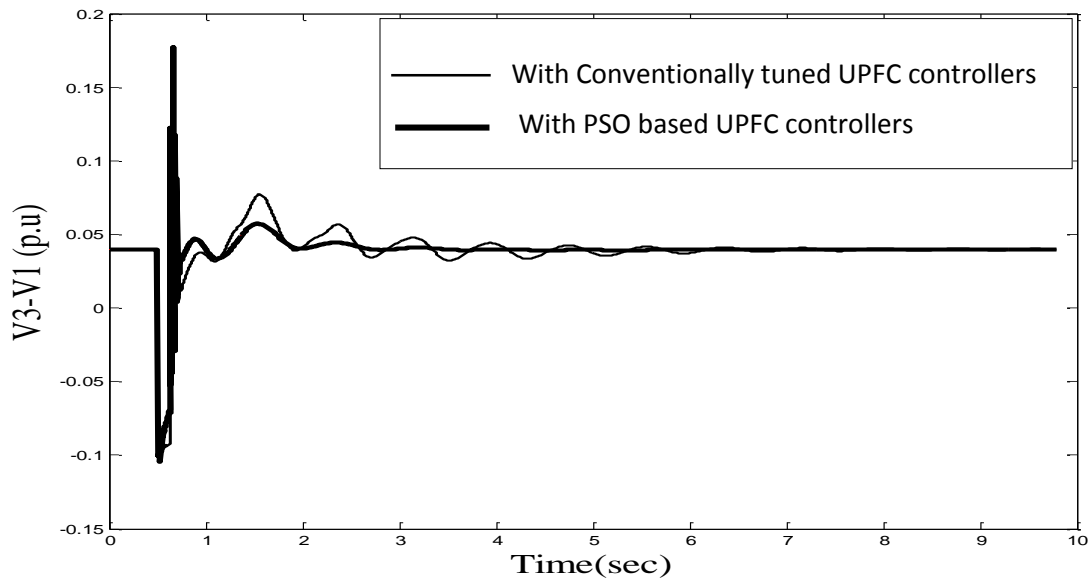


Fig. 6.54 Time response of Generator terminal voltage deviation ( $v_3-v_1$ ) (with conventionally tuned and with PSO based UPFC controllers)

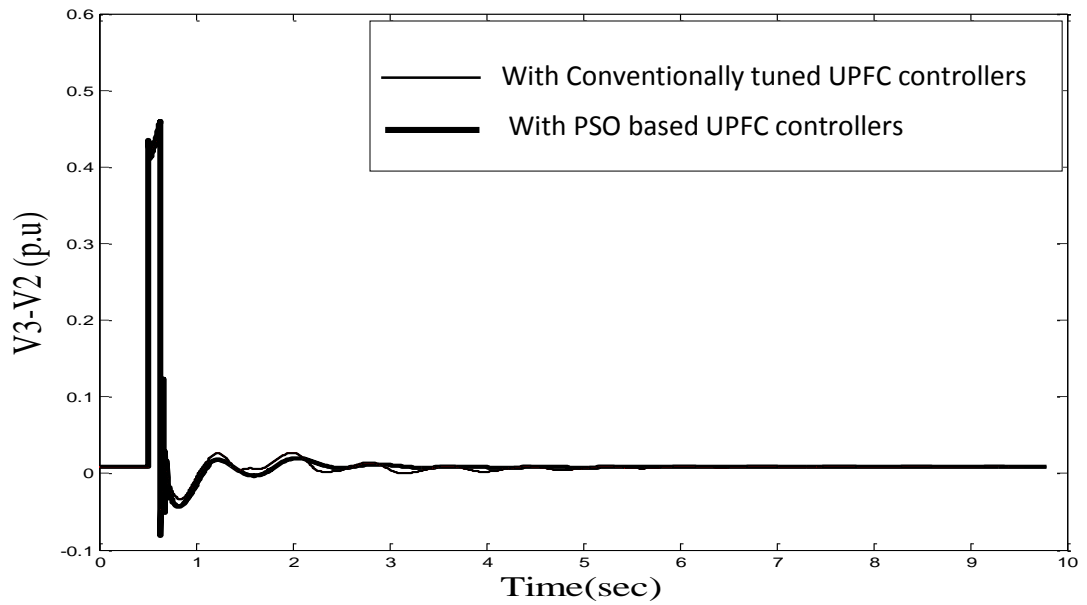


Fig.6.55 Time response of Generator terminal voltage deviation ( $v_3-v_2$ ) (with conventionally tuned and with PSO based UPFC controllers)

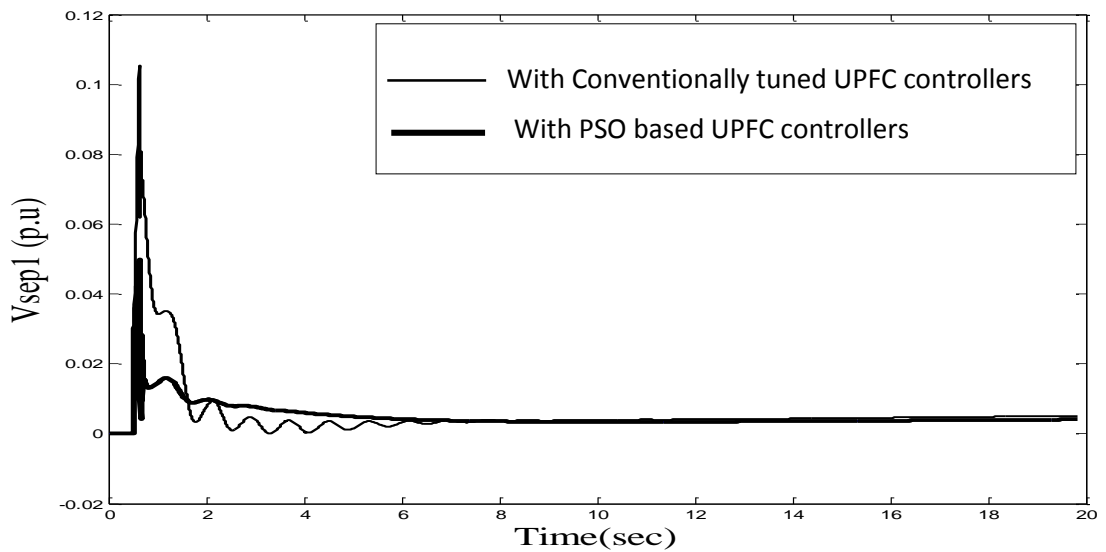


Fig. 6.56 Time response of in phase component of series voltage injection of UPFC 1 (with conventionally tuned and with PSO based UPFC controllers)

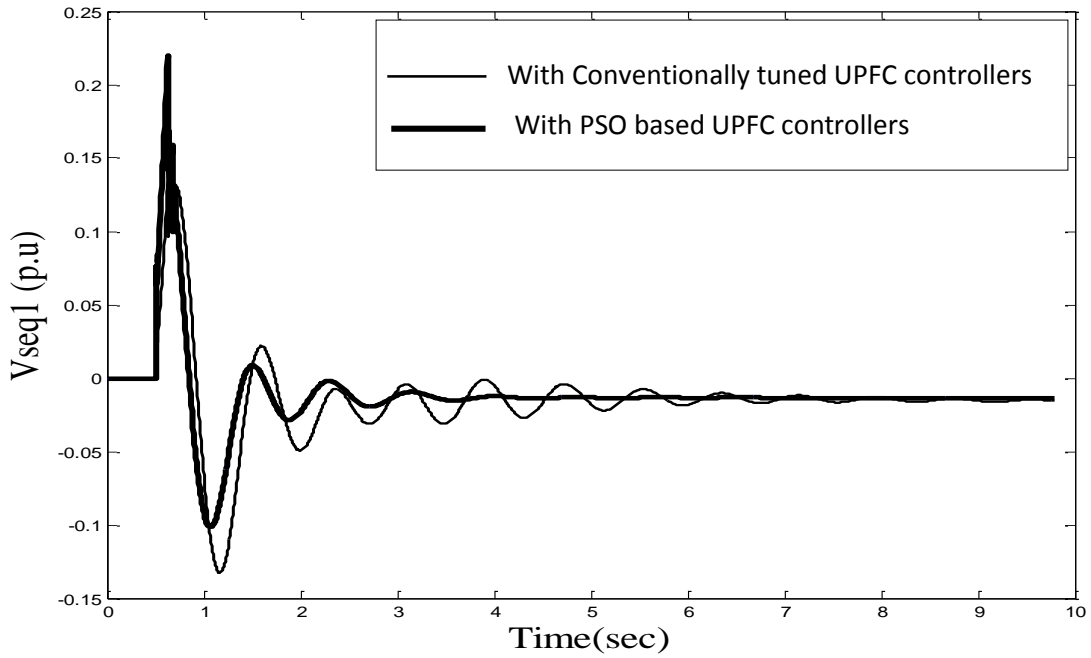


Fig. 6.57 Time response of quadrature component of series voltage injection of UPFC 1 (with conventionally tuned and with PSO based UPFC controllers)

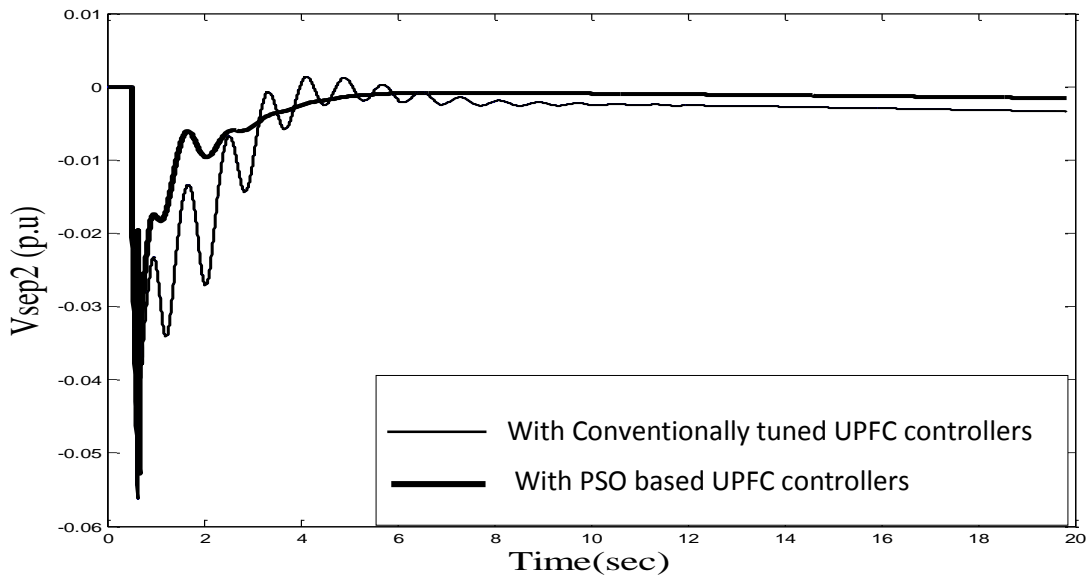


Fig. 6.58 Time response of quadrature component of series voltage injection of UPFC 2 (with conventionally tuned and with PSO based UPFC controllers)

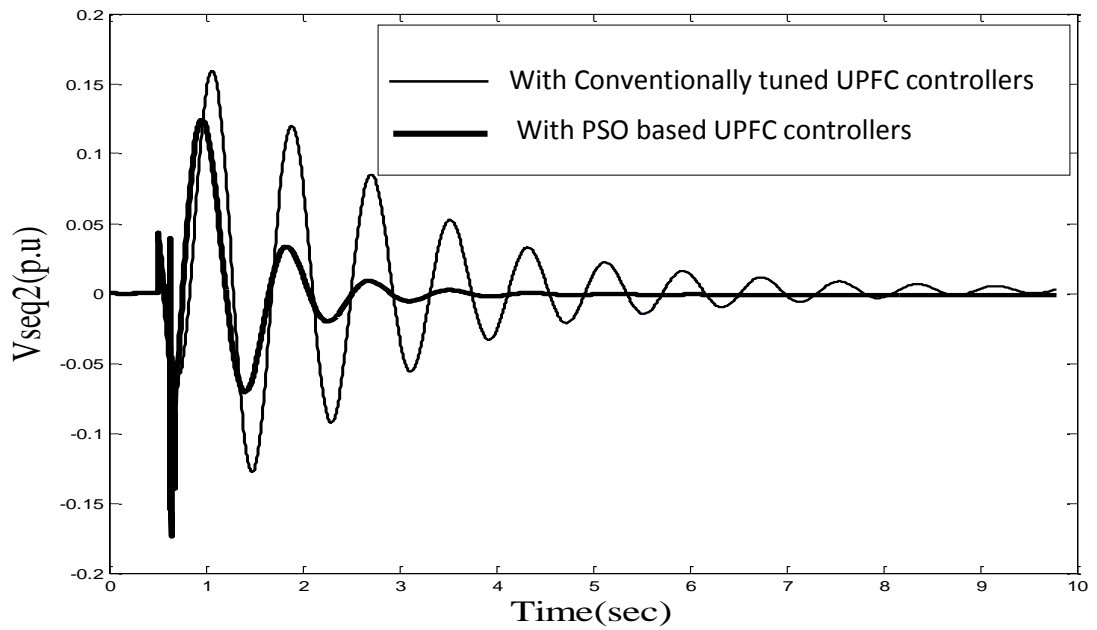


Fig. 6.59 Time response of in phase component of series voltage injection of UPFC 2 (with conventionally tuned and with PSO based UPFC controllers)

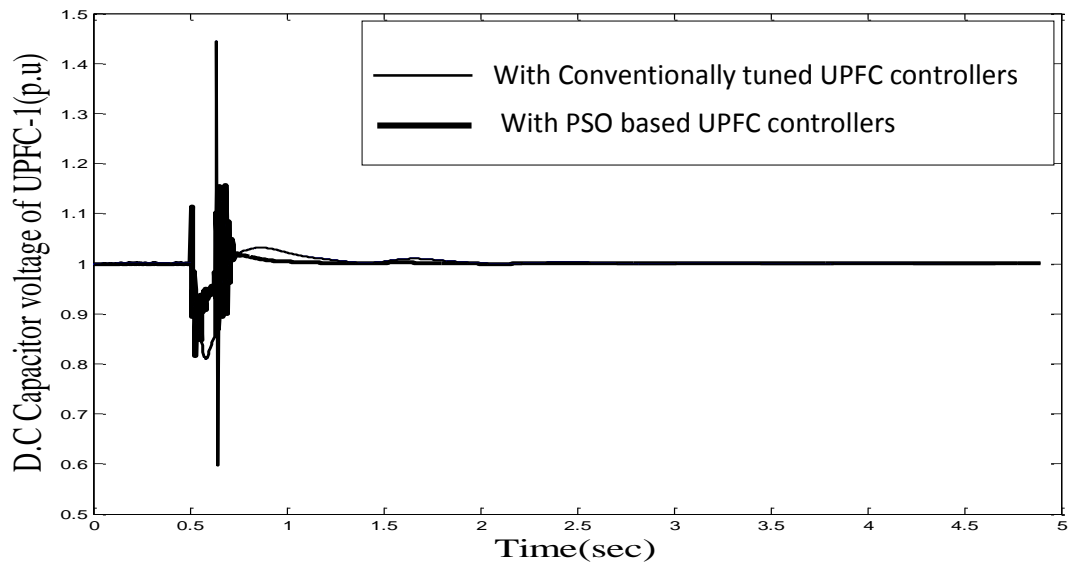


Fig. 6.60 Time response of D.C voltage of UPFC-1 (with conventionally tuned and with PSO based UPFC controllers)

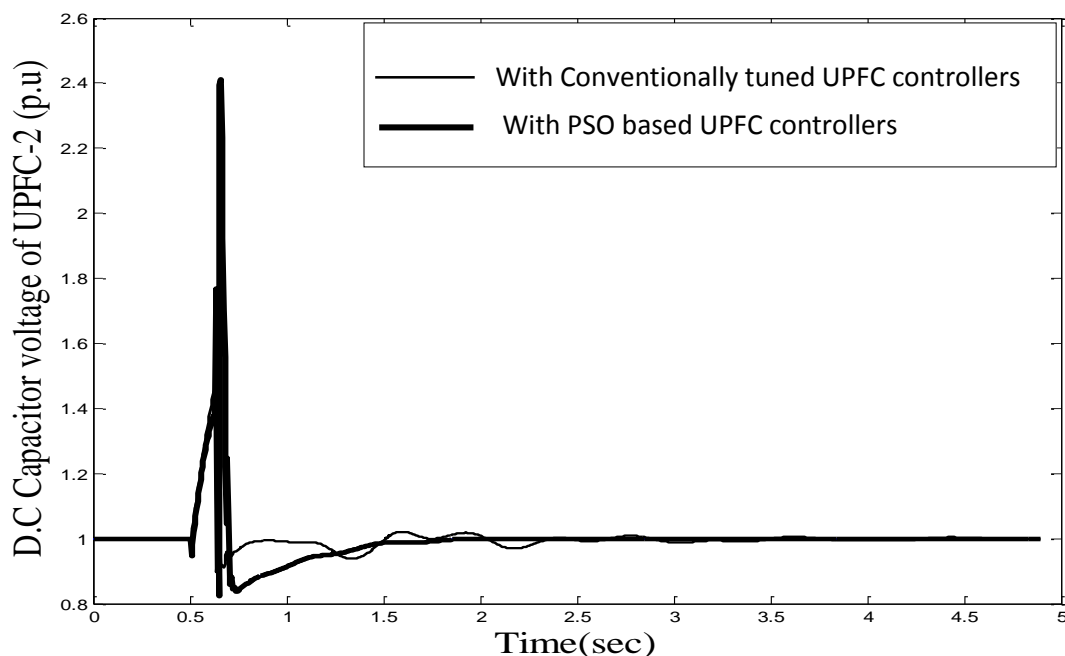


Fig. 6.61 Time response of D.C voltage of UPFC-2 (with conventionally tuned and with PSO based UPFC controllers)

## 6.16. DISCUSSION

In this case study, modeling of multi-machine system is done and all loads are converted into the equivalent admittances and are included in the  $Y_{BUS}$ . Two UPFC's connected are converted into the power injection model and the equivalent loads obtained are converted into the equivalent admittances and thus modifies the bus admittance matrix which is further used for load flow study. On the occurrence of the fault in the line, the bus admittance is further modified. A systematic procedure is developed as discussed in section 6.12. Conventional PI controller is used for UPFC FACTS device. The controller parameters are then optimized using both conventional technique and Particle Swarm Optimization algorithm for improving the transient stability of the multi-machine power system. From the responses, it is well established that the proposed PSO based UPFC controller is highly robust in its performance in damping the power system oscillations under transient disturbances in comparison to the conventional technique.

# **CHAPTER-7**

## **CONCLUSIONS**

### **7.1 GENERAL**

Today there is a need of secure and reliable power system network that comprises of long transmission line and a large number of generators. This requires the researchers to design different types of controllers for fast mitigation of power oscillations after a transient disturbance. With the advancement in the field of power electronics, FACTS devices have been introduced which allow additional power transfer on the existing lines without overloading them and also improve the steady state, dynamic stability and transient stability of the power system network after the disturbance. This thesis presents the design of various FACTS controllers whose parameters are optimized using various Swarm Intelligent techniques and an evolutionary technique to improve the damping performance for modal oscillations in interconnected power systems and also for SMIB system. The 21<sup>st</sup> century will certainly see a revolution in the control philosophy with a motivation towards intelligent FACTS controllers.

### **7.2 OVERALL ASSESSMENT**

As mentioned earlier, the choice of controller for FACTS devices is a challenging task due to inherent non-linearity and high degree of uncertainty in the field of power system. Various controllers implemented for FACTS controllers in this thesis are PI controllers, lead lag compensators and PI with lead lag compensators. Since conventional techniques for optimizing their parameters are time consuming and sometimes may not converge and cannot perform satisfactorily in damping electromechanical oscillations over a wide range of power system operating conditions. This has motivated for the formulation of AI based controllers for FACTS devices and circumvent the above mentioned drawbacks, the author has applied Swarm intelligent control for synchronous generator excitation control, control of Static Var System, control of series reactance of TCSC and the series and shunt voltage source converter control for the UPFC. The results obtained are quite inspiring and justify the work undertaken. The digital simulation results conclude the following:

- The auxiliary SVC controller has enhanced the transient stability by mitigating the power oscillations effectively in comparison to SVC controller only. These FACTS controllers are found to be effective for both SMIB and multi-machine power system network. Eigen value analysis has also been done to establish the dynamic stability of the power system network. Voltage stability enhancement is also analyzed using SVC controller in the multi-machine power system network. By optimizing the controller parameters using AI techniques, steady state, dynamic stability and transient stability are further enhanced. For the search of global minima in the m-dimensional search space, various variants of PSO have been implemented and found PSO-TVAC to be highly effective. BFO and GA based FACTS controllers are found to be comparable while the hybrid technique, a synergy of BFO and PSO proved to be the best for optimizing the controller parameters.
- TCSC, another FACTS controller is incorporated in both SMIB and multi-machine system for improving the steady state and transient stability of the power system network. Continuously varying reactance of TCSC model incorporated in an SMIB system (represented by a linearized model) has been designed and implemented for steady state stability enhancement. PSO based TCSC controller is designed for making the power network more reliable. Co-ordination control of multi-machine system using both SVC and TCSC controller has been implemented for further improvement in the performance enhancement of power system network.
- UPFC controller, combination of both series and shunt controllers has been designed. The performance of the new controller is investigated in both single machine and multi-machine environment. The superb damping capability of this FACTS controller is clearly traced from the transient responses. Besides, this controller improves the critical clearing time of the power systems. The performance of the controller is evaluated by subjecting the single machine power system with different transient disturbances and for different generator loadings. AI based UPFC controller are more effective as seen from the results. BFO, PSO and GA techniques are comparable while the hybrid technique proves to be more effective due to vast search of global minima in the m-dimensional search space.



Hybrid BFO-PSO has been implemented for optimizing the auxiliary SVC controller parameters and Hybrid BFO-PSO with TVAC has been implemented for optimizing the UPFC controller parameters. These techniques found to be more effective than other basic Swarm Intelligent techniques in controlling the controller parameters for improving the power oscillation damping. Further, UPFC performs the best compared to all the other treated FACTS devices due to control of both real and reactive power flow in the line. The proposed new UPFC controller is simple enough to be implemented in real time operation. Further the proposed controller can also be applicable to large power system by suitably selecting the objective function and the parameters of FACTS controllers.

However, the real time application of the proposed FACTS controllers face the difficulties for implementation in practice are marketability, availability of expertise and required development time. Research has still to go a long way to prove the worth of intelligent controller both technically and economically.

### **7.3 FUTURE SCOPES**

The author would like to note the following areas which need further investigation:

- Both Fuzzy and Neural controllers for FACTS devices can be tried and their performance may be investigated.
- Other Hybrid techniques like PSO with evolutionary technique or ant colony optimization technique based FACTS controllers may be investigated for the improvement in the mitigation of power oscillations.
- The performance of UPFC controller in voltage regulation mode may be investigated.

## REFERENCES

01. N. G. Hingorani, L. Gyugyi, "Understanding FACTS Concepts and Technology of Flexible AC Transmission Systems, IEEE Press Book, Standard Publications, Distributors, Delhi, 2001."
02. P. Kundur, "Power System Stability and Control", Tata McGraw-Hill, 2006.
03. P.M Anderson and A.A. Fouad, "Power system control and stability", Iowa State University Press, U.S.A., 1977.
04. K. R. Padiyar, Power System Dynamic stability and control, second edition, B. S. Publications, Hyderabad, 2002.
05. P. R. Sharma, Ashok Kumar and Narender Kumar, "Optimal Location for Shunt Connected FACTS Devices in a Series Compensated Long Transmission Line", Turk J Elec Engin, VOL.15, no.3, 2007.
06. Edris Abdel-Aty, "Controllable VAR Compensator: A Potential Solution to Load ability Problem of Low Capacity Power Systems. "IEEE Trans. on Power Systems, Vol. PWRS-2, pp. 561-567, Aug, 1987.
07. Haque M. H., "Maximum Power Transfer Capability within the Voltage Stability Limit of Series and Shunt Compensation Scheme for AC Transmission Systems", Elsevier Science Sa Lausanne, Electric Power Systems Research; pp: 227-235, Vol: 24
08. M.N. Sahadat, N. Al Masood, M.S. Hossain, G. Rashid and A.H. Chowdhury, "Real Power Transfer Capability Enhancement of Transmission Lines Using SVC", Asia-Pacific Power and Energy Engineering Conference (APPEEC), 25-28 March 2011.
09. C. Bulac, C. iaconu, M. Eremia, B. Otomega, I. Pop, L. Toma and I. Tristiu "Power Transfer Capacity Enhancement using SVC", , 2009 IEEE Bucharest Power Tech Conference, June 28th - July 2nd, Bucharest, Romania
10. Hauth R. L., Miske S. A. and Nozari F., "The role and Benefits of Static VAR Systems in High Voltage Power System Applications", IEEE Trans. on PAS, Vol. PAS-101, pp. 3761-3770, Oct, 1982.

11. Hauth R. L., Haman T. and Newell R. J., Application of a Static VAR System to Regulate System Voltage in Western Nebraska”, IEEE Trans. Vol. PAS-97, No.5, Sept. /Oct. 1978, pp. 1951-1962.
12. Bhatti T.S. and Kothari D. P., “Compensation of Long Distance Transmission Lines”, Proc. N.S.C.-90 A.M.U. Aligarh (India) pp. 63.
13. B. Vishwanathan, “Effect of series compensation on the Voltage stability of E.H.V. long lines, Electric Power System Research J. 6 (1983) 185-191.
14. Mayordomo, J. G. Izzeddine, M Asensir R., “Load and Voltage balancing in harmonic Power flows by means of static VAR compensators, “IEEE Trans. on Power Delivery Vol. 17, No. 3 (2002), 761-769.
15. Huayuan Chen, Youyi Wang and Rujing Zhou, “Voltage Stability Boundary affected by Nonlinear SVC control” Electric Machines and Power Systems, 2000.
16. D. Thukaram, Abraham Lomi, “Selection of Static VAR Compensator Location and size for System Voltage Stability improvement” Electric Power System Research 54 (2000) pp. 139-150.
17. Trang Phuong nam, Dinh Thanh Viet and La van Ut “Application of SVC for voltage regulation in real time power market”, IEEE Conference on Industrial Electronics and Applications (ICIEA), 2013.
18. Mehrdad Ahmadi Kamarposhti, Mostafa Alinezhad, Hamid Lesani, Nemat Talebi, “Comparison of SVC, STATCOM, TCSC, and UPFC Controllers for Static Voltage Stability Evaluated by Continuation Power Flow Method”, IEEE conference on Electrical Power & Energy, 2008
19. M. Sailaja Kumari, and M. Sydulu “A Novel Load Flow approach for Voltage Stability Index Calculation and adjustment of Static VAR Compensator Parameters”, Power India Conference, 2006 IEEE.
20. O. L. Bekri and M.K. Fella, “Optimal Location of SVC and TCSC for Voltage Stability Enhancement”, 4th International Power Engineering and Optimization Conference (PEOCO2010), Shah Alam, Selangor, MALAYSIA. 23-24 June 2010.
21. S.C. Kapoor, “Dynamic Stability of Static Compensator - Synchronous Generator Combination” IEEE Transactions on Power Apparatus and Systems, 05/1981

22. Ramar K. and Srinivas A., "Suppression of Low Frequency Oscillations Using Static VAR Compensator Controls, *Electric Machines and Power Systems*, vol. 17, 1989, pp. 109-121.
23. Nelson Martins, Leonardo T. G. Lima, "Determination of Suitable Locations of Power System Stabilizers and Static VAR Compensator for Damping Electromechanical oscillations in Large Scale Power Systems", *IEEE Trans. on Power Systems*, Vol. 5, No. 4, Nov. 1990, pp. 1455-1469.
24. Lerch E., Povh D., Xu L., "Advanced SVC Control for Damping power System Oscillations", *IEEE Trans. On Power Systems*, vol. 6 No. 2, May 1991, pp. 524-535.
25. Padiyar K. R. and Verma R. K. "Damping Torque Analysis of Static VAR System Controllers", *IEEE Trans. on Power Systems*, Vol. 6, No. 2, /May 1991, pp. 458-465
26. Lee Shun., Liu Chun-Chang. "An Output Feedback Static VAR Controller for Damping of Generator Oscillations", *Electric Power System Research*, Vol. 29, 1994, pp. 9-16.
27. Zhou E.Z. "Applications of Static VAR Compensators to Increase Power System Damping", *IEEE Trans. On Power Systems*, Vol. 8, No. 2, May 1993, pp. 655-701.
28. A. R. Messina, M. O. Begovich, "Analytical Investigation of the use of Static VAR Compensators to aid Damping of Inter area Oscillations, "Electric Power System Research 21(1999) 199-210.
29. A. R. Messina and E. Barocio, "Nonlinear analysis of inter area Oscillations: effect of SVC voltage support" *Electric Power System Research*, Vol. 64, (2003), pp. 17-26.
30. P.R. Sharma and Poonam Singhal," A New Static Var System Auxillary Controller for Damping Sub synchronous Resonance Oscillations in Series Compensated power Systems" National Conference on role of computers and electronics in power system 13-15 July,2007 Jaipur
31. Mathur R.M. and Hammad A. E., "A new Generalized Concept for the Design of Thyristor Phase-Controlled VAR compensators Part II: Transient Performance", *IEEE Trans. on PAS*. Vol. PAS-98, pp. 227-231, Jan. / Feb. 1979.

32. Hsu Y.Y., Liu Chuan sheng, Lin C. J. and Huang C.T., "Application of power System Stabilizers and Static VAR Compensators on a Longitudinal Power System", IEEE Trans. on Power Systems, Vol.3, No.4, 1988, pp. 1464-1469.
33. Murthy A.S.R, Balasubramanyam P. V., and Parmaswaran, S., "Performance Evaluation of Static VAR Compensated System with Auxiliary Controls." Electric Machines and Power Systems, Vol. 19, 1991, pp. 251-270
34. P.K. Muttik, P.Wang and M.W.H. Minchin, "Detailed Simulation of SVC Transient Performance Using PSCAD", International Conference on Power System Technology (Power Con), 2000
35. Nor Azwan Mohamed Kamari, Ismail Musirin and Muhammad Murtadha Othman "Computational Intelligence Technique Based PI Controller using SVC", Power Engineering and Automation Conference (PEAM), 2011 IEEE (Volume: 2)
36. Y. P. Wang, D. R. Hur, H. H. Chung, N. R. Watson, J. Arrillaga and S.S. Maitair, "A Genetic Algorithms Approach to Design an Optimal PI Controller for Static Var Compensator," International Conference on Power System Technology (Power Con 2000), Vol.3, 2000, pp.1557 –1562.
37. Rusejla Sadikovic, Petr Korba and Goran Andersson, "Application of FACTS Devices for damping of power system oscillations", IEEE Power Tech2005, Russia, June 2005
38. IEEE Committee Report, "First Supplement to a Bibliography for the Study of Sub-synchronous Resonance between Rotating Machines and Power Systems", IEEE Trans. on PAS, Vol. PAS-98, pp. 1872-1875, Nov. /Dec. 1979.
39. IEEE SSR Working Group, "Countermeasures to Sub-synchronous resonance Problems", IEEE Trans. on PAS, Vol. PAS-99, pp. 1810-1818, Sept./Oct. 1980.
40. Hammad A. E., "Analysis of Power System Stability Enhancement by Static VAR Compensators", IEEE Trans. on Power Systems, Vol. PWRS-1, pp. 222-227, Nov. 1986.
41. Lee Shun., Lin Chun-cheng, "A Single Input Multi Output Excitation Controller Via Eigen structure Assignments for Damping the Sub-synchronous Resonance of a Turbo-generator", Electric Power System Research, Vol. 26, 1993, pp. 109-116.

42. A. F. Abdou, A. Abu-Siada, and H. R. Pota , “Application of SVC on Stabilizing Torsional Oscillations and Improving Transient Stability”, Power and Energy Society General Meeting, 2012.
43. Li Wang, “Stabilizing torsional oscillations using a shunt reactor controller”, IEEE Transactions on Energy Conversion,10/1991.
44. Sujit Purushothaman and Francisco de Leon, “Eliminating Sub-synchronous oscillations with an Induction Machine Damping unit (IMDU)”IEEE Transaction on Power Systems, Vol.26, No.1, February 2011.
45. B. K. Keshavan Nagesh Prabhu, Damping of Sub-synchronous oscillations using STATCOM –A FACTS Device, Transmission and Distribution Conference and Exposition, 2001 IEEE/PES 1, pp. 1-7
46. Alberto D. Del Rosso, Claudio A. Cañizares and Victor M. Doña, “A Study of TCSC Controller Design for Power System Stability Improvement” IEEE Transactions On Power Systems, Vol. 18, No. 4, November 2003.
47. A.O Anele, J. T. Agee, A. A. Jimoh” Investigating the Steady State Behavior of Thyristor Controlled Series Capacitor”, IEEE
48. Nicklas P. Johansson, Lennart Angquist, Hans-Peter Nee, “Adaptive Control of Controlled Series Compensators for Power System Stability Improvement” Power Tech, 2007 IEEE Lausanne.
49. A.M. Kulkarni and K. R.Padiyar “Performance Evaluation of Unified Power Flow Controller using Transient Simulation” in International Conference on Power Electronics and Drive Systems (PEDS-97), May 1997.
50. H.W Ngan and Wanliang Fang,“Coordinated Power Control Strategy for Flexible AC Transmission System” Proceedings of the IEEE Conference PEDS '1999
51. R.L.Arnez and L.C. Zanetta,“Unified Power Flow Controller (UPFC): its versatility in handling power flow and interaction with the network.”IEEE 2002
52. Manju P and Subbiah V,“Intelligent Control Of Unified Power Flow Controller For Stability Enhancement Of Transmission Systems” International Conference on Advanced Computer Control (ICACC), 2010, Volume 3.
53. S.Rai, S. Ghosh, D.S. Babu and P.S Venkataramu,., “Line congestion relief using UPFC”, International Conference on Power, Energy and Control (ICPEC), 2013

54. R.S.Lubis S.P.Hadi Tumiran,” Modeling of the generalized unified power flow controller for optimal power flow”, International Conference on Electrical Engineering and Informatics (ICEEI), 2011
55. M.A. Abido, A.T. AL-Awami and Y.L.Abdel-Magid,“Analysis and Design of UPFC Damping Stabilizers for Power System Stability Enhancement”, International Symposium on Industrial Electronics, 2006, Volume 3
56. H.F. Wang, “Damping function of unified power flow controller, ”IEE Proceedings-C, vol. 146, no. 1, p. 81, Jan. 1999.
57. H.F. Wang and F.J. Swift, “A unified model for the analysis of FACTS devices in damping power system oscillations Part I: Single machine infinite-bus power systems,” IEEE Trans. Power Del., vol. 12, no. 2, pp. 941-946, April 1997.
58. E. Babaei, A.Mokari Bolhasan, M. Sadeghi and S.Khani,“An improved PSO and Genetic Algorithm based damping controller used in UPFC for power system oscillation damping” ICEMS, 2011
59. Eskandar Gholipour and Shahrokh Saadate“ Improving of Transient Stability of Power Systems using UPFC”,IEEE Transactions on Power Delivery, Vol. 20,No2, April 2005.
60. Sunina Kaul and Sheela Tiwari, “Model Predictive Control for improving Small Signal Stability of a UPFC Equipped SMIB system” International Conference on Engineering (NUICONE), 8-10 Dec 2011.
61. R.C. Eberhart and Y.shi “Comparing Inertia Weights and Constriction Factors in Particle Swarm Optimization” Proceedings of the 2000 Congress on Evolutionary Computation, 2000, pp. 84 - 88 vol.1.
62. Ganesh K. Venayagamoorthy, “Optimal Control parameters for a UPFC in a multi-machine using PSO” Proceedings of the International Conference on Intelligent Systems Application to Power Systems (ISAP), 2005.
63. A.Kazemi and M.V. Sohrforouzani, “Power system damping using Fuzzy controlled FACTS devices”, POWERCON 2004.
64. Mondal, D. Chakrabarti, A., Sengupta, A., “PSO based location and parameter setting of advance SVC controller with comparison to GA in mitigating small signal

- oscillations”, International Conference on Energy, Automation, and Signal (ICEAS), 2011.
65. Mahyar Zarghami, and Mariesa. L. Crow, ”The Effect of Various UPFC Operating Points on Transient Stability.” North American Power Symposium (NAPS), 2006.
  66. G.Li., T.T. Lie, G. B. Shrestha and K.L. Lo, “Design and Applications of Co-ordinated multiple FACTS Controllers” IEE Proc. Gener. Trans. Distrib. Vol. 147, No. 2, March 2000.
  67. H.F.Wang,” “State Synchronous Series compensator to damp Power System Oscillations”, Electric Power System Research 5, 4 (2000) 133-199.
  68. Y. L. Kang, G. B. Shrestha, T. T. lie, “ Improvement of Power System dynamic Performance with the Magnitude and Phase angle control of Static Phase Shifter” Electric Power Systems Research 55(2000) 121-128.
  69. W.M. Korani, H.T. Dorrah and H.M. Emar” Bacterial foraging oriented by Particle Swarm Optimization strategy for PID tuning”, IEEE International Symposium on Computational Intelligence in Robotics and Automation (CIRA), 2009
  70. A. Muruganand S. Thamizmani, “A new approach for voltage control of IPFC and UPFC for power flow management”, International Conference on Energy Efficient Technologies for Sustainability (ICEETS), 2013.
  71. A.F. Abdou A. Abu-Siada and H.R. Pota, “Application of a STATCOM for damping sub-synchronous oscillations and transient stability improvement”, Australasian Universities Power Engineering Conference (AUPEC), 2011
  72. S. R. Khuntia and S. Panda, “A comparative study of PSO-technique and fuzzy based SSSC controller for improvement of transient stability performance”. International Conference on Communication Control and Computing Technologies (ICCCCT), 2010.
  73. Iravani M. R. and Mathur R. M., “Suppressing Transient Shaft Stresses of Turbine Generators Using a Static Phase Shifter”, IEEE Trans. on Energy Conversion, Vol. EC-1, pp. 186-192, March, 1986.
  74. Noroozian, N. Ghadhari, M. Andersson, G. Gronquest, J. Hiskens “A robust control strategy for shunt and series reactive compensators to damp electromechanical



- Oscillations”, IEEE Trans. on Power Delivery, Vol. 16, No. 4, Oct (2000), 812-817.
75. Cheng C.H. and Hsu Y.Y., “Damping of Generator oscillations using an Adaptive Static VAR Compensator”, IEEE Trans. On Power Systems, Vol.7, No. 2, May 1992 pp. 718-724
  76. Hammad A. E., M.EL-Sadek, “Applications of Thyristor Controlled VAR Compensator for Damping Subsynchronous Oscillations in Power Systems,” IEEE Trans. on PAS, Vol. PAS-103, No. 1, Jan. 1984.
  77. Hamouda R. M., Iravani M. R. and Hackam R., “Coordinated Static VAR Compensators and Power System Stabilizers for Damping Power System Oscillation”, IEEE Trans. on Power Systems, Vol. PWRS-2, pp. 1059-1067.
  78. A. H. M. A. Rahim, S. A. Al-Baiyat and H.M.Al –Maghrabi, “Robust damping controller design for static compensator” IEE Proc. Generation Transm. Distrib. 149, 4(2002), pp. 491-496.
  79. Byerly B. T., Pozaniak D. T., and Taylor E. R. “Static Reactive Compensation for Power Transmission Systems,” IEEE Trans. On PAS, Vol. PAS-101, pp. 3997-4005, OCT. 1982.
  80. L. Gyugyi,”Unified power flow concept for Flexible AC transmission systems”, IEE Proc. C, Vol139, No. 4, July 1992, pp.323-332.
  81. L. Gyugyi, T.R. Rietman, A. Edris, C. D. Shauder, D. R. Torgerson, S.L. Williams,’The Unified Power Flow Controller:A new approach to power transmission control”, IEEE Trans. On Power Delivery, Vol.10, No.2, April 1995, pp. 1085-1097.
  82. L.Gyugyi,” Dynamic Compensation of AC transmission lines by Solid-State Synchronous Voltage sources”, IEEE Trans. on power delivery, Vol 9, no. 2, April 1994.
  83. Nabavi-Niaki, A., and Iravani, M.R.: ‘Steady-state and dynamic models of unified power flow controller (UPFC) for power system studies’. Presented at 1996 IEEE iPES Winter Meeting, Baltimore, 1996 pp. 447-454

84. Seyed Ali Nabavi-Niaki, M. R. Iravani, "Visualization and Investigation of Unified Power Flow Controller (UPFC) Non-linearity in Power Flow" in the proceedings of IEEE 2003 pp 812-817.
85. W. G. Heffron and R. A. Phillips, "Effect of modern amplidyne voltage regulators on under-excited operation of large turbine generator," AIEE Transactions on Power Apparatus and Systems, Aug 1952, pp. 692-697.
86. D.J. Gotham," FACTS device models for power flow and stability simulations", IEEE 96 winter meeting, paper 96WM 258-4pwr1994.
87. C.Shauder and H.Mehta, "Vector analysis and control of advanced static VAR compensators", IEE Proc, 140, No. 4, July 1993.
88. B. Geethalakshmia, , P. Dananjayan," Investigation of performance of UPFC without DC link capacitor",Electric power system research, volume 78,Issue4, April 2008,pp736-746.
89. Singh, Arvind Kumar; Prasad, Upendra; Pudur, Rajen; Satyendra Kumar," Modelling Of Single Phase UPFC without DC Capacitor", International Journal of Engineering Science & Technology,2011, Vol. 3 Issue 5, p3732.
90. Y. Liu, and K. M Passino, "Biomimicry of social Forging for Distributed optimization: Models, principles for Emergent Behaviour" JOTA, vol 115, no. 3, pp 603-623, Dec 2002.
91. S. Panda, N. P. Padhy, "Comparison of Particle Swarm Optimization and Genetic Algorithm for TCSC-based Controller Design" International Journal of Computer Science and Engineering Volume 1 No. 1.
92. K. M Passino, "Biomimicry of bacterial forging for distributed optimization and control", IEEE Control System Magazine, Vol 22, no. 3 pp 52-67, June, 2002.
93. Swagatam Das, Arjit Biswas, Sambarta Dasgupta "Bacterial Foraging Optimization Algorithm: Theoretical Foundation, Analysis & Application."
94. Sidhartha Panda and Narayana Prasad Padhy,"Power system with PSS and FACTS controller: modelling, Simulation and simultaneous tuning employing Genetic Algorithm", World Academy of Science, Engineering and Technology, IJEESE,Vol.1, No.3, 2007.

95. Yong Hua Song and Allan T. Johns, "Flexible AC Transmission Systems (FACTS)", IET, 2009.

## APPENDIX A

### MODEL 1

#### Generator Data:

G1: 100 MVA, 16.5 KV, 60Hz,  $x_d = 0.1460$  p.u,  $x_d' = 0.0608$ p.u,  $x_q = 0.0969$ ,  $x_q' = 0.0969$ ,

$T_{d0}' = 8.96$ sec,  $T_{q0}' = 0.310$ sec,  $H = 23.64$ sec

G2: 250 MVA, 18 KV, 60Hz,  $x_d = 0.8958$  p.u,  $x_d' = 0.11980$  p.u,  $x_q = 0.8645$ ,  $x_q' = 0.1969$ ,

$T_{d0}' = 6$ sec,  $T_{q0}' = 0.5350$ sec,  $H = 6.4$ sec

G3: 100 MVA, 13.8 KV, 60Hz,  $x_d = 1.3125$  p.u,  $x_d' = 0.1813$  p.u,  $x_q = 1.2578$  p.u,

$x_q' = 0.25$ p.u

$T_{d0}' = 5.89$ sec,  $T_{q0}' = 0.6$ sec,  $H = 3.01$ sec

#### Transformer Data:

Transformer 1: 100MVA, 16.5/230 kV,  $X_L = 0.0576$ p.u

Transformer 2: 100MVA, 18/230 kV,  $X_L = 0.0625$ p.u

Transformer 3: 100MVA, 13.8/230 kV,  $X_L = 0.0586$ p.u

#### Line Data:

Line	R (p.u)	X (p.u)	B(p.u)
7-8	0.0085	0.072	0.1490
8-9	0.0119	0.1008	0.2090
6-9	0.039	0.170	0.358
6-4	0.017	0.092	0.158
4-5	0.01	0.85	0.176
5-7	0.032	0.161	0.306

Load at buses 5, 6 and 8 =  $(1+j0.35)$ p.u

#### SVC controller Data:

$K_r = 100$ p.u,  $T_r = 10$ sec,  $V_{Ref} = 1.0$  p.u,  $B_{max} = 1$  and  $B_{min} = -1$

#### TCSC controller Data:

$K_r = 10$ p.u,  $T_r = 0.5$ sec,  $K_p = 5$ ,  $K_i = 1$ ,  $X_l = 0.2$ p.u and  $X_c = 0.1$ p.u

## MODEL 2

### Generator Data:

$x_d = 1.6 \text{ p.u.}$ ,  $x_q = 1.55 \text{ p.u.}$ ,  $x_d' = 0.32 \text{ p.u.}$ ,  $T_{do}' = 6 \text{ p.u.}$ ,  $H = 5.0 \text{ sec}$ ,  $f = 60 \text{ Hz}$ ,  $x_e = 0.4 \text{ p.u.}$ ,  $D = 0$

Expressions for computing model constants:

$$K1 = \frac{V_b E_{qo} \cos \delta_o}{(x_T + x_q)} + \frac{(x_q - x_d)}{(x_T + x_d')} V_b i_{qo} \sin \delta_o$$

$$K2 = \frac{x_T + x_q}{(x_T + x_d')} i_{qo} = \frac{V_b \sin \delta_o}{(x_T + x_d')}$$

$$K3 = \frac{x_T + x_d'}{x_d + x_T}$$

$$K4 = \left( \frac{x_d - x_d'}{(x_d' + x_T)} \right) V_B \sin \delta_o$$

$$K5 = \frac{-x_q v_{do} V_b \cos \delta_o}{(x_T + x_q) V_{T0}} - \frac{x_d' v_{qo} V_b \sin \delta_o}{(x_T + x_d') V_{T0}}$$

$$K6 = \frac{x_T}{(x_T + x_d')} \left( \frac{v_{qo}}{V_{T0}} \right)$$

### Exciter data:

$K_E = 200$ ,  $T_E = 0.05 \text{ sec}$

### SVC Controller data:

$K_a = 80$ ,  $T_a = 0.025 \text{ sec}$ ,  $T_g = 0.0371 \text{ sec}$ ,  $T_c = 0.0375 \text{ sec}$

$Z_{th} = 0.02 \text{ p.u.}$ ,  $T_m = 0.000795 \text{ seconds}$

### PSO based SVC Controller data:

Population=50,  $c1=2.0$ ,  $c2=2.0$ , itermax=10,  $k_{min} = [60, 0]$ ,  $k_{max} = [100, 0.5]$

$K_a = 72.6369$  and  $T_a = 0.0056 \text{ sec}$

### Conventionally tuned parameters of auxiliary SVC controller:

$K_p = 0.5$ ,  $k_i = 0.1$ ,  $k_d = 0.01$

### PSO based auxiliary SVC controller parameters:

Population=50,  $c1=2.05$ ,  $c2=2.05$ , itermax=10,  $k_{min} = [0.5 -0.5 0.01]$ ,  $k_{max} = [0.7 -0.3 0.02]$ ,

$K_p = 0.5$ ,  $k_i = -0.500$ ,  $k_d = 0.0180$

**PSO-SFIWA based auxiliary SVC controller Parameters:**

Population=50,  $c_1=2.05$ ,  $c_2=2.05$ , itermax=10, SF/CF=0.73,  $w_{\max}=0.9$ ,  $w_{\min}=0.4$ ,  
 $k_{\min} = [0.5 \ -0.5 \ 0.01]$ ,  $k_{\max} = [1.0 \ -0.3 \ 0.05]$   
 $K_p= 0.9$ ,  $k_i= -0.46937$ ,  $k_d= 0.0455$

**PSO-TVAC based auxiliary SVC controller Parameters:**

Population=50,  $c_1=2.05$ ,  $c_2=2.05$ , itermax=10,  $c_{1i}=2.5$ ,  $c_{2f}=0.5$ ,  $c_{2i}=0.5$ ,  $c_{2f}=2.5$ ,  
 $w_{\max}=0.9$ ,  $w_{\min}=0.4$ ,  $k_{\min} = [0.5 \ -0.5 \ 0.01]$ ,  $k_{\max} = [1.0 \ -0.3 \ 0.05]$   
 $K_p= 0.6969$ ,  $k_i= -0.5$ ,  $k_d=0.02$

**Bacterial Foraging based auxiliary SVC controller Parameters:**

No. of Bacteria=20,  $N_c= 10$ ,  $N_s=3$ ,  $P_{ed}=0.02$ ,  $depth_{attractant}=0.01$ ,  $width_{attractant}=0.04$ ,  
 $height_{repellant}= 1 * depth_{attractant}$ ,  $width_{repellant}=10$ ;  
 $K_p= 1.0289$ ,  $k_i=1.4573$ ,  $k_d=0.0690$ ,  $K_a=76.5628$ ,  $T_a=0.0026$

**Hybrid BF-PSO based auxiliary SVC controller Parameters:**

No. of Bacteria=10,  $N_c= 10$ ,  $N_s=4$ ,  $N_{re}=4$ ,  $N_{ed}=2$ ,  $P_{ed}=0.25$ ,  $c_1=2.5$ ,  $c_2=1.5$   
 $K_p= 0.7900$ ,  $k_i= -0.4201$ ,  $k_d= 0.0180$ ,  $K_a=75$ ,  $T_a=0.0145$

**Genetic Algorithm based auxiliary SVC controller Parameters:**

Population=10, itermax=100,  $P_e=0.1$ ,  $P_c=0.85$ ,  $P_m=0.005$ ,  
 $K_p= 0.93812$ ,  $k_i=0.46937$ ,  $k_d= 0.0759$ ,  $K_a=99.37500$ ,  $T_a= 0.00166$

## APPENDIX B

### MODEL 1

**Generator data:**  $P=600\text{MVA}$ ,  $V_T=22\text{KV}$ ,  $f=60\text{Hz}$ ,  $X_d=1.305\text{p.u.}$ ,

$X_d'=0.246\text{p.u.}$ ,  $X_d''=0.252\text{p.u.}$ ,  $X_q=0.474\text{p.u.}$ ,  $X_q'=0.474\text{p.u.}$ ,  $X_q''=0.243\text{p.u.}$ ,  $H=6.5$ ,

$T_{do}'=1.01\text{sec}$ ,  $T_{do}''=0.053\text{sec}$ ,  $T_{qo}''=0.1\text{sec}$

**Voltage regulator parameters:**

$K_a=200$ ,  $T_a=0.02\text{sec}$

**Exciter parameters:**

$K_e=1$ ,  $T_e=0\text{sec}$ ,  $0 \leq E_{fd} \leq 7.0$

**Transformer parameter:**

$P=600\text{MVA}$ ,  $f=60$ ,  $V_1/V_2=22/500\text{KV}$ ,  $R_1=0.06\Omega$ ,  $L_1=0$ ,  $V_2=500\text{KV}$ ,  $R_2=0.06\Omega$ ,

$R_m=X_m=500\text{ p.u}$

**Transmission line parameters:**

$R_1=0.074\text{p.u.}$ ,  $X_1=0.08\text{p.u.}$ ,  $R_m=0.022$ ,  $X_m=0.24\text{p.u.}$ ,  $R_2=0.0067$ ,  $X_1=0.0739\text{p.u.}$ ,

$R_m=0.0186$ ,  $X_m=0.210\text{p.u}$

**TCSC parameters:**  $C_{TCSC}=21.977\mu\Omega$ ,  $X_{TCSC}=0.043\text{H}$ ,  $T_{TCSC}=4\text{ ms}$ ,  $K_p=0.8$ ,  $K_i=4.6$ ,

$T_1=0.05\text{sec}$  and  $T_2=0.016\text{sec}$

### MODEL 2

**Generator data:**

$2220\text{ MVA}$ ,  $24\text{KV}$ ,  $60\text{ Hz}$ ,  $R_a=0.003\text{p.u.}$ ,  $X_a=0.15\text{p.u.}$ ,  $H=3.5\text{ sec}$ ,  $x_d=1.81\text{p.u.}$ ,

$x_d'=0.3\text{p.u.}$ ,  $x_d''=0.23\text{p.u.}$ ,  $x_q=1.76\text{p.u.}$ ,  $x_q'=0.65\text{p.u.}$ ,  $x_q''=0.25\text{p.u.}$ ,  $T_{do}'=8\text{sec}$ ,

$T_{do}''=0.03\text{ sec}$ ,  $T_{qo}'=1\text{sec}$ ,  $T_{qo}''=0.07\text{ sec}$

**Transformer parameters:**

$2220\text{MVA}$ ,  $24/400\text{KV}$ ,  $x_l$  (leakage reactance)  $=0.15\text{p.u}$

**Transmission line parameters:**

$Z_{line1}=j0.5\text{p.u.}$ ,  $Z_{line2}=0.01+j0.8\text{p.u.}$ ,  $Z_{line3}=j0.13\text{p.u}$

**TCSC parameters:**

$K_r=10$ ,  $T_r=0.5\text{sec}$ ,  $K_p=0.1$ ,  $K_i=1$ ,  $X_L=0.2\text{p.u.}$ ,  $X_C=0.1\text{ p.u}$

### **MODEL 3**

#### **Generator data:**

$H=5\text{sec}$ ,  $D=0$ ,  $f=60\text{ Hz}$ ,  $X_d=1.6$ ,  $X_d'=0.32\text{p.u.}$ ,  $X_q=0.32\text{p.u.}$ ,  $T_{d0}'=6\text{sec}$ ,  $R_a=0$ ,  $P_g=0.5\text{p.u.}$ ,  
 $\delta^0=47.24^\circ$

#### **Exciter data:**

$K_R=2$ ,  $T_R=0.0015\text{ sec}$

#### **Transmission line:**

$R_T=0$ ,  $X_T = 0.8125\text{p.u.}$ ,  $X_{TR}$  (Transformer) =  $0.1364\text{p.u.}$ ,  
 $X_{TH}=0.13636$

#### **TCSC Controller:**

$L=6.63\text{mH}$ ,  $C=53\mu\text{F}$ ,  $T_{TCSC} = 15\text{ ms}$ ,  $\alpha_0=146.5^\circ$

#### **Conventionally tuned TCSC parameters:**

$K_T=32$ ,  $T_{WT}=10\text{sec}$ ,  $T_{1T}=1\text{sec}$ ,  $T_{2T}=2\text{sec}$ ,  $K_p = 10$ ,  $K_i=0.01$ ,  $K_R = 2$ ,  $T_R = 0.0015\text{sec}$

PSO based Excitation and TCSC Controller parameters:

#### **PSO Parameters:**

Population=50,  $c_1=2.0$ ,  $c_2=2.0$ ,  $\text{iter}_{\max}=10$ ,  $w_{\max}=0.9$ ,  $w_{\min}=0.4$ ,  $T_{1T}=1\text{sec}$ ,  $T_{2T}=2\text{sec}$ ,  
 $K_p = 10$ ,  $K_i=0.01$ ,  $K_r = 4.0219$ ,  $T_r = 0.0251\text{sec}$ ,



## APPENDIX C

### MODEL 1

#### Generator Data:

$$X'_d = 0.17 \text{ p.u.}, X'_q = 0.3 \text{ p.u.}, X'_{do} = 0.15 \text{ p.u.},$$

$$X_d = 1.9 \text{ p.u.}, X_q = 1.6, T_{do}' = 6.314 \text{ p.u.}, H = 5 \text{ s}$$

#### Exciter data:

$$K_E = 50, T_E = 0.1 \text{ s}$$

#### UPFC Data:

$$V_{dc\text{base}} = 30.5 \text{ kV}, MVA_{\text{base}} = 100, C = 3500 \mu\text{F}$$

#### Conventional Controller Data:

$$kp1 = 0.9, ki1 = 3.0, kp2 = 0.1, ki2 = 6.9$$

#### Bacterial Foraging parameters:

depthattractant= 0.02, widthattractant=0.04, heightrepellant=1\*depthattractant, widthrepellant=10, runlengthunit=.068,  $N_s$  (swim length)=3,  $P_{ed}$  (probability of elimination and dispersal)=0.2, No.of bacteria=8,  $N_c$  (chemotaxis step)=10 and  $N_{re}$  (reproduction steps)=15

#### BFO based UPFC controller parameters:

$$kp1 = 0.2340, ki1 = 2.0114, kp2 = 0.3891, ki2 = 1.4039$$

#### PSO parameters:

$w_{max} = 0.5$ ,  $w_{min} = -0.5$ ,  $it_{max} = 50$ ,  $c1 = 2$ ,  $c2 = 2$  and no. of particles=30

#### PSO based UPFC controller parameters:

$$kp1 = 0.3185, ki1 = 2.7387, kp2 = 0.3891, ki2 = 1.9115$$

#### Hybrid BF-PSO-TVAC parameters:

$S$  (The number of bacteria) =10,  $N_c$  (Number of chemotactic steps)=10,  $N_s$ (swim length)=4,  $N_{re}$ (number of reproduction steps)=4,  $N_{ed}$ (number of elimination-dispersal events)=2,  $S_r$ (number of bacteria reproductions (splits))= $s/2$ ,  $P_{ed} = 0.25$ ,  $c1 = 1.2$ ,  $c2 = 0.5$

#### Hybrid BF-PSO-TVAC based UPFC controller parameters:

$$kp1 = -0.2702, ki1 = 10.9063, kp2 = 1.6105, ki2 = 9.4152$$

**GA parameters:**

Population size=50, No. of bits=30, itermax=50,  $P_e$  (Elitism probability) =0.1,  $P_c$  (crossover probability)=0.8,  $P_m$  (mutation Probability)=0.05

**GA based UPFC controller parameters:**

$k_{p1} = 0.3269$ ,  $k_{i1} = 2.1141$ ,  $k_{p2} = 0.2949$ ,  $k_{i2} = 0.9280$

**MODEL 2****Generator 1:**

$X_{d1} = 0.1468$  p.u,  $X_{d1}' = 0.0608$  p.u ,  $X_{q1} = 0.0969$ p.u ,  $X_{q1}' = 0.0969$ p.u,  $T_{do1}' = 8.96$ sec,  
 $H1 = 5$ sec

**Generator 2:**

$X_{d1} = 0.8958$  p.u,  $X_{d1}' = 0.1198$  p.u ,  $X_{q1} = 0.8645$  p.u ,  $X_{q1}' = 0.1969$ ,  $T_{do1}' = 0.1969$ ,  
 $H2 = 4$ sec

**Generator 3**

$X_{d1} = 1.3125$ p.u,  $X_{d1}' = 0.1813$  p.u ,  $X_{q1} = 1.2578$  p.u ,  $X_{q1}' = 0.25$ ,  $T_{do1}' = 0.25$ ,  
 $H3 = 4$ sec

**Exciter Data:**

$K_{E1} = 25$ ,  $T_{E1} = 0.05$ sec,  $K_{E2} = 25$ ,  $T_{E2} = 0.02$  sec,  $K_{E3} = 25$ ,  $T_{E3} = 0.06$ sec

**Transmission line Data:**

$z_{24} = j0.068$ ,  $z_{37} = j0.068$ ,  $z_{84} = jz_{37}$ ,  $z_{78} = 0.1 * z_{37}$ ,  $z_{45} = j0.07$ ,  $z_{56} = 0.1 * z_{45}$ ,  $z_{61} = j0.07$

**Equivalent Load Reactance:**

$Y_{L5} = 0$ ,  $Y_{L6} = 0$ ,  $Y_{L7} = 0$ ,  $Y_{L1} = 6.261 - j1.044$ ,  $Y_{L2} = 0.0877 - j0.029$ ,  $Y_{L3} = 0.0877 - j0.0292$ ,  
 $Y_{L4} = 0.9690 - j0.3391$

**UPFC Data:**

$C = 3500$   $\mu$ F,  $B_{se} = 142.85$ siemens,  $V_{dc}$  base=31.5 kV

**Conventional controller parameters:**

$k_{p1} = 0.02$ ,  $k_{i1} = 0.3$ ,  $k_{pp1} = 0.02$ ,  $k_{ii1} = 0.3$ ,  $k_{p2} = 0.02$ ,  $k_{i2} = 0.3$ ,  $k_{pp2} = 0.02$ ,  $k_{ii2} = 0.3$

**PSO parameters:**

No. of Particles=,  $c1 = 0.2$ ,  $c2 = 0.4$ ,  $w_{max} = 0.5$ ,  $w_{min} = -0.5$  and  $it_{max} = 30$

**PSO based controller parameters:**

$k_{p1} = 0.045$ ,  $k_{i1} = 0.3245$ ,  $k_{pp1} = 0.0511$ ,  $k_{ii1} = 0.2211$   $k_{p2} = 0.015$ ,  $k_{i2} = 0.1021$ ,  
 $k_{pp2} = 0.0115$ ,  $k_{ii2} = 0.310$

## LIST OF PUBLICATIONS OUT OF THESIS

### List of Published Papers

S.No.	Title of Paper	Name of Journal where published	No.	Volume & Issue	Year	Pages
1	Advanced Adaptive Particle Swarm Optimization based SVC Controller for Power System Stability	International Journal of Intelligent System Applications (IJISA)	1	7	2014	101-110
2	Transient Stability Enhancement of a Multi-Machine System using Particle Swarm Optimization based Unified Power Flow Controller	International Journal of Engineering Research and Applications (IJERA)		Vol-4, Issue-7	2014	121-131
3	Optimization of UPFC Controller Parameters Using Bacterial Foraging Technique for Enhancing Power System Stability	International Journal of Advancements in Technology (IJOAT)	2	5	2014	61-70
4	Transient Stability Enhancement of a Power System using	International Review on Modelling and Simulations (IREMOS)	5	6	2013	1558-1569

	Unified Power Flow Controller					
5	Stability Enhancement of a Multi-Machine Power System using Static VAR Compensator	International Journal of Advanced and Innovative Research (IAIR),		Vol-2, Issue 2	2013	495-502